CHANGES IN ENDOSOME-LYSOSOME pH ACCOMPANYING PRE-MALIGNANT TRANSFORMATION

by

JENNIFER GOUWS JACKSON

B.Sc. (Hons)

Submitted in fulfilment of the
academic requirements for the degree of
Doctor of Philosophy
in the
Department of Biochemistry
School of Biochemistry, Genetics, Microbiology and Plant Pathology
University of KwaZulu-Natal
Pietermaritzburg

October 2005

PREFACE

The experimental work described in this thesis was carried out in the Department of Biochemistry, University of KwaZulu-Natal, Pietermaritzburg, from January 1999 to December 2004, under the supervision of Dr. Edith Elliott.

These studies represent original work by the author and have not been submitted in any other form to another university. Where use was made of the work of others, it has been duly acknowledged in the text.

Jennifer Gouws Jackson

Dr. Edith Elliott (supervisor)

ABSTRACT

The mechanisms by which altered processing, distribution and secretion of proteolytic enzymes occur, facilitating degradation of the extracellular matrix in invasive and metastatic cells, are not fully understood. Studies on the MCF-10A breast epithelial cell line and its premalignant, c-Ha-*ras*-transfected MCF-10AneoT counterpart have shown that the *ras*-transfected cell line has a more alkaline pH. The objective of this study was to determine which organelles of the endosome-lysosome route were alkalinized and shifted to the cell periphery after *ras*-transfection. Antibodies to the hapten 2,4-dinitrophenyl (DNP), required for pH studies, were raised in rabbits and chickens using DNP-ovalbumin (DNP-OVA) as immunogen. Cationised DNP-OVA (DNP-catOVA) was also inoculated to increase antibody titres. Anti-hapten and carrier antibody titres were assessed. In rabbits, cationisation seems useful to increase anti-DNP titres if a non-self carrier protein (OVA) is used. In chickens, cationisation of DNP-OVA seems necessary to produce a sustained anti-OVA (anti-self) response (implying a potential strategy for cancer immunotherapy). Oregon Green® 488 dextran pulse-chase uptake and fluorescent microscopy, and (2,4-dinitroanilino)-3'-amino-*N*-methyldipropylamine (DAMP) uptake, immunolabelling for DNP (a component of DAMP) and unique markers for the early endosome (early endosome antigen-1, EEA1), the late endosome (cation-independent mannose-6-phosphate receptor, CI-MPR) and the lysosome (small electron dense morphology and lysosome-associated membrane protein-2, LAMP-2) and electron microscopy was performed. The pH of late endosomes and lysosomes in the *ras*-transfected MCF-10AneoT cell line were found to be relatively alkalinised and lysosomes shifted toward the cell periphery. The acidic pH of late endosomes is required to release precursor cysteine and aspartic proteases from their receptors (e.g. CI-MPR), process the precursors to active proteases and to allow receptor recycling. The more alkaline pH observed potentially explains the altered processing of proteases in *ras*-transfected cells. Alkalinisation of the cytosol may affect the cytoskeleton responsible for, among other things, the positioning and trafficking of various organelles, causing relocation of lysosomes toward the cell periphery and actin depolymerisation. This may enable fusion of lysosomes with the plasma membrane and the release of proteolytic enzymes, facilitating the observed invasive phenotype.

ACKNOWLEDGEMENTS

I would like to express my appreciation to the following people for their contribution to this thesis:

Dr. Edith Elliott, my supervisor, for her guidance and drive throughout the duration of this study, for her ideas and discussions, for providing the necessary infrastructure for research, and a thorough appraisal of this thesis.

My parents, for bearing with me during this long and sometimes arduous process. My mother, for always standing by me with encouragement. My father, for his encouragement, providing me with logic when mine failed, and his financial generosity.

The members of staff in the Department of Biochemistry for interesting discussions and the loan of reagents in case of dire emergency.

Prof. Theresa Coetzer for arranging chickens for this study.

Prof. Bonnie Sloane, Wayne State University, Detroit, for supplying the MCF-10A and MCF-10AneoT cell lines, without which this study would not have been possible.

The staff of the Centre for Electron Microscopy, University of KwaZulu-Natal, Pietermaritzburg, Tony Bruton, Vijay Bandu, Belinda White and Pricilla Donelly for running an excellent unit, for skilled advice and assistance with anything microscopic or photographic, and for their cheerfulness and interest.

The administrative and technical staff, Charmaine Ahrens for dealing with admin problems, Jennifer Ender for ordering and tracking reagents, Denzil Lackay for always being available to troubleshoot equipment problems, Agnes Zondi and Richard Shabalala for maintaining lab cleanliness and helping to move equipment from one lab to another.

The staff of the electronic and mechanical workshops for fixing and creating new equipment.

Tertia Erusmus and her staff at Pannar Laboratory Services (Pty) Ltd., for their assistance with IEF.

My fellow lab inmates, Celia, Mary-Anne, Jackie, Amanda, Jess, for sharing papers and for good times.

Lizette and Alan, for being great friends and many marvellous philosophical discussions

Brendon, for laughs during the good times and a shoulder to cry on in the bad.

My other friends, scattered all over the world, for being great friends and making e-mail a pleasure to read.

The National Research Foundation for financial support.

CONTENTS

LIST OF TABLES

LIST OF FIGURES

ABBREVIATIONS

α_2-M	α_2-macroglobulin
α_2-MR	α_2-macroglobulin receptor
µg	microgram
µl	microlitre
3D	three-dimensional
ABTS	2,2'-azino-di-(3-ethyl)-benzthiozoline sulfonic acid
ARNO	ADP-ribosylation factor nucleotide binding site opener
Ag	antigen
AP2	adaptor protein-2
APC	antigen presenting cell
ASGPR	asialoglycoprotein receptor
ATP	adenosine triphosphate
Av	Avidin
Av-biotHRP	Avidin biotinylated HRP
BAD	pro-apoptotic protein of Bcl-2 family
biotHRP	biotinylated HRP
BSA	bovine serum albumin
BSA-PBS	bovine serum albumin in phosphate buffered saline
BSA-TBS	bovine serum albumin in Tris buffered saline
Ca^{2+}	calcium ion
catBSA	cationised bovine serum albumin
catOVA	cationised ovalbumin
CCD	charge-coupled device
CCP	clathrin coated pits
CD-MPR	cation-dependent mannose-6-phosphate receptor
Cdk	cyclin-dependent kinase
CHO	Chinese hamster ovary cells
CI-MPR	cation-independent mannose-6-phosphate receptor
Cl^-	chloride ion
CPT1	carnitine palmitoyl transferase of the outer mitochondrial membrane

c-*ras*	cellular *ras*
CTL	cytotoxic T lymphocyte
CURL	compartment for uncoupling of receptor and ligand
d.H_2O	distilled water
DAB	diaminobenzidine
DAG	1,2-diacylglycerol
DAMP	(2,4-dinitroanilino)-3'-amino-*N*-methyldipropylamine
dd.H_2O	double distilled water
DHSS	dinitrophenyl hapten sandwich staining
DIC	differential interference contrast
DMEM	Dulbecco's minimal essential medium
DNFB	2,4-dinitrofluorobenzene
DNP	2,4-dinitrophenyl
DNP-BGG	DNP-bovine gamma globulin
DNP-catOVA	cationised 2,4-dinitrophenyl ovalbumin
DNP-KLH	DNP-keyhole limpet haemocyanin
DNP-OVA	DNP-ovalbumin
ECM	extracellular matrix
ECV	endosome carrier vesicle
EDC	1-ethyl-3-[(3-dimethylaminopropyl)-carbodiimide hydrochloride]
EDTA	ethylenediaminetetraacetic acid
EE	early endosome
EEA1	early endosome antigen 1
EF	elongation factor
EGF	epidermal growth factor
EGFR	epidermal growth factor receptor
EGTA	ethylene glycol-bis(β-aminoethylether)-*N*,*N*,N',N',-tetraacetic acid
ELISA	enzyme-linked immunosorbent assay
EM	electron microscopy
ER	endoplasmic reticulum
ERK	extracellular signal-related kinase
ERM	ezrin, radixin, and moesin
Et-CoA	etomoxir-CoA
F-actin	filamentous actin

FBG	fish skin gelatin, bovine serum albumin, glycine
Fc	fragment, crystallisable
FITC	fluorescein isothiocyanate
fp	filopodia
FPP	farnesylpyrophosphate
FTase	farnesyltransferase
FTI	farnesyltransferase inhibitor
g	gram
G-actin	globular actin
GAP	GTPase activating protein
GCR	G protein-coupled receptor
GDI	guanine nucleotide dissociation inhibitor
GDP	guanosine diphosphate
GEF	guanine nucleotide exchange factor
GGPP	geranylgeranylpyrophosphate
GGTase	geranylgeranyltransferase
GlcNAc	*N*-acetyl glucosamine
GTP	guanosine triphosphate
GTPase	guanosine triphosphatase
h	hour(s)
H^+	proton
Ha-*ras*	Harvey-*ras*
HBSS	Hanks' balanced salt solution
HEPES	*N*-2-hydroxyethyl-piperazine-N'-2-ethane sulfonic acid
HMG-CoA	3-hydroxy-3-methylglutaryl-coenzyme A
HPTS	8-hydroxypyrene-1,3,6-trisulfonic acid
HRP	horseradish peroxidase
IEF	isoelectric focussing
IFN	interferon
IGF2	insulin-like growth factor-2
IGF2R	insulin-like growth factor-2 receptor
IgG	gamma immunoglobulin
IgY	yolk immunoglobulin
IL	interleukin

JNK	Jun amino-terminal kinase
JNKK	JNK kinase
K^+	potassium ion
kDa	kiloDalton
Ki-*ras*	Kirsten-*ras*
KLH	keyhole limpet heamocyanin
L	litre
LAMP	lysosome-associated membrane protein
LBPA	lysobisphosphatidic acid
LDLR	low density lipoprotein receptor
LE	late endosome
lgp	lysosomal glycoprotein
lp	lamellapodia
LPA	serum lysophosphatidic acid
MDR	multidrug resistance
M-6-P	mannose-6-phosphate
Lys	lysosome
MAP	microtubule associated protein
MAPK	mitogen activated protein kinase
MCF	Michigan Cancer Foundation
MCF-10A	MCF-10, attached
MEK	MAPK kinase
MEKK	MAPK kinase kinase
mg	milligram
Mg^{2+}	magnesium ion
MHC	major histocompatibility complex
mIg	membrane immunoglobulin
min	minute(s)
ml	millilitre
MLC	myosin light chain
MLCK	myosin light chain kinase
MMP	matrix metalloproteinase
MPR	mannose-6-phosphate receptor
mRNA	messenger ribonucleic acid

MT-MMP	membrane type matrix metalloproteinase
MVB	multivesicular body
Na^+	sodium ion
nBSA	native bovine serum albumin
neoT	neomycin resistant
NH_2	amino group
NHE	Na^+/H^+-exchanger
NSF	*N*-ethylmaleimide sensitive factor
OGD	Oregon Green® 488 dextran
OVA	ovalbumin
PAG	protein A-gold
PAK	p21 associated kinase
PBS	phosphate buffered saline
PDGF	platelet derived growth factor
PDGFR	platelet derived growth factor receptor
PEG	polyethylene glycol
PHEM	PIPES, HEPES, EGTA and $MgCl_2$
PI(3)K	phosphatidylinositol 3-kinase
PI(3)P	phosphatidylinositol 3-phosphate
PIPES	piperazine-*N*,*N*'-bis(2-ethanesulfonic acid)
PKA	protein kinase A
PKC	protein kinase C
PKN	protein kinase N
PLA_2	phospholipase A_2
PLC	phospholipase C
PLD	phospholipase D
PLGA NP	poly(lactide-co-glycolide) nanoparticle
PM	plasma membrane
R^2	correlation coefficient
r.p.m.	revolutions per minute
Rac	Ras actin
Ras	Rous sarcoma
RER	rough endoplasmic reticulum
Rho	Ras homologous

ROK	Rho binding kinase
RT	room temperature
RTK	receptor tyrosine kinase
sd.H_2O	sterile distilled water
SDS-PAGE	sodium dodecylsulfate polyacrylamide gel electrophoresis
sf	stress fibres
sIg	soluble immunoglobulin
SNAFL	seminaphthofluorescein
SNARE	*N*-ethylmaleimide sensitive factor-attachment protein receptor
SNARF	seminaphthorhodafluor
SOS	son of sevenless
TBS	Tris buffered saline
TGF	transforming growth factor
TGN	*trans* Golgi network
Th	T helper
TIL	tumour-infiltrating lymphocyte
TIP47	Tail-interacting 47-kDa protein
tPA	tissue-type plasminogen activator
TR	transferrin receptor
T_{Reg} cells	$CD4^+CD25^+$ T cells
t-SNARE	target *N*-ethylmaleimide sensitive factor-attachment protein receptor
UDP	uridine diphosphate
uPA	urokinase-type plasminogen activator
uPAR	urokinase-type plasminogen activator receptor
UV	ultra violet
V-ATPase	vacuolar H^+-ATPase
v-*ras*	viral *ras*

CHAPTER 1

INTRODUCTION

1.1 Malignant transformation

Transformation to the malignant phenotype is a multi-step process requiring a minimum of three mutations at the gene level. The primary mutation in premalignant transformation usually results in immortalisation due to mutation of genes such as the p53 gene, responsible for programmed cell death, the second mutational activation of an oncogene such as *ras* and the final mutation usually resulting in uncontrolled proliferation, tumour formation and metastasis (Vogelstein *et al.*, 1988). Malignancy is also associated with metastasis or tumour dissemination, facilitated by the secretion of proteolytic enzymes (proteases), the degradation of the basement membrane and invasion into- and back out of the blood vascular system.

The mechanism by which upregulation and altered trafficking of proteases is associated with the malignant, invasive phenotype is not fully understood. Early studies using *ras*-transformed fibroblasts were the first to implicate *ras* mutations in the altered trafficking and secretion of proteases. In such model systems, transfection with mutated Harvey-*ras* (Ha-*ras*) was seen to cause the hypersecretion of procathepsin L, while transfection with mutated Kirsten-*ras* (Ki-*ras*) was seen to result in the upregulation and secretion of urokinase-type plasminogen activator (uPA) (Dong *et al.*, 1989).

The MCF-10A breast cancer cell line and its *ras*-transfected MCF-10AneoT derivative was, however, the first human model used to investigate the effects of *ras*-transformation on progression to a premalignant phenotype (Soule *et al.*, 1990; Basolo *et al.*, 1991). Transfection with mutationally activated c-Ha-*ras* has been shown to cause cells to become invasive (Basolo *et al.*, 1991; Tait *et al.*, 1990; Russo *et al.*, 1991; Ochieng *et al.*, 1991) and results in altered trafficking of lysosomal proteases, such as cathepsins B, D, and L (Moin *et al.*, 1994; Sameni *et al.*, 1995). Since these changes accompany the acquisition of an invasive phenotype, an understanding of the pathways by which such phenotypic changes may be induced could be important for the development of therapeutic strategies.

The following section, therefore, describes the role of the Ras protein superfamily in the Ras signalling pathway that becomes constitutively active after *ras*-transfection.

1.1.1 Ras, the Ras-family proteins and the transformed phenotype

The Ras superfamily of proteins belongs to a large family of membrane-associated guanine nucleotide-binding proteins functioning in receptor-mediated processes that include growth-related signal transduction, regulation of the cytoskeleton, and membrane trafficking (Fig. 1.1) (Lowry and Willumsen, 1993; Prendergast and Gibbs, 1993). These proteins undergo post-translational modifications essential for their biological functions (Casey, 1995; Rando, 1996). The C-terminal amino acids of Ras family proteins form a CaaX motif (C = cysteine, a = any aliphatic amino acid, X = carboxy terminal amino acid), which directs the attachment of either a farnesyl or geranylgeranyl moiety onto the cysteine residue via a thioether linkage. The presence of either Ile or Leu at position X directs geranylgeranylation by geranylgeranyltransferase I (GGTase I), while Met or Ser at position X directs farnesylation by farnesyltransferase (FTase) (Tamanoi, 1993; Cox *et al.*, 1994).

Ras-family proteins exist in two conformational states: GDP-bound (inactive) and GTP-bound (active) and have GTPase activity (Barbacid, 1987). The activity of Ras-like proteins is further regulated by guanine nucleotide exchange factors (GEFs) that activate Ras by allowing exchange of GDP for GTP, GTPase activating proteins (GAPs) that increase GTP hydrolysis and hence downregulate Ras activity, and guanine nucleotide dissociation inhibitors (GDIs) that block both GAP inhibition and GEF activation of Ras GTPase (Tamanoi, 1993; Cox *et al.*, 1994).

Mutations at amino acid positions 12, 13, 14 and 61 decrease the activity of the GTPase and render Ras constitutively active. These point mutations have been identified in both viral (v-*ras*) and cellular (c-*ras*) *ras* oncogenes (Barbacid, 1987). Introduction of oncogenic c-*ras* into the NIH 3T3 fibroblast cell line has been shown to result in a fully transformed phenotype, i.e. a distinct cellular morphology, anchorage-independent growth, reduced serum requirements, and tumour formation when injected into susceptible animals (Egan *et al.*, 1989; Der *et al.*, 1986; Muschel *et al.*, 1985). In primary rat embryo fibroblasts, however, c-Ha-*ras* induces the morphological changes associated with

transformation but cells are not immortalised, and usually do not induce tumourigenesis when injected into nude mice (Land *et al.*, 1983; Ruley, 1983). Transfection with both oncogenic *ras* and *myc* (or other nuclear oncogenes), however, leads to fully transformed, immortal cell lines that are tumourigenic. If *ras* is provided with retroviral long terminal repeat sequences, which act as strong promoters and enhancers, the altered *ras* will immortalise cell lines (Chang *et al.*, 1982; McKay *et al.*, 1986). In the immortal MCF-10A cell line, used in the present study, c-Ha-*ras*-transfection alone results in transformation of the cell line, as well as many of the phenotypic changes seen in the NIH 3T3 fibroblasts (Basolo *et al.*, 1991), including a more fibroblast-like morphology and increased chemotactic and invasive potential (Basolo *et al.*, 1991; Ciardiello *et al.*, 1990; Russo *et al.*, 1991; Ochieng *et al.*, 1991).

Ras regulates at least three downstream signal transduction pathways: the extracellular signal-related kinase (ERK) or mitogen activated protein kinase (MAPK) pathway of serine/threonine kinases that regulates gene transcription, the Rac/Rho pathway that controls the cytoskeletal organisation of the cell and vesicle trafficking, and the Akt pathway involved in the inhibition of apoptosis (Fig.1.1) (Prendergast and Gibbs, 1993; Sahai and Marshall, 2002; Haluska *et al.*, 2002). Although the pathways regulate distinct cellular processes, evidence suggests the possibility of cross-talk between them (Takai *et al.*, 1995; Vojtek and Cooper, 1995). Mutationally activated Ras proteins may, therefore, lead to the overexpression or overactivation of the ERK and MAPK pathways and their downstream products (e.g. Rac and Rho). This could result in morphological and functional alterations in the cell, like those observed in the MCF-10A cell line after *ras*-transfection (Basolo *et al.*, 1991; Ciardiello *et al.*, 1990; Russo *et al.*, 1991; Ochieng *et al.*, 1991).

The Ras subfamily proteins include Rac, Rho, Cdc42Hs and Tc10 that share at least 50% amino acid sequence identity (Dutartre *et al.*, 1996). Functional Rac, Rho, and Cdc42Hs proteins have been shown to be essential for the progression of cells through the G1 phase of the cell cycle and hence for DNA replication and cell proliferation (Olson *et al.*, 1995) (Fig. 1.1).

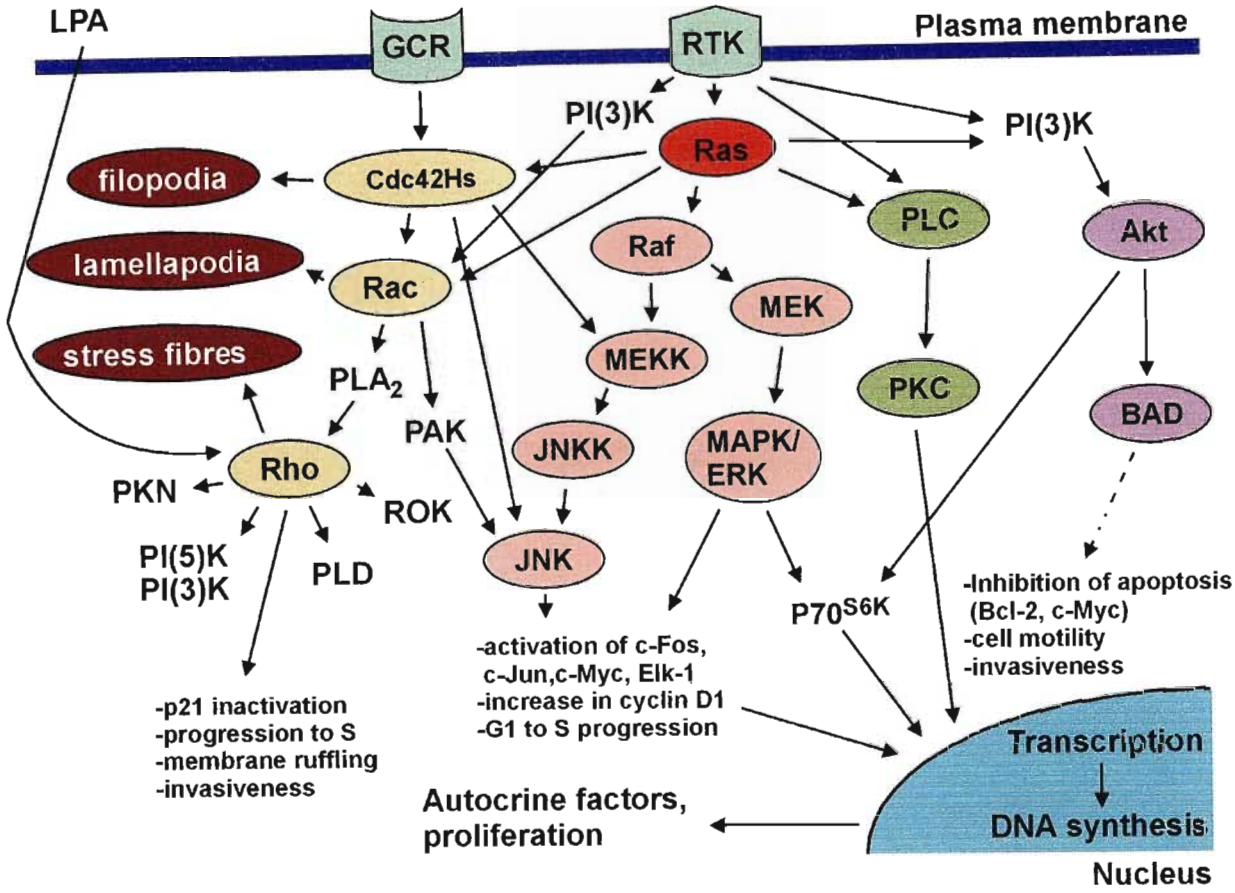

Figure 1.1 **The signal transduction pathways of Ras family GTPases.**
Oncogenic Ras controls both the ERK/MAPK and Rac/Rho pathways to cause cell transformation. Ras is translocated to the plasma membrane following the binding of a ligand to its respective receptor tyrosine kinase. Raf protein kinase is the first intermediate protein of the ERK pathway, which stimulates transcription by the phosphorylation of transcriptional activators, e.g. c-*myc,* and translation by phosphorylation of the S6 protein of the eukaryotic 40S ribosomal subunit. Ras is thought to act in parallel with PI(3)K in activating the Akt pathway, responsible for inhibition of apoptosis, and Rac1 GTPase. Cdc42Hs, activated by ligand binding to G protein coupled receptors, initiates filopodia formation and activates Rac1. Rac1 initiates the formation of lamellapodia, the activation of the PAK, and subsequently, the JNK pathway and activation of Rho via PLA_2. Rho may be alternatively activated by serum lysophosphatidic acid. Rho activation alters the actin cytoskeleton by catalysing the formation of focal adhesions and actin stress fibres. Focal adhesion formation allows for ECM binding mainly via the integrin family of proteins. The different MAPK modules activated by Ras, Rac, and Rho are integrated at the level of transcription factors. Transcriptional activation in turn leads to the production of autocrine factors (in some cells) and initiation of DNA synthesis (adapted from Symons, 1996; Haluska *et al.*, 2002). Abbreviations: LPA = lysophosphatidic acid; GCR = G protein-coupled receptor; RTK = receptor tyrosine kinase; PI(3)K = phosphatidylinositol 3-kinase; PI(5)K = phosphatidylinositol 5-kinase; MAPK = mitogen activated protein kinase; MEK = MAPK kinase; ERK = extracellular-signal regulated kinase; PAK = p21 associated kinase; MEKK = MAPK kinase kinase; JNK = Jun amino terminal kinase; JNKK = JNK kinase; PLA_2 = phospholipase A_2; PLD = phospholipase D; ROK = Rho binding kinase; PKN = protein kinase N; PKC = protein kinase C; $p70^{s6k}$ = ribosomal s6 kinase; BAD = pro-apoptotic protein of Bcl-2 family.

Rac is involved in membrane ruffling and the formation of lamellapodia, as dominant inhibitory Rac proteins have been shown to inhibit these events in platelet derived growth factor (PDGF) or epidermal growth factor (EGF) stimulated fibroblasts (Ridley *et al.*, 1992). In addition, Rac1 is responsible for lysophosphatidic acid-mediated activation of Rho via phospholipase A_2 (PLA_2), and activates the p21 associated kinase (PAK) pathway. The PAK pathway, in turn, stimulates gene transcription by activating the Jun upstream transcriptional enhancer element via Jun amino-terminal kinase (JNK) (Fig. 1.1). Overexpression of Rac1 may, therefore, be indirectly involved in the production of increased levels of proteases, such as cathepsin B, occurring in the *ras*-transfected MCF-10AneoT cell line (Elliott and Sloane, 1996).

Rho proteins seem to have profound effects on the cell morphology and phenotype as they stimulate the formation of actin stress fibres and focal adhesion points (Nobes *et al.*, 1995; Ridley and Hall, 1992; 1994; Chrzanowska-Wodnicka and Burridge, 1996). Upregulation of receptor tyrosine kinases (RTKs) by *ras*-transfection, results in p120 Cas replacing β-catenin for cadherin binding to adherens junctions, resulting in weaker binding of actin to the proteins associated with adherens junctions (Kinch *et al.*, 1995). Furthermore, overexpression of phosphatidylinositol 3-kinase [PI(3)K] (a downstream product of *ras* transfection) (Fig. 1.1) is sufficient to induce ruffling and stress fibre breakdown (Martin *et al.*, 1996a,b; Siddhanta *et al.*, 1998). *Ras*-transfection of the MCF-10A cell line, therefore, seems to result in stress fibre breakdown (Kinch *et al.*, 1995). The regulation of stress fibre formation, however, seems to be cell line dependent. In most fibroblast cell lines (e.g. NIH 3T3), the growth factors signalling through RTKs cause the disassembly of stress fibres, whereas in Swiss 3T3 cells assembly of stress fibres is induced by the same signal (Ridley and Hall, 1992; 1994). Furthermore, in one report using Swiss 3T3 cells, Cdc42 (a Ras-independent activator of Rac) was shown to activate Rho (Nobes and Hall; 1995), but by contrast, in another study, employing a different strain of Swiss 3T3 fibroblasts, Cdc42 caused disassembly of stress fibres (Kozma *et al.*, 1995). The effects of Ras and Rho proteins seem, therefore, to be cell-specific and may also differ between different lines of the same cell type (e.g. NIH 3T3 fibroblasts and Swiss 3T3 fibroblasts). The results obtained from various research groups are also highly dependent on the experimental approaches adopted.

Intact and cell-free assays suggest that Rho regulates the reorganisation of the actin cytoskeleton through the formation of phospholipid metabolites (Takai *et al.*, 1995). Hydrolysis of PI(4,5)P by phospholipase C (PLC) results in actin depolymerisation by releasing sequestered actin binding proteins, while enhanced formation of PI(4,5)P induces actin polymerisation. The activity of PI(4)P-5-kinase, which produces PI(4,5)P, is enhanced by Rho. Decreasing PI(4,5)P levels are paralleled by enhanced 1,2-diacylglycerol (DAG) synthesis that regulates actin dynamics via protein kinase C (PKC) (Jakab *et al.*, 2002). Rho is further required for contractile ring assembly during cytokinesis after cell nuclear division (Dutatre *et al.*, 1996; Olson *et al.*, 1995).

In some cell types, Rho proteins control additional actin-based structures and processes. In polarised epithelia (such as the MCF-10A breast epithelial cell line) Rho is involved in the regulation of tight junctions (Symons, 1996). At the plasma membrane, GTP-Rho has been found to associate with actin filaments, integrin, vinculin, ERM proteins (ezrin, radixin, and moesin) and the cell surface glycoprotein CD44, a receptor for collagen (type I or VI) and hyaluronic acid, facilitating cellular adhesion to the extracellular matrix (ECM) (Kreis and Vale, 1993). Inhibition of Rho activity may, therefore, alter ECM adhesion and thus assist metastasis (Takai *et al.*, 1995).

Rho proteins are also involved in the loss of epithelial polarity evident in benign tumours (also seen in the MCF-10AneoT cell line) and are thought to be important in the epithelial-mesenchymal (fibroblast-like) transition observed in more aggressive tumours (Sahai and Marshall, 2002; Malliri and Collard, 2004). Since Rac signalling is required for E-cadherin-mediated adhesion (Hordijk *et al.*, 1997), the downregulation of Rac activity with the consequent activation of Rho, results in loss of the epithelial phenotype and the acquisition of a more fibroblast like morphology. Rac antagonizes Rho activity by the Rac-mediated production of reactive oxygen species that inhibit the low-molecular-weight protein tyrosine phosphatase, resulting in phosphorylation and activation of p190Rho GAP, an inhibitor of Rho activity (Nimnual *et al.*, 2003). Rac1 and Rho thus play an important role in cell motility, and hence may be important for cell migration and invasion. Rac1 mediates the formation of lamellapodia at the leading edge of cells and Rho is involved in cell attachment at the leading edge and detachment at the trailing edge.

Rac1 and RhoA are also thought to be involved in endocytosis, and RhoD to regulate endosome dynamics (Lamaze *et al.*, 1996; Murphy *et al.*, 1996). Rac1 may act by binding to synaptojanin2, a phosphatidylinositol phosphate involved in the regulation of endocytosis (Malecz *et al.*, 2000). RhoA, RhoG, Rac1 and Cdc42 have been shown to bind kinectin, which is involved in anchoring vesicles to microtubules (Hotta *et al.*, 1996; Vignal *et al.*, 2001). Rho proteins might, therefore, regulate the movement of vesicles along microfilament networks (Sahai and Marshall, 2002). Upregulation of the Rho proteins may, therefore, give rise to the altered trafficking of proteases seen in the *ras*-transfected MCF-10AneoT cell line. This may also give rise to the features associated with the pre-malignant phenotype found in the MCF-10AneoT cell line, e.g. the appearance of peripheral active-enzyme-containing organelles and increased secretion and association of proteases with the cell surface (Moin *et al.*, 1994).

Tc10 is a Rho-family protein involved in GLUT4 (a glucose transporter) translocation and glucose uptake (Chiang *et al.*, 2001). This is interesting since glucose deprivation may result in reversible dissociation of the subunits of the V-ATPase proton pumps of the endosome-lysosome system, decreasing their activity and potentially resulting in an increase in vesicular pH (Myers and Forgac, 1993). *Ras*-transfection appears to result in cellular alkalinisation (Sloane *et al.*, 1994b). An altered cytosolic pH could affect many components of the cell, including the cytoskeleton and possibly the cytoskeleton-assisted movement or trafficking of organelles, leading to a change in vesicle distribution (Heuser, 1989). There is also evidence that the processing, trafficking and secretion of proteases in *ras*-transfected fibroblasts is affected by the alkalinisation of acidic organelles usually responsible for the processing of pro-enzymes to the mature active form (Dong *et al.*, 1989). This may also be the case for the *ras*-transfected MCF-10AneoT cells. pH alterations may similarly affect trafficking of proteases by affecting enzyme glycosylation patterns, or by affecting elements of the endosome-lysosome system, specifically receptor-binding and release of newly synthesised proteases. The aim of this study was to establish whether the pH of the endosome-lysosome organelles involved in protease processing and trafficking is altered by Val-12 mutationally activated c-Ha-*ras*. The aim was also to determine the identity of organelles found in the cell periphery after *ras*-transfection. Before this study is described, however, the organelles of the endosome-lysosome system and the pathway by which normal trafficking and processing of proteases occurs will be reviewed.

1.2 The endosome-lysosome system

Molecules taken up into cells, via a process known as "endocytosis", include a variety of small and macromolecules, small insoluble particles and some viruses. The uptake of bacteria, cell fragments and whole cells, i.e. larger particles, is termed "phagocytosis". There is practically no limit to what can be introduced into the endocytic/phagocytic system, a feature that makes these systems ideal targets for drug therapies.

This study will be confined to the "endocytic system", which consists of both an "endocytic-digestive pathway" and an "endocytic-recycling pathway" (Fig. 1.2). The endocytic-digestive pathway is responsible for handling material intended for degradation and for lysosomal enzyme processing (Fig. 1.2, Path 1), while the endocytic-recycling pathway is responsible for the recycling of internalised plasma membrane receptors back to the cell surface (Fig. 1.2, Path 2). A further biosynthetic pathway, originating from the endoplasmic reticulum (ER) and Golgi, ensures that the correct protein constituents and lipids are trafficked to the correct organelles in the endocytic system, or the cell surface (Fig.1.2, Path 3).

Molecules are taken up at different rates via the two endocytic-digestive routes: the constitutive (or fluid-phase) endocytic route that leads to the digestive pathway, and the receptor mediated endocytic route that leads to both the digestive and recycling pathways (Fig. 1.2) (Mullock *et al.*, 1994).

The early endosome is the first compartment reached by plasma membrane receptor-ligand complexes and fluid-phase molecules during endocytosis. It is, therefore, the major sorting compartment of the endocytic pathway. During receptor-mediated endocytosis, the ligands dissociate from their receptors due to the mildly acidic pH of the early endosome, and the receptors recycle back to the cell surface via the recycling endosome (Fig. 1.2, Path 2) (Mellman, 1996; Mukherjee *et al.*, 1997; Clague, 1998; Pillay *et al.*, 2002). Receptor recycling is so efficient that only approximately 3% of all internalised receptors are delivered to the late endosome (Haylett and Thilo, 1986; Draye *et al.*, 1987). Fluid-phase molecules (and ligands which have dissociated from their receptors) subsequently move, via an intermediate endosome carrier vesicle (ECV), to the late endosome for digestion (Fig. 1.2, Path 1).

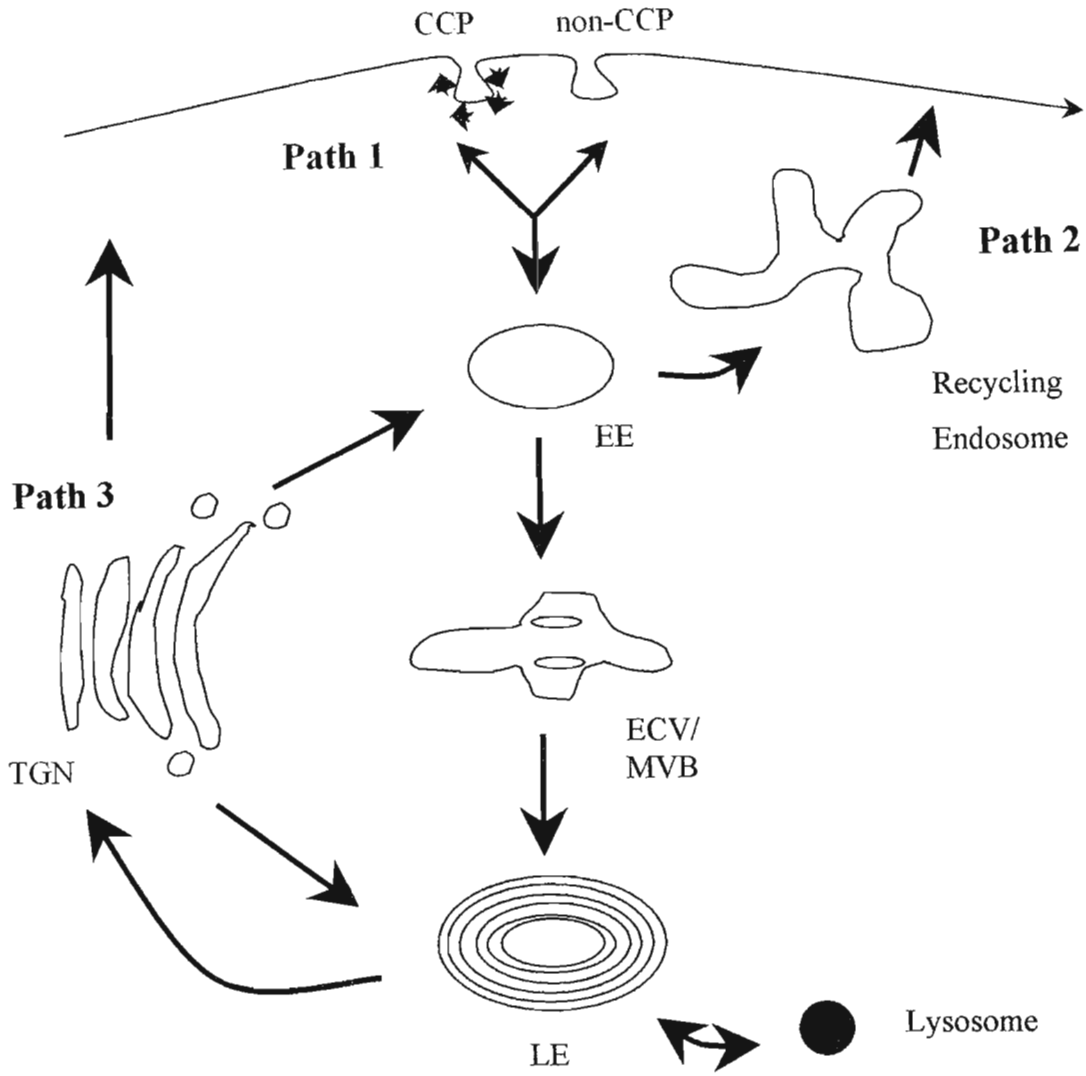

Figure 1.2 **A model of the biosynthetic, endocytic-digestive/processing and recycling pathways.**
Path 1) The endocytic-digestive route is the major endocytic traffic route from the plasma membrane, via either CCP or non-CCP, to the early endosome, and via ECV, moving on microtubules, to the late endosome. The lysosome fuses with the late endosome, and presumably releases proteolytic enzymes into the late endosome. Path 2) The endocytic-recycling route is the pathway by which endocytosed receptors are recycled from the early endosome back to the cell surface. Path 3) The biosynthetic pathway, emanating from the TGN, delivers newly synthesised lysosomal membrane glycoproteins or enzymes to their destinations via the plasma membrane or endosomal compartments. Traffic routes back to the TGN from endosomal compartments are also indicated (adapted from Luzio *et al.*, 2000; Clague, 1998). Abbreviations: TGN = *trans* Golgi network; CCP = clathrin coated pits; EE = early endosome; ECV = endosome carrier vesicle; MVB = multivesicular body; LE = late endosome.

The membrane trafficking pathway from early to late endosomes has been studied extensively (reviewed by Gruenberg and Maxfield, 1995; Gu and Gruenberg, 1999; Gruenberg, 2001; 2003) but the membrane traffic between late endosomes and lysosomes has been difficult to elucidate, mainly because both organelles have similar properties. Both these organelles are acidic, have similar densities, and contain similar lysosomal enzymes and subsets of lipid components in their membranes. Additionally, the lysosome has no unique, easily demonstrable markers, except that the cation-independent mannose-6-phosphate receptor (CI-MPR) is not found in the lysosome (Griffiths, 1996). This difficulty has led to the adoption of various strategies to distinguish and study the mechanism of trafficking between these organelles. Such strategies include: membrane labelling, endocytic uptake of fluid-phase markers, morphological studies, labelling of plasma membrane receptors involved in receptor-mediated endocytosis, and others.

1.2.1 Fluid-phase and membrane lipid and protein trafficking studies

Early studies of the endocytic pathway concentrated on the uptake and delivery of macromolecules, via the early endosome, to a digestive body initially known as the "lysosome" (Thilo, 1985) and subsequently identified as the late endosome (Stinchcombe and Griffiths, 1999). Confusion in nomenclature and in the distinction between the late endosome and lysosome complicates interpretation of much of the earlier literature. The function and role of the lysosome is now also perceived to be different (as will be outlined in Section 1.2.2.1) to that of the digestive body (the late endosome) (Griffiths, 1996). For this reason, where the "lysosome" is mentioned as the final digestive destination of endocytosed material in early studies, the words "digestive body" or "digestive organelle" will be substituted.

Early quantitative studies using fluid-phase uptake of horseradish peroxidase (HRP) showed that HRP becomes distributed throughout the early endosomal compartments in <2 min. Thereafter, no significant increase in the number of labelled compartments containing HRP occurs, but the concentration within the system steadily increases over 15-20 min as the digestive body fills with the fluid-phase marker (Thilo, 1985; Griffiths *et al.*, 1989). Such studies proved that the internalised fluid-phase tracer reaches the digestive body (late endosome) within 60 min (Thilo, 1985; Steinman *et al.*, 1976; Griffiths *et al.*, 1989). The markers distinguishing this organelle as a late endosome and

not a lysosome are: CI-MPR (Section 1.3) and the regulatory domain of a cAMP-dependent protein kinase found in late endosomes (Griffiths, 1996).

Early fluid-phase and membrane lipid and protein trafficking studies gave rise to a hotly debated "maturation model" that postulates that the early endosomal body "matures" into a lysosome via a vesicular delivery process, carrying proteolytic enzymes into the maturing organelle, and a vesicular recycling process, carrying membranes and plasma membrane receptors back to the cell surface (Griffiths and Gruenberg, 1991; Roederer *et al.*, 1987; Stoorvogel *et al.*, 1991; Murphy, 1991; Griffiths, 1996). Two schools of thought have subsequently emerged, the one steadfastly proposing the "maturation model" (Murphy, 1991; Stoorvogel *et al.*, 1991) and the other proposing a "pre-existing" organelle model, in which the organelles in the endocytic route are stable, pre-existing compartments (Griffiths and Gruenberg, 1991). These compartments, it is argued, have specific fusion capabilities, i.e. capable only of homotypic fusion and fusion with their specifically associated "shuttle" vesicle populations. These vesicle populations are responsible for carrying membrane and fluid-phase components between the specific pre-existing organelles (Griffiths and Gruenberg, 1991; Griffiths, 1996). The school proposing the existence of pre-existing organelles argues that the complexity of the organelles of the endosome-lysosome system precludes a maturation process. Their argument is based on evidence from fusion studies on subcellularly fractionated vesicular populations (described in Section 1.2.2.1 and 1.4), and the requirement of specific distinct fusion proteins, known as the Rabs, for fusion between specifically associated vesicle and organelle populations (Gruenberg and Griffiths, 1991; Griffiths, 1996). Additionally, the different organelle populations are also enriched with different phosphoinositides (Fig. 1.3) (Gruenberg, 2003).

Studies on the recycling of plasma membrane receptors have also shed some light on the identity of organelles from which receptors recycle (the endocytic recycling route) (Fig. 1.2, Path 2). Plasma membrane proteins involved in receptor-mediated endocytosis do not reach the digestive organelle and only approximately 0.1% of the endocytosed plasma membrane receptors were found in the digestive compartment. Surface receptors, such as the transferrin receptor (TR), low density lipoprotein receptor (LDLR), α_2-macroglobulin receptor (α_2-MR) and asialoglycoprotein receptor (ASGPR), therefore, recycle back to the plasma membrane with >99% efficiency (Goldstein *et al.*, 1985; Salzman and Maxfield, 1988). It has also been estimated that an amount of plasma

membrane equal to the entire cell surface is internalised and recycled every 1-2 h (Steinman *et al.*, 1976; Griffiths *et al.*, 1989). Kinetic data also showed that membrane and receptor recycling was occurring from more than one compartment of the endocytic system. Studies on fluid-phase markers and plasma membrane receptor recycling showed that the early endosome is involved in the initial sorting of internalised materials, while a "recycling endosome" is involved in the recycling of a specific subset of cell surface receptors back to the plasma membrane. The early endosome involved in sorting is accessible to fluid-phase markers, while the recycling endosome is not (van Deurs *et al.*, 1989; Courtoy, 1991).

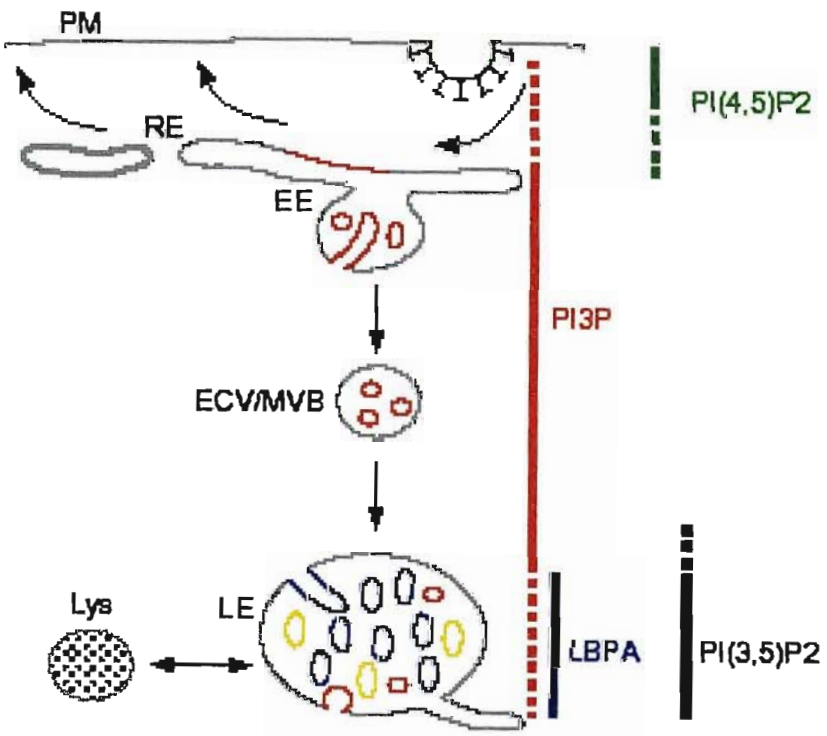

Figure 1.3 **Lipid territories in the endocytic pathway.**
The outline shows the distribution of endocytic lipid territories. Whereas PI(4,5)P2 (green) is thought to be predominantly found at the PM and plays a role in the formation of clathrin-coated pits, PI(3)P (red) and PI(3,5)P2 (black) are believed to be abundant in endosomes. In EEs, PI(3)P is presumably generated from phosphatidylinositol by a Vps34p complex, and accumulates within ECV/MVB internal membranes. Then, the lipid is either degraded, presumably by myotubularin, or converted into PI(3,5)P2 by PIK, although the precise distribution of PI(3,5)P2 is not known. LEs contain large amounts of LBPA (blue), generated via an unknown biosynthetic pathway. This lipid is abundant within LE internal membranes, which appear to be distinct from the remaining PI(3)P containing vesicles. In addition to LBPA and PI(3)P domains, LE internal membranes might also contain other membrane domains (yellow), including, cholesterol-enriched membranes and rafts (Gruenberg, 2003). Abbreviations: PM = plasma membrane; PI(x)P = phosphatidylinositol x-phosphate, where x is a number; EE = early endosome; ECV = endosome carrier vesicle; MVB = multivesicular body; PIK = phosphatidylinositol kinase; LE = late endosome; LBPA = lysobisphosphatidic acid; Lys = lysosome.

1.2.1.1 Use of temperature to study fluid-phase marker trafficking

Recycling receptors reach early endosomes (Dunn *et al.*, 1989) and are still able to do so when the temperature is lowered to 20°C, or when the microtubule cytoskeleton is depolymerised (Marsh *et al.*, 1983; Gruenberg and Howell, 1989). Since these treatments prevent fluid-phase tracers from penetrating further along the digestive route than the early endosome, this provides a useful means of identifying the organelle (i.e. the early, sorting endosome) to which rapidly recycling receptors migrate. The next compartment in the endocytic-digestive pathway has been termed the late endosome or prelysosome, the former because it is believed that sorting events continue within this compartment and the latter because the compartment also contains typical lysosomal proteins such as the acidic, highly glycosylated membrane proteins, the lysosomal glycoproteins (lgps), also called lysosome-associated membrane proteins (LAMPs). Low temperatures also prevent the recycling of the CI-MPR back to the Golgi (Ludwig *et al.*, 1991). The accumulation of receptors under such conditions indicates that the late endosome is also the organelle to which newly synthesised lysosomal enzymes and CI-MPR are ultimately delivered.

1.2.2 Morphological studies of organelles involved in trafficking of fluid-phase markers (the endocytic-digestive pathway)

Vesicles budding inward from the plasma membrane were initially shown to fuse with an interconnected system of pleiomorphic vacuoles and tubular compartments that lead to larger, more spherical vacuolar compartments (Geuze *et al.*, 1983; Marsh *et al.*, 1986; Hopkins *et al.*, 1990; Tooze and Hollinshead, 1991; Wilson *et al.*, 1991). Material internalised via fluid-phase endocytosis, therefore, accumulates within spherical early endosomal compartments, roughly 0.5-1.0 μm in diameter (Yamashiro *et al.*, 1984; Salzman and Maxfield, 1988). Maxfield and co-workers, studying CHO cells using light microscopy, first termed these vacuoles collectively the "sorting endosome" (Yamashiro *et al.*, 1984; Salzman and Maxfield, 1988; Dunn *et al.*, 1989; Dunn and Maxfield, 1992; Mayor *et al.*, 1993). At the EM level, these structures correspond to the compartments that have been termed "receptosomes", "compartment for uncoupling of receptor and ligand" (CURL), "multivesicular endosomes" or "early endosomes" (Courtoy 1991; Gruenberg and Howell, 1989). In this thesis the term "early endosome" will be used for the sorting endosome (Fig. 1.2).

Sorting in the early endosome appears to be effected by the "pinching" off of membranes into long tubular cisternae, containing receptors bound for the recycling endosome. The fluid-phase content, membranes, and receptors for degradation, on the other hand, may be inwardly pinched off to form the ECV or multivesicular body (MVB) (Hopkins, 1990; Clague, 1998; Murphy, 1991). The ECV or MVB is usually a spherical organelle (0.4-0.7 μm), often filled with vesicle-like membrane-bound bodies and carries material from the early endosome to the late endosome in a microtubule-dependent fashion (Griffiths, 1996; Gruenberg *et al.*, 1989) (Fig. 1.2, Path 1).

The late endosome or prelysosomal compartment (0.5-0.8 μm) contains cisternal, tubular and vesicular regions with many membrane invaginations (Griffiths *et al.*, 1988; Piper and Luzio, 2001) and usually, therefore, appears to be either multivesicular or multilamellar (Fig. 1.2, Path 1). The pleiomorphic internal membrane ultrastructure of both the ECV/MVB and late endosome is difficult to preserve (McDowall *et al.*, 1989), contributing to the confusion of organelle classification in the literature, and leading many authors to disregard morphology as a means of identifying these organelles. Since the late endosome and lysosome also share almost all their membrane lipids [e.g. lysobisphosphatidic acid (LBPA), also found in the ECV (Fig. 1.3)], proteins (e.g. LAMPs) and cytosolic proteins or enzymes and no reliable marker proteins [except that lysosomes do not contain CI-MPR or the regulatory domain of a cAMP-dependent protein kinase] have been identified (Griffiths, 1996), the late endosome has often been wrongly identified as a lysosome and *vice versa*. This led to the idea that the lysosome, and not the late endosome, was the site of digestion of endocytosed materials. Now that more specific markers (e.g. Rabs) are available and ultrastructure preservation methods have improved, morphological and immunolabelling identification of these organelles has become more reliable.

The lysosome, once regarded as the terminal degradation compartment of the endocytic pathway, is an organelle of approximately 0.5 μm diameter with an electron-dense core and is devoid of recycling receptor molecules (Holtzmann, 1989; Griffiths *et al.*, 1988; Geuze *et al.*, 1988; Kornfeld and Mellman, 1989). The mechanisms by which lysosomes may secrete their contents into the late endosome have recently been revealed

(Section 1.2.2.1), explaining why the late endosome and lysosome both contain similar proteases and share many membrane proteins. The lysosome is currently, therefore, considered a storage organelle that releases its contents into late endosome and autophagosomes (or extracellularly) when required to facilitate digestion (or invasion) (Stinchcombe and Griffiths, 1999; Luzio *et al.*, 2000; 2003).

1.2.2.1 Late endosome-lysosome fusion

Earlier hypotheses proposing the maturation of late endosomes to lysosomes (Roederer *et al.*, 1990; Murphy, 1991) could not explain either ligand transport from late endosome to lysosome, or lysosome biogenesis (Mullock *et al.*, 1994; 1998). The establishment of a cell-free system has, however, shown that mixing of fluid-phase and other contents and/or exchange of membrane proteins occurs between late endosomes (Aniento *et al.*, 1993), between lysosomes (Bakker *et al.*, 1997; Ward *et al.*, 1997), and between late endosomes and lysosomes (Mullock *et al.*, 1998).

Three different hypotheses were, therefore, formulated to explain content mixing seen between these organelles (Fig. 1.4). The first hypothesis assumes vesicular transport between the organelles and is based on extrapolating the existence of the many vesicular traffic steps found in both the secretory and endocytic pathways, to the existence of such a system in late endosome to lysosome transport (Rabinowitz *et al.*, 1992). The second hypothesis is termed 'kiss and run' and proposes that late endosomes and lysosomes undergo continuous and transient fusion (Storrie and Desjardins, 1996). The third hypothesis proposes direct and complete fusion between late endosomes and lysosomes to form a hybrid organelle, from which the lysosomes can be recovered for re-use (Griffiths, 1996).

To date, the vesicular trafficking model (the first hypothesis) does not seem to have found much support, as no evidence of vesicular transport between late endosomes and lysosomes has been reported. In the rat hepatocyte cell-free system devised by Mullock *et al.* (1994), content mixing between late endosomes and lysosomes occurs in an organelle of density intermediate to those of the late endosome and lysosome, a possible intermediate form in the "kiss and run" (Storrie and Desjardins, 1996) or the hybrid organelle proposed by Griffiths (1996). These two hypotheses are further supported by experiments showing

direct fusion of late endosomes and lysosomes, isolation of the late endosome-lysosome hybrid from rat liver, and electron microscopy (EM) experiments on cultured cells (Casciola-Rosen and Hubbard, 1991; Tjelle *et al.*, 1996; Futter *et al.*, 1996; Bright *et al.*, 1997; 2005). Late endosome-lysosome fusion may, therefore, explain the observed heterogeneity of late endocytic compartments, the similar protein and lipid composition of both the late endosome and lysosome, and the fact that proteolysis of ligands appears to occur in the late endosome (Casciola-Rosen and Hubbard, 1991; Tjelle *et al.*, 1996; Mullock *et al.*, 1998).

This scenario, besides being the one that seems to be supported by the most research data, is similar to that first proposed by de Duve (1983). His hypothesis was that primary lysosomes, containing digestive enzymes, fused with a body (the late endosome), containing substrate, to give rise to the digestive organelle (the hybrid organelle), which he called the secondary lysosome (de Duve, 1983). It would now seem that either a complete or partial reversion of this process is possible after digestion of endocytosed material has occurred (Gruenberg, 2001).

1.3 Normal trafficking and processing of lysosomal enzymes via the biosynthetic pathway

Normal trafficking of newly synthesised lysosomal enzymes (including cysteine and aspartic proteases) from the ER to lysosomes is usually directed via the presence of a mannose-6-phosphate (M-6-P) moiety on the asparagine-linked (Asn-linked) oligosaccharide side chains of such proteins. This moiety binds to mannose-6-phosphate receptors (MPR) and is used in sorting lysosomal enzymes from other proteins in the Golgi (Kornfeld and Mellman, 1989). Two types of MPR are known to perform the function of directing the trafficking of lysosomal enzymes to late endosomes and, indirectly, to lysosomes: a large (275 kDa) cation-independent receptor (CI-MPR) and a small (47 kDa) cation-dependent receptor (CD-MPR) (Kornfeld, 1992). Both receptors, which seem to have different affinities for various lysosomal enzymes, bind their ligands in the Golgi complex and exit the *trans* Golgi network (TGN) via clathrin-coated pits (CCP) (Lobel *et al.*, 1989; Kornfeld, 1992).

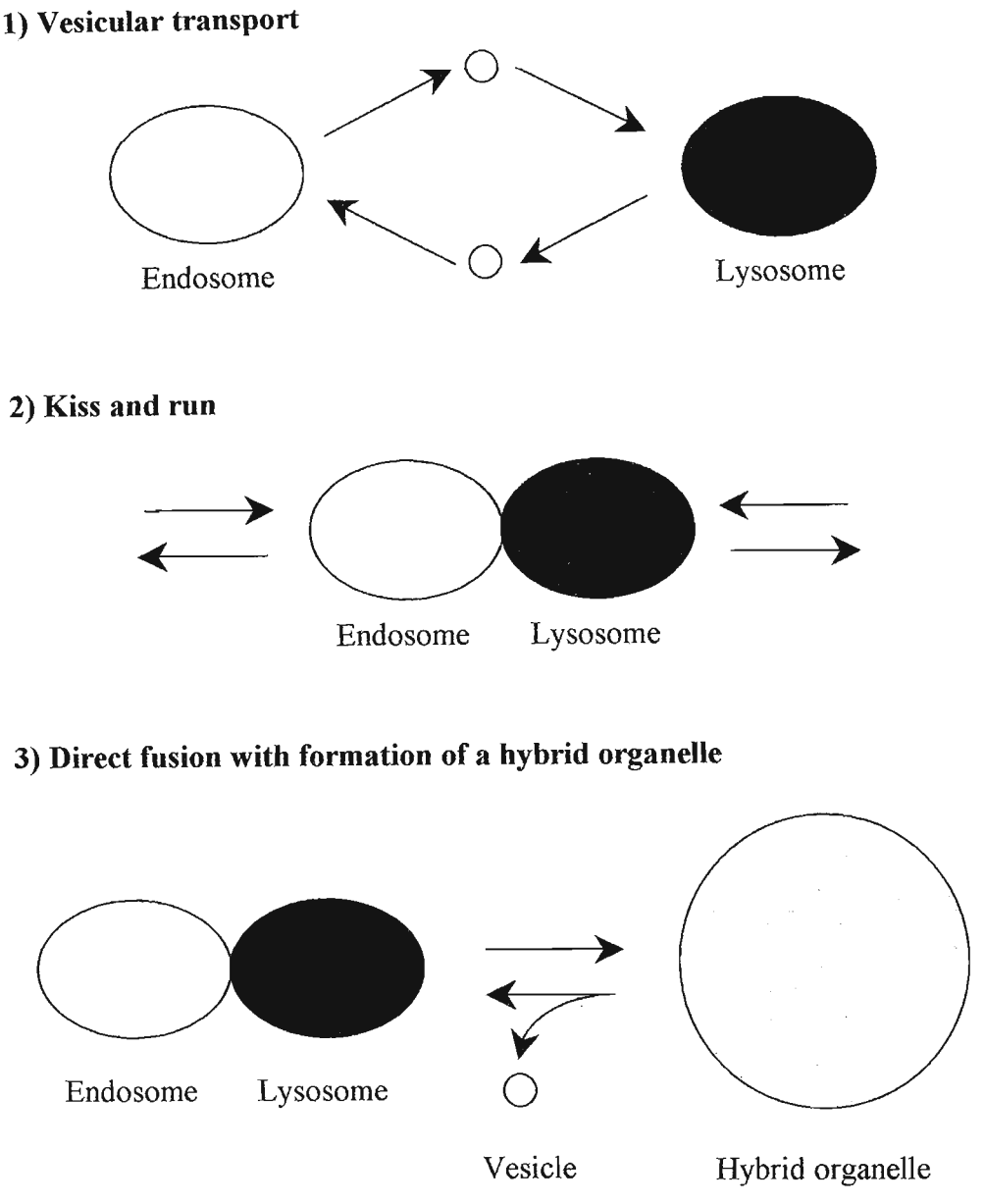

Figure 1.4 **Three hypotheses to explain content mixing between late endosomes and lysosomes.**
1) Vesicular transport, for which no evidence has been found. In this model retrograde traffic of v-SNAREs and other proteins to endosomal compartments after fusion of vesicles with lysosomes is anticipated. 2) Kiss and run, in which transient fusion pores are formed between late endosomes and lysosomes to allow exchange of content. 3) Direct fusion between late endosomes and lysosomes to form hybrid organelles, followed by subsequent re-formation of lysosomes. The latter should require recondensation of hybrid content as well as recycling of v-SNAREs and other proteins to endosomal compartments, presumably by vesicular transport (adapted from Luzio *et al.*, 2000). Abbreviation: v-SNARE = vesicular *N*-ethylmaleimide sensitive factor-attachment protein receptor.

Lysosomal enzymes are glycoproteins that are synthesised via a biosynthetic pathway similar to that used to synthesise secretory and membrane glycoproteins. Newly synthesised lysosomal enzymes are inserted into the lumen of the rough endoplasmic reticulum (RER), their signal sequences are cleaved, and an Asn- and lipid-linked oligosaccharide that contains three glucoses, nine mannoses, and two *N*-acetylglucosamines (GlcNAc) is transferred to the polypeptide. While the polypeptide is still in the RER, the glucoses and two mannose residues are removed and the polypeptide is transported to the Golgi where GlcNAc-1-phosphotransferase (phosphotransferase) transfers GlcNAc-1-phosphate from UDP-GlcNAc to mannose residues of lysosomal enzymes. The phosphotransferase recognises a distinct domain in lysosomal enzymes, ensuring that phosphorylation occurs only on these enzymes (Baranski *et al.*, 1990). The resulting GlcNAc, attached to mannose by a phosphodiester bond, is removed by GlcNAc-1-phosphodiesterase, leaving a phosphate attached to C-6 of the mannose residues (Cuozzo and Sahagian, 1994). The newly formed M-6-P-tagged enzymes are recognised by MPRs and trafficked from the TGN to the late endosome via early endosomes (Ludwig *et al.*, 1991; Rijnboutt *et al.*, 1992; Press *et al.*, 1998). The pH required for the release of lysosomal enzymes from the MPR is more acidic than for ligand dissociation from plasma membrane receptors, and the receptors are, therefore, transported to the more acidic late endosome before releasing the lysosomal proteins. After release of the newly synthesised enzymes, the receptors are recycled back to the TGN (Kornfeld, 1992; Rohrer *et al.*, 1995). The lysosomal enzymes lose their pro-sequences in the acidic environment of the late endosome and the mature enzymes are trafficked to the lysosome where they are now thought to be stored (Griffiths *et al.*, 1988; Griffiths, 1996).

As mentioned, the two MPRs differ in their affinity for lysosomal enzymes, neither having an exclusive affinity for one of several lysosomal enzymes and neither MPR can substitute *in vivo* for the loss of the other. Differences in the cytoplasmic tail regions of the two receptors determine their final destination within the cell: the CI-MPR to the late endosome and the CD-MPR to both the late endosome and lysosome (Lobel *et al.*, 1989; Nair *et al.*, 2003). The CD-MPR contains a 159-residue luminal domain, a single 25-residue transmembrane region, and a 67-residue cytoplasmic domain, has one binding site for M-6-P and appears to function as a dimer. The CI-MPR contains a large 2219-residue luminal domain, a single 23-residue transmembrane domain and a

163-residue cytoplasmic domain. The luminal domain is composed of 15 contiguous repeating segments, and these repeats appear to be the minimum size for binding of M-6-P. Of these repeating segments, two are involved in actual binding of M-6-P. Furthermore, each repeating segment is homologous to the luminal domain of CD-MPR (Dahms *et al.*, 1989; Kornfeld and Mellman, 1989). Therefore, the CD-MPR binds to one M-6-P as a dimer, while the two different repeating segments of CI-MPR bind to two M-6-Ps. Recent work on the crystal structure of CI-MPR, has resolved the architecture of the 2 high affinity M-6-P binding pockets (Olson *et al.*, 2004a,b) and that of a third low-affinity M-6-P binding site (Reddy *et al.*, 2004). The CI-MPR also binds to diphosphorylated oligosaccharides with a much stronger affinity than the CD-MPR (Tong and Kornfeld. 1989). The varying posttranslational processing of different lysosomal enzymes, which results in heterogeneity of the M-6-P recognition marker, has resulted in the evolution of two MPRs with complementary binding properties to ensure an efficient targeting of lysosomal proteins (Pohlmann *et al.*, 1995).

Any disturbance of the activity of glycosylating enzymes and the post-translational processing of the M-6-P recognition signal on lysosomal enzymes may potentially result in default secretion of the precursor form, such as occurs in I-cell disease (Glickman and Kornfeld, 1993). Studies on the MCF-10A model system have, however, shown that glycosylation of lysosomal enzymes, such as cathepsins B, D and L, appears unaltered (Sloane *et al.*, unpublished data), though their trafficking is altered by *ras*-transfection (Lah *et al.*, 2000; Rozhin *et al.*, 1994; Moin *et al.*, 1994; Sloane *et al.*, 1994a). The number and distribution of CD-MPR also appears similar in the MCF-10A and its *ras*-transfected counterpart (MCF-10AneoT), though the number of the CI-MPR may be slightly reduced in the transfected cell line (Sloane *et al.*, unpublished data), which may lead to an increase in default secretion of the precursor forms of lysosomal enzymes, since insufficient numbers of CI-MPR are available to traffic these enzymes to the late endosome.

Though there seems to be a slowing of processing and a decrease in the number of CI-MPR available for trafficking of lysosomal enzymes in the *ras*-transfected MCF-10AneoT cell line (Sloane *et al.*, unpublished data), there seems to be an increased number of peripheral organelles carrying mature active cathepsin B and D (Moin *et al.*, 1994). As this phenomenon seems to accompany progression to a premalignant, invasive

phenotype, this also implies that such enzymes may be involved in invasion. The identity and mechanism by which the enzymes are trafficked to these peripheral organelles and processed is thus far unknown. In order to determine the differences in trafficking induced by *ras*-transfection it is, therefore, essential to identify such organelles. For this reason, a review of the current markers used to identify endocytic organelles, including the currently accepted pH values for the various organelles is given in the following Section.

1.4 Markers of the endosome-lysosome system

Marker proteins found exclusively in a specific organelle are preferred for immunolabelling. Their identification (and raising antibodies to such proteins), however, usually requires organelle isolation. This was always problematic in early investigations, since endosomes and lysosomes are difficult to isolate using the standard cell fractionation and density gradient centrifugation techniques because their general properties are similar to many other organelles (e.g. Golgi, ER and plasma membrane).

The 275 kDa CI-MPR was the first marker isolated. It was discovered during studies on lysosomal storage diseases and easily purified for antibody production using M-6-P affinity chromatography (Kornfeld and Mellman, 1989). CI-MPR is a type I transmembrane glycoprotein that carries lysosomal enzymes from clathrin-coated buds on the TGN to elements of the endosome-lysosome system (Kornfeld and Mellman, 1989). Initial studies showed that CI-MPRs were concentrated in a distinctive type of organelle (Griffiths *et al.*, 1988). Since these organelles were thought to lie beyond the early endosome because they could not be labelled with a fluid-phase endocytic tracer at 20°C, and lysosomes containing active hydrolases lack CI-MPR, the organelle was identified as the late endosome (Kornfeld and Mellman, 1989). Several studies have shown that newly synthesised CI-MPR is trafficked from the TGN to the late endosome via early endosomes (Ludwig *et al.*, 1991; Rijnboutt *et al.*, 1992; Press *et al.*, 1998) and recycling endosomes (Lin *et al.*, 2004). Recycling of the CI-MPR back to the TGN occurs with the aid of the mammalian retromer complex (Arighi *et al.*, 2004; Seaman, 2004) and seems to require interaction with the Tail-interacting 47-kDa protein (TIP47), Rab9 and cholesterol (Orsel *et al.*, 2000; Umeda *et al.*, 2003; Hanna *et al.*, 2002; Ganley *et al.*, 2004; Miwako *et al.*, 2001). The CI-MPR appears to be the primary receptor for the major lysosomal aspartic protease cathepsin D (Pohlmann *et al.*, 1995; Press *et al.*, 1998). The receptor also

functions to internalise extracellular M-6-P-ligands, and the M-6-P-independent binding and internalisation of insulin-like growth factor-2 (IGF2), transforming growth factor-β (TGF-β), plasminogen and urokinase-type plasminogen activator receptor (uPAR) (Dahms, 1996; Kiess *et al.*, 1988; Morgan *et al.*, 1987; Olson *et al.*, 2004b) and is possibly the most reliable marker for the late endosome.

The next major markers to be found for the late endosome-lysosome system were LAMP-1 and LAMP-2. The earlier procedures for isolation of organelles for marker identification relied on endogenous or exogenous perturbants to selectively modify the density of endosomal compartments (Courtoy *et al.*, 1984; Hornick *et al.*, 1985), immunoadsorption (Meuller and Hubbard, 1986), or on a lengthy series of physical fractionation techniques (Dickson *et al.*, 1983; Wall and Hubbard, 1985). These crude techniques, however, led to the discovery and isolation of LAMP-1 (Carlsson *et al.*, 1988; Chen *et al.*, 1985; Lewis *et al.*, 1985; Barriocanal *et al.*, 1986) and LAMP-2 (Ho and Springer, 1983; Chen *et al.*, 1985). At first, LAMPs were considered present only in the lysosome, but were later proven to be present in the late endosome also (Kornfeld and Mellman, 1989).

LAMP-1 is also called Limp III (Barriocanal *et al.*, 1986), lgp 120 (Howe *et al.*, 1988), and LEP-100 (Lippincott-Schwarts and Fambrough, 1987), whereas LAMP-2 is also called Limp IV and lgp110. The amino acid sequence and protein chemistry of LAMP-1 and LAMP-2, isolated from human cells, revealed that LAMPs are type I membrane proteins consisting of a large luminal domain (that is heavily *N*-glycosylated), a single transmembrane domain (the two domains separated by a hinge-region which is *O*-glycosylated) and a short cytoplasmic domain near the C-terminus (Howe *et al.*, 1988; Himeno *et al.*, 1989; Noguchi *et al.*, 1989; Granger *et al.*, 1990; Carlsson and Fukuda, 1989; 1990; Carlsson *et al.*, 1993). A soluble form of LAMP-2 has, however, been isolated from rat liver (Jadot *et al.*, 1996; Akasaki and Tsuji, 1998). Although LAMP-1 and LAMP-2 evolved from the same gene, these genes are located on different chromosomes, and both of these proteins share more homology across species than to each other (Mattei *et al.*, 1990; Manoni *et al.*, 1991). These results suggest that they have distinct functions.

The LAMP molecule itself is protected from proteolytic degradation by its high glycosylation state, which also prevents hydrolases from reaching and degrading the

lysosomal membrane. LAMPs are negatively charged until approximately pH 4 and in lysosomes, which have a low pH, proteolytic enzymes are positively charged. It is, therefore, presumed that the lysosomal enzymes bind electrostatically to LAMPs and are immobilised, protecting the lysosomal enzymes and membrane from degradation (Jadot *et al.*, 1997). When the lysosome fuses with the late endosome the pH possibly increases, the proteolytic enzymes become less positively charged and are released from the LAMP molecule, allowing proteolysis to occur (Fukuda, 1994; Hunziker and Geuze, 1996). In LAMP-1 and LAMP-2 knockout mice, LAMP-2 mutants seemed to suffer the greater impairment of function and mortality, showing extensive accumulation of autophagic vacuoles (Tanaka *et al.*, 2000). For this reason the role of LAMP-2 seems more critical than that of LAMP-1 and LAMP-2 was, therefore, chosen as a marker for the present study.

The late endosome has a high content of LAMPs, CI-MPR, acid phosphatase and a pH range significantly lower than the early endosome (pH 4.0-5.0 for the late endosome and pH 6.0-6.2 for the early endosome) (Maxfield and Yamashiro, 1991; Kornfeld and Mellman, 1989). It can easily be separated from the TR-containing early and recycling endosome compartments by a variety of preparative methods. These methods have demonstrated that the late endosome has a greater buoyant density and carries a more cationic surface charge (Brunner *et al.*, 1977; Wall and Hubbard, 1985).

Lysosomes are similarly enriched in LAMPs, acid hydrolases and acid phosphatase but usually have a pH range significantly lower than the early endosome and apparently similar to that of the late endosome (pH 4.0-5.0) (Maxfield and Yamashiro, 1991; Kornfeld and Mellman, 1989; Griffiths *et al.*, 1990b). This range may, however, fluctuate as suggested by Butor *et al.* (1995), Fukuda (1994) and Hunziker and Geuze (1996). pH alone, therefore, may not be a definitive distinguishing feature, though the lysosomal pH may be slightly more acidic than that of the late endosome (Kornfeld and Mellman, 1989).

Since the late endosome and lysosome share many enzymes and membrane surface proteins (e.g. LAMPs and acid phosphatase), have a similar lipid composition and density, and are also both distinctly more acidic than organelles of the rest of the endocytic system (Griffiths *et al.*, 1990b; Thilo, 1985), a combination of pH and marker protein labelling, as

well as fluid-phase uptake, has been used in identifying these organelles. Early studies used HRP pulse-chased into cells as a time-dependent marker, the presence of HRP being detected by incubation with substrate diaminobenzidine (DAB), and the product made electron-dense through osmication. Uptake of BSA-gold in a pulse-chase fashion also proved popular, as the gold itself is electron-dense so does not require extra treatments to render it visible at the EM level. Labelling times for the various organelles were found to be approximately 5 min for the early endosome, 30–45 min for the late endosome, 1–2 h for the lysosome and overnight pulse-chase showing an equal distribution between late endosome and lysosome (Griffiths *et al.*, 1990b). The rate of trafficking, however, was also shown to vary between cell types (Mullock *et al.*, 1994) and, therefore, additional markers are required.

With the advent of density shift (in which the density of an organelle is changed through artificial means), in conjunction with free flow electrophoresis (in which organelles are separated according to their charge) and density gradient centrifugation, the organelles of the endosome-lysosome system could finally be purified with no detectable cross-contamination (Marsh *et al.*, 1987). Immunoisolation of organelles of the endosome-lysosome system has also been greatly improved by using antibodies to either the cytosolic domain of CI-MPR, or to the endocytosed transmembrane G-protein of the Semliki Forest virus, the latter being artificially integrated into the plasma membrane using low pH conditions (White *et al.*, 1980; Gruenberg and Howell, 1985).

The improved isolation of the various organelles of the endocytic pathway allowed the *in vitro* study of fusion events between elements of the endocytic system (Altstiel and Branton, 1983; Davey *et al.*, 1985; Gruenberg and Howell, 1986; 1987; Braell, 1987; Diaz *et al.*, 1988; Woodman and Warren, 1988). In this system, a fluid-phase marker, avidin (Av), is internalised in "acceptor" cells and biotinylated HRP (biotHRP) in "donor" cells. Fractions prepared from these cells are mixed in the cell-free assay. The binding affinity of Av for biotin is used to quantify fusion. If fusion occurs, a labelled Av-biotHRP complex forms. Complex formation is quantified, after detergent-solubilisation of donor and acceptor populations, in the presence of excess unlabelled biotin using an enzyme-linked immunosorbent assay (ELISA). The ELISA plate is coated with an antibody against avidin to trap and immobilise any labelled and unlabelled complexes formed. The amount of labelled biotin captured by this method gives an indication of the extent of fusion, since

the excess unlabelled biotin effectively out-competes any biotHRP from unfused organelles during the solubilisation procedure (Braell, 1987; Cook and Davidson, 2001).

These studies of fusion events between the vesicles and organelles of the endocytic system, led to the discovery of a family of GTPases, the Rabs, necessary for vesicle fusion, and their specific effector proteins, e.g. the early endosome antigen-1 (EEA1) for Rab5. Table 1.1 provides a summary of the Rab proteins relevant to the endocytic system (known to date). With the use of Rabs, it is possible to distinguish the early endosome (Rab5 positive), the recycling endosome (Rab11 positive) and the late endosome (Rab7 positive). To date, however, no Rab protein has been found that distinguishes the lysosome from the late endosome and, therefore, a combination of markers must be used to distinguish the lysosome (CI-MPR negative, LAMPs positive, Rab7 negative) from the late endosome (CI-MPR positive, LAMPs positive, Rab7 positive).

Table 1.1 Localisation and functional properties of Rab proteins in mammalian cells.

Protein	Localisation	Function
Rab4[1,2,3]	Early endosomes	Recycling pathway from endosomes to plasma membrane
Rab5[4,5,6]	Plasma membrane, clathrin-coated vesicles, early endosomes	Plasma membrane to early endosome transport, homotypic fusion between early endosomes
Rab7[7,8,9]	Late endosomes	Transport from early to late endosomes and lysosomes
Rab9[10,11,12]	Late endosomes and TGN	Transport from late endosomes to TGN
Rab11[13,14]	TGN, constitutive secretory vesicles, secretory granules, recycling endosomes	Transport through recycling endosomes
Rab17[15,16]	Recycling endosomes	Regulation of transcytosis from apical to basolateral cell surface

References: 1. Daro *et al.*, 1996; 2. van der Sluijs *et al.*, 1992; 3. Bottger *et al.*, 1996; 4. Gorvel *et al.*, 1991; 5. Bucci *et al.*, 1992; 6. McLauchlan *et al.*, 1998; 7. Feng *et al.*, 1995; 8. Méresse *et al.*, 1995; 9. Chavrier *et al.*, 1990; 10. Soldati *et al.*, 1994; 11. Riederer *et al.*, 1994; 12. Diaz *et al.*, 1997; 13. Ullrich *et al.*, 1996; 14. Trischler *et al.*, 1999; 15. Lütcke *et al.*, 1993; 16. Hunziker and Peters, 1998.

The Rab5 effector protein, EEA1, is a 162 kDa protein consisting of a long coiled coil dimer flanked by two FYVE zinc-binding 'finger' domains and two Rab5 binding domains (Mu *et al.*, 1995; Callaghan *et al.*, 1999; Merithew *et al.*, 2003). The lengthy α-helical motif shows homology with the myosin heavy chain, rabaptin-5 and to p115, a protein implicated in Golgi transport (Sapperstein *et al.*, 1995). This effector protein acts as a tethering protein in early endosome fusion. It moves freely through the cytosol, until recruited to help facilitate fusion (Mills *et al.*, 1998; Simonsen *et al.*, 1998; Christoforidis *et al.*, 1999a). Fig. 1.5 shows the function of EEA1 and other effector proteins to promote early endosome fusion.

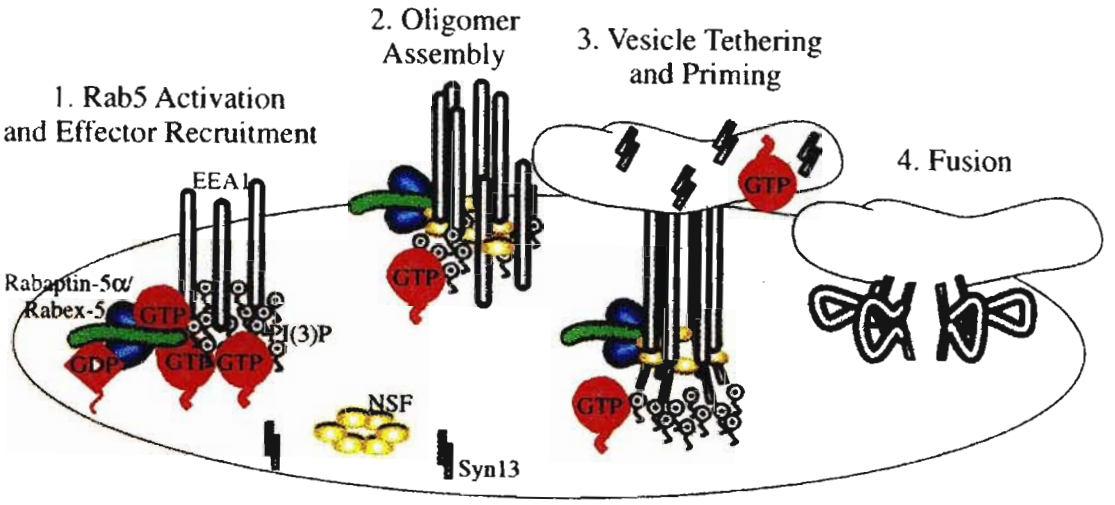

Figure 1.5 **Model of events leading to endosome fusion.**
1) Rab5 activation and effector recruitment. Rab5:GDP is delivered to the membrane where Rabex-5 mediates nucleotide exchange. Rabaptin-5 (complexed to Rabex-5) stabilises Rab:GTP, which can subsequently recruit EEA1. 2) EEA1 oligomer assembly. EEA1 requires PI(3)P for stable membrane recruitment, which may participate in the assembly of oligomers containing NSF, Rabaptin-5, and Rabex-5. 3) Docking and priming. EEA1 mediates vesicle docking, which can be directly coupled to SNARE priming since NSF is incorporated within the docking complex. 4) EEA1-syntaxin 13 interaction for fusion. Docking is intimately linked to fusion, since EEA1 transiently incorporates syntaxin 13 into the large oligomers perhaps to form a fusion pore reminiscent of viral fusion pores (McBride *et al.*, 1999). Abbreviations: EEA1 = early endosome antigen-1; PI(3)P = phosphatidylinositol 3-phosphate; NSF = *N*-ethylmaleimide sensitive factor; SNARE = *N*-ethylmaleimide sensitive factor-attachment protein receptor.

EEA1 associates with early endosomal membranes via its Rab5 binding domains and its FYVE finger domains that bind to PI(3)P in the early endosome membrane (see Fig. 1.3) (Stenmark *et al.*, 1996; Burd and Emr, 1998; Christoforidis *et al.*, 1999a; Kutateladze *et al.*, 1999). Rab5 promotes the localised generation of PI(3)P by interacting with the

PI(3)K (Christoforidis *et al.*, 1999b). Membrane-bound EEA1 forms part of a large complex that includes Rabaptin5-Rabex5, *N*-ethylmaleimide sensitive factor (NSF) and the target *N*-ethylmaleimide sensitive factor-attachment protein receptor (t-SNARE) syntaxin 13 (McBride *et al.*, 1999). EEA1 also interacts with syntaxin 6, a SNARE implicated in TGN to early endosome transport (Simonsen *et al.*, 1999). The multiple protein–protein interactions of EEA1 suggest that it may function as a scaffolding protein bringing the various proteins necessary for fusion into close proximity, or that it has a coordinating role in regulating membrane fusion. Since there are more molecules of EEA1 than Rab5 involved in early endosome fusion (Fig. 1.5), and antibodies to EEA1 would potentially give more reliable results, EEA1 was chosen preferentially over Rab5 as an early endosome marker.

Table 1.2 shows a summary of the different marker proteins currently used to identify endocytic compartments. As can be seen in the table, there is still no definitive marker for the lysosome, although the recent characterization of the major integral membrane protein complement of the lysosome (Bagshaw *et al.*, 2005) may reveal a unique lysosomal marker protein. For the purposes of this study, however, three of these markers were selected to identify the endosome-lysosome organelles of interest: EEA1 for the early endosome, CI-MPR for the late endosome, and LAMP-2 for the late endosome and lysosome. Since both the late endosome and lysosome contain LAMP-2, it was decided to distinguish these on their differing morphology (the lysosome being defined as a small electron-dense organelle while the late endosome as a larger organelle with extensive internal morphology, Section 1.2.2) (Holtzmann, 1989; McDowall *et al.*, 1989). It was anticipated that identification of these organelles using markers and morphology would allow the relative pH of the endosome-lysosome system in the model cell line, the MCF-10A, and its *ras*-transfected premalignant counterpart, the MCF-10AneoT cell line, to be determined. Of particular interest to this study, is the pH and marker identity of the peripheral organelles found in the MCF-10AneoT cell line (Sameni *et al.*, 1995). The organelles of lower pH occur later in the endocytic pathway, and are usually distributed more perinuclearly. The pH and marker complement of the peripheral organelles found in the MCF-10AneoT cell line may thus give an indication of whether these organelles are of late endosome-lysosome system origin.

Table 1.2 **Established marker proteins for endocytic compartments (adapted from Clague, 1998).**

Recycling endosome	Early endosome	Late endosome	Lysosome
Rab11	Rab5	Rab7, Rab9	
	EEA1	CI-MPR	
TR, other recycling receptors		LAMP-1, LAMP-2, LBPA	
	Ligands directed to lysosome (e.g. LDL)		

1.5 Aims of the study

The overall aims of this study were to: 1) develop and characterise antibodies for the measurement of pH at the EM level, 2) apply these antibodies to the MCF-10A and *ras*-transfected MCF-10AneoT cell lines, 3) determine the pH and morphology of the early endosome, late endosome and lysosome (using specific markers), in order to determine the compartment most affected by alkalinisation after *ras*-transfection, 4) establish the identity of the peripheral organelles that appear after *ras*-transfection.

In Chapter 2 the general methodology used is described, while Chapter 3 covers the production, characterisation and affinity purification of antibodies to 2,4-dinitrophenyl (DNP) used for pH determinations described in Chapter 4. In Chapter 4 the pH values of the early endosome, late endosome and lysosome in the MCF-10A and MCF-10AneoT cell lines were compared. In Chapter 5 a closer look is taken at the morphology and intracellular location of the endocytic compartments, and the identity of the peripheral organelle seen in the MCF-10AneoT cell lines. Chapter 6 is a general discussion that presents interpretations and offers insights supported by the results of this study.

CHAPTER 2

MATERIALS AND METHODS

2.1 Introduction

The principles of biochemical techniques and reagents commonly used in a few sections of this thesis are described in this chapter. Methods for preparing reagents are described under the "Reagents" section for each method, whereas reference is made under the "Procedure" section, to those reagents that do not require preparation. The reagents used throughout this study are listed under the heading of "Materials" below.

2.2 Materials

The majority of common chemicals used in this study were of analytical grade and obtained from BDH, Boeringer, Merck or Sigma. Nigericin, (2,4-dinitroanilino)-3'-amino-*N*-methyldipropylamine (DAMP), Oregon Green® 488 dextran (OGD, Mr 10000) and SlowFade™ were from Molecular Probes Inc. (Eugene, OR). Serva Blue G was from Serva Chemicals (Heidelberg, Germany). 7X-PF was from ICN Biomedicals Ltd. (Irvine, Scotland). Anhydrous ethylene diamine, bovine serum albumin (BSA), N-2-hydroxyethyl-piperazine-N'-2-ethane sulfonic acid (HEPES) and paraformaldehyde were from BDH (Poole, UK). 2,2'-Azino-di-(3-ethyl)-benzthiozoline sulfonic acid (ABTS), 4-chloro-1-naphthol, 2,4-dinitrofluorobenzene (DNFB), 2,4-dinitrophenyl-ε-lysine (DNP-lysine), Dulbecco's minimal essential medium (DMEM):Ham's F-12 medium, 1-ethyl-3-[(3-dimethylaminopropyl)-carbodiimide hydrochloride] (EDC), ethylene glycol-bis(β-aminoethylether)-N,N,N',N',-tetraacetic acid (EGTA), fish skin gelatin, Freund's complete and incomplete adjuvants, Hanks' balanced salt solution (HBSS), horseradish peroxidase (HRP), hydrocortisone, insulin, isoelectric focussing (IEF) Mix 3.6-9.3, ovalbumin (OVA, Grade V), piperazine-N,N'-bis(2-ethanesulfonic acid) (PIPES), saponin and trypsin-EDTA solution (x 1) were from Sigma Chemical Co. (St. Louis, MO). Fungizone (0.25 mg/ml) and horse serum were from Gibco (Paisley, UK). Epidermal growth factor (EGF) was from Biomedical Technologies Inc. (Stoughton, MA). Glutaraldehyde was from Merck

(Midrand, RSA). Foetal calf serum was from Delta Bioproducts (Kempton Park, RSA). Medium grade LR White was from London Resin Company (Reading, UK). CY-3-linked donkey anti-IgY was from Jackson ImmunoResearch Pharmaceuticals (West Grove, PA). Monoclonal mouse anti-EEA1 IgG was from Transduction Laboratories (Lexington, KY). Rabbit anti-mouse IgG (BioYeda) was from the Weizmann Institute (Rehovot, Israel). Rabbit anti-CI-MPR was from Dr. B Hoflack (European Molecular Biology Laboratory, Heidelberg, Germany). Mouse anti-LAMP-2 was from Dr. T August (Developmental Studies, Hybridoma Bank, University of Iowa, IA). Protein A-gold (PAG) was from the Department of Cell Biology, University of Utrecht, Netherlands. The AminoLink™ affinity column used was from Pierce (Rockford, Illinois). Enzyme-linked immunosorbent assay (ELISA) Nunc-Immuno Maxisorp F96 plates, 12-well Multiwell plates and sterile plastic culture-ware were from Nunc Intermed (Roskilde, Denmark). Nitrocellulose (Hybond-TC) membranes were from Amersham International (Buckinghamshire, UK). The MCF-10A and MCF-10AneoT cell lines used in this study were provided by Dr Bonnie Sloane (Wayne State University, Detroit, MI) as part of a collaborative study. Elite fat-free milk powder was from a local supermarket. Nickel grids (hexagonal, 100 mesh) were from SCI Science Services (Munich, Germany). Ultra-pure water (dd.H_2O) was produced using a Milli-Q Plus filtration unit supplied by Microsep (Durban, RSA).

2.3 Methods of protein concentration

During some procedures it is necessary to concentrate protein solutions for further use.

2.3.1 Lyophilisation

Lyophilisation (freeze-drying) is used to concentrate frozen protein samples by removing water and other volatile molecules via sublimation. This allows direct vaporisation of water from the frozen state, and is accomplished by producing both a temperature and vapour pressure gradient. The protein solution is frozen in a thin layer in a vessel (-20°C) and attached to the lyophiliser (freeze drier) under a vacuum. The temperature differential between the sample (-20°C) and the condensing chamber (-40°C), combined with the overall low pressure of the lyophiliser (0.1-0.5 mm Hg), allows sublimation of the frozen water. The frozen water component of the sample, which has a vapour pressure greater

than the ambient pressure within the lyophiliser and less than that in the condensing chamber, will sublime in the sample chamber and condense in the condensing chamber, progressively dehydrating (freeze-drying) the sample (Boyer, 1993; Dennison, 2003).

2.3.2 Concentrative dialysis

Where concentration of large volumes of dilute protein solutions is required, dialysis against a substance that has high osmotic pressure when in solution, such as sucrose or polyethylene glycol (PEG), can be utilised. The sample is concentrated due to a concentration gradient that is established between the protein solution contained in the dialysis membrane and the substance at the exterior surface of the membrane. Water and buffer ions move out of the membrane, slowly saturating the sucrose or PEG, while proteins larger than the membrane molecular weight cut-off limit are retained. The overall volume in which the protein is dissolved is thus reduced, and the process is halted when the required degree of protein concentration has been reached.

Sucrose, which is inexpensive, is most often used in this process but has the disadvantage that it is small enough to diffuse into the dialysis tubing and contaminate protein sample preparations. When concentrated, sucrose-free protein solutions are required, therefore, dialysis against PEG (20 kDa) is generally employed. PEG has a molecular weight greater than the size cut-off of the dialysis membrane usually used (10-12 kDa) and will thus not move through the dialysis membrane and contaminate the sample.

2.4 Protein concentration determination

Various procedures require methods for determining protein concentrations. These methods need to be rapid, specific, and sensitive. Spectrophotometry, at 280 nm (A_{280}), and calculations using specific extinction coefficients may be used to quickly determine the protein concentration. This method can, however, only be applied to pure proteins of known extinction coefficient. Methods for determining the concentration of mixed proteins, based on dye-binding to non-specific proteins, are often inaccurate due to interference from PEG or detergents (e.g. Triton), variability of results, or insensitivity. The Bradford dye-binding assay, however, overcomes most of these problems (Bradford, 1976).

2.4.1 Bradford dye-binding assay

The Bradford assay is based on the principle that Coomassie brilliant blue G-250 dye exists in two colour forms, red (λ_{max} = 470 nm) and blue (λ_{max} = 590 nm), the red form predominating at low pH and converting to the blue form upon binding of the dye to protein. Due to its rapidity, the assay is suitable for processing large sample numbers. Colour development is essentially complete within 2 min of the addition of the dye reagent to the protein sample and remains stable for up to 1 h.

The important advantage of the assay is the lack of interference by most chemicals tested. Small effects due to Tris, acetic acid, 2-mercaptoethanol, sucrose, glycerol, EDTA, trace amounts of Triton X-100 and sodium dodecyl sulfate can be eliminated by using the appropriate buffer blank. Detergents at concentrations of 1% or greater, however, produce too much interference to be overcome.

The greatest disadvantage of the dye-binding assay is the wide variation of colours generated in response to different standard proteins (Read and Northcote, 1981). This may affect the validity of measurements extrapolated from calibration curves generated using such standard proteins. When determining the concentration of purified proteins, this problem is best overcome by using the pure protein to be measured as its own standard for generating calibration curves, although this is seldom feasible due to the wastefulness of such an approach. To reduce such variation, Read and Northcote (1981) modified the dye-binding method by substituting Coomassie brilliant blue G-250 with Serva Blue G, and by increasing the dye concentration or decreasing the phosphoric acid concentration. It was found, however, that modification of dye and phosphoric acid concentrations caused the dye to precipitate.

The reagent finally employed in this study was the same as that of Bradford (1976), except that Serva blue G replaced Coomassie brilliant blue G-250. The only disadvantage of the reagent employed compared to that of Read and Northcote (1981), is evidence of non-linearity at protein amounts greater than 25 μg per assay, presumably due to dye depletion. This can easily be overcome by diluting protein samples to within the

5-25 μg working range of the assay. For the determination of lower protein concentrations (1-5 μg), however, or to minimise the amount of protein used in the assay, a micro-assay procedure (Read and Northcote, 1981) can be used.

2.4.1.1 Reagents

Dye reagent. Serva blue G (50 mg) was dissolved with stirring in phosphoric acid [50 ml of 89% (v/v)]. Absolute ethanol (23.5 ml) was added and stirred for 1 h. The solution was made up to 500 ml with d.H_2O, stirred for a further 30 min and filtered through Whatman No.1 filter paper. The dye reagent can be stored in a brown bottle at room temperature for several months.

100 mM Phosphate buffer, pH 7.6. $NaH_2PO_4.H_2O$ (13.8 g) was dissolved in 800 ml of d.H_2O, adjusted to pH 7.6 with NaOH and made up to 1 litre.

Standard protein solution. Standard protein, (e.g. OVA, or pure IgG or IgY lyophilised in phosphate buffer) was dissolved at 1 mg/ml in d.H_2O. This was diluted to 100 μg/ml for the micro-assay.

2.4.1.2 Procedure

A standard protein solution was diluted to 0-5 μg/ml (0-50 μl of the 100 μg/ml solution made up to a final volume of 50 μl with phosphate buffer). Dye reagent (950 μl) was added to standard solutions, samples and blanks, vortexed and allowed to stand for 2 min. The absorbance was read at 595 nm in 1 ml plastic micro-cuvettes against the buffer blank. A standard curve of absorbance at 595 nm versus the standard protein concentration was generated for each new batch of reagent, and subjected to linear regression analysis, and was used to calculate the protein concentration of unknown protein samples.

2.4.2 Concentration determination using extinction coefficients

Spectrophotometry and calculation of protein content using extinction coefficients represents a useful method of determining the concentration of pure protein. Different

proteins absorb light to a different extent at 280 nm and, therefore, each protein requires the use of its own unique extinction coefficient in order to determine the protein concentration. Determination of the concentrations of pure proteins, such as IgG and IgY can, therefore, be determined by using their extinction coefficients at 280 nm (1.43 and 1.25 ml/mg/cm, respectively) (Hudson and Hay, 1980; Coetzer, 1985).

2.4.2.1 Procedure

Pure protein solutions were diluted (1/40 (v/v) in phosphate buffer) prior to reading their absorbance at 280 nm on a spectrophotometer in a 1 cm quartz cuvette against a phosphate buffer blank. The protein concentration was calculated by rearrangement of the formula:

$$A = \varepsilon l c$$

to $c = A / \varepsilon l$

where A = absorbance at 280 nm

$\varepsilon^{0.1\%}$ = extinction co-efficient (absorbance of a 0.1% solution (i.e. 1 mg/ml) solution in a 1 cm cuvette path length)

c = protein concentration in mg/ml.

l = length of light path (1 cm)

2.5 General inoculation protocol for antibody production

Rabbits were each injected intradermally with antigen, emulsified in a 1:1 (v/v) ratio in Freund's complete adjuvant. Further inoculations were administered in a similar manner, using Freund's incomplete adjuvant, in subsequent weeks 2, 6 and 10. Blood was collected from the marginal ear vein at weeks 3 and 8, and by lethal cardiac puncture, under anaesthesia, at 12 weeks. The blood was allowed to clot overnight and the serum was separated and stored frozen.

Chickens were inoculated intramuscularly (in their large breast muscle) with antigen, emulsified in Freund's complete adjuvant. Further inoculations were similarly administered, using Freund's incomplete adjuvant, at weeks 2, 6 and 10. Eggs were collected at weeks 3, 8 and 12 and stored (4°C).

2.6 Fractionation of IgG and IgY

A simple and convenient method of purification of IgG and IgY uses the protein precipitating properties of polyethylene glycol (PEG), a water-soluble linear polymer. Polson *et al.* (1964) found that relatively low concentrations of high molecular weight polymers were able to precipitate proteins, whereas high concentrations of low molecular weight species are required to effect the same degree of precipitation. PEG is a mild precipitating agent that acts by steric exclusion of proteins from the aqueous phase, the proteins being concentrated in the extrapolymer space, until they exceed their solubility limit. It was found that the concentration of the polymer required to precipitate a protein is a function of the net charge on the protein, as determined by the pH of the medium in which it is dissolved. The optimum amount of PEG required to precipitate IgG was less than for ammonium sulfate precipitation and, therefore, the protocol chosen to purify IgG from rabbit serum was that of Polson *et al.* (1964). The method used for antibody purification from egg yolks (IgY) was a modification of this protocol (Polson *et al.*, 1985; Rowland *et al.*, 1986).

2.6.1 Reagents

10 mM Sodium borate buffer, pH 8.6. Boric acid (2.16 g), NaOH (0.2g), HCl [0.62 ml of 37% (v/v)] and NaCl (2.19 g) were added to d.H_2O and made up to 1 litre. At this point the pH should be 8.6.

100 mM Phosphate buffer, 0.02% (w/v) NaN_3 pH 7.6. $NaH_2PO_4.H_2O$ (13.8 g) and NaN_3 (0.2 g) were dissolved in 800 ml of d.H_2O, adjusted to pH 7.6 with NaOH and made up to 1 litre.

2.6.2 Procedure

Isolation of IgG from rabbit serum

Rabbits were bled from the marginal ear vein and the blood allowed to clot overnight at 4°C. Supernatant serum was carefully drawn off the clot, and remaining serum recovered by centrifugation (3 000 x g, 10 min, RT) and removal from above the clot. The serum was preserved with NaN_3 [0.02% (w/v)]. Rabbit serum (1 volume) was diluted with borate

buffer (2 volumes). PEG [14% (w/v), 6 kDa] was dissolved in the protein solution with stirring and the resulting IgG precipitate sedimented by centrifugation (12 000 x g, 10 min, RT). The pellet was dissolved in phosphate buffer (3 volumes) and the precipitation procedure repeated to remove remaining contaminants. The final pellet was dissolved in half the initial serum volume with phosphate buffer. In determination of IgG concentration, a 1/40 dilution of IgG in phosphate buffer was made and the absorbance read at 280 nm in a quartz cuvette against a buffer blank using the extinction coefficient of 1.43 ml/mg/cm as previously described (Section 2.4.2.1).

Isolation of IgY from chicken eggs

Individual yolks were freed of adhering albumin (egg white) by careful washing in a stream of water. The yolk sac was punctured, the yolk volume measured and phosphate buffer, equivalent to 2 volumes of yolk, was added and thoroughly mixed. Solid PEG (6 kDa) was added to a final concentration of 3.5% (w/v of diluted yolk). The PEG was dissolved with stirring and the mixture was centrifuged (4 420 x g, 30 min, RT) to separate three phases, a casein-like vitellin fraction, then a clear fluid, and a lipid layer on the surface. The supernatant fluid contaminated with some of the lipid layer was filtered through a loose plug of cottonwool placed in the neck of a funnel. The volume of clear filtrate was measured and the PEG concentration increased to 12% (w/v). The precipitated IgY fraction was centrifuged (12 000 x g, 10 min, RT), the pellet dissolved in phosphate buffer to the volume after filtration, and the IgY again precipitated [12% (w/v) PEG] and centrifuged (12 000 x g, 10 min, RT). The final IgY pellet was dissolved in a volume of phosphate buffer equal to one sixth of the original yolk volume. IgY concentration was determined as described in Section 2.4.2.1 using an extinction coefficient of 1.25 ml/mg/cm.

2.7 Enzyme-linked immunosorbent assay

Immunoassays use the specific interaction of an antibody with an antigen to provide information about antibody (or antigen) concentration. In principle, chemical conjugation of an enzyme, for which a chromogenic substrate is available, to either the antibody or antigen in a particular system, allows the detection of antibody-antigen interactions formed on a solid phase. This forms the basis of the enzyme-linked immunosorbent assay

(ELISA), first introduced by Engvall and Perlmann (1971). One of the simplest and most commonly used ELISAs for the detection of antibodies, is a three-layer system. Briefly, antigen is coated to the plastic surface of the wells of polystyrene microtitre plates, and the primary antibodies (to be quantified) allowed to form a complex with the immobilised antigen. After excess antibody has been washed away, the amount of reactivity is quantified with an appropriate detection system. In an ELISA this would take the form of an enzyme conjugated to a secondary antibody that recognises the primary antibody bound to the immobilised antigen. The enzyme reacts with a substrate, yielding a coloured product that can be measured spectrophotometrically. This quantitative system complements dot blotting, which gives qualitative information about antibody specificity. During the course of this work, an ELISA was most commonly used as a means to monitor the progress of immunisation of rabbits and chickens, and to compare antibody titres produced by modifying the antigen.

2.7.1 Reagents

Phosphate buffered saline (PBS), pH 7.4. NaCl (8.0 g), KCl (0.2 g), $Na_2HPO_4.2H_2O$ (1.15 g) and KH_2PO_4 (0.2 g) were dissolved in 800 ml of $d.H_2O$, adjusted to pH 7.4 with HCl and made up to 1 litre.

0.5% (w/v) BSA in PBS (BSA-PBS). BSA (0.5 g) was dissolved in PBS and made up to 100 ml.

0.1 % (v /v) Tween 20 in PBS (PBS-Tween). Tween 20 (1 ml) was diluted to 1 litre in PBS.

Substrate buffer (150 mM citrate-phosphate, pH 5.0). $Na_2HP0_4.2H_2O$ (2.84 g) and citric acid (2.29 g) were each dissolved in $d.H_2O$ and made up to 100 ml. The citric acid solution was titrated against the Na_2HPO_4 (50 ml) solution to pH 5.0.

Substrate solution [0.05% (w/v) ABTS and 0.0015% (v/v) H_20_2 in citrate-phosphate buffer]. For each ELISA plate ABTS (7.5 mg) and H_2O_2 (7.5 µl) were dissolved in citrate-phosphate buffer, pH 5.0 (15 ml).

Stop solution [0.1% (w/v) sodium azide in 150 mM citrate-phosphate buffer, pH 5.0]. For each ELISA plate NaN_3 (15 mg) was dissolved in citrate-phosphate buffer (15 ml).

2.7.2 Procedure

ELISAs were used to assess the response to inoculation. Before antibody response could be assessed, however, the antigen coating levels on the microtitre plates had to be optimised. This was accomplished by coating with a variety of antigen concentrations (5–20 μg/ml, 100 μl) and using antibodies from the week 8 response in the same ELISA procedure as outlined below. Coating levels that produced the most linear, steepest titration curve were used to assess the antibody response at weeks 3, 8 and 12. To this end, microtitre plates were coated overnight at 4°C with antigen (100 μl) in PBS. The wells were blocked with BSA-PBS (200 μl, 1 h, 37°C) and washed three times with PBS-Tween. Serial twofold dilutions of antibodies, diluted in BSA-PBS, were added to the plate (150 μl). The plates were incubated (2 h, 37°C) and washed three times with PBS-Tween. The appropriate secondary antibody, diluted in BSA-PBS (150 μl), was added to each well and incubated (1 h, 37°C). The plates were washed three times in PBS-Tween. Substrate solution was added to each well (150 μl) and the colour was allowed to develop in the dark (approximately 20 min, 37°C). Addition of stop solution (50 μl) stopped the enzyme reaction. The absorbance at 405 nm of each well was measured on a Bio-Tek EL307 ELISA plate reader. In controls, either the antigen, blocking step, primary antibody or secondary antibody steps were omitted to assess the efficiency of blocking steps, any possible crossreaction, and the specificity of each step in the procedure. Titration curves were constructed from the spectrophotometric values.

2.8 Dot blots

The accessibility of a resolved protein mixture on the surface of a nitrocellulose membrane allows the use of a variety of detection methods to label proteins in the western blot procedure of Towbin *et al.* (1979). The dot blot procedure is a modification of this procedure in which the pure protein solutions are blotted onto nitrocellulose. Due to the use of pure proteins, prior separation of crude preparations of target antigens by sodium dodecylsulfate polyacrylamide gel electrophoresis (SDS-PAGE) in order to obtain a pure protein band is unnecessary. A secondary antibody that is conjugated to an enzyme-

reporter system may subsequently detect antibody recognition and binding. The action of the conjugated enzyme generates a coloured reaction product from a specific colourless substrate, precipitating the product on the nitrocellulose. This can usually be easily visualised against the white background of the membrane.

2.8.1 Reagents

Tris buffered saline (TBS: 20 mM Tris-HCl, 200 mM NaCl, pH 7.4). Tris base (2.42 g) and NaCl (11.68 g) were dissolved in about 900 ml of d.H_2O, adjusted to pH 7.4 with HCl and made up to 1 litre.

Blocking agent [5% (w/v) fat-free milk powder in TBS]. Fat-free milk powder (5 g) was dissolved in about 90 ml of TBS and made up to 100 ml.

0.5% (w/v) BSA in TBS (BSA-TBS). BSA (0.4 g) was dissolved in TBS and made up to 80 ml.

0.1% (v/v) Tween 20 in TBS (TBS-Tween). Tween 20 (0.5 ml) was diluted to 500 ml in TBS.

4-Chloro-l-napthol substrate solution [0.06% (w/v) 4-chloro-l-napthol, 0.0015% (v/v) H_2O_2]. 4-chloro-l-napthol (0.03 g) was dissolved in methanol (10 ml). This solution (2 ml) was diluted with TBS (10 ml). Hydrogen peroxide [4 µl of 35% (v/v)] was added just before use.

0.1% (w/v) Sodium azide in TBS. NaN_3 (0.03 g) was dissolved in TBS (30 ml).

2.8.2 Procedure

Antigens were dot-blotted onto nitrocellulose strips and allowed to dry. The strips were placed into separate containers and soaked in blocking agent with gentle rocking to saturate non-specific protein binding sites (1 h). The membranes were washed with TBS (3 x 5 min) and antibody diluted in BSA-TBS added. Controls consisted of pre-immune IgG or IgY preparations substituted in the labelling system for each specific antibody, at the same concentration. After incubation in the primary antibody (2 h or overnight), the nitrocellulose was washed with TBS-Tween (3 x 5 min), the detergent decreasing

non-specific binding of antibody molecules to the nitrocellulose surface via hydrophobic interactions. The nitrocellulose was subsequently incubated in the appropriate secondary antibody-HRP conjugate (1 h, diluted in BSA-TBS), washed in TBS-Tween (3 x 5 min) and incubated in the dark with freshly prepared substrate solution. Incubation in substrate was allowed to proceed until an optimal colour differential between specifically targeted antigens and background, judged by non-immune incubations, was achieved. The reaction was stopped by briefly rinsing the membranes in NaN_3 [0.1% (w/v), in TBS]. Blots were allowed to dry, photographed, and stored in the dark to prevent yellowing.

2.9 Cell culture

The MCF-10A and MCF-10AneoT cell lines, supplied for collaboration with Dr. Sloane (Department Pharmacology, Wayne State University, Detroit, MI), were cultured exactly as in their source laboratory to ensure that the cell phenotype maintained was consistent with that laboratory, as this protocol differs slightly from that used by other workers. The passage numbers of cells were similarly kept as low as possible. All glassware was washed in 7X-PF detergent solution and copiously rinsed in tap water and d.H_2O before autoclaving.

2.9.1 Reagents

Hanks' balanced salt solution (HBSS). Powdered HBSS and sodium hydrogen carbonate (1.2 g) were consecutively dissolved in about 900 ml of dd.H_2O, adjusted to pH 7.3 with NaOH and made up to 1 litre. HBSS was filtered through a 0.22 μm filter into sterile autoclaved bottles under sterile conditions and stored at 4°C.

Epidermal growth factor (EGF, 50 μg/ml). EGF (100 μg) was dissolved in sd.H_2O (2 ml) and stored at -20°C.

Insulin (600 μg/ml). Insulin (10.2 mg) was dissolved in HBSS (16.5 ml) with the addition of 0.1M NaOH (500 μl) and used immediately.

Hydrocortisone (3.33 mg/ml). Hydrocortisone (10 mg) was dissolved in absolute ethanol (3 ml) and stored at -20°C.

Fungizone (250 µg/ml). Fungizone (5 mg) was dissolved in sd.H_2O (20 ml) and stored at -20°C.

DMEM:Ham's F-12 complete medium [DMEM:Ham's F-12, hydrocortisone (0.5 µg/ml), insulin (10 µg/ml), EGF (20 ng/ml), horse serum (5%, v/v), fungizone (0.25 µg/ml), pH 7.3]. Powdered medium and sodium hydrogen carbonate (1.2 g) were consecutively dissolved in about 900 ml dd.H_2O, adjusted to pH 7.3 with NaOH and made up to 1 litre. Medium was filtered through a 0.22 µm filter into sterile autoclaved bottles under sterile conditions and horse serum (50 ml), hydrocortisone (150 µl), insulin (17 ml), EGF (400 µl) and fungizone (10 ml) were aseptically added. Complete medium was stored at 4°C.

2.9.2 Procedure

Cells were cultured at 37°C in 25 cm^3 flasks in complete medium in a humidified atmosphere containing 5% CO_2, fed every 3-4 days and passaged upon reaching 80% confluence. To this end, cells were washed with HBSS (3 x), rinsed in trypsin-EDTA, just enough to cover the monolayer, and incubated at 37°C until the cells detached. Cells were diluted in complete medium, split in a ratio of 1:3 for each passage and seeded into new flasks.

2.10 Fixation and pre-embedding processing of cells

Fixation is used to quickly arrest cellular processes and preserve the location of proteins and other molecules. The most commonly used method for arresting cellular activity is chemical fixation, involving either precipitation of proteins within the cells (e.g. alcoholic fixation) or covalent cross-linking of proteins (e.g. aldehyde fixatives) (Griffiths, 1993). The best fixatives for immunocytochemistry are those which fix the specimen in position in an insoluble form, preserve the antigen binding site in a form recognised by the antibody, do not mask epitopes by excessive cross-linking, and preserve the structure of the tissue as much as possible.

Unfortunately, different fixative types give rise to different levels of denaturation of antigens, and increasing fixative concentrations and fixation times increase these effects. The choice of fixative, fixative concentration and length of fixation need to be optimised for each cell type to ensure antigenic preservation, mechanical stability, and quick penetration rates (Griffiths, 1993). Alcoholic fixation results in considerable extraction of membrane lipids and protein precipitation that generally destroys antigenicity. In addition, alcohol destroys the ultrastructure, making alcoholic fixation unsuitable for electron microscopy (EM). Osmium tetroxide is commonly used for EM secondary fixation but is not used in conjunction with immunocytochemistry as it denatures antigens excessively. Aldehyde fixatives are popular as they immobilise proteins and are compatible with a number of buffers. Fixation by aldehydes is also considered less harmful to epitopes, though covalent linkages formed by the fixatives may lead to alterations in protein conformation (Griffiths, 1993).

Paraformaldehyde reacts with uncharged primary amine groups, amides and aromatic amino acid residues. It penetrates tissues very quickly but fixes slowly in comparison to glutaraldehyde, and at concentrations below 2%, paraformaldehyde cross-linking is reversible. Paraformaldehyde fixation is not as destructive to antigenic epitopes as glutaraldehyde but generally gives poor preservation of ultrastructure. Glutaraldehyde penetrates tissues more slowly than paraformaldehyde but cross-links at a faster rate. Cross-linking is irreversible and involves reactions with amino, amido, aromatic, carboxyl, amidozole and sulfhydryl groups. Due to this high reactivity, glutaraldehyde preserves the tissue ultrastructure better than paraformaldehyde, but at high concentrations may result in loss of antigenicity due to extensive cross-linking of epitopes (Griffiths, 1993).

For the best results, a combination of paraformaldehyde and glutaraldehyde is generally used. Robertson *et al.* (1992) investigated the problem of fixation, i.e. the concentrations and duration of fixation that would result in the preservation of sufficient ultrastructure and antigenicity to be suitable for immunocytochemistry. The results indicated that specimens (including a cell monolayer) fixed for 60 min in a mixture of 2% (m/v) paraformaldehyde and 0.05% (v/v) glutaraldehyde gave uniformly good ultrastructural preservation and labelling characteristics. Specimens fixed for 30 min in 4% (m/v) paraformaldehyde and 0.05% (v/v) glutaraldehyde also showed good results. The low concentration of

glutaraldehyde imparts some irreversible mechanical strength to the cell while avoiding extensive oxygen consumption (and possibly anoxia) that occurs during glutaraldehyde fixation (Rash, 1986). A mixture of 4% (m/v) paraformaldehyde and 0.05% (v/v) glutaraldehyde was, therefore, chosen for EM studies.

The buffer used in conjunction with the fixative plays an important role in ensuring minimal extraction of cytoplasmic components and phospholipids. Phosphate buffers are generally unsuitable for fixation as they can form precipitates with cytoplasmic calcium, and prolonged fixation in phosphate buffers can lead to increased protein leaching. Cacodylate buffers have been used successfully, but the cacodylate-derived arsenic induces oxygen starvation that causes tissue anoxia. The zwitterionic Good's buffers, PIPES and HEPES, are optimal buffer components for fixatives since they penetrate cell membranes easily (due to their charge neutrality) and do not extract phospholipids (Schiff and Gennaro, 1979). For this reason Good's buffers were used, although Tris, HEPES and PIPES have the potential to form antigen-damaging free-radicals (Grady *et al.*, 1988).

2.10.1 Reagents

800 mM HEPES stock solution, pH 7.3. HEPES (43.68 g) was dissolved in 180 ml of d.H_2O, adjusted to pH 7.3 with NaOH and made up to 200 ml. The solution was aliquotted and stored frozen. Prior to use, the buffer was diluted to 200 mM, and the pH adjusted if necessary.

16% (m/v) Paraformaldehyde stock solution. Paraformaldehyde (16 g) was dissolved in 90 ml d.H_2O, warmed to a maximum of 60°C, cleared with a minimum amount of 1 M NaOH and made up to 100 ml. The solution was stored at -10°C until required.

8% (m/v) Paraformaldehyde in 200 mM HEPES, pH 7.3. Paraformaldehyde stock solution (25 ml) was added to HEPES stock solution (12.5 ml), adjusted to pH 7.3 with 1 M HCl and made up to 50 ml with d.H_2O. The solution was stored at -10°C until required.

4% (m/v) Paraformaldehyde, 0.05% (v/v) glutaraldehyde in 200 mM HEPES, pH 7.3. Paraformaldehyde stock solution (25 ml) and glutaraldehyde [200 µl of 25% (v/v)] was

added to HEPES stock solution (25 ml) and made up to 90 ml with d.H_2O. The pH was adjusted to pH 7.3 with 1 M HCl and the volume made up to 100 ml. The solution was stored at -10°C until required.

20 mM Glycine in 200 mM HEPES, pH 7.3. Glycine (0.015 g) was dissolved in 200 mM HEPES and made up to 10 ml.

10% (m/v) Gelatin in 200 mM HEPES, pH 7.3. Microbiological grade gelatin (10 g) was added to 200 mM HEPES (100 ml) and dissolved by heating. The volume was made up to 100 ml if necessary with d.H_2O, chilled rapidly on ice and stored at 4°C.

2.10.2 Procedure

MCF-10A and MCF-10AneoT cells were fixed with 4% (m/v) paraformaldehyde, 0.05% (v/v) glutaraldehyde in 200 mM HEPES (30 min, RT). The fixative was removed and replaced with 8% (m/v) paraformaldehyde in 200 mM HEPES. The monolayers were carefully scraped off the bottom of the flasks using a rubber policeman, transferred to Eppendorf tubes and stored overnight in fixative (4°C). The cells were gently pelleted, the excess fixative removed and any remaining free aldehyde groups quenched with 20 mM glycine in 200 mM HEPES (2 x 15 min). The cells were pelleted, excess glycine removed and infiltrated with 10% (m/v) gelatin in 200 mM HEPES (2 h, 37°C). The cells were pelleted, excess gelatin removed and the cell pellet was chilled rapidly on ice. A thin layer of buffer was placed over the gelatin-infiltrated cell pellet to prevent drying out. The pellet was cut into 1 mm^3 cubes that were dehydrated and embedded in LR White resin for sectioning and immunolabelling for EM as described in Sections 2.11, 2.12 and 2.13.

2.11 LR White embedding of cells

The polyhydroxy aromatic acrylic resin, LR White, was developed specifically to combine hydrophilic characteristics with a cross-linking capacity that is stable under an electron beam. The resin may either be heat-cured at 50°C, room temperature-cured using an aromatic tertiary amine accelerator, or microwave cured using benzoyl peroxide as accelerator (Causton, 1984; Hillmer *et al.*, 1991). The cross-link density of the resin is

critical for good immunocytochemical results, the best results obtained using a slow heat cure at 50°C (Causton, 1984).

LR White is hydrophilic; therefore, full penetration of aqueous solutions can occur on ultrathin sections. The tissues need only be partially dehydrated to 70% ethanol, which retains antigenicity (Newman *et al.*, 1982; 1983). The degree to which LR White dissolves lipids is significantly lower than that of hydrophobic resins and therefore membranes and organelles are easily distinguishable, even when the tissue is not post-fixed in osmium. The resin itself does not bind antibodies as some hydrophobic resins do, nor does it prevent antibodies from binding to tissue antigens. It does not require low temperatures, or ultra violet (UV) light for polymerisation and no etching with H_2O_2 or other chemicals, or protease digestion, is required to expose antigens. The resin is not, however, highly stable in the electron beam and, therefore, a supporting film on the grid is generally used (Newman and Jasani, 1984). A greater extent of antibody binding is allowed with the use of LR White than with hydrophobic resins, as antigens throughout the thickness of the sections should theoretically be available to antibodies, whereas etching of hydrophobic resins is required to expose only a few superficial epitopes. More recent reports, however, show that antibodies may not be able to penetrate through the LR White resin (Brorson *et al.*, 1994). Gold labelling reagents are usually too large to diffuse through the resin and, therefore, only antigen-antibody complexes on the surface of the resin can be detected using this type of immunocytochemistry (Newman and Jasani, 1984).

The method used here for LR White embedding was modified from that of Newman *et al.* (1983), in that the sample was fully dehydrated to 100% ethanol, to ensure complete infiltration of the embedding media.

2.11.1 Reagents

25% (v/v) Ethanol. Ethanol (2.5 ml) was made up to 10 ml with d.H_2O.

50% (v/v) Ethanol. Ethanol (5 ml) was made up to 10 ml with d.H_2O.

70% (v/v) Ethanol. Ethanol (7 ml) was made up to 10 ml with d.H_2O.

90% (v/v) Ethanol. Ethanol (9 ml) was made up to 10 ml with d.H_2O.

Resin:ethanol (1:1). LR White (2.5 ml) was mixed with an equal amount of absolute ethanol (2.5 ml).

Resin:ethanol (2:1). LR White (4 ml) was mixed with absolute ethanol (2 ml).

2.11.2 Procedure

The gelatin blocks were dehydrated in a graded ethanol series (25%, 50%, 70%, 90% and 100% ethanol for 15 min, 15 min, 1 h, 30 min and 30 min, respectively). The dehydrated blocks were transferred to increasing amounts of LR White resin (1:1 and 2:1, for 30 min each, followed by undiluted resin for 30 min, 30 min and 1 h respectively). The gelatin blocks were transferred to fresh undiluted embedding media and allowed to further infiltrate overnight. Fresh resin was dispensed into gelatin capsules. The samples were placed on top of the resin, taking care to minimise resin carryover, and allowed to sink to the bottom of the capsule. The capsules were quickly closed, making sure that no air bubbles were present, as oxygen prevents polymerisation, and allowed to polymerise (24 h, 50°C).

2.12 Grid preparation, glass knife production and sectioning of LR White blocks

Ultrathin sections of resin embedded material are required for immunocytochemistry for EM. The grids used to pick up the sections must also receive a protective coating, to impart some mechanical strength to the section during immunolabelling procedures, and to stabilise the sections under the electron beam. Before these sections can be cut, however, glass knives must be prepared. Once the grids and glass knives have been prepared, ultrathin sections can be cut and placed onto the grids.

2.12.1 Reagents

0.25% (m/v) Formvar in chloroform. Formvar (0.25 g) was dissolved in chloroform (100 ml).

2.12.2 Procedure

For the preparation of formvar-coated grids, a dish (20 x 10 x 10 cm) was completely filled with d.H_2O. A clean glass microscope slide was dipped into the formvar solution, the excess allowed to drain and the remaining film dried. The dried film was loosened around the edges of the slide with a razor-blade, and floated onto the surface of the d.H_2O. Nickel grids (hexagonal, 100 mesh) were placed, shiny side up, on the floating film and, using a rectangular piece of wire mesh as a support, the film was recovered using a scooping motion. The grids, adhered to the underside of the film, were allowed to dry. Formvar-coated grids were removed from the wire mesh by carefully perforating the formvar film surrounding individual grids.

For the preparation of glass knives a glass strip was cleaned with detergent and water, dried using tissue paper and positioned on a Type 7801B LKB Knife Maker (Morewood *et al.*, 1992) with the ridged imperfect edge facing downwards. The glass strip was repeatedly scored and fractured in the middle until square pieces were produced. Each square was placed in the glass holder at a 45° angle, scored quickly through the middle and fractured into two right-angled triangles. Usually, the one triangle has a sharp usable edge while the other has the blunt counter face, if the fracture line was not perfectly linear through the apices of the opposite sides of the square. A trough to hold the d.H_2O upon which cut sections would be floated out was made below the sharpest knife-edge using silver adhesive tape. The knives were stored in a dust-free container for subsequent use.

Prior to sectioning, the LR White blocks were trimmed into a trapezoid using a fine hacksaw. The blocks were further trimmed with a glass knife on an RMC MT6000XL ultramicrotome. The trough of the previously prepared knife was filled with sufficient d.H_2O to ensure that the d.H_2O just reaches the knife-edge. Silver-gold ultrathin sections (80-100 nm) were cut and floated onto the water trough for retrieval onto formvar coated nickel grids. Grids were dried and could be stored indefinitely before immunolabelling.

2.13 Immunolabelling of LR White sections

Both monoclonal and polyclonal antibodies can be used in immunocytochemistry. Monoclonal antibodies (mAbs) have the advantage that they recognise and bind to a single epitope of the antigen of interest. This helps ensure that recognition and binding of the mAb will occur only with the correct antigen and that non-specific binding is minimised. However, if the fixation protocol denatures the single epitope of the antigen targeted by the mAb, recognition of the epitope by the mAb will not occur and labelling will be unsuccessful.

Polyclonal antibodies are a mixture of antibodies raised against various epitopes of a whole protein. This may be advantageous, since polyclonal antibodies have the potential to bind a number of epitopes, even if some epitopes have been denatured or masked by the fixation protocol. Although polyclonal antibody production is less costly than mAb production, the polyclonal preparations may contain antibodies that are crossreactive with the epitopes of other proteins. Such non-specific antibodies are, however, usually of low titre. High titre specific antibodies and the appropriate pre-immune antibody controls at the same low antibody concentration that is used for the specific antibody in the labelling procedure are, therefore, used to ensure specificity of labelling.

The final consideration in immunocytochemistry is the choice of the detection system used to identify and localise the antibody-antigen complex. The two most common detection systems produce either diffuse staining (e.g. enzyme-coupled secondary antibodies using histochemical detection with substrates that produce electron-dense products), or punctate staining (e.g. gold colloids or ferritin molecules) (Griffiths, 1993; Slot and Geuze, 1985; Leunissen and de Mey, 1989; Slot *et al.*, 1989). HRP-linked secondary antibodies that react with the substrate diaminobenzidine (DAB) to produce a product, which is made electron-dense through osmication, are usually used for diffuse staining. A combination of protein A bound to colloidal gold and rabbit primary antibodies may be used to produce punctate labelling at the EM level.

Protein A from *Staphylococcus aureus* recognises and binds the Fc region of the rabbit IgG on the CH_2 and CH_3 domains (Forsgren and Sjöquist, 1966; Diesenhofer, 1981). The binding occurs in a 1:1 ratio and does not interfere with the stability of the immune complex (Slot *et al.*, 1989). Protein A can bind Fc regions of other IgG species, such as

human, guinea pig and dog, and, with lesser affinity, IgG from goat, sheep, rat and chicken (Forsgren and Sjöquist, 1966; Diesenhofer, 1981). If the primary antibody was from an animal species that exhibits low protein A affinity, a linker rabbit anti-species IgG may be used, which is detected with protein A. Use of a linker antibody also allows an increase in labelling density (i.e. signal amplification) since more than one rabbit anti-species IgG binds to a primary antibody molecule (Merighi, 1992).

2.13.1 Reagents

Phosphate buffered saline (PBS), pH 7.4. NaCl (8.0 g), KCl (0.2 g), $Na_2HPO_4.2H_2O$ (1.15 g), KH_2PO_4 (0.2 g) and NaN_3 (0.2 g) were dissolved in 800 ml of $d.H_2O$, adjusted to pH 7.2 with NaOH and made up to 1 litre.

1% (m/v) BSA in PBS (BSA-PBS). BSA (0.2 g) was dissolved in PBS and made up to 20 ml.

0.1% (m/v) BSA in PBS (BSA-PBS). 1% BSA-PBS (1 ml) was added to PBS (9 ml).

1% (v/v) Glutaraldehyde in PBS. 25% Glutaraldehyde (40 µl) was added to PBS (960 µl).

20 mM Glycine in PBS. Glycine (15 mg) was dissolved in PBS and made up to 10 ml.

1% (v/v) Fish skin gelatin, 0.8% (m/v) BSA, 20 mM glycine in PBS (FBG). Fish skin gelatin (5 ml), BSA (4 g) and glycine (0.75 g) was made up to 500 ml in PBS. Impurities were sedimented (10 000 x g, 4 h), the supernatant aliquotted and stored frozen.

2% (m/v) Uranyl acetate. Uranyl acetate (1 g) was dissolved in $d.H_2O$ (50 ml), the addition of 95% ethanol (1 ml) assists solubility. The uranyl acetate solution was stored in the dark at 4°C.

1 M NaOH. NaOH (0.4 g) was dissolved in $d.H_2O$ and made up to 10 ml.

Lead citrate. Lead nitrate (1.33 g) and trisodium citrate.$2H_2O$ (1.76 g) were added to 40 ml freshly boiled and cooled $d.H_2O$ and shaken intermittently for 30 min. 1 M NaOH (± 8 ml)

was added to clear the milky solution. The solution was made up to 50 ml with freshly boiled and cooled d.H_2O and stored in the dark at 4°C in an air-tight container.

2.13.2 Procedure

Immunolabelling was performed by incubation of grids, section-side down, on droplets of reagents on a layer of Parafilm spread onto a bench. Grids were transferred from reagent to reagent with a 1 mm nichrome wire loop on the end of a thin wooden stick. The same loop was used for each immunolabelling procedure optimised, as the loop carries a small volume of liquid from droplet to droplet, which introduces a dilution factor.

Immunogold labelling was performed according to the following procedure:

1) Non-specific antibody binding was blocked by treatment with 1% BSA-PBS (10 min).
2) Grids were incubated with specific antibody diluted in 1% BSA-PBS (1 h).
3) Grids were washed with 0.1% BSA-PBS (5 x 2 min).
4) If the primary antibody had a weak binding capacity for PAG, grids were incubated with secondary rabbit anti-species antibody diluted in 1% BSA-PBS (1 h).
5) Grids were washed with 0.1% BSA-PBS (5 x 2 min).
6) Grids were incubated with PAG (5 nm) freshly diluted in 1% BSA-PBS (1 h).
7) Grids were washed with 0.1% BSA-PBS (5 min).
8) Grids were washed with PBS (5 x 5 min).
9) The antigen:antibody:PAG complex was stabilised with 1% glutaraldehyde in PBS (5 min).
10) Grids were washed with PBS (2 x 5 min).
11) In case of double labelling, after quenching excess fixative with 20 mM glycine in PBS (5 x 2 min), steps 1-10 were repeated using a different antibody and 10 nm PAG.
12) Grids were washed with dd.H_2O (5 x 12 min) and dried.
13) Grids were counterstained with uranyl acetate (10 min) and washed with dd.H_2O by gentle pipetting.
14) Grids were counterstained with lead citrate in a closed dish containing NaOH pellets to remove CO_2 (5 min), washed with dd.H_2O by gentle pipetting and dried.

As a control, the labelling protocol was also performed using a pre-immune antibody preparation instead of specific antibody. During optimisation of the gold probe level, the

primary antibody was substituted with diluting buffer to detect labelling due to non-specific binding of the gold probe. Additional controls included single labelling with each probe for each antigen in the presence and absence of primary antibody, and double labelling for both antigens with both sizes of probe.

If a high concentration (>100 μg/ml) of antibodies was required for optimal labelling, excess background was eliminated with the use of the superior blocking agent FBG (instead of BSA-PBS) in steps 1-7.

CHAPTER 3

PREPARATION AND CHARACTERISATION OF ANTI-DNP ANTIBODIES FOR *pH* DETERMINATIONS

3.1 Introduction

In 1953, the successful determination of the amino acid sequence of insulin by Sanger established a technique for the analysis of the primary structure of proteins (Sanger and Thompson, 1953). The technique introduced by Sanger used 2,4-dinitrofluorobenzene (DNFB, also called Sanger's reagent), which selectively and covalently reacts with the amino (NH_2) groups in a polypeptide, allowing the identification of the N-terminal amino acid residue (Fig. 3.1) (Sanger, 1945; Sanger and Thompson, 1953). After DNFB treatment, acid hydrolysis yields the N-terminal and ε-NH_2 groups of lysyl residues as 2,4-dinitrophenyl derivatives (DNP-amino acid). The DNP-amino acid can be identified by chromatographic procedures, using known DNP-amino acid derivatives as standards. An N-terminal lysyl residue can be distinguished from an internal Lys residue as the former contains 2 DNP moieties. This chemistry, first used for the sequencing of proteins, was to have far reaching direct and indirect applications, not only in protein sequencing, but also in immunological methods and studies on the immune system.

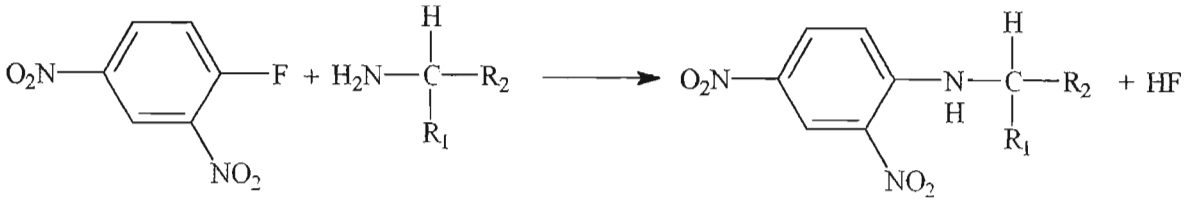

Figure 3.1 **Reaction of 2,4-dinitrofluorobenzene (DNFB) with amino groups to form 2,4-dinitrophenyl (DNP) derivatives.**

For immunological methods, antibodies to DNP are required. Monoclonal anti-DNP antibodies have been successfully produced using murine hybridoma clones (Scott and Fleishman, 1982; Anderson and Pathak, 1985; Orci *et al.*, 1985; Esser *et al.*, 1993) and splenocytes (Schilizzi *et al.*, 1992). Polyclonal anti-DNP has been successfully raised in many species, including mice (Scott and Fleishman, 1982; Maeji *et al.*, 1992; Segre and

Segre, 1994; Vajdy and Lycke, 1995), rabbits (Segre and Segre, 1994), cattle (Corbeil *et al.*, 1997) and humans (Berd, 2001; 2003).

The use of DNP-conjugates and anti-DNP antibodies, allowed the development of the dinitrophenyl hapten sandwich staining (DHSS) procedure, which has a wide variety of immunocytochemical and immunoassay applications (Jasani *et al.* 1981). In this system DNP, conjugated to the primary antibody that has bound to the target antigen in a tissue sample, is detected using an anti-DNP IgM antibody coupled to either peroxidase or glucose oxidase (secondary antibody). Each of the five antigen binding sites of the pentameric IgM can potentially bind to one or two DNP-linked primary antibodies, giving rise to signal amplification. DHSS, in which a peroxidase molecule is conjugated to the secondary antibody, can also be applied to light microscopy by using a peroxidase chromogenic substrate, or electron microscopy (EM) by adding osmium tetroxide to make the substrate product electron-dense (Jasani *et al.*, 1981; 1992).

Wojtkowiak *et al.* (1983) developed a sensitive DNFB/DNP staining technique for proteins western-blotted onto nitrocellulose. This method is approximately 100 times more sensitive than Coomassie brilliant blue or amido black staining. In this method, the blotted proteins are exposed to DNFB and the resultant DNP-labelled proteins (Fig. 3.1) are detected with anti-DNP antibodies and visualised with peroxidase-coupled secondary antibodies. Esser *et al.* (1993) used a similar strategy for the detection and protein isolation of mitochondrial carnitine palmitoyl transferase-1 (CPT1) found in the outer mitochondrial membrane. Previous isolation protocols had been unsuccessful, as CPT1 is detergent-labile and, therefore, could not be isolated in a catalytically active form. The enzyme is also highly hydrophobic and is very difficult to separate from other mitochondrial membrane proteins. Isolation procedures were improved when DNP was conjugated to etomoxir-CoA (Et-CoA), an inhibitor of CPT1. This allowed the fractions containing CPT1 to be identified with anti-DNP antibodies, in western blots of fractions from chromatography columns, and subsequently purified and analysed (Esser *et al.*, 1993).

DNP-proteins and their antibodies have also found use in endocytic studies. Diaz *et al.* (1988) used DNP-glucuronidase and anti-DNP antibodies to study the fusion of endocytic vesicles in a cell-free system following receptor-mediated endocytosis. Similarly,

DNP-proteins have also been used as pulse-chase markers of the endocytic route, their presence detected with anti-DNP antibodies (e.g. Larsson *et al.*, 1997). Of interest to this study is that antibodies to DNP have also been used for pH determination of acidic organelles using the (2,4-dinitroanilino)-3'-amino-*N*-methyldipropylamine (DAMP) system (described in the next chapter).

The fact that DNFB couples covalently to the $-NH_2$ groups in proteins, yielding highly immunogenic DNP-protein derivatives, resulted in the DNFB reagent becoming popular for producing immunogens for studies of the immune response. For example, Gallagher and Voss (1969) used DNP-bovine gamma globulin (DNP-BGG) as an immunogen for the determination of the molecular weight, and the chemical and other physical properties of chicken IgG. DNP-ovalbumin (DNP-OVA) has been used to demonstrate that carrier-specific T cell hybridomas can be used for *in vitro* immunisation procedures to increase the production of hapten specific antibody-forming B-lymphocytes (Schilizzi *et al.*, 1992). Such conjugates have also been used to examine auto- and polyreactivity of IgG in human sera (Berneman *et al.*, 1993), and to prove that interleukin-12 (IL-12) increases the humoral immune response through both interferon-γ (IFN-γ) dependent and independent mechanisms (Metzger *et al.*, 1997). Other conjugates have been used to study pulmonary alveolar macrophage suppression of mouse IgM, IgG and IgE antibody production (Steele and Herscowitz, 1993). DNP conjugated to OVA, bovine serum albumin (BSA), keyhole limpet haemocyanin (KLH), or Ficoll has been used to study the idiotypic and anti-idiotypic immune response (Segre and Segre, 1994). The use of DNP-KLH allowed characterisation of the long-term mucosal memory B cells of mice generated after oral immunisation (Vajdy and Lycke, 1995).

DNP-modified self-antigens have recently been used as immunotherapeutics for cancer treatment (Berd, 2001; 2003). Tumour cells are usually weakly immunogenic (Pardoll, 1999) and DNP-haptenisation of these cells induces an autoimmune response to both native and modified tumour antigens (Berd, 2001). This response is only apparent after intensive inoculation, once a week for six weeks, augmented by cyclophosphamide, and leads to remission in some cases (Berd, 2001; 2003).

Besides the use of DNP-modification, adjuvants or carrier proteins, an alternate approach to increasing the immunogenic response to a particular immunogen has been to cationise

the immunogen. Cationisation of non-self antigens increases their rate of uptake by antigen presenting cells (APCs), increases antibody titres (Koyama *et al.*, 1986a,b; Bass *et al.*, 1990; Muckerheide *et al.*, 1987a,b; 1990; Apple et al., 1988, Michael, 1991; Farmer *et al.*, 1993) and produces antibodies that recognize both the native and modified antigen (Muckerheide *et al.*, 1987a,b; 1990). On the other hand, cationisation of antibodies increases their rate of endocytosis, systemic clearance and organ uptake (Hong *et al.*, 1999, 1998; Triguero *et al.*, 1991), enhances transport of antibodies across biological barriers (Girod *et al.*, 1999; Bickel *et al.*, 1994; Hong *et al.*, 2000), and has found use in antibody therapy for cancer (Lee and Pardridge, 2003; Pardridge *et al.*, 1995; 1998), AIDS (Pardridge *et al.*, 1994a; 1994b; 1994c) and in the development of vaccines (e.g. Farmer *et al.*, 1993).

In the present study, the aim was to attempt to enhance the immune response (using cationisation of DNP-OVA) to produce higher titres of anti-DNP antibodies in chickens and rabbits for use in the DAMP pH determination system (described in Section 4.3). Rabbits and chickens have similar immune systems, in that both produce antibody diversity through a process that includes gene conversion (Reynaud *et al.*, 1994; Knight and Crane, 1994; Vajdy *et al.*, 1998). OVA is, however, a self-antigen in chickens so the possible induction of autoantibodies by DNP-modification and cationisation is also of interest, since this may have implications for breaking self-tolerance. The results of this study, therefore, suggest possible strategies for increasing anti-hapten (as opposed to anti-carrier protein) antibody yield and for eliciting autoantibodies for cancer therapy.

Before such a study could be commenced, however, a secondary immunological detection system, in the form of rabbit anti-IgY, needed to be raised and conjugated to horseradish peroxidase (HRP) for the detection of IgY antibodies raised in chickens.

3.2 Preparation of rabbit anti-IgY

Rabbit anti-IgY was required as a secondary antibody for use in both the enzyme-linked immunosorbent assay (ELISA) and for EM procedures where an IgY primary antibody was used. For ELISA purposes, the rabbit anti-IgY was coupled to HRP for the detection of IgY antibodies bound to the target antigen. The EM detection system used in this study was protein-A gold (PAG) labelling. Protein-A does not, however, bind to IgY but does

bind to rabbit IgG (Roth, 1984). Thus a secondary antibody, rabbit anti-IgY, was required for use when IgY primary antibodies, such as the anti-DNP antibodies produced in this study, were used.

3.2.1 Isolation of IgY and inoculation of rabbits

As a source of IgY for the production of rabbit anti-IgY, the eggs of healthy non-immunised chickens were used. The resultant IgY isolate was injected into two healthy rabbits to increase the chance of achieving a good immune response in at least one animal.

3.2.1.1 Reagents

Reagents for IgY isolation as described in Section 2.6.1.

3.2.1.2 Procedure

IgY was isolated from the eggs of non-immunised chickens using PEG precipitation as described in Section 2.6.2. Two rabbits were inoculated intradermally with 1 mg IgY in phosphate buffer (without azide) emulsified in Freund's adjuvant as described in Section 2.5.

3.2.2 Assessment of antibody response

The antibody response of rabbits inoculated with IgY would be anticipated to be fairly substantial because of the evolutionary distance between rabbits and chickens. The IgY antibodies would, therefore, be recognised as foreign by the rabbit's immune system and an immune response generated.

3.2.2.1 Reagents

Reagents for ELISA as described in Section 2.7.1.

Reagents for isolation of rabbit IgG as described in Section 2.6.1.

3.2.2.2 Procedure

The antibody response of rabbits inoculated with IgY was assessed at weeks 3, 8, and 12 using sera, harvested during the relevant week, in an ELISA system. After optimisation of the coating levels (Section 2.7.2), microtitre plates were coated overnight with IgY (2 μg in 100 μl PBS per well). A serial two-fold dilution of rabbit serum, starting at 1 in 20 in BSA-PBS, was used as primary antibody. HRP-linked sheep anti-rabbit IgG (diluted 1 in 450 in BSA-PBS) was used as secondary antibody. The procedure and controls were as described in Section 2.7.2. The serum from the week showing the greatest reactivity against IgY was subjected to PEG precipitation (Section 2.6.2) to isolate the rabbit anti-IgY. The purified rabbit anti-IgY was used "as is" in immunolabelling procedures (Section 2.13.2), or used to prepare rabbit anti-IgY-HRP conjugates (Section 3.2.3.2).

3.2.2.3 Results

The antibody response to the inoculated IgY peaked at week 12 with negligible difference in titre between weeks 8 and 12 (Fig. 3.2).

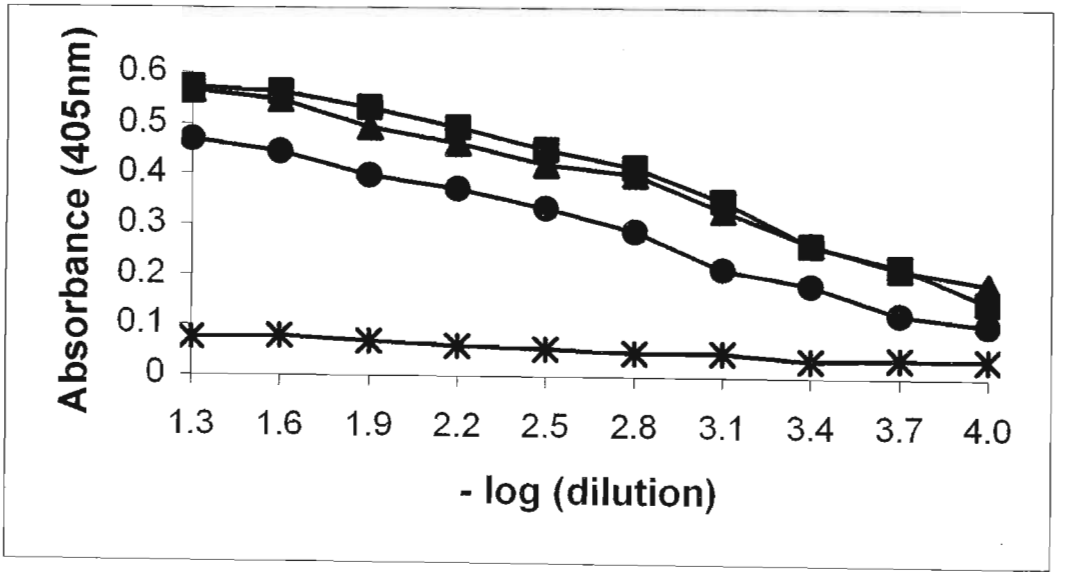

Figure 3.2 **Immune response to IgY of rabbits inoculated with IgY as determined by ELISA.**
IgY was coated at 20 μg/ml to the microtitre plate and incubated with serial two-fold dilutions of sera collected after 3 (●), 8 (▲) and 12 (■) weeks and pre-immune serum (✳). Binding was visualised by incubation with sheep anti-rabbit-HRP conjugate and ABTS as described in Section 2.7. Each point is the mean absorbance at 405 nm of duplicate samples.

3.2.3 Preparation of horseradish peroxidase-linked rabbit anti-IgY

A two-step procedure for the coupling of HRP to rabbit anti-IgY, using glutaraldehyde, is advantageous for the preparation of conjugates with peroxidase, a protein that shows low reactivity with glutaraldehyde because of the small number of free amino groups it contains. The HRP-conjugates obtained show homogeneity of 90%, with some free molecules of antibody and peroxidase, and produce a 1:1 coupling of antibody to peroxidase (Ternynck and Avrameas, 1990). The procedure was altered slightly from that of Ternynck and Avrameas (1990), in that dialysis against 0.15 M NaCl was used to effect the buffer exchange. This replaced passage through a column of Sephadex G-25 fine, equilibrated with 150 mM NaCl, and pooling the fractions containing the "activated" peroxidase (Ternynck and Avrameas, 1990).

3.2.3.1 Reagents

100 mM Phosphate buffer, pH 6.8. $NaH_2PO_4.H_2O$ (13.8 g) was dissolved in 800 ml of $d.H_2O$, adjusted to pH 6.8 with NaOH and made up to 1 litre.

1% (v/v) Glutaraldehyde in 100 mM phosphate buffer, pH 6.8. Glutaraldehyde [8 µl of 25% (v/v)] was added to phosphate buffer (192 µl).

150 mM NaCl. NaCl (8.78 g) was dissolved in $d.H_2O$ and made up to 1 litre.

1 M Na_2CO_3. Na_2CO_3 (5.3 g) was dissolved in $d.H_2O$ (50 ml).

1 M $NaHCO_3$. $NaHCO_3$ (4.2 g) was dissolved in $d.H_2O$ (50 ml).

1 M Carbonate-bicarbonate buffer, pH 9.5. 1 M $NaHCO_3$ (20 ml) was adjusted to pH 9.5 with 1 M Na_2CO_3.

1 M Lysine. Lysine-HCl (182 mg) was dissolved in $d.H_2O$ (1 ml).

Phosphate buffered saline (PBS), pH 7.4. NaCl (8.0 g), KCl (0.2 g), $Na_2HPO_4.2H_2O$ (1.15 g) and KH_2PO_4 (0.2 g) were dissolved in 800 ml of $d.H_2O$, adjusted to pH 7.4 with HCl and made up to 1 litre.

Reagents for ELISA as described in Section 2.7.1.

3.2.3.2 Procedure

Activated HRP was prepared by dissolving HRP (10 mg) in glutaraldehyde [0.2 ml of 1% (v/v) in phosphate buffer]. The preparation was allowed to react (18 h, RT), dialysed overnight against 150 mM NaCl and concentrated to 1 ml using PEG as described in Section 2.3.2. Rabbit anti-IgY antibody solution (1 ml of 5 mg/ml in 150 mM NaCl) was added to the activated HRP. Carbonate-bicarbonate buffer (0.2 ml) was added and the reaction allowed to proceed (24 h, 4°C). The reactivity of the fixative was quenched with lysine (0.2 ml, 2 h). The preparation was dialysed against PBS (overnight, 4°C), after which an equal volume of glycerol was added. The HRP-linked antibodies were stored at 4°C. The optimal dilution of HRP-conjugated rabbit anti-IgY to use for any specific coating concentration was determined using a checkerboard ELISA. This procedure is similar to that described in Section 2.7.2, except that both the IgY coating levels (serial dilutions starting from 10 μg in 100 μl PBS) and the HRP-linked rabbit anti-IgY concentrations (serial dilutions starting from 1 in 50 in BSA-PBS) were varied.

3.2.3.3 Results

A checkerboard ELISA gave the optimal dilution of HRP-anti-IgY to be used as secondary antibody in ELISA as 1 in 750.

3.3 Preparation of DNP-OVA

A hapten is a small molecule, which will bind to a pre-formed antibody (e.g. the surface receptor of a B cell). However, the hapten alone is too small to cross-link B cell surface receptors and therefore will not stimulate B cell differentiation to plasma cells and antibody production. In addition, the B cell response to antigen, in most cases, requires co-operation by T-lymphocytes (T cells). Due to the small size of the hapten, it cannot stimulate both lymphocytes simultaneously. However, if the hapten is conjugated to an immunogenic protein, the T cells will recognise the protein, or carrier molecule, and so

co-operate with B cells to produce anti-hapten (as well as anti-carrier) antibodies (Roitt, 1994).

The hapten used in this study was DNP. At physiological pH, free 2,4-dinitrophenol ionises into DNP which is toxic, as it acts as an uncoupler of the oxidative phosphorylation pathway by acting as a proton scavenger in the mitochondria, thereby preventing ATP formation (Darnell *et al.*, 1986). Conjugation of DNP to a carrier protein prevents DNP from entering the mitochondria of cells by permeation, counteracting the toxic effect. Due to the small size and toxicity of DNP, the molecule was conjugated to OVA using DNFB chemistry, prior to inoculation (Altmann, 1993).

3.3.1 Reagents

1 M Na_2CO_3. Na_2CO_3 (5.3 g) was dissolved in d.H_2O (50 ml).

3.3.2 Procedure

Fraction V OVA (5 g) was dissolved in Na_2CO_3 (50 ml), and DNFB (1.25 ml) added. The mixture was incubated in the dark on a platform shaker (100 r.p.m., 1 h, 37°C). Unconjugated DNFB was removed by dialysis against d.H_2O (4 changes of 5 litre, 24 h) and the conjugates were lyophilised as described in Section 2.3.1. The DNP substitution ratio was determined as described in Section 3.5.

3.4 Preparation of DNP-catOVA

Studies have demonstrated that enhanced targeting of the immunogen to antigen presenting cells (APCs) is associated with enhanced activation of T helper (Th) cells (Casten and Pierce, 1988; Snider and Segal, 1989). Therefore, modification of native antigens, so that they are more efficiently bound by APCs, has been proposed to result in an improved immune response. In this context, the effect of cationisation of BSA, on uptake and presentation by immune cells, has been extensively studied using an *in vitro* mouse model system (Muckerheide *et al.*, 1987a; 1987b; 1990). Cationisation of BSA, i.e. increasing the pI of the resultant protein from 5.5 to >9.5, has been reported to result in a molecule which induces the production of increased levels of antibody to both cationised BSA

(catBSA) and native BSA (nBSA). CatBSA enhances the activation of T cells, requiring 500-fold less catBSA, than that needed for activation by nBSA, to optimally activate T cells, possibly due to enhanced uptake and processing of the antigen by APCs. This occurs as a result of the cationised antigen binding electrostatically to the anionic membranes of APCs, possibly due to association with negatively charged phospholipids and sialic acid residues (Apple *et al.*, 1988). Another model suggests that cationisation destroys the determinants on the antigen necessary for the induction of suppressor T cells, while still allowing the display of many of the B cell epitopes present in the native protein (Ferguson *et al.*, 1983; Michael, 1991).

Cationisation not only alters the charge of a protein, but also its conformation, possibly exposing new epitopes and increasing the immunogenicity of the protein (Bass *et al.*, 1990). In human systems the enhanced immune response of cationised proteins was found to be dependent on $CD4^+$ Th cells, accompanied by increased production of IL-1β, IL-2 and IFN-γ, and dependent on HLA-DR for antigen presentation (Farmer *et al.*, 1993). Of interest to this study is that cationisation of DNP-modified foreign proteins has been shown to increase anti-hapten as well as anti-carrier antibody production in sheep and mice (Altmann, 1993). In this study, therefore, antibodies to DNP-OVA and DNP-cationised OVA (DNP-catOVA) conjugates were raised in rabbits and chickens, with the use of adjuvant, in order to assess whether cationisation of the antigen would increase the immune response to DNP in these species, (and at the same time, generate antibodies for the determination of intracellular pH using the DAMP system) and to monitor the possible induction of autoantibodies to OVA in chickens.

The cationisation of DNP-OVA was performed using the water-soluble activating, or coupling agent 1-ethyl-3-(3-dimethylaminopropyl)-carbodiimide (EDC) according to the method of Border *et al.* (1982), where the reaction between EDC and ethylene diamine replaces the carboxyl groups on proteins with ethylamine groups (Fig. 3.3). Since the DNP moiety contains no carboxyl groups, only the carrier protein (OVA) would become cationised.

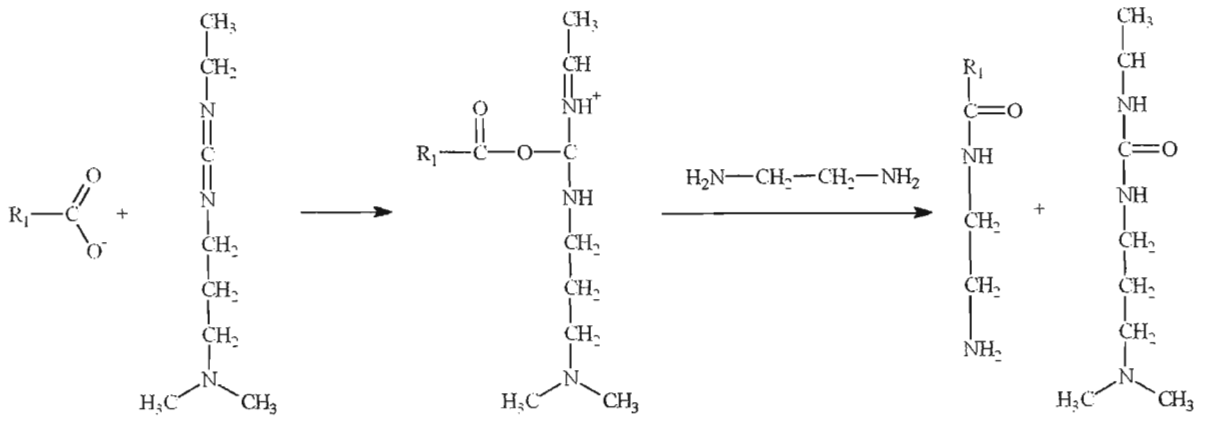

Figure 3.3 **Reaction of 1-ethyl-3-(3-dimethylaminopropyl)-carbodiimide (EDC) and ethylene diamine to replace carboxyl groups with ethylamine groups.** The *N*-substituted carbodiimide reacts with the carboxylic groups of the C-terminus, Glu and Asp side-chain carboxyl groups, to form a highly reactive *O*-acylisourea ester derivative. This activated species then reacts with a primary amine group of ethylene diamine, forming a peptide bond and thereby effectively replacing carboxyl groups with ethylamine groups hence producing a protein which remains cationic at most pH's. The *O*-acylisourea by-product is soluble in water and can easily be removed by dialysis (adapted from Hermanson *et al.*, 1992).

3.4.1 Reagents

1 M Anhydrous ethylene diamine, pH 4.75. Anhydrous ethylene diamine (13.4 ml) was added to 150 ml d.H_2O, adjusted to pH 4.75 with 6 M HCl and made up to 200 ml.

4 M Acetate buffer, pH 4.75. Acetic acid (22.64 ml) was added to 50 ml d.H_2O, adjusted to pH 4.75 with NaOH and made up to 100 ml.

3.4.2 Procedure

DNP-OVA (1 g) was dissolved in d.H_2O (5 ml) and added to anhydrous diaminoethane (200 ml) while stirring. EDC (0.36 g) was slowly added and the cationisation reaction was allowed to proceed (120 min, 25°C). The reaction was stopped by the addition of acetate buffer (6 ml). The product was dialysed against d.H_2O (6 changes of 5 litre, 72 h) and lyophilised as described in Section 2.3.1. The DNP substitution ratio was determined as described in Section 3.5. CatOVA was required for use in ELISAs and was prepared the same way as described above.

3.5 Calculation of the dinitrophenyl substitution ratio

DNFB reacts with the free amino, phenolic-hydroxyl and thiol groups of amino acid residues in a protein under basic conditions. The fluoro group of DNFB acts as a leaving group, covalently binding a dinitrophenyl group to the protein, producing a yellow coloured product (maximally detected at 360 nm). The DNP-tyrosine residues formed by the reaction with phenolic-hydroxyl groups are, however, colourless (Sanger, 1945). Though this could lead to an underestimation of the substitution ratio, the formulae used by Good *et al.* (1980) and used in this study at least gives some guidance as to the substitution ratio.

The extinction co-efficient ($\varepsilon^{0.1\%}$) of DNP was determined at 360 nm (the absorption maximum of DNP) using 1 mg/ml DNP-lysine and that of OVA at 280 nm using 1 mg/ml OVA. The DNP substitution ratio, i.e. the number of molecules DNP per molecule of OVA, was determined spectrophotometrically according to the method of Good *et al.* (1980) using the formulae:

$$[DNP] = \{A_{360} - (0.01)(A_{280})\} / \varepsilon^{0.1\%}$$

$$[OVA] = \{A_{280} - (0.316)(A_{360})\} / \varepsilon^{0.1\%}$$

$$\text{Substitution ratio} = [DNP] / [OVA]$$

3.5.1 Results

The substitution ratio was calculated to be 4.8 molecules of DNP per molecule of OVA. Subsequent cationisation of DNP-OVA did not alter the substitution ratio.

3.6 pI determination of OVA, catOVA, DNP-OVA and DNP-catOVA

The pI of a protein is defined as the pH at which the protein has a net charge of 0 (Dennison, 2003), i.e. all the positive and negative charges of the protein are balanced. The protein will, therefore, be positively charged at pH values below the protein's pI and negatively charged at pH values above the pI. The pI of a protein can be determined using isoelectric focussing (IEF) in which the protein migrates through a pH gradient gel (IEF gel) till it reaches its pI.

The pH gradient in the gel is established with the use of a mixture of ampholytes (synthetic polyamino-polycarboxylic acids, in which amino and carboxyl groups are randomly added to a carbon backbone). When an electrical current is passed through a gel containing ampholytes, the ampholytes will migrate towards either the anode (which has an acidic pH) or cathode (which has a basic pH), depending on their charge, until they reach a pH at which they have zero charge. Each ampholyte will, therefore, establish the pH at its pI value, thus creating a pH gradient (Dennison, 2003).

A protein sample applied to the pH gradient gel will migrate through zones of changing pH, either losing negative charges as it migrates towards the anode, or losing positive charges as it migrates towards the cathode. Once the protein has migrated to a point on the pH gradient that is the same as its pI, the nett charge on the protein will be zero and it will stop migrating (Fig. 3.4) (Dennison, 2003). The pI of the unknown protein can then be established with the use of standard proteins of known pI, also run on the same IEF gel.

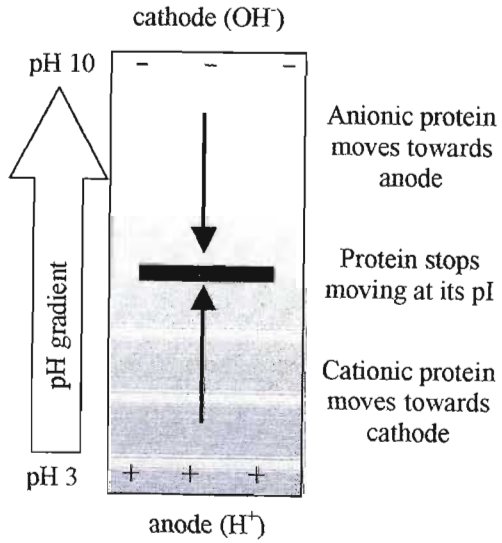

Figure 3.4 **Schematic diagram of the principles of isoelectric focussing.**
The IEF gel contains a pH gradient. A protein applied to the IEF gel loses negative charges (anionic protein) as it migrates towards the anode, or loses positive charges (cationic protein) as it migrates towards the cathode. Once the protein has migrated to a point on the pH gradient that is the same as its pI, the nett charge on the protein will be zero and it will stop migrating

3.6.1 Reagents

10 mg/ml OVA. OVA (10 mg) was dissolved in d.H_2O (1 ml).

10 mg/ml catOVA. catOVA (10 mg) was dissolved in d.H_2O (1 ml).

10 mg/ml DNP-OVA. DNP-OVA (10 mg) was dissolved in d.H_2O (1 ml).

10 mg/ml DNP-catOVA. DNP-catOVA (10 mg) was dissolved in d.H_2O (1 ml).

Fixing solution [12% (m/v) trichloroacetic acid]. Trichloroacetic acid (60 g) was dissolved in d.H_2O (500 ml)

Destaining solution [50% (v/v) ethanol, 10% (v/v) acetic acid]. Ethanol [500 ml of 100% (v/v)] was mixed with acetic acid [100 ml of 100% (v/v)] and made up to 1 litre with d.H_2O.

Staining solution [0.25% Coomassie blue R-250, 50% (v/v) ethanol, 10% (v/v) acetic acid]. Coomassie blue R-250 (0.5 g) was dissolved in destaining solution (200 ml).

3.6.2 Procedure

The samples (10 mg/ml OVA, catOVA, DNP-OVA and DNP-catOVA) were further diluted 1/5, 1/10, 1/20 and 1/50 and loaded onto a ProtMaai001© gel-type (range of pI 3-10) IEF gel (12 µl). The pI marker proteins from the IEF Mix 3.6-9.3 were also loaded onto the gel (8 µl). Isoelectric focusing was performed according to the manufacturer's instructions (Copyright Proteios BV, Netherlands). The gel was fixed with fixing solution (1 h) and washed with destaining solution to remove the ampholytes (which would also stain) (10 min). The gel was incubated in staining solution (30 min) and destained with destaining solution until the background colour was removed. The pI values of OVA, catOVA, DNP-OVA and DNP-catOVA were subsequently determined using standard proteins of known pI.

3.6.3 Results

The pI of OVA was between 4.0 and 4.5 (Fig. 3.5, lanes 5,10,15,20). Cationisation of OVA increased the pI to greater than 9.5 (Fig. 3.5, lanes 4,9,14,19), since negatively charged carboxyl groups were replaced with positively charged ethylamine groups. DNP modification of OVA lowered the pI to less than 3 (Fig. 3.5, lanes 3,8,13,18), which is below the detection limits of the IEF gel so that bands of DNP-OVA are not visible, since positively charged amino groups were neutralized by the addition of non-charged DNP groups. Cationisation of DNP-OVA increased the pI to between 8.6 and 9.2 (Fig. 3.5, lanes 2,7,12,17), due the exchange of negative charges for positive charges.

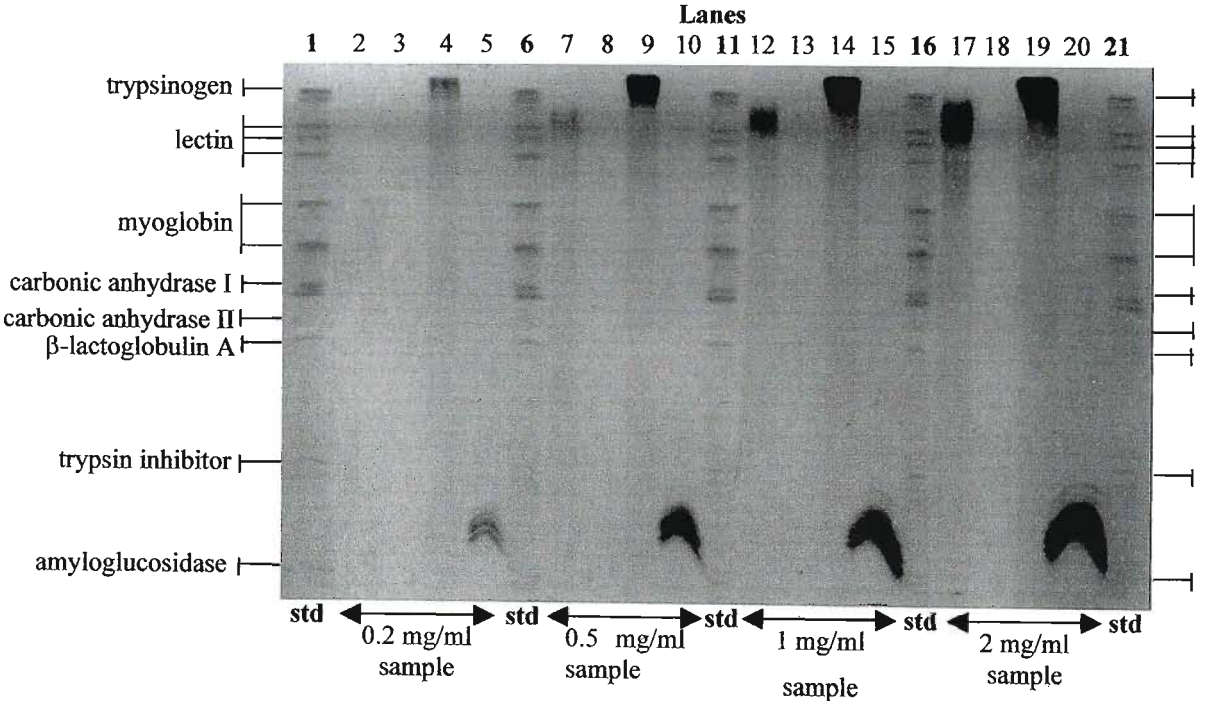

Figure 3.5 **Isoelectric focussing to determine the pI of OVA, CatOVA, DNP-OVA and DNP-catOVA.**

Samples were loaded onto a ProtMaai001© isoelectric focussing gel. Lanes 2,7,12,17 = DNP-catOVA; lanes 3,8,13,18 = DNP-OVA; lanes 4,9,14,19 = catOVA; lanes 5,10,15,20 = OVA; lanes 1,6,11,16,21 = pI standards (std). Lanes 2-5 were loaded with 0.2 mg/ml sample; lanes 7-10 were loaded with 0.5 mg/ml sample; lanes 12-15 were loaded with 1 mg/ml sample; lanes 17-20 were loaded with 2 mg/ml sample. The standards consisted of trypsinogen (pI 9.3), lectin from *Lens culinaris* (pI 8.8, 8.6, 8.2), myoglobin (pI 7.2, 6.8), carbonic anhydrase I (pI 6.6), carbonic anhydrase II (pI 5.9), β-lactoglobulin A (pI 5.1), trypsin inhibitor (pI 4.6) and amyloglucosidase (pI 3.6). The bands were visualised using Coomassie staining.

3.7 Anti-DNP-OVA and anti-DNP-catOVA production in rabbits and chickens

Intravenous injection of cationised proteins may give rise to chronic glomerular nephritis and renal failure. The positively charged antigen has been shown to bind mainly to peripheral capillary walls, due to interaction with the polyanion layer of the glomerular basement membrane, resulting in membrane damage (Gauthier *et al.*, 1982; Koyama *et al.*, 1986a; Bass *et al.*, 1990). To ensure the health of the experimental animals, therefore, intravenous inoculation was not considered and intradermal inoculation was used.

Intradermal and intramuscular inoculations allow the use of adjuvants, which when emulsified with the antigen, provide a depot effect in which the antigen is slowly and persistently leaked into the surrounding tissue, challenging the immune system continuously. Besides its lower toxicity in this case, the intradermal inoculation method is preferred to intravenous inoculation, as the antigen is not cleared out of the system as quickly, allowing a prolonged stimulation of the immune response (Hudson and Hay, 1980) and was, therefore, used in the present study.

3.7.1 Procedure

Rabbits were inoculated intradermally and chickens were inoculated intramuscularly in their large breast muscle with 100 μg DNP-OVA or DNP-catOVA in phosphate buffer (without azide) emulsified in Freund's adjuvant as described in Section 2.5.

3.8 Assessment of immune response

The sera (rabbits) or egg yolk extracts (chickens) of the two animals of each species were pooled to provide average response data. Rabbit serum or diluted egg yolk extracts, i.e. crude unpurified preparations containing antibodies, were used to assess the immune response of rabbits and chickens to inoculation with DNP-OVA or DNP-catOVA over weeks 3, 8 and 12. Dilutions of egg yolk was used to assess response titres, using an ELISA system, as such samples give results comparable to those obtained using isolated IgY (Coetzer, 1985). Such dilutions, and whole serum, were used to select serum or egg yolks of weeks showing the highest anti-DNP response for isolation of IgG and IgY, to facilitate the comparison of titre (i.e. the relative amount of total antibody produced against DNP-OVA to that produced against DNP-catOVA). Since the hapten DNP is relatively

uncharged, a DNP-lysine derivative was used to coat ELISA plates, the lysine component improving binding to ELISA plates due to its charge.

3.8.1 Reagents

Reagents for ELISA as described in Section 2.7.1.

100 mM Phosphate buffer, pH 7.6. $NaH_2PO_4.H_2O$ (13.8 g) was dissolved in 800 ml of $d.H_2O$, adjusted to pH 7.6 with NaOH and made up to 1 litre.

3.8.2 Procedure

To assess the response of rabbits inoculated with DNP-OVA, microtitre plates were coated overnight with DNP-OVA, OVA, or their cationised equivalents or DNP-lysine (1 μg in 100 μl). Pooled rabbit sera, diluted serially twofold starting at 1 in 20 in BSA-PBS, were used as the primary antibody. HRP-linked sheep anti-rabbit IgG (diluted 1 in 450 in BSA-PBS) was used as secondary antibody. The procedure and controls used were as described in Section 2.7.2, and ELISAs for the comparison of various equivalent antisera, i.e. cationised and non-cationised, were performed simultaneously.

A similar experiment was performed to asses the immune response of chickens, except that pooled egg yolks were diluted with two volumes of phosphate buffer and used as the primary antibody (diluted serially twofold thereafter starting at 1 in 20 in BSA-PBS). HRP-linked rabbit anti-IgY was used as secondary antibody (diluted 1 in 750 in BSA-PBS).

The addition of DNP groups, or the replacement of carboxyl groups with ethylamine groups (all very low molecular weight), was calculated to change the molecular mass of a protein insignificantly, and thus the molar masses of DNP-OVA, DNP-catOVA, OVA and catOVA were judged to be similar enough to coat all conjugates at 1 μg (OVA = 45 kDa; DNP-OVA ≈ 45 kDa; catOVA ≈ 45 kDa; DNP-catOVA ≈ 45 kDa). In order to ensure that the differences in antibody titre were not due to differential binding of the different antigens to the microtitre plates, the amount of antigen actually coated was determined

spectroscopically (at 280 nm) by subtracting the amount of antigen remaining in solution after overnight coating from the amount loaded into the wells (1 μg per well, in 12 replicates).

3.8.3 Results

The molar masses of DNP-OVA, DNP-catOVA, OVA and catOVA conjugates are similar (OVA = 45 kDa; DNP-OVA ≈ 45 kDa; catOVA ≈ 45 kDa; DNP-catOVA ≈ 45 kDa), since the addition of DNP groups, or the replacement of carboxyl groups with ethylamine groups (all very low molecular weights), would not change the molecular mass of the protein in the kDa range. It was found that there is a 0.68% difference in coating levels between OVA and catOVA and 1% difference in coating levels between DNP-OVA and DNP-catOVA (considered statistically non-significant, meaning that the number of molecules coated should differ only marginally). The immune responses against the various conjugated immunogens in either chickens (Fig. 3.6A,B,C,D) or rabbits (Fig. 3.7A,B,C,D) may, therefore, be semi-quantitatively compared within each species. The molecular weight of DNP-lysine (≈ 400 Da) differs by more than 1000 fold from the protein-based conjugates, however, so the results obtained from ELISAs where the microtitre plates were coated with DNP-lysine (Fig. 3.6E,F and Fig. 3.7E,F) cannot be compared to results obtained using the protein conjugates. The trends of each graph can, however, be compared across antigens and across species.

In chickens inoculated with DNP-OVA, the average response against DNP-OVA (Fig. 3.6A), OVA (Fig. 3.6C) and DNP (Fig. 3.6E) appears to peak at week 8 and subsequently decreases significantly. With inoculation using DNP-catOVA, on the other hand, the response to DNP-catOVA (Fig. 3.6B) and catOVA (Fig. 3.6D) peaks at week 12, producing apparently higher titres than those raised against DNP-OVA (Fig. 3.6A,C). Against DNP (Fig. 3.6F), however, a weak response, apparently lower than that seen with inoculation with DNP-OVA (Fig. 3.6E), is seen at 8 weeks, with the response decreasing at week 12. The response in chickens inoculated with DNP-OVA conjugate appears to be mainly directed towards the hapten DNP (Fig. 3.6A,C). This is verified in the ELISA against the DNP antigen (Fig. 3.6E). The response to inoculation with DNP-catOVA

would seem to be mostly towards catOVA (Fig. 3.6B,D). This is confirmed by results against DNP (Fig. 3.6F).

In rabbits inoculated with DNP-OVA, the average response to DNP-OVA (Fig. 3.7A), OVA (Fig. 3.7C) and DNP (Fig. 3.7E) peaks at week 12 and gives a minimal response towards OVA (Fig. 3.7C). The response to DNP-catOVA (Fig. 3.7B), catOVA (Fig. 3.7D) and DNP (Fig. 3.7F) in rabbits inoculated with DNP-catOVA also peaks at 12 weeks, and the response is greater than that of their non-cationised counterparts.

Since the maximum titres of anti-DNP antibodies were obtained from week 12 in rabbits (Fig. 3.6) and from week 8 in chickens (Fig. 3.7), the rabbit sera from week 12 and the chicken egg yolk from week 8 were selected for purification and further analysis.

3.9 Crossreactivity between DNP-OVA and DNP-catOVA antibodies

Cationisation is reported to increase the immune response (Muckerheide *et al.*, 1987a; 1987b; 1990). Such a response is useful only if the antibodies to the cationised immunogen can bind to the native antigen. For this reason the crossreactivity of anti-DNP-OVA and anti-DNP-catOVA antibodies to the antigens, DNP-OVA and DNP-catOVA, was also determined. Since the antigens, as well as the hapten and carrier molecules were available in pure form, simple dot blot procedures were used to determine whether antibodies crossreacted with cationised and non-cationised conjugates.

3.9.1 Reagents

Reagents for antibody isolation as described in Section 2.6.1.

Reagents for dot blotting as described in Section 2.8.1.

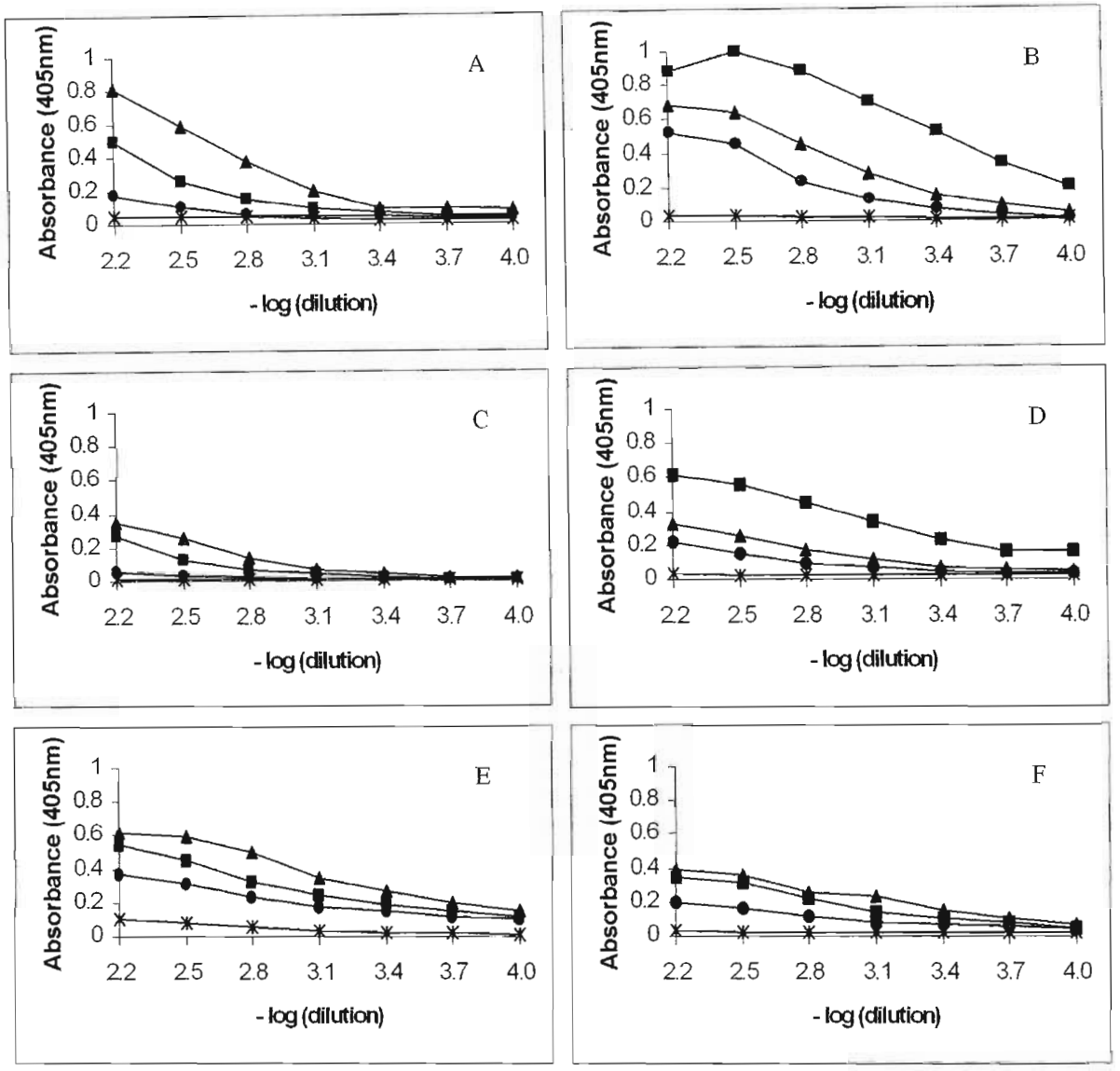

Figure 3.6 **Immune response of chickens inoculated with DNP-OVA or DNP-catOVA as determined by ELISA.**

DNP-OVA (A), DNP-catOVA (B), OVA (C), cat OVA (D) or DNP-lysine (E and F) was coated at 10 μg/ml on the microtitre plates and incubated with serially two-fold dilutions of egg yolk from chickens inoculated with DNP-OVA (A,C,E) or DNP-catOVA (B,D,F) collected after 3 (●), 8 (▲) and 12 (■) weeks and pre-immune IgY (✳). Binding was visualised by incubation with rabbit anti-IgY-HRP conjugate and ABTS. Each point is the mean absorbance at 405 nm of duplicate samples.

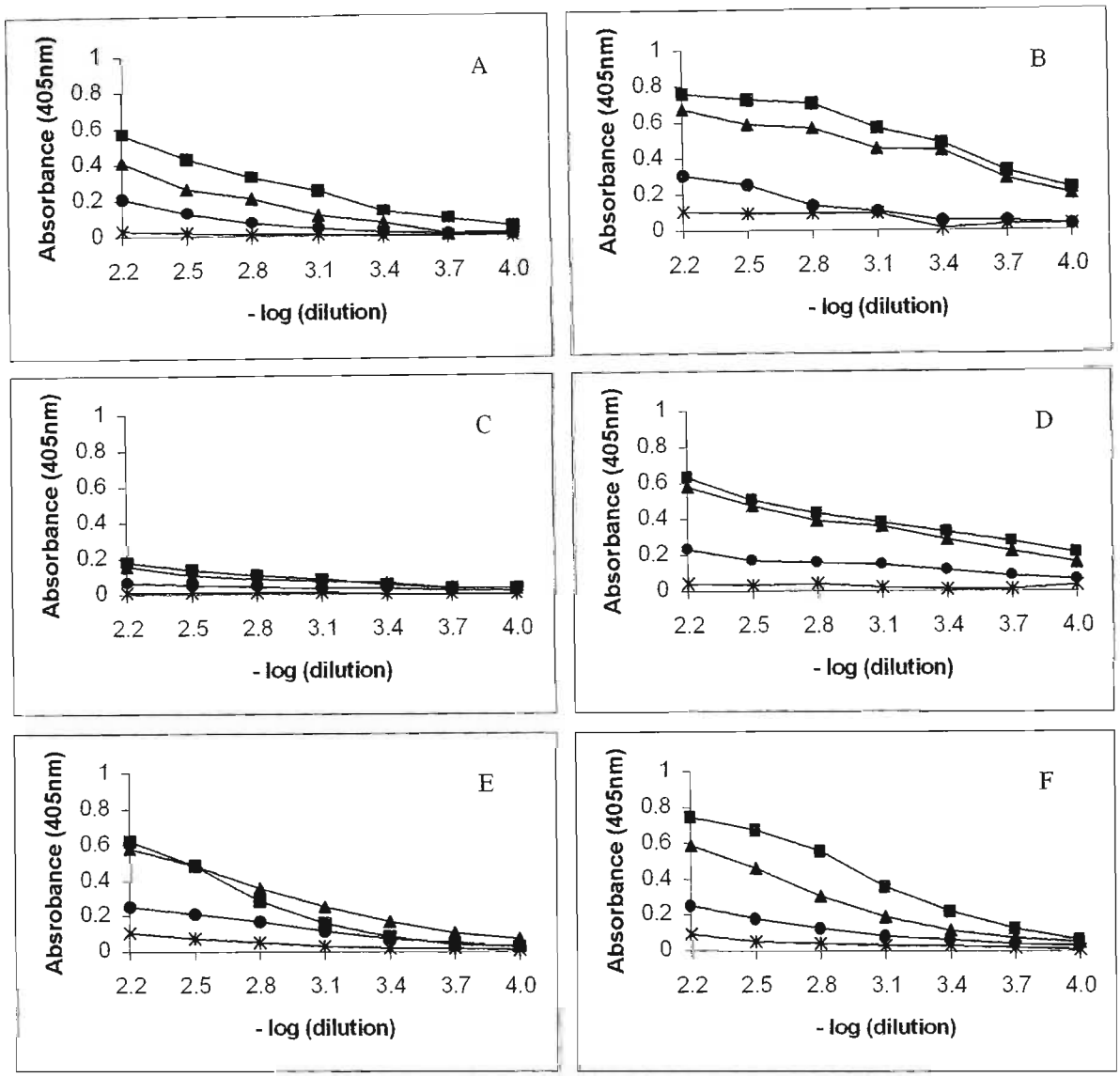

Figure 3.7 **Immune response of rabbits inoculated with DNP-OVA or DNP-catOVA as determined by ELISA.**

DNP-OVA (A), DNP-catOVA (B), OVA (C), cat OVA (D) or DNP-lysine (E and F) was coated at 10 μg/ml on the microtitre plates and incubated with serially two-fold dilutions of sera from rabbits inoculated with DNP-OVA (A,C,E) or DNP-catOVA (B,D,F) collected after 3 (●), 8 (▲) and 12 (■) weeks and pre-immune IgY (✳). Binding was visualised by incubation with sheep anti-rabbit-HRP conjugate and ABTS. Each point is the mean absorbance at 405 nm of duplicate samples.

3.9.2 Procedure

IgG and IgY were purified from rabbit sera or chicken egg yolk from week 12 and week 8, respectively, as described in Section 2.6.2. Nitrocellulose (Hybond-TC) strips were dot blotted with 0.5 μg DNP-lysine, OVA, catOVA and BSA (as control) and allowed to dry. The strips were placed into separate containers and treated with blocking agent (1 h, with gentle rocking). The membranes were washed with TBS (3 x 5 min) and primary antibody (either anti-DNP-OVA or anti-DNP-catOVA from either rabbits or chickens similarly diluted in BSA-TBS, 1 h) added. Subsequent washes, secondary antibodies and substrate reactions were performed as described in Section 2.8.2, using the relevant controls.

3.9.3 Results

The level of reactivity and cross-reactivity of the purified antibodies produced by inoculation with DNP-OVA and DNP-catOVA is summarized in Table 3.1. The week 8 IgY in chickens and week 12 IgG in rabbits detect DNP-lysine (DNP) equally well (fully cross-reactive) and show the maximal reactivity with DNP (assigned a value of +++++) compared to other antigens probed.

In chickens the IgY antibodies raised against the self-carrier protein DNP-OVA conjugate, whether cationised or not, seem to exhibit the same level of cross-reactivity with the unmodified (self or OVA) protein. IgY antibodies raised against DNP-catOVA cross-react with catOVA (++) apparently equally as well with unmodified OVA (++), whereas those raised against DNP-OVA are less cross-reactive with catOVA (+) than with the unmodified OVA protein (++) (Table 3.1).

In rabbits, where OVA is a foreign protein, IgG antibodies raised against the DNP-OVA conjugate seem to exhibit a greater level of cross-reactivity with the unmodified OVA protein (+++) than against catOVA (+). IgG antibodies raised against DNP-catOVA, on the other hand, cross-react less well with the unmodified OVA (++) than with catOVA (+++) and are less cross-reactive with unmodified OVA (++) than antibodies raised against DNP-OVA (+++) (Table 3.1).

In summary, for both chickens and rabbits the antibodies produced to the carrier protein OVA, whether cationised or not, are cross-reactive, although antibodies to DNP-catOVA are more cross-reactive with OVA than antibodies to DNP-OVA are with catOVA.

Table 3.1 Crossreactivity of antibodies raised to DNP-OVA and DNP-catOVA.

Species	Antibody	Antigen			
		DNP-lysine*	OVA*	catOVA*	BSA*
Rabbit	Anti-DNP-OVA	+++++	+++	+	none
	Anti-DNP-catOVA	+++++	++	+++	none
	Pre-immune	none	none	none	none
Chicken	Anti-DNP-OVA	+++++	++	+	none
	Anti-DNP-catOVA	+++++	++	++	none
	Pre-immune	none	none	none	none

*A value was assigned to each dot based on the darkness of the dot produced relative to a maximum of DNP

3.10 Affinity purification of anti-DNP antibodies

Affinity chromatography procedures are used extensively for the purification of biological molecules, and take advantage of the binding interactions that can occur on a protein's surface, allowing specific antigens to be covalently coupled to an insoluble matrix such as cellulose, agarose or glass beads. Such solid-phase antigen reagents can subsequently provide valuable methods for the isolation of specific antibodies. The commercial AminoLink™ product used in the present study consists of an agarose support, activated to yield aldehyde groups. These react with primary amine groups of the antigen to form Schiff bases. Reductive amination forms a stable covalent linkage of antigen to the support (Peng *et al.*, 1986). A solution containing a mixture of antibodies is applied to the solid-phase antigen, the antibodies specific to the antigen binding to the insoluble matrix. Contaminating (unbound) antibodies are subsequently washed off and the bound antibodies eluted from the column by lowering the pH of the suspending buffer sufficiently to disrupt the antigen-antibody complex, but not the covalent antibody-matrix linkage (Hermanson *et al.*, 1992). The low pH of the elution buffer may, however, denature the high affinity antibodies, which are the most difficult to elute but are preferred for immunocytochemistry. Antibodies with high affinity to the antigen are, therefore, sometimes lost as they are not easily eluted from affinity columns.

Anti-DNP antibodies were required for use in later immunolabelling studies, and the results of ELISAs performed on both chickens and rabbits (Fig. 3.6 and 3.7) indicated that anti-DNP-OVA antibodies contain less contaminating anti-OVA antibodies than do anti-DNP-catOVA antibodies. It was, therefore, decided to purify the anti-DNP antibodies by coupling OVA to an AminoLink™ column, thus removing unwanted contaminating anti-OVA antibodies and retaining the anti-DNP antibodies. In this case anti-DNP antibodies would pass through the column, while the anti-OVA antibodies would bind to the OVA-coupled matrix. The success of the affinity purification was determined via dot blot, using nitrocellulose strips coated with decreasing amounts of DNP-lysine and OVA, successful purification being indicated by DNP-lysine reactivity and a lack of reactivity for OVA.

3.10.1 Reagents

AminoLink™ affinity column. An AminoLink™ column coupled to OVA was prepared using an ImmunoPure® Ag/Ab Immobilization Kit (Pierce) according to manufacturer's instructions.

Sample buffer [100 mM phosphate buffer, 0.02% (w/v) NaN_3 pH 7.6]. $NaH_2PO_4.H_2O$ (13.8 g) and NaN_3 (0.2 g) were dissolved in 800 ml of $d.H_2O$, adjusted to pH 7.6 with NaOH and made up to 1 litre.

Elution buffer (0.1M glycine, pH 2.8). Glycine (7.51 g) was dissolved in 800 ml $d.H_2O$, adjusted to pH 2.8 with HCl and made up to 1 litre.

Neutralisation buffer (1 M Tris-HCl, pH 9.5). Tris (12.11g) was dissolved in 70 ml $d.H_2O$, adjusted to pH 9.5 with HCl and made up to 100 ml.

The reagents for dot blotting as described in Section 2.8.1.

3.10.2 Procedure

By measuring the amount of OVA applied to the column (20 mg per 10 ml activated agarose support) and the amount of OVA eluted after coupling (1 mg per 10 ml activated agarose support) the coupling efficiency of OVA to the activated matrix was calculated as 95%. The binding capacity (i.e. the amount of antibody that can bind to the column) was calculated from the coupling efficiency by calculating the amount of OVA coupled to the column. A small column (1.6 x 3.1 cm) was packed under gravity and equilibrated with 5 column volumes of sample buffer. An undersaturating amount of anti-DNP-OVA IgG (0.3 ml of 25 mg/ml) or IgY (0.2 ml of 37.5 mg/ml) was loaded onto the column and the column was washed (8.14 cm/h) with 5 column volumes of sample buffer. Contaminating anti-OVA antibodies were eluted off with elution buffer and fractions (0.5 ml) collected. The pH of the eluted fractions was increased with neutralisation buffer (25 µl per fraction) added to the tubes before fractions were collected. The fractions containing anti-DNP antibodies, obtained before elution, were pooled and concentrated using PEG (20 kDa) as described in Section 2.3.2.

The success of the removal of anti-OVA antibodies was monitored via dot blot, using nitrocellulose (Hybond-TC) strips coated with DNP-lysine and OVA (0.5 µg, 0.25 µg, 0.1 µg, 0.075 µg, 0.05 µg, and 0.025 µg), and the affinity purified anti-DNP antibodies as primary antibody as described in Section 2.8.2.

3.10.3 Results

All contaminating anti-OVA antibodies were apparently removed as no antibodies to OVA were detected on the dot blot (Fig. 3.8). Furthermore, the antibody reactivity decreased as the amount of DNP-lysine coated decreased. Taken together, this indicates that the antibody reactivity with DNP is not due to non-specific protein-protein interactions.

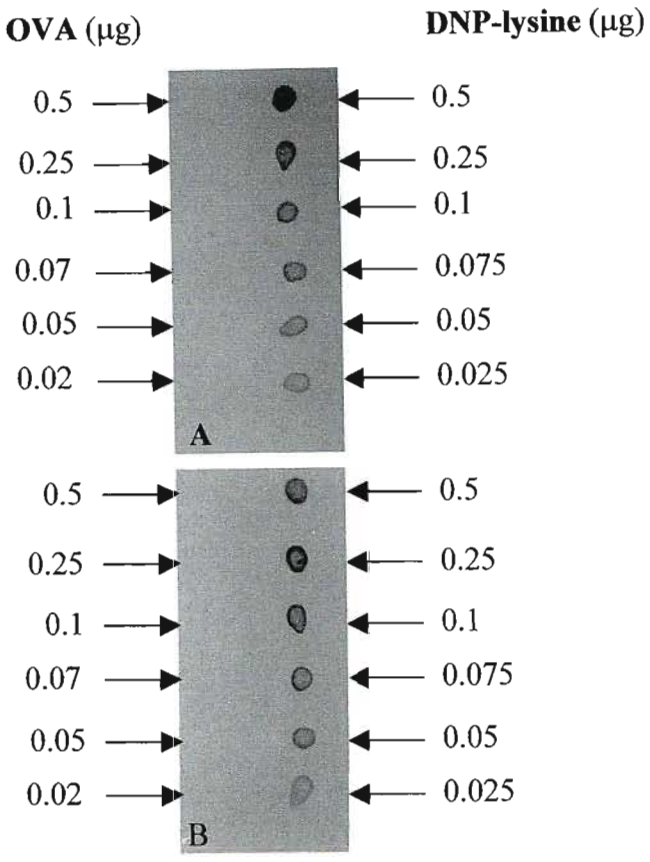

Figure 3.8 **Dot blot to assess whether all anti-OVA has been successfully removed by affinity chromatography.**
Varying amounts of DNP-lysine and OVA were dot blotted onto nitrocellulose strips and incubated in affinity purified rabbit anti-DNP IgG (A) or chicken anti-DNP IgY (B). Areas of antibody binding were detected using HRP-linked anti-species and 4-chloro-1-naphthol as substrate as described in Section 2.8.

3.11 Discussion

The immune system seems to be more concerned with "danger" than the distinction between self and non-self (Matzinger, 1994). To distinguish between "dangerous" and "harmless" self or non-self molecules, the emphasis is shifted away from the recognition and specificity of individual lymphocytes towards the interaction between lymphocytes and the interaction between lymphocytes and antigens associated with infection (e.g. heat shock proteins) or tissue damage (Matzinger, 1994; 2002). In the case of "dangerous" antigens, peptide:MHC complexes found on APCs must be presented to naïve T cells, for the T cells to differentiate into antigen-specific $CD4^+$ T cells that will react with same-antigen primed B cells, to stimulate antibody production (Janeway Jr, 2001). "Harmless" antigens, including self-antigens, generally do not result in an immune response.

Tolerance to self-antigens is generally maintained by the removal (via clonal deletion or receptor editing) or inactivation (via anergy or tuning) of self-reactive B and T cells, to prevent autoimmune disease (Goodnow *et al.*, 2005).

Immature B cells that have high affinity for self-antigens undergo clonal deletion or receptor editing. Those with low affinity, or with no contact with inaccessible tissue-specific antigens, however, survive and mature (Goodnow *et al.*, 1995). When the self-reactive mature B cells encounter their self-antigen in the periphery, they become anergic (inactive). The anergic B cells are either eliminated directly through apoptotic signals in the lymph node, or indirectly if a T cell specific for a peptide from that self-antigen, which stimulates apoptosis through interaction with the Fas ligand on the T cell is encountered (Goodnow *et al.*, 1995; 2005; Rathmell *et al.*, 1995).

The survival of immature self-reactive T cells, after clonal deletion and receptor editing of high self-antigen affinity T cells, seems to be dependent on the amount of self-peptides presented by MHC molecules on APCs. In the thymus, most self-peptides are presented at too low a level to bind Th cells, yet at high enough levels to induce clonal deletion of the immature self-reactive T cells (Goverman *et al.*, 1993; Kurts *et al.*, 1999). Some of the immature self-reactive T cells normally destined for clonal deletion, however, are positively selected to become regulatory $CD4^{+}CD25^{+}$ T cells (T_{Reg} cells) that inhibit autoimmune responses (Kawahata *et al.*, 2002). Other immature self-reactive T cells are not deleted in the thymus, due to antigen inaccessibility, but mature to naïve T cells that become anergic once they encounter the self-peptide presented on tissue cell MHC class I molecules. The anergic T cells are not necessarily eliminated (as is the case for B cells), but persist to possibly compete with other naïve non-anergic T cells to bind (without inducing a response) foreign antigens that mimic self-peptide:MHC complexes, preventing the accidental activation of autoreactive T cells by low levels of infectious agents (Greenfield *et al.*, 1998). These mechanisms, established by investigation of mouse and human systems are similar in chickens, the species of interest in this study (Corbel, 1996). In summary, therefore, tolerance to self is maintained by the removal or inactivation of self-reactive B and T cells. Additionally, self-antigens at low levels or in immunologically privileged sites are ignored by the immune system. When levels of self-antigens are increased by infection or disease, however, short-term autoimmunity may result to fight the infection, reject tumour cells, or repair tissue damage (Matzinger, 1994; 2002;

Lanzavecchia, 1995; Cohen, 1991; 1992). This response declines when the antigen levels fall (e.g. due to antigen removal by the stromal system), mature dendritic cell cross-presentation to naïve T cells in the draining lymph nodes decreases, gradual removal and inactivation of self-reactive B and T cells occurs and $CD4^+CD25^+$ T cell (T_{Reg} cell) activation induces tolerance to the auto-antigen (Spiotto *et al.*, 2003; Steinhoff *et al.*, 1994; von Boehmer, 2003).

In this study, the IgY response to OVA and DNP in chickens seems to be short-term, peaking at week 8 and thereafter decreasing. The anti-OVA response is reminiscent of the antibody responses associated with molecular mimicry, where the inoculated antigen contains peptide sequences identical or similar to that of the host. In such cases, $CD4^+$ T cells may induce a B cell response to the foreign epitopes, producing antibodies that are crossreactive with host epitopes, potentially causing B cells to act as APCs and activate naïve self-reactive T cells (Lin *et al.*, 1991; Mamula *et al.*, 1992). Also, DNP-modified peptide sequences similar to those of the host may provide sufficiently elevated levels of modified self-antigen to cause an increase in MHC:self-peptide presentation, allowing dendritic cell maturation, self-reactive naïve T and B cells activation and the induction of an autoantibody and anti-modified self response. Tolerance is, however, re-established once receptor desensitisation, induced by suppression of receptor-initiated signals (biochemical tuning), increases the activation threshold for both T and B cells (Abbas *et al.*, 2004; Lohr *et al.*, 2005). This prevents the activation of further lymphocytes and causes activated autoreactive T and B cells to become anergic (Abbas *et al.*, 2004; Lohr *et al.*, 2005). The activation of T_{Reg} cells also assists in establishing and maintaining tolerance, even after subsequent inoculation with the modified self-antigen (von Boehmer, 2003; Singh *et al.*, 2002), as seen in the declining anti-OVA ELISA response in chickens inoculated with DNP-OVA in this study.

The short-term anti-DNP IgY response in chickens inoculated with either DNP-OVA or DNP-catOVA seems similar to responses previously seen in trinitrophenyl-induced autoimmune reactions. In such instances co-elicited $CD8^+$ T cells initiate suppression of the hapten-specific $CD4^+$ T cell response, resulting in a decrease in hapten-specific antibody production (also seen in DNP-OVA or DNP-catOVA inoculated chickens) and an increase in $CD8^+$ T cell-dependent cytotoxic effects (Martin *et al.*, 2004). The short-term response may also possibly be due to hapten-specific tolerance induced by T_{Reg} cells,

responding to the presence of the self-protein carrier in the DNP-OVA or DNP-catOVA conjugate (Morimoto *et al.*, 1983; Zoller and Andrighetto, 1988).

The chicken immune response to the catOVA component of DNP-catOVA, on the other hand, seems to be more sustained, i.e. still increasing at week 12, and produces high-titre anti-catOVA antibodies that are crossreactive with unmodified OVA. Cationisation of DNP-OVA significantly increases the pI, indicating alterations in charge (positive to negative) after C-terminal, glutamic and aspartic carboxyl groups are replaced with ethylamine groups. This may also potentially disrupt the secondary structure of the DNP-catOVA by disrupting normal hydrogen-bonding and exposing both cryptic and altered epitopes. These epitopes may be recognized by $CD4^+$ T cells as "non-self" on the polymorphic histocompatability loci of dentritic cells as such peptides usually differ from self by several amino acids, whereas $CD8^+$ T cells generally recognize peptides differing by a single amino acid (Sahara and Shastri, 2003). Recent work has also shown that mutations in self-peptides (as in the case of certain cancer antigens) give rise to altered self (heteroclitic epitopes) that can enhance binding and extend the duration of MHC:peptide complex presentation by APCs to naïve T cells (Houghton *et al.*, 2001; Houghton and Guevara-Patiño, 2004; Guevara-Patiño *et al.*, 2003). The altered side-chains present in DNP-catOVA may resemble heteroclitic epitopes that are more efficient at triggering a sustained $CD4^+$ T cell response. Cationisation may furthermore compromise the epitopes on the self-antigen necessary for the induction of T_{Reg} cells (Muckerheide *et al.*, 1990; Michael, 1991), preventing the establishment of $CD4^+$ T cell tolerance, and giving rise to a sustained response against catOVA.

An increase in the cationic charge of antigens, as in the case of DNP-catOVA in this study, has previously been shown to increase the rate of antigen uptake into APCs (Koyama *et al.*, 1986a,b; Bass *et al.*, 1990; Muckerheide *et al.*, 1987a,b; 1990; Apple *et al.*, 1988; Michael, 1991; Farmer *et al.*, 1993), resulting in higher levels of MHC-mediated antigen presentation than for non-cationised antigens. This potentially reduces the amount of antigen required to induce a $CD4^+$ T cell-mediated immune response, so that inoculation with the same amount of antigen (cationised or non-cationised) produces higher antibody titres to the cationised antigen (in this case catOVA) (Apple *et al.*, 1988; Farmer *et al.*, 1993).

In rabbits, where OVA is not a self-protein, inoculation with DNP-OVA elicits a minimal IgG response to the OVA component, despite the fact that there is almost no sequence homology between OVA and rabbit albumin. Previous work (Naim and van Oss, 1991) has, however, suggested that the conjugation of a hapten to the primary amino groups of OVA may diminish the $CD4^+$ T cell response to the carrier, thus preventing significant IgG antibody production against OVA. Additionally, OVA has significant allergenic potential (Dearman *et al.*, 2000) and an IgE (rather than an IgG) response could have been elicited. APC presentation of epitopes containing DNP, however, seems unaffected by the use of an OVA carrier, giving rise to a significant anti-DNP IgG immune response. Cationisation of DNP-OVA seems to increase the antibody titres of both anti-DNP and anti-OVA IgG antibodies. The modified epitopes may increase the immunogenicity of the carrier and the increase in cationic charge may have the same effect as observed in previous studies (Koyama *et al.*, 1986a,b; Bass *et al.*, 1990; Muckerheide *et al.*, 1987a,b; 1990; Apple *et al.*, 1988; Michael, 1991; Farmer *et al.*, 1993), and as described earlier.

In conclusion, from these preliminary results, it would seem that if cationisation of DNP-OVA is to be used for the purpose of producing higher anti-DNP antibody titres for laboratory use, it may be wiser to use rabbits (instead of chickens), in which the carrier protein OVA is non-self. The reasons for such a low response to OVA in rabbits bears further investigation, since it could have significant impact on desensitisation treatment for allergies, if cationisation of OVA causes an antibody class switch from IgE to IgG production.

To induce anti-self IgY antibodies in chickens, DNP-modification of OVA does not seem to be sufficient to produce a sustained $CD4^+$ T cell-mediated anti-OVA response and haptenisation, in conjunction with cationisation, seems necessary. The mechanisms whereby cationisation of OVA overcomes self-tolerance and the epitopes presented on MHCs that are involved in the autoimmune response, however, require clarification.

DNP-modification of tumour antigens produces a response only with the use of cytotoxic drugs and intensive inoculation schedules (Berd, 2001; 2003). DNP-modification in conjunction with cationisation of altered self antigens (tumour antigens) may, similar to the results seen in this study, enhance and prolong $CD4^+$ T cell-mediated anti-modified self (anti-cancer) responses, although the effects of haptenisation and cationisation on $CD8^+$

T cell cytotoxic responses should be explored as such effects are also desirable for tumour immunotherapeutic strategies. Whether $CD4^+$ T cell-mediated cross-reactive anti-OVA (unmodified self) responses decline when inoculations with DNP-catOVA cease should be determined, as this would indicate whether autoimmune disease has been induced, an unwanted side-effect of cancer therapy. This seems unlikely as, by week 12 in chickens, no pathological sequelae were observed and the chickens did not stop laying eggs. Inoculation of cationised antigens into monoclonal systems could also prove useful for faster, high titre antibody production for use in passive immunotherapies, where the antibodies to tumour antigens are introduced into the patient.

According to Koyama *et al.* (1986a), although cationisation of the antigen produces higher titres of antibodies, these antibodies may have lower avidity than those produced to non-cationised proteins, and may also prove difficult to affinity purify due to non-specific electrostatic binding of the antibodies to a cationised antigen-coupled affinity column. The titres of anti-DNP antibodies present in IgY preparations raised against anti-DNP-catOVA, although higher than those present in anti-DNP-OVA preparations, were not that significantly higher to warrant the additional complications of using a catOVA affinity column for adsorption of anti-catOVA contaminating antibodies. Although there was a significant increase in rabbit anti-DNP IgG titre after cationisation of the immunogen, it was considered impractical to affinity purify these antibodies, for the above-mentioned reasons. Only anti-DNP antibodies affinity purified from anti-DNP-OVA were, therefore, used in the DAMP system for pH determination described in the following Chapter. Of these antibodies, the chicken antibodies may be of higher titre (Section 3.8) and hence superior for the determination of the pH of endosome-lysosome organelles.

CHAPTER 4

pH DETERMINATION OF ORGANELLES IN THE ENDOSOME-LYSOSOME SYSTEMS OF NORMAL AND *RAS*-TRANSFECTED BREAST EPITHELIAL CELLS

4.1 Introduction

Mutations in various *ras* genes have been associated with different cancers and pre-malignant transformation of many cell types (Sloane *et al.*, 1994a; 1994b). Two *ras* genes were originally isolated from the Harvey (Ha-) and Kirsten (Ki-) murine sarcoma viruses, and have subsequently been found in human, avian, and non-vertebrate species. Mutants of Ha-*ras* genes are most commonly found in bladder, lung and mammary carcinomas, while mutants of Ki-*ras* are responsible for >50% of colon and >90% of pancreatic cancers, and have also been associated with gall bladder, ovarian, gastric, and renal wall carcinomas. Mutations of N-*ras*, a third member of the *ras* family, has been found in human neuroblastomas (N-), various forms of leukaemia and sarcoma cell lines (Burck *et al.*, 1988; Gibbs, 1991). The effects of the *ras* genes are, therefore, of interest since their genetic mutation produces protein products that are constitutively activated and which may have serious effects on the Ras signalling pathway (Fig. 1.1). Constitutively active Ras may thus affect the activity of the Ras protein subfamilies, i.e. Rho, Rac, Rab, and Arf. Rho and Rac are involved in many cellular processes, such as cytoskeleton organisation, cell proliferation, regulation of movement of vesicles along microtubules and endocytosis (Prendergast and Gibbs, 1993; Sahai and Marshall, 2002). Rab and Arf proteins are mainly involved in endo- and exocytic vesicular transport (Prendergast and Gibbs, 1993) (Section 1.1.1). Mutationally activated *ras* may, therefore, be responsible for the changes in the trafficking and secretion of proteases, changes in phenotype and invasiveness observed in many cancer cells (Basolo *et al.*, 1991; Elliott and Sloane, 1996).

The MCF-10A breast epithelial cell line and its pre-malignant MCF-10AneoT derivative (transfected with Val-12 point mutationally activated c-Ha-*ras*), give rise to a model system in which "normal" and pre-malignantly transformed cells can be compared,

providing a unique opportunity to study the effects of constitutively activated Ras in pre-malignant transformation.

4.1.1 The MCF-10A cell line and its pre-malignant derivative, MCF-10AneoT

The MCF-10A cell line used in this study was established from mastectomy tissue of a 36 year old pre-menopausal woman, with no family history of breast malignancy, diagnosed with extensive fibrocystic disease. Histological examination showed increased mammary fibrous stroma, numerous dilated mammary ducts, benign apocrine metaplasia, and small confocal areas of intraductal hyperplasia with no evidence of atypia. The mastectomy tissue and patient were free of malignancy (Soule *et al.*, 1990).

Decreased Ca^{2+} concentrations usually increase the *in vitro* longevity of normal epithelial cells in culture (Soule *et al.*, 1990). The MCF-10A cell line, however, is an immortal cell line that arose spontaneously, without viral or chemical intervention. The diploid mortal cells, MCF-10M, senesce when passaged in 1.05 mM Ca^{2+}. The immortal cell lines, designated MCF-10A (attached cells) and MCF-10F (floating cells), display near-diploidy and proliferate for years in medium containing normal Ca^{2+} (1.05 mM) or low Ca^{2+} concentrations (0.04 mM) (Soule *et al.*, 1990). None of the known oncogenic mutations (c-*erbB*-1/*HER*-2/*neu*, c-*erbA*-1, *int*-2, and c-Ha-*ras*-1) that could be responsible for immortalisation were initially detected (Basolo *et al.*, 1991). The cell line contains functionally active wild-type p53 (Shekhar *et al.*, 1997; Merlo *et al.*, 1995) and the leucine zipper transcription factor USF, required for insulin-like growth factor-2 receptor (IGF2R) transcription and responsible for proliferation and regulation of cathepsin D expression (Qyang *et al.*, 1999; Szentirmay *et al.*, 2003). Recently, however, genetic abnormalities commonly associated with the *in vitro* culture of mammary epithelial cells, including deletion of the locus containing *p16* and *p14ARF* and amplification of *myc* have been described in the MCF-10A cell line (Stampfer and Yaswen, 2000; Elenbaas *et al.*, 2001; Debnath *et al.*, 2003). p16 is a cyclin-dependent kinase (Cdk) inhibitor that affects the control of G1/S transition (Hengst *et al.*, 1994; Hengst and Reed, 1996) while p14ARF regulates p53-mediated cell cycle arrest and apoptosis (Huang *et al.*, 2003), so that the deletion of their loci could result in cell proliferation and immortalisation. The role that *myc* amplification plays is not fully understood, although it is hypothesized to reduce growth-factor requirements, contribute to immortalisation, provide resistance to

anti-mitogenic factors and contribute to genetic instability that promotes secondary mutations and affects the ploidy of cells (Lutz *et al.*, 2002).

The MCF-10A cell line, however, exhibits the characteristics of normal breast epithelium: 1) it does not form tumours in nude mice, 2) it shows no three-dimensional (3D) growth in collagen, 3) proliferation in culture is dependent on hormones and growth factors, 4) it shows no signs of anchorage-independent growth or dome formation in confluent cultures (Soule *et al.*, 1990; Tait *et al.*, 1990; Martin *et al.*, 2003). MCF-10A cells also form acinar structures after 15 days in 3D culture that exhibit low levels of proliferation, the acinar size and number of cells remaining constant, an important characteristic of glandular epithelium *in vivo* (Debnath *et al.*, 2002; Muthuswamy *et al.*, 2001; Debnath *et al.*, 2003).

Transfection of the parental MCF-10A cells with the plasmid Homer 6 containing the human Val-12-mutated c-Ha-*ras* oncogene and a neomycin resistance gene, however, produces a pre-malignant equivalent of the MCF-10A line, named the MCF-10AneoT cell line (Basolo *et al.*, 1991), in which many of the features associated with transformation to the malignant, invasive phenotype are apparent, i.e. cells: 1) become larger and form three-dimensional colonies in collagen (i.e. exhibit loss of polarity), 2) show no growth hormone or growth factor-dependence, 3) show increased migratory and chemotactic ability and high invasive potential, 4) form tumours in nude mice, 5) show increased secretion of transforming growth factor-α (TGFα), 6) contain increased numbers of mitochondria and vesicles containing digestive enzymes, possibly lysosomes, 7) exhibit increased levels of c-Ha-*ras* mRNA transcripts and, therefore, increased levels of activated p21 (*ras* related protein products), 8) show increased cathepsin B and L mRNA and protein expression and increased activity of these proteases (Basolo *et al.*, 1991; Ciardiello *et al.*, 1990; Russo *et al.*, 1991; Ochieng *et al.*, 1991; Kinch *et al.*, 1995; Premzl *et al.*, 2003; Premzl and Kos, 2003; Lah *et al.*, 2000). An additional difference, significant to this study, is the relative alkalinisation of MCF-10AneoT cells compared to the MCF-10A cell line (Sloane *et al.*, 1994b), since this could affect the processing, trafficking and secretion of proteases involved in invasion.

It has not yet been established how such alkalinisation may arise and what effect transfection with activated *ras* may have on factors and intermediates involved in endo- and exocytic vesicular trafficking. Interference with vesicular and membrane trafficking

(including the various pumps necessary to maintain the acidic pH of these organelles) could lead to the alkalinisation of organelles of the endosome-lysosome system and possibly explain the altered processing and trafficking of proteases observed in the MCF-10AneoT cell line (Moin *et al.*, 1992; Sameni *et al.*, 1995). In order to explore this, and other possible causes of vesicular alkalinisation, details of the pumps involved in vesicular acidification of the endosome-lysosome system, their mode of action and potential regulation were reviewed.

4.1.2 The ATPase pumps and maintenance of pH of the endosome-lysosome system

An acidic lumen is vital for the dissociation of certain receptor-ligand complexes during receptor-mediated endocytosis and receptor recycling, the movement and maturation of organelles, the activity of membrane transporters that have acidic pH optima and activation of lysosomal hydrolases and proteolysis (Tjelle *et al.*, 1996; Pisoni and Theone, 1991; Hasilik, 1992). The acidification of a variety of intracellular organelles, including clathrin-coated vesicles, endosomes, lysosomes, Golgi and secretory vesicles is due to activity of a family of ATP-driven proton pumps, the vacuolar H^+-ATPases (V-ATPases) (Forgac, 1998; Kane and Stevens, 1992). Improper functioning of the V-ATPases has been shown to cause cellular acidosis, promoting the activation of endonucleases and apoptosis in a variety of normal cells, leading to cell death (Arends *et al.*, 1990; Barry and Eastman, 1992; Gottlieb *et al.*, 1996; Akifusa *et al.*, 1998). The degree of malfunction of the V-ATPases in such cases is difficult to assess, as there are many levels at which V-ATPase function may be altered or regulated. In cancer cells, however, altered V-ATPase expression, regulation and/or trafficking inhibit apoptosis by removing protons from the cytoplasm thus preventing cellular acidosis (Shekar *et al.*, 1997; Izumi *et al.*, 2003).

The V-ATPase pumps responsible for the acidification of the endosome-lysosome system require both ATP and Mg^{2+}-binding in order to function but can function nearly as well with GTP as with ATP (Schneider, 1981; Okhuma *et al.*, 1982) and consists of two discrete domains. The catalytic cytosol-facing hydrophilic domain (V_1) is composed of at least 8 different subunits (A-H) that contain 3 catalytic sites for ATP hydrolysis formed from the A and B subunit (Sun-Wada *et al.*, 2003; 2004). The B subunit also contains an F-actin binding domain that binds F-actin when phosphatidylinositol 3-kinase [PI(3)K] activity is blocked (Chen *et al.*, 2004). The E subunit also interacts with mSOS-1, which plays a role

in the activation of Ras and Rac1 (Miura *et al.*, 2001) and the H subunit has been shown to bind to the adaptor protein-2 (AP2) complex, which is involved in the internalisation of proteins from the plasma membrane to the early endosome (Pearse and Robinson, 1990). The transmembrane domain (V_0) contains up to 5 subunits (a, c, c', c'', d) that form the proton-conducting channel and are thus responsible for proton translocation across membranes (Gruber, 2003; Sun-Wada *et al.*, 2003; 2004).

Other ion transport proteins are also necessary for acidification. Addition of ATP to the cytosolic side of the vesicle initiates pumping of protons across the vesicle membrane. A corresponding build-up of negative charge on the outer membrane, however, creates an electrical potential across the membrane that would eventually oppose further movement of protons from the cytosol into the vesicle lumen. In order for the vesicle lumen to further acidify, therefore, either an equal number of anions must be moved in the same direction, or an equal number of cations must be moved in the opposite direction (Nelson, 1992).

In early endosomes, the Na^+/K^+-ATPase transporter pump, present on the plasma membrane, is taken into the organelle where it regulates the pH. The increased positive membrane potential generated by the presence of the Na^+/K^+-ATPase pump favours the operation of the Na^+/K^+-ATPase pump and opposes V-ATPase-dependent acidification in early endosomes, maintaining a mild pH $\approx$ 6.0–6.2 (Fuchs *et al.*, 1989). The Na^+/K^+-ATPase pump is recycled from the early endosome to the cell surface, decreasing the membrane potential and allowing further acidification in the late endosome and lysosome via the V-ATPase pump (Corley-Cain *et al.*, 1988). Inhibition of the V-ATPase in early endosomes results in reduced rates of endocytic uptake, recycling to the plasma membrane and transport of ligands to the late endosome (van Weert *et al.*, 1995). This implies that acidification via the V-ATPase and recycling of the Na^+/K^+-ATPase must occur before trafficking can continue to the late endosome.

The V-ATPase pump maintains a pH of $\approx$ 4.0-5.0 in the late endosome and lysosome and in late endosomes is found on the outer limiting membrane (Toyomura *et al.*, 2003). An influx of Cl^- ions through a Cl^- channel, eliminates membrane potential (Ohkuma *et al.*, 1982; van Dyke, 1988; van Dyke and Belcher, 1994). This facilitates the development of a proton gradient and results in a more acidic pH (Moriyama and Nelson, 1989; Futai *et al.*, 2000), a process regulated by (protein kinase A) PKA-dependent phosphorylation (Bae and

Verkman, 1990; Forgac 1998). Acidification of late endosomes and lysosomes does not require an active influx of protons once an equilibrium has been reached, but the acidification process can be abolished by cations such as K^+ and Na^+ (Moriyama *et al.*, 1992).

Factors that affect the initial rate of vesicle acidification or steady state pH, the electrochemical gradient, or both, could alter endosome-lysosome pH. These factors include: 1) differential regulation of V-ATPases or the presence of different isoforms of V-ATPases (Timchak *et al.*, 1986; Wang and Gluck, 1990; Kawasaki-Nishi *et al.*, 2001), 2) alterations in the regulated assembly of V_0 and V_1 domains (Kane, 1995; Sumner *et al.*, 1995), 3) changes in vesicle conductance for Cl^- (Bae and Verkman, 1990; Barasch *et al.*, 1991; Xie *et al.*, 1989), 4) differences in cation permeability (Fuchs *et al.*, 1989) or proton leakage (Hilden *et al.*, 1990), 5) the presence of other competing electrogenic transporters such as Na^+/K^+-ATPase pumps (Corley-Cain and Murphy, 1988; Corley-Cain *et al.*, 1988), 6) differences in vesicle buffering capacity, surface-to-volume ratio, and/or the number of membrane pumps relative to vesicle surface area or volume (van Dyke and Belcher, 1994). All the above factors could be caused or influenced by alterations in vesicular and protein trafficking, especially the trafficking of proton- and other ATPase pumps.

The focus of the present study is to establish the pH and hence the extent of alkalinisation, if any, of the various organelles responsible for processing and trafficking of various lysosomal proteases in the MCF-10A and MCF-10AneoT cell lines, and to establish the identity of the peripherally located organelles found in the MCF-10AneoT cell line. The pH of the peripheral organelles may assist in their identification. These peripheral organelles seem to contain mature, active cathepsin B and D (Elliott, unpublished results) and, if found to be acidic, could be hypothesised to be either secretory or storage lysosomes. Their appearance seems to accompany, and be necessary for the acquisition of the invasive phenotype. Their identity and characterisation may, therefore, be important in understanding the invasive phenotype, and may shed light on the mechanism by which altered distribution or trafficking of proteases may occur due to *ras*-transfection. The changes in trafficking may, in turn, lead to insight into how the various signal transduction intermediates (Section 1.1.1) may give rise to such a phenotype, and what inhibitors of signal transduction may be targeted for the therapeutic reversion of the invasive phenotype to the "normal" non-malignant phenotype.

In order to gain an overview of the relative pH of the organelles of the endosome-lysosome system, a fluorescent pH determination method was initially used, followed by a more discriminating, higher resolution electron microscopy (EM) based technique of pH determination.

4.2 Oregon Green® dextran pulse-chase and pH determination using fluorescence microscopy

The *in vivo* pH of the endocytic system has often been determined using cell-permeant fluorescent pH indicators and fluorescence microscopy (e.g. Tanaka *et al.*, 1997). The pH indicators may also be made impermeant by coupling to carrier molecules, such as α_2-macroglobulin (α_2-M) or dextran (a polysaccharide synthesised by *Leuconostoc* bacteria) for use in pH studies specific to the endosome-lysosome system (e.g. Montcourrier *et al.*, 1994).

Most fluorescent pH indicators are phenolic compounds and can be acidic, basic or neutral with their fluorescence depending on the ionisation, or non-ionisation, of particular groups within the indicator molecule. The alteration in charge reconfigures the indicator's π-electron system, resulting in pH-dependent fluorescence (Johnson, 1992). Three properties characterise the most satisfactory fluorescent pH indicators: 1) they should be highly fluorescent, so that their presence can be revealed at low concentrations, and the fluorescence should be lasting and resistant to quenching effects of oxygen or tissue constituents, 2) they should absorb light strongly between 350 and 500 nm, so that excitation can be achieved by light of wavelengths not themselves highly damaging to living cells, 3) the emitted fluorescence should be in the visible spectrum (380-780 nm) and so readily visible using a fluorescent microscope (Allison and Young, 1969).

Fluorescent techniques that provide accurate measurement of the intracellular pH use the fluorescent readings as the ratio of fluorescence intensities at two wavelengths, rather than the absolute intensity at a single wavelength. This ratio can be determined from either two excitation wavelengths at a constant emission wavelength [e.g. coumarins, pyranines, fluoresceins, rhodols or seminaphthofluorescein (SNAFL)], or two emission wavelengths at a constant excitation wavelength [e.g. SNAFL or seminaphthorhodafluor (SNARF)]. A

number of variables (e.g. non-uniform intracellular dye concentrations, probe leakage, dye bleaching and cell thickness) that perturb pH measurements are eliminated using such ratios, since these variables have similar effects on intensities at both wavelengths (Haugland, 1992).

The biggest drawback to the ratio method is the lengthy calibrations that must be performed in order to equate a dual-excitation or dual-emission ratio to a specific pH, and the requirement for specialised software, microscopy equipment and cameras. Intracellular (*in situ*) calibration of the fluorescence response of pH indicators is usually performed using the K^+/H^+ ionophore nigericin (Fig. 4.1) in buffers of defined pH (e.g. Levitz *et al.*, 1999), causing equilibration of intracellular and extracellular pH by catalysing K^+-H^+ exchange in the presence of high concentrations of extracellular K^+ (Galloway *et al.*, 1983). This allows a dual-excitation or dual-emission ratio to be equated with a certain pH.

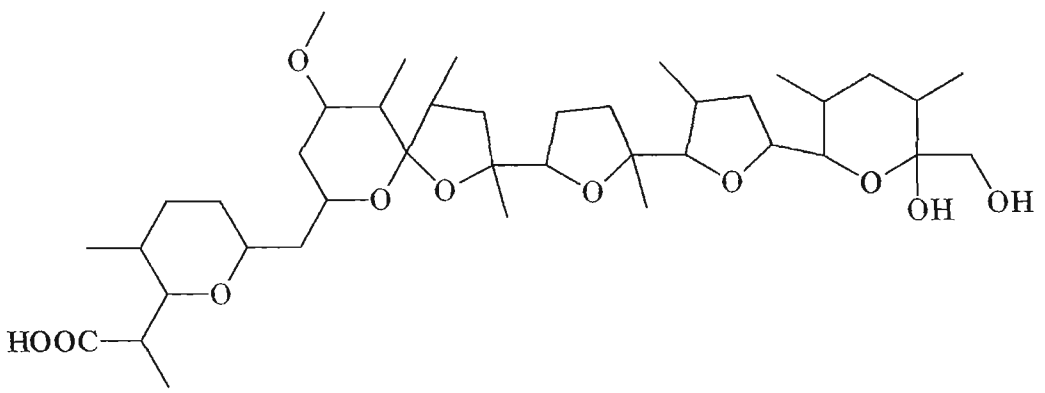

Figure 4.1 Structure of nigericin.

For the purpose of this study, the fluorescein derivative 2',7'-difluorofluorescein dextran (10 kDa), commonly known as Oregon Green® 488 dextran (OGD), was chosen as pH indicator. The structure of Oregon Green® 488 is given relative to the structure of fluorescein in Fig. 4.2. OGD was derived by the introduction of electron-withdrawing groups into fluorescein, resulting in a molecule with a lower pKa (pKa $\approx$ 4.7) than that of fluorescein (pKa 5-7, depending on its degree of ionisation), which would provide more accurate pH determination for the more acidic late endosome and lysosome. The high molecular weight of the dextran component of OGD (10 kDa) ensures that the molecule is too big to permeate through membranes so that uptake is limited to the endocytic pathway, allowing pulse-chase uptake of OGD into either early endosomes ($\pm$ 10 min) or late endosomes/lysosomes (overnight) [prolonged incubations have shown that endocytosed

materials distribute equally between late endosomes and lysosomes (Griffiths *et al.*, 1990a) and fluorescence microscopy does not provide sufficient resolution to distinguish them visually]. Dextran is also water-soluble, has very low toxicity, is relatively inert and contains 1,6-polyglucose linkages that are resistant to cleavage by most endogenous cellular glycosidases. The pH-dependent spectral characteristics of OGD, however, remain very similar to fluorescein, i.e. the emission spectrum at 510 nm is pH sensitive when excited at 490 nm and pH insensitive when excited at 440 nm, allowing ratio imaging that is independent of probe concentration (Haugland, 2002).

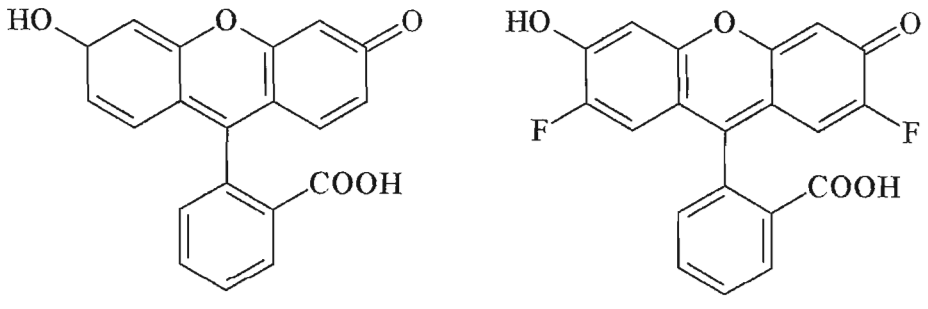

Fluorescein 2',7'-Difluorofluorescein

Figure 4.2 Structure of fluorescein and 2',7'-difluorofluorescein (Oregon Green® 488)

Once the pH standards have been calibrated using *in situ* methods, the pH of early endosomes and late endosomes/lysosomes can be determined, once background fluorescence from unloaded cells has been subtracted, using either regression analysis from a calibration curve or the formula:

$$pH = pKa + \log\left(\frac{R_a - R}{R - R_b}\right)$$

where R_a is the 450/490 excitation ratio at the most acidic calibration point, R_b is the 450/490 excitation ratio at the most basic calibration point and R is the 450/490 excitation ratio of the organelle of interest (Vergne *et al.*, 1998). Since the *in situ* pKa of OGD was not known, the pH of the early endosomes and late endosomes/lysosomes of the MCF-10A and MCF-10AneoT cell lines was determined using regression analysis from a standard pH calibration curve (Haugland, 2002).

4.2.1 Reagents

Reagents for cell culture as described in Section 2.9.1.

Oregon Green® 488 dextran (OGD) solution. Oregon Green® 488 (2 mg) was dissolved in DMEM:Ham's F-12 complete medium (2 ml) and sterile filtered through a 0.22 μm filter.

Calibration stock solution (1.5 M KCl, 0.5 M $NaH_2PO_4.H_2O$, 0.25 mM nigericin). KCl (5.6 g), $NaH_2PO_4.H_2O$ (3.45 g) and nigericin (10 mg) was dissolved in dd.H_2O and made up to 50 ml.

pH 3.5 Calibration working solution (150 mM KCl, 50 mM $NaH_2PO_4.H_2O$, 25 μM nigericin, pH 3.5). Calibration stock solution (5 ml) was added to dd.H_2O (30 ml). The pH was adjusted to pH 3.5 with HCl and the volume made up to 40 ml.

pH 4.0 Calibration working solution (150 mM KCl, 50 mM $NaH_2PO_4.H_2O$, 25 μM nigericin, pH 4.0). Calibration stock solution (5 ml) was added to dd.H_2O (30 ml). The pH was adjusted to pH 4.0 with HCl and the volume made up to 40 ml.

pH 5.0 Calibration working solution (150 mM KCl, 50 mM $NaH_2PO_4.H_2O$, 25 μM nigericin, pH 5.0). Calibration stock solution (5 ml) was added to dd.H_2O (30 ml). The pH was adjusted to pH 5.0 with HCl and the volume made up to 40 ml.

pH 5.5 Calibration working solution (150 mM KCl, 50 mM $NaH_2PO_4.H_2O$, 25 μM nigericin, pH 5.5). Calibration stock solution (5 ml) was added to dd.H_2O (30 ml). The pH was adjusted to pH 5.5 with HCl and the volume made up to 40 ml.

pH 6.0 Calibration working solution (150 mM KCl, 50 mM $NaH_2PO_4.H_2O$, 25 μM nigericin, pH 6.0). Calibration stock solution (5 ml) was added to dd.H_2O (30 ml). The pH was adjusted to pH 6.0 with HCl and the volume made up to 40 ml.

pH 6.5 Calibration working solution (150 mM KCl, 50 mM $NaH_2PO_4.H_2O$, 25 μM nigericin, pH 6.5). Calibration stock solution (5 ml) was added to dd.H_2O (30 ml). The pH was adjusted to pH 6.5 with HCl and the volume made up to 40 ml.

4.2.2 Procedure

Cells were seeded (Section 2.9) at a low density into 12-well Nunc Multiwell plates, each well containing a 15 mm sterile glass coverslip, and allowed to adhere. To detect early endosomes, two coverslips were incubated in OGD solution (5 min, 37°C), washed with media and incubated in fresh media (5 min, 37°C). Coverslips were inverted onto a small drop of complete medium on a glass slide and viewed in an Olympus A70 microscope equipped with two fluorescence dichroic mirrors producing: 1) excitation with a 470-490 nm narrow band pass filter and emission with a 515-550 nm band pass barrier filter, 2) excitation with a 420-440 nm narrow band pass filter, a 460 nm beam splitter, and emission with a 515 nm long pass filter. Representative cells (at least five per organelle type) were photographed with an AnalySIS® F-view low-light charge-coupled device (CCD) black and white digital camera for both excitation wavelengths to produce paired photographs. To detect late endosomes and lysosomes, two coverslips were incubated in OGD solution (1 h, 37°C), washed with media and incubated in fresh media (overnight, 37°C). Coverslips were inverted onto a small drop of complete medium on a glass slide, viewed and photographed as described above.

In order to establish the pH standards, coverslips (two per pH standard) of MCF-10AneoT cells were incubated in OGD solution (overnight, 37°C), washed twice with the relevant calibration working solution (pH 3.5, 4.0, 5.0, 5.5, 6.0 or 6.5) and incubated in fresh calibration working solution (10 min). The coverslips were mounted, viewed and photographed as described above.

The images were analysed using the AnalySIS® software imaging system. The greyscale pixel intensity was measured for each randomly selected fluorescent organelle (pH 3.5 n = 57; pH 4.0 n = 74; pH 5.0 n = 126; pH 5.5 n = 102; pH 6.0 n = 149; pH 6.5 n = 156 where n is the number of organelles in a minimum of five randomly selected cells used for calibration) on the paired photographs, to produce paired data points of fluorescent

intensity at both excitation wavelengths (440 nm and 490 nm). The 440/490 excitation ratio was determined by dividing the pixel intensity at excitation 440 nm with that obtained at 490 nm and the background excitation ratio from cells not loaded with OGD was subtracted. A standard curve equating the 440/490 excitation ratio to pH was established using the results obtained from cells incubated in the various pH calibration buffers. The pH of randomly selected early endosomes (MCF-10A n = 8; MCF-10AneoT n = 13) and late endosome/lysosomes (MCF-10A n = 95; MCF-10AneoT n = 62) was subsequently determined using regression analysis from the standard curve. The pH values obtained for each cell line were averaged to provide an overall pH value for a specific type of organelle (early endosome or late endosome/lysosome) and the standard deviation from the mean determined. The pH values obtained were also subjected to one-tailed student's t-test analysis, in order to determine if the differences in pH between organelles and cell lines was >95% significant.

For visual representation in this thesis, the photograph pairs were artificially coloured using red to represent the fluorescence at excitation 440 nm and green to represent the fluorescence at excitation 490 nm using the AnalySIS® software imaging system. The coloured paired photographs were then combined to produce a coloured composite photograph.

4.2.3 Results

The calibration curve produced by plotting the average 440/490 excitation ratio of MCF-10AneoT cells incubated with OGD and calibration buffers of various pH, containing the ionophore nigericin is shown in Fig. 4.3. Representative fluorescent images of these standards are depicted in Fig. 4.4 (A,B,C,G,H,I). Since the fluorescence at excitation 440 nm is pH independent, the amount of red in each composite should remain the same. The fluorescence at excitation 490 nm is pH dependent with the fluorescence intensity increasing as the pH increases, meaning that the amount of green in the composite photographs increases with increasing pH. The combination of red and green in fluorescence microscopy produces yellow. Thus, as seen in Fig. 4.4 (A,B,C,G,H,I), the fluorescence becomes more intense and the colour changes from red to orange to yellow to green as the pH increases.

Using regression analysis (Fig. 4.3), the pH of the early endosome in the MCF-10A (pH 6.0 ± 0.3) and MCF-10AneoT (pH 6.1 ± 0.4) cell lines was determined. The slight pH difference between the early endosomes of the MCF-10A and MCF-10AneoT cells was found to be statistically non-significant (from a one-tailed student's t-test with a confidence interval of 95%), indicating the early endosomes of both *ras*-transfected and non-transfected cell lines have a similar pH. This can be seen in Fig. 4.5 (A and C), where the colour (yellow) and brightness of the fluorescent early endosomes are similar. These images are of whole cells (not optical sections as would be seen with a confocal microscope) and the fluorescent early endosomes are found in the periphery of the cell, although early endosomes present at the top of the cell may appear to be perinuclear (Fig.4.5A and C). Although there are large amounts of red fluorescence visible in Fig. 4.5C, this can be attributed to insufficient washing to remove excess OGD.

Using regression analysis (Fig. 4.3), the pH of the late endosome/lysosome in the MCF-10A (pH 4.8 ± 0.6) and MCF-10AneoT (pH 5.5 ± 0.6) cell lines was determined. The late endosome and lysosome can unfortunately not be distinguished morphologically using fluorescence microscopy, due to insufficient resolution, and prolonged incubations (18-24 h), as done in this study, have shown that endocytosed materials distribute equally between these organelles (Griffiths *et al.*, 1990a). There is, furthermore, also no fluorescent marker available that can distinguish the late endosome from the lysosome in live cells (immunolabelling requiring cells to be fixed, a process incompatible with fluorescent methods for pH determination). Since late endosomes cannot be distinguished from lysosomes, and lysosomes generally have a pH slightly lower than that of the late endosome (Kornfeld and Mellman, 1989), this may have contributed to the large standard deviation in pH values observed for the late endosome/lysosome organelles in the two cell lines. Overall, the pH of the late endosomes/lysosomes of the MCF-10AneoT cell line increased by 0.7 pH units relative to that of the MCF-10A cell line. Despite the large standard deviation, this pH difference was found to be statistically significant (from a one-tailed student's t-test with a confidence interval of 95%), indicating that the late endosomes/lysosomes of the *ras*-transfected MCF-10AneoT cell line are more alkaline than those of the "normal" MCF-10A cell line. This can be seen in Fig. 4.6 (A and C), where in Fig. 4.6A the organelles of the MCF-10A cells are orange and fluoresce less intensely than in Fig. 4.6C, where the organelles of the MCF-10AneoT cells are yellow and fluoresce more intensely.

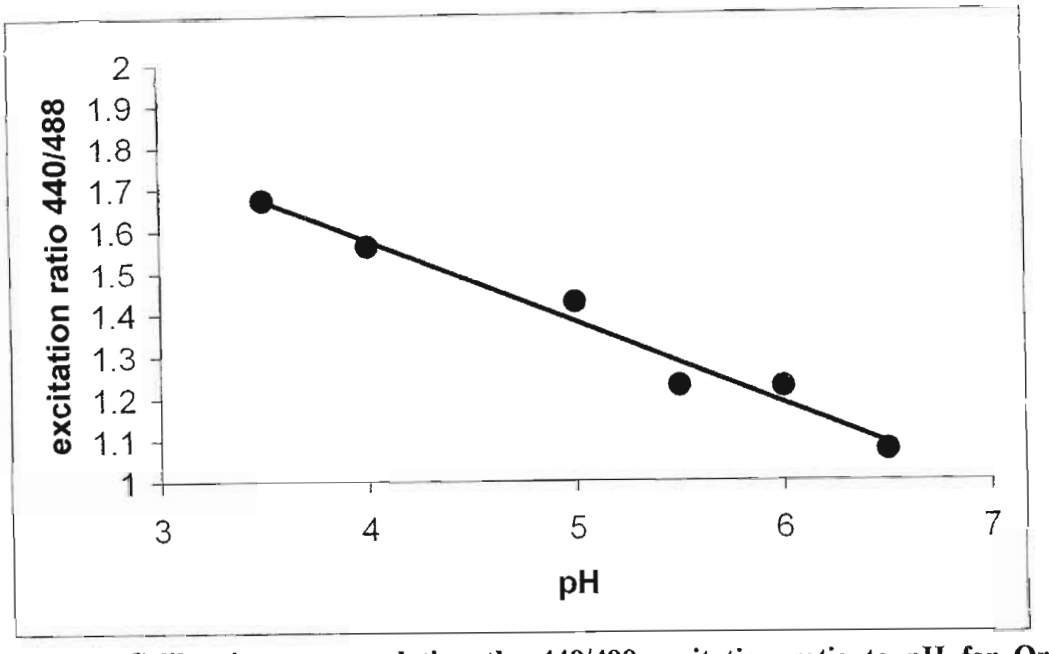

Figure 4.3 **Calibration curve relating the 440/490 excitation ratio to pH for Oregon Green® 488 dextran (OGD).**
MCF-10AneoT cells containing the fluorescent pH indicator OGD were incubated with calibration solution (pH 3.5, 4.0, 5.0, 5.5, 6.0 and 6.5) containing the K^+/H^+ ionophore nigericin to equilibrate the intracellular pH to that of the calibration solution. The average 440/490 excitation ratio for randomly selected organelles was determined (pH 3.5 n = 57; pH 4.0 n = 74; pH 5.0 n = 126; pH 5.5 n = 102; pH 6.0 n = 149; pH 6.5 n = 156 where n is the number of organelles in a minimum of 5 randomly selected cells) and plotted against pH to establish a calibration curve. Regression analysis gave the equation for the straight line as $y = -0.1951x + 2.3552$ with a correlation coefficient (R^2) of 0.97.

4.3 DAMP uptake and pH determination using electron microscopy

de Duve *et al.* (1974) showed that weak bases, which become positively charged at acidic pH, become concentrated in lysosomes. Concentration occurs as these chemicals diffuse freely through hydrophobic membranes in their unprotonated state at neutral pH and become protonated at acidic pH in lysosomes and hence trapped there. Using this knowledge, Anderson *et al.* (1984) developed a weak base (2,4-dinitroanilino)-3'-amino-*N*-methyldipropylamine (DAMP), a basic congener of 2,4-dinitrophenyl (DNP), which allowed identification of acidic organelles under the electron microscope, using antibodies to DNP and immunolabelling.

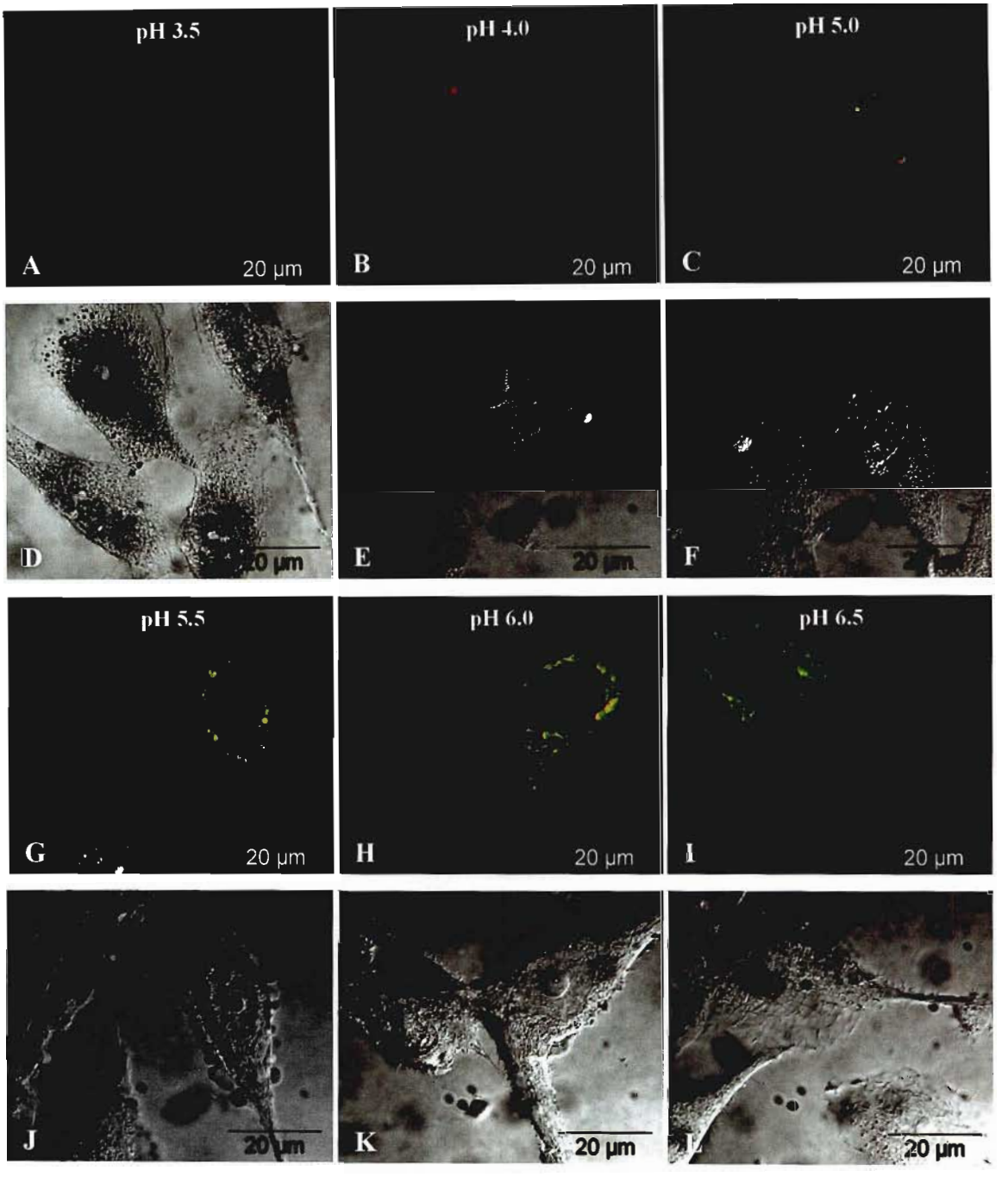
pH 3.5
A
20 µm
pH 4.0
B
20 µm
pH 5.0
C
20 µm
D
20 µm
E
20 µm
F
pH 5.5
G
20 µm
pH 6.0
H
20 µm
pH 6.5
I
20 µm
J
20 µm
K
20 µm
20 µm

Figure 4.4 **Oregon Green® dextran (OGD) uptake into MCF-10AneoT cells with calibration solution treatment to produce pH standards.**
Cells were incubated overnight in OGD, followed by incubation in calibration solutions of various pHs containing the K^+/H^+ ionophore nigericin to equilibrate the intracellular pH with that of the calibration solution. A,B,C,G,H,I are fluorescent composite images of the fluorescence produced by OGD at excitation 440 nm (red) emission 510 nm at which the fluorescence is pH independent and at excitation 490 nm (green) emission 510 nm at which the fluorescence is pH dependent. A,B,C,G,H,I thus show the fluorescence intensity and composite colour of OGD at pH 3.5 (A), pH 4.0 (B), pH 5.0 (C), pH 5.5 (G), pH 6.0 (H) and pH 6.5 (I). D,E,F,J,K,L are the corresponding DIC images (shown below their respective fluorescent images). DIC = differential interference contrast.

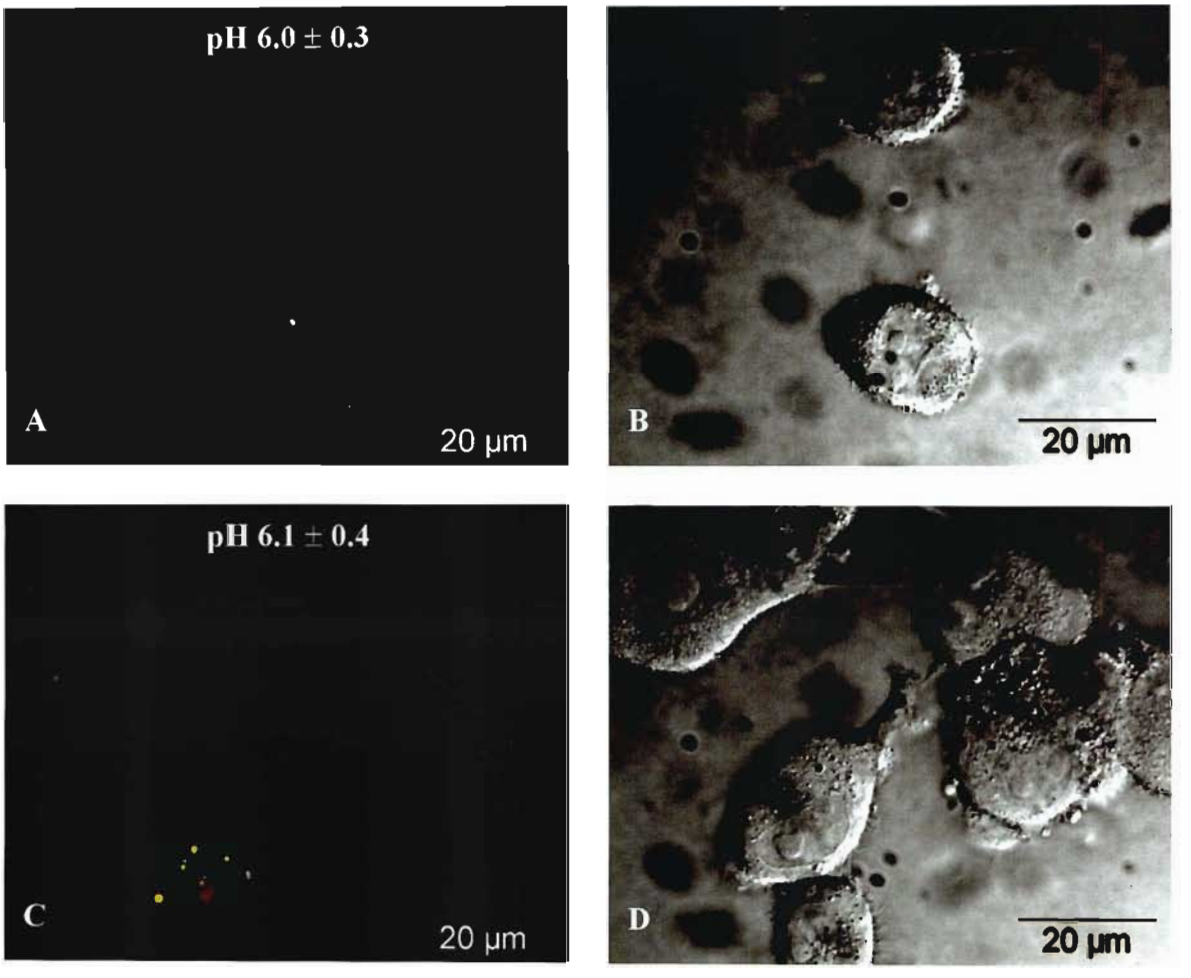
pH 6.0 ± 0.3
A
20 µm
B
20 µm
pH 6.1 ± 0.4
C
20 µm
D
20 µm

Figure 4.5 **Oregon Green® dextran (OGD) uptake into early endosomes of MCF-10A and MCF-10AneoT cells.**

A, and C are composite images of the fluorescence produced by OGD at excitation 440 nm (red) emission 510 nm where the fluorescence is pH independent and at excitation 490 nm (green) emission 510 nm where the fluorescence is pH dependent. B and D are the corresponding DIC images (shown to the right of their respective fluorescent images). A shows the fluorescence intensity and composite colour in MCF-10A cells after a 5 min pulse of OGD followed by a 5 min chase with fresh media. The average pH of early endosomes in the MCF-10A cell lines was found to be pH 6.0 ± 0.7 (n = 8). C shows the fluorescence intensity and composite colour in MCF-10AneoT cells after similar pulse-chase exposure. The average pH of early endosomes in the MCF-10AneoT cell lines was found to be pH 6.1 ± 0.4 (n = 13). n = the number of organelles used for pH determination in a minimum of 5 randomly selected cells. DIC = differential interference contrast.

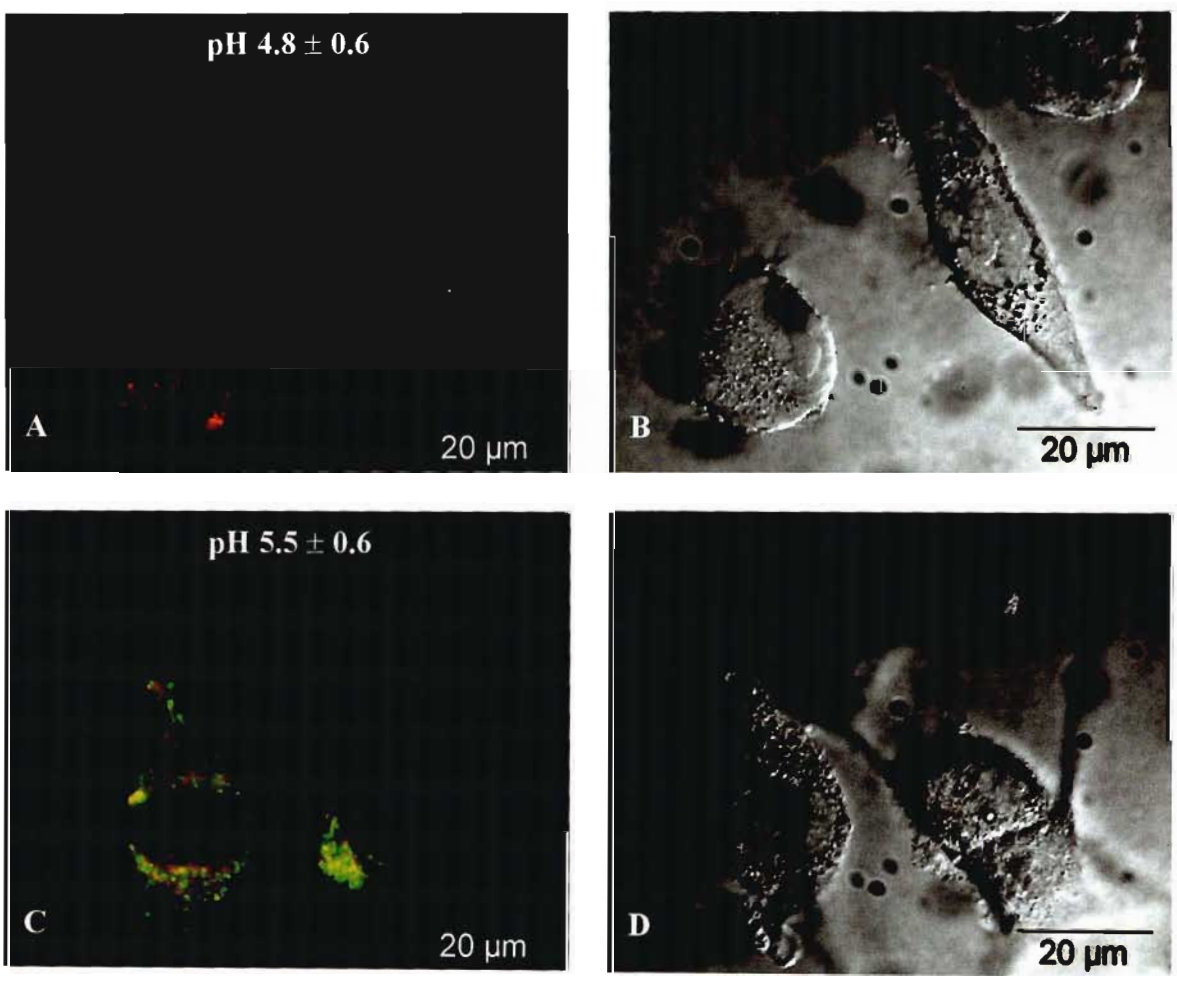
pH 4.8 ± 0.6
A
20 µm
B
20 µm
pH 5.5 ± 0.6
C
20 µm
D
20 µm

Figure 4.6 **Oregon Green® dextran (OGD) uptake into late endosomes/lysosomes of MCF-10A and MCF-10AneoT cells.**

A, and C are fluorescent composite images of the fluorescence produced by OGD at excitation 440 nm (red) emission 510 nm where the fluorescence is pH independent and at excitation 490 nm (green) emission 510 nm where the fluorescence is pH dependent. B and D are the corresponding DIC images (shown to the right of their respective fluorescent images). A shows the fluorescence intensity and composite colour in MCF-10A cells after a 1 hour pulse of OGD followed by an overnight chase with fresh media. The average pH of late endosomes/lysosomes in the MCF-10A cell lines was found to be pH 4.8 ± 0.6 (n = 95). C shows the fluorescence intensity and composite colour in MCF-10AneoT cells after similar pulse-chase exposure. The average pH of late endosomes/lysosomes in the MCF-10AneoT cell lines was found to be pH 5.5 ± 0.6 (n = 62). n = the number of organelles used for pH determination in a minimum of 5 randomly selected cells. DIC = differential interference contrast.

DAMP contains primary and tertiary amino groups that become protonated and positively charged at acidic pH, allowing the molecules to become trapped in acidic vesicles (Fig. 4.7). The primary amino group also enables DAMP molecules to be covalently linked to proteins by aldehyde fixatives, such as glutaraldehyde, allowing DAMP to be retained *in situ* after fixation (Anderson *et al.*, 1984; Anderson, 1989) so that the dinitroarene group (DNP) can be detected using anti-DNP antibodies. This allows DAMP localization, and thus the presence of acidic organelles, to be detected immunocytochemically.

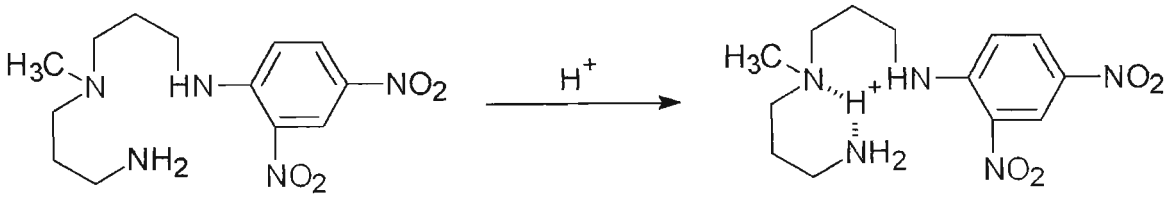

Figure 4.7 Structure of DAMP in its unprotonated (left) and protonated (right) forms.

DAMP may be used in fluorescent microscopy to mark acidic organelles at lower magnifications, when the secondary antibody is conjugated to an appropriate fluorochrome (e.g. Kataoka *et al.*, 1995). Using this system, the pH of labelled cells may be determined using fluorescent microscopy (e.g. Montcourrier *et al.*, 1994), spectrofluorometry (e.g. Millot *et al.*, 1997), flow cytometry (e.g. Li and Eastman, 1995), or a fluorescence-activated cell sorter (e.g. Barasch *et al.*, 1988). Using DAMP uptake and double immunolabelling techniques it is also possible to determine the co-localisation of antigens in acidic vesicles (e.g. Hanson *et al.*, 1997; Mwandumba *et al.*, 2004). Since DAMP relies on immunolabelling for the detection of acidic organelles, the technique can also be applied to EM, which provides the resolution required to distinguish organelles and their morphology. Using EM, DAMP can be exploited as an acidic organelle marker, in conjunction with any type of electron-dense diffuse staining (e.g. Polyak *et al.*, 1997) or punctate staining (labelling) using gold particles (e.g. Orci *et al.*, 1987) which allows the labelling to be quantified, thus enabling pH determination using EM (e.g. Hayashi *et al.*, 2002). To determine the pH of acidic vesicles, it is assumed that DAMP accumulation in these vesicles is directly proportional to the H^+ concentration and that aldehyde fixation quantitatively retains DAMP at its site of accumulation. Two important properties of DAMP support these assumptions: 1) titration experiments indicate that DAMP behaves as an amine, where protonation involves the interaction of a single proton with both the

primary and tertiary amine groups of one DAMP molecule, 2) fixation involves the cross-linking of the primary amine groups with proteins in the lumen of the acidic vesicle (Anderson *et al.*, 1984). The number of gold particles (representing anti-DNP antibodies binding to DAMP) per area (i.e. the labelling density) can be used to calculate pH according to the formula:

$$pH = 7.0 - \log (D_1/D_2)$$

where D_1 is the density of DAMP-specific gold particles in the compartment being analysed and D_2 is the density of gold particles in a neutral (pH 7.0) compartment such as the nucleus (Anderson and Orci, 1988). This EM method thus allows both pH determination and identification of the acidic organelles of the endosome-lysosome system (with the use of markers and morphology) to be performed simultaneously and was, therefore, chosen for the present study.

The DAMP system, however, has some shortcomings. The formula given for the estimation of pH is not appropriate for all circumstances, as DAMP may not always penetrate all organelles to the same extent, e.g. specific cisternae of the Golgi (Anderson and Pathak, 1985). Also, since DAMP, as well as other weak bases, cause swelling of acidic compartments, the size of the acidic compartment may appear larger than usual (Mallya *et al.*, 1992). DAMP molecules are fixed through cross-linking with nearby proteins: therefore, if the vesicles of interest contain few proteins, DAMP might not be fixed readily enough to keep it in place (Augenbraun *et al.*, 1990). Although thorough penetration of DAMP into tissue samples is problematic, the DAMP system is ideal for use in living cell culture systems (Anderson, 1989).

The DAMP immunolabelling system for pH determination requires a control to verify labelling specificity. The control consists of perturbation of the cellular pH with ionophores, weak bases, or pharmaceutical drugs and determining if this alters the labelling density observed in acidic organelles. The most common chemicals used as controls with DAMP uptake are monensin, ammonium chloride or chloroquine.

Monensin (Fig. 4.8) is a monovalent carboxylic ionophore, which is capable of carrying protons as well as being selective for Na>>K>Rb>Li>Cs ions (Pressman, 1976) and can

also induce an increase in cytosolic Ca^{2+} concentrations (Savina *et al.*, 2005). In animal cells it disrupts the movement of membrane vesicles from the Golgi apparatus to the plasma membrane and between the *medial* and *trans* Golgi. This is caused by disrupting the ion gradient required for the budding of vesicles from the Golgi apparatus (Griffiths *et al.*, 1983). The Golgi cisternae also swell and appear as large vacuoles (Tartakoff and Vassalli, 1978; Boss *et al.*, 1984). In cells treated with monensin, the secretion of soluble and plasma-membrane enzymes and proteins is blocked, and the growth hormone receptors and recycling of surface receptors for receptor-mediated endocytosis is also disrupted (Strous and Lodish, 1980; Basu *et al.*, 1981; Wang *et al.*, 2002; Veyrat-Durebex *et al.*, 2004; Mitchell *et al.*, 2004). Monensin also causes alkalinisation of lysosomes and endocytic vesicles (Maxfield, 1982; Yamashiro *et al.*, 1983), which can result in increased secretion of proteolytic enzymes (Achkar *et al.*, 1990). Recently, monensin has also been used to overcome drug resistance in human breast tumour cell lines (Shaik *et al.*, 2004) and to inhibit the proliferation of various cancer cell lines (Park *et al.*, 2002a,b; 2003a,b,c).

Ammonium chloride is a weak base that results in the alkalinisation of acidic vesicles (Johnson *et al.*, 1979; Galloway *et al.*, 1983) and vesicular swelling (Ohkuma and Poole, 1978; Busch *et al.*, 1994). The ammonium ion deprotonates to ammonia, which crosses the vesicle membrane and reassociates with an internal proton, causing an increase in pH (Fishkes and Rudnick, 1982) and inhibiting the action of enzymes with an acidic pKa (Decker *et al.*, 1985; Neumann *et al.*, 1993; Orci *et al.*, 1994). This alkalinisation of acidic organelles may also divert enzymes from a regulated to a constitutive secretory pathway, by preventing the newly synthesised enzymes from interacting with their sorting receptors during passage through the Golgi complex and thus defaulting to the constitutive pathway (Caplan *et al.*, 1987). Furthermore, ammonium chloride treatment inhibits the synthesis of mannose-6-phosphate (M-6-P) groups on lysosomal proenzymes and also inhibits MPR-dependent trafficking by preventing acidic pH-dependent dissociation of MPR/lysosomal enzyme complexes (Capony *et al.*, 1994; Isidoro *et al.*, 1997).

Chloroquine (Fig. 4.8) is also a weak base that enters the cell and acidic vesicles at a rapid rate through permeation and causes swelling and alkalinisation of acidic organelles, though its accumulation can be suppressed by monensin (van Bambeke *et al.*, 2004). It has been shown to stabilise lysosomal membranes while causing an increase in their luminal pH

(de Duve *et al.*, 1974). In addition, chloroquine decreases the secretion of enzymes whose action relies on the acidity of their secretory vesicles (Fuller *et al.*, 1995).

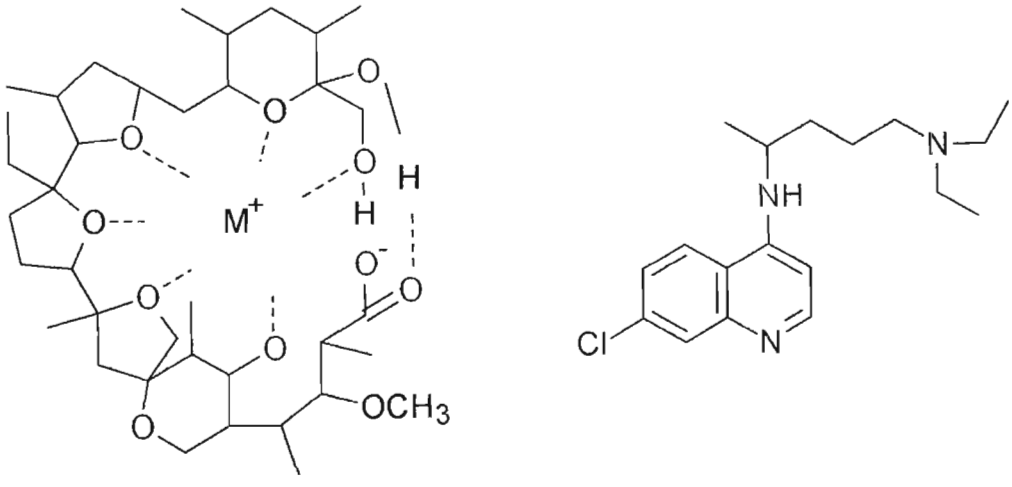

Monensin Chloroquine

Figure 4.8 Structure of the ionophore monensin and the weak base chloroquine.

All three of these pH perturbants have found a wide range of applications, particularly in studies of endocytic and secretory trafficking pathways. They are also usually included as controls when trying to determine the pH of acidic vesicles. Since the incubation times for these controls is very short (5 min), their effects on protein trafficking was anticipated to be negligible. Ammonium chloride was used in this study, as it was readily available and cheaper than either monensin or chloroquine. Fixation was also carried out directly after treatment to prevent too much distortion of ultrastructure.

The labelling densities of gold probes during immunolabelling have, at best, a maximum labelling efficiency (i.e. one gold probe per antigen) of 10% (Griffiths, 1993). Fixation between each labelling step during double immunolabelling (i.e. labelling for two antigens, in this case DNP to detect DAMP uptake and an organelle marker protein) potentially decreases the antigenicity of the section, and thus the detection of each subsequent antigen. Steric hindrance can also decrease labelling density, larger probes generally producing a lower labelling density. For all these reasons, triple labelling can be even more problematic, lowering the labelling density or possibly extinguishing labelling of certain antigens. Since lysosome-associated membrane protein-2 (LAMP-2) and cation-independent mannose-6-phosphate receptor (CI-MPR) are membrane proteins that have a

very low labelling density, even during single labelling, triple labelling for LAMP-2, CI-MPR and DNP to distinguish lysosomes (LAMP-2 positive, CI-MPR negative) from late endosomes (LAMP-2 positive, CI-MPR positive) was not considered.

From a review of the literature (Section 1.2), however, it was anticipated that early endosomes would have a diameter of 0.5-1.0 μm, a pH of 6.0-6.2 and be devoid of internal structure, late endosomes would contain an extensive internal morphology and have a pH of 4.0-5.0, and lysosomes would be distinctive organelles of approximately 0.5 μm and have a similar but possibly lower pH than the late endosome. It was, therefore, decided that labelling for DAMP (for acidity) and one other marker antigen (double immunolabelling) would allow satisfactory identification of all the major organelles in the endosome-lysosome pathway. The recycling endosomes and endosome carrier vesicles (ECVs) could, however, not be identified, even if double labelling for two of the currently selected markers [early endosome antigen 1 (EEA1), CI-MPR and LAMP-2] was to be performed. Late endosomes were thus classified as any organelle that was acidic, labelled for CI-MPR and had a complex internal morphology. Any acidic, small, electron-dense organelle that labelled for LAMP-2 was termed a lysosome. Early endosomes, it was anticipated, would be easily distinguishable, being the least acidic and the only organelles that label for EEA1.

4.3.1 Reagents

Reagents for cell culture as described in Section 2.9.1.

100 mM DAMP stock solution. DAMP (3.8 mg) was dissolved in sd.H_2O (100 μl) and stored at -20°C.

50 μM DAMP working solution. DAMP stock solution (25 μl) was added to DMEM:Ham's F-12 complete medium (50 ml).

100 mM NH_4Cl stock solution. NH_4Cl (1.6 mg) was dissolved in sd.H_2O (200 μl)

50 μM NH_4Cl working solution. NH_4Cl stock solution (25 μl) was added to DMEM:Ham's F-12 complete medium (50 ml).

Reagents for fixation and processing of cells as described in Section 2.10.1.

Reagents for LR White embedding as described in Section 2.11.1.

Reagents for preparation of formvar-coated nickel grids as described in Section 2.12.1.

Reagents for immunolabelling as described in Section 2.13.1.

Antibodies. Rabbit anti-DNP antibodies were used at 250 μg/ml, chicken anti-DNP antibodies and rabbit anti-IgY antibodies were used at 25 μg/ml, monoclonal mouse anti-EEA1 antibodies were used at 5 μg/ml, rabbit anti-CI-MPR antiserum was used at 1/40 dilution, rabbit anti-mouse antiserum was used at 1/200 dilution, mouse anti-LAMP-2 ascites fluid antibodies were used at 1/200 dilution. All antibody dilutions were made using either 1% (m/v) BSA-PBS or 1% (v/v) fish skin gelatin, 0.8% (m/v) BSA, 20 mM glycine in PBS (FBG) (Section 2.13.1).

Protein A-gold (PAG). 5 nm PAG was used at 1/300 dilution, 10 nm PAG was used at 1/300 dilution, dilutions being made in either 1% (m/v) BSA-PBS or FBG immediately before use.

4.3.2 Procedure

MCF-10A and MCF-10AneoT cells were seeded at a low density into 75 cm^2 flasks (Section 2.9.2). DAMP uptake was performed before cells reached approximately 80% confluence. Flasks were incubated with DAMP working solution (10 ml, 30 min, 37°C) and washed in fresh medium (2 x 5 min, 37°C). Control cells were further incubated with NH_4Cl working solution (10 ml, 5 min, 37°C). The cells were fixed, processed and embedded in LR White for electron microscopy as described in Section 2.10.2 and Section 2.11.2. LR White blocks were sectioned and retrieved onto formvar-coated nickel grids as described in Section 2.12.2.

Double immunolabelling for markers and DAMP was performed as described in Section 2.13.2. The EEA1, CI-MPR or LAMP-2 marker proteins are all membrane bound and, therefore, immunolabelling for these, using the smaller 5 nm PAG probe, was performed first. The smaller probe would enhance their low labelling density and prevent possible steric hindrance effects, which would be marked should a large probe and labelling for DAMP be performed first. This was followed by immunolabelling for the presence of DAMP using either rabbit or chicken IgY anti-DNP antibodies and a 10 nm PAG. The immunolabelling was optimised, and the optimised antibody concentrations and labelling protocols were used for labelling of both MCF-10A and MCF-10AneoT cell lines simultaneously, so that similar labelling conditions for both cell lines would allow comparison of results.

Labelling was first performed using BSA-PBS (Section 2.13.2, steps 1-7). High levels of background, however, were subsequently eliminated using the superior blocking agent FBG instead of BSA-PBS.

To avoid any misclassification of organelles, a strictly defined set of populations was sampled for pH determination. Only organelles that labelled positively for their respective markers: EEA1 for the early endosome, CI-MPR for the late endosome, and LAMP-2 for the lysosome were considered for pH determination. Since LAMP-2 labels both the late endosome and lysosome, only acidic small electron-dense organelles that labelled for LAMP-2 were considered to be lysosomes, according to the definition of Holtzman (1989).

After photographing various random sections of labelled grids at 20 500x to 32 000x magnification, the photographs were scanned into a digital (JPEG) format. The surface areas of the early endosome (electron-translucent, EEA1 positive organelle), late endosome (CI-MPR positive organelle with some internal morphology) and lysosome (LAMP-2 positive, small electron-dense organelle) were determined using the AnalySIS® software imaging system. DNP labelling on a minimum of five randomly selected organelles of each organelle type was used for statistical analysis. By counting the number of gold probes per organelle and calculating labelling density, i.e. the number of gold probes per μm^2, the pH was determined according to the formula:

$$pH = 7.0 - \log (D_1/D_2)$$

where 7.0 is the pH at neutrality, D_1 is the density of DAMP-specific gold particles in the compartment being analysed and D_2 is the density of gold particles in a neutral (pH 7.0) compartment, i.e. the pH of each organelle was determined relative to that of the cell's nucleus (Anderson and Orci, 1988). The calculated pH values of at least five random sections containing such organelles were averaged to provide an overall pH value for a specific type of organelle (early endosome, late endosome or lysosome). In order to provide some indication of the labelling densities for each type of organelle, these values were also averaged. Standard deviation from the mean was determined for the average labelling densities and calculated pH values. The pH values obtained were also subjected to one-tailed student's t-test analysis, in order to determine if the differences in pH between organelles and cell lines was >95% significant.

Since all cells have small pH fluctuations (0.1-0.3 pH units) depending on the stage of the cell cycle (Madhaus, 1988), it was anticipated that the labelling density of the acidic organelles would, when averaged, show a larger standard deviation than would be reflected in the pH values obtained, due to the method by which the pH values were calculated.

4.3.3 Results

Optimal labelling for DAMP uptake into acidic organelles was found to require the use of 25 μg/ml chicken anti-DNP IgY and 250 μg/ml rabbit anti-DNP. The ten-fold increase in antibody concentration necessary for optimal labelling using the rabbit antibodies possibly indicates the low affinity of the antibody for DNP. For labelling using the rabbit anti-DNP antibodies, therefore, a superior blocking agent (FBG) was required to decrease background labelling, especially in the nucleus. Such a high background labelling may be caused by protein-protein interactions [due to the use of high concentrations (>100 μg/ml) of antibodies] and could potentially influence the pH values determined. The use of FBG instead of BSA-PBS as blocking agent decreased the rabbit anti-DNP background labelling density of the nucleus from 9.8 ± 3.6 gold probes/μm^2 (n = 10) to 4.4 ± 0.5 gold probes/μm^2 (n = 16) in MCF-10A cells, and 5.3 ± 0.5 gold probes/μm^2 (n = 10) to 2.0 ± 0.8 gold probes/μm^2 (n = 20) in MCF-10AneoT cells, where n = the number of

organelles used. In order to produce more comparable results, FBG was also used as a blocking agent in DAMP labelling procedures using IgY anti-DNP antibodies.

Labelling for EEA1 in both MCF-10A and MCF-10AneoT (Fig. 4.9, arrows) shows that the early endosomes are electron-translucent, and contain few DNP groups (Fig. 4.9, arrowheads), indicating their mild acidity. As anticipated, EEA1 labelling (Fig. 4.9, arrows) is localised to the outer membrane of the early endosome. The organelles labelling for EEA1 in the MCF-10A (Fig. 4.9A and B) and MCF-10AneoT (Fig. 4.9C and D) appeared morphologically similar, although the relative size of these organelles was not statistically determined, as serial sectioning and stereography was not performed. These organelles do, however, appear to be smaller than the 0.5-1.0 μm diameter reported in the literature (Yamashiro *et al.*, 1984; Salzman and Maxfield, 1988), with diameters of approximately 0.2-0.6 μm. Fig. 4.9A shows three electron-translucent vesicles labelling for EEA1 (early endosomes), one of which did not label for DAMP (Fig. 4.9A, left), and also a small electron-dense organelle which did not label for EEA1 but contains a fairly high labelling density for DAMP (Fig. 4.9A, arrowheads, lower left). This latter organelle can be characterised as a small, acidic, electron-dense organelle and is, therefore, most likely a lysosome. The diameter of this organelle is smaller than the reported 0.5 μm (Holtzmann, 1989), though it is similar in diameter and morphology to other lysosomes of both the MCF-10A and MCF-10AneoT cell lines (Fig. 4.11).

The presence of the marker CI-MPR (Fig. 4.10, arrows) is used to distinguish the late endosome from other organelles in both MCF-10A (Fig. 4.10A and B) and MCF-10AneoT cells (Fig. 4.10C and D). Late endosomes, identified by the CI-MPR marker in MCF-10A cells, show that these organelles contain large amounts of DAMP labelling (Fig. 4.10A and B, arrowheads) and have a distinct internal membranous morphology. This multilamellar morphology was largely disrupted in the MCF-10AneoT cells (Fig. 4.10C and D). The diameter of the late endosome was approximately 0.3-0.6 μm in the MCF-10A cell line and 0.3-0.7 μm in the MCF-10AneoT cell line. This range of diameters was smaller than the 0.5-0.8 μm reported in the literature (Griffiths, 1996; Gruenberg *et al.*, 1989; Hopkins, 1981). Other acidic organelles that did not label for CI-MPR, but due to their multilamellar or multivesicular morphology could possibly be late endosomes or endosome carrier vesicles (ECVs) are found in both the MCF-10A (Fig. 4.10B, centre top) and

MCF-10AneoT cell lines (Fig. 4.10C, centre top). These organelles were not, however, used for pH calculations, as their identity was not confirmed by the presence of the CI-MPR marker.

Since both the late endosome and lysosome (but not ECVs) label for LAMP-2 (Fig. 4.11, arrows), labelling for LAMP-2 in conjunction with the morphological features of the organelle was used to distinguish the lysosome (lysosomes being defined as small electron-dense organelles). These lysosomes also have a high labelling density for DAMP (Fig. 4.11, arrowheads), indicating their low pH. The late endosomes in both the MCF-10A and MCF-10AneoT cells, while labelling for LAMP-2 (Fig. 4.11A and C, arrows) and DAMP (Fig. 4.11A and C, arrowheads) are larger and more electron-translucent than the lysosomes and are, therefore, easily distinguished (Fig. 4.11A, lower left and Fig. 4.11C, centre). The lysosomes of the MCF-10AneoT cell line also appear to be situated closer to the cell surface, i.e. more peripherally located (Fig. 4.11C and D).

Despite repeated optimisation of procedures, comparison of the labelling densities using rabbit and chicken antibodies (Table 4.1), show that the rabbit antibodies produce a higher labelling density on the nucleus. This labelling density has a larger standard deviation, and combined with the generally lower labelling density on other organelles, indicates that despite the use of a superior blocking agent these antibodies still produce high non-specific labelling. The pH values calculated from such results could, therefore, be less accurate than those giving a lower background and higher specific labelling density, i.e. than the values calculated using the chicken anti-DNP IgY. The pH values calculated using rabbit anti-DNP do, however, show that the different types of organelles investigated become more acidic from early endosome to late endosome to lysosome for both cell types (Table 4.1).

The pH of the early endosome, late endosome and lysosome of MCF-10A and MCF-10AneoT cell lines, determined from the DNP labelling density using both rabbit and chicken anti-DNP antibodies, showed similar trends. The pH of the late endosome of MCF-10AneoT cells differed most from that of the MCF-10A cell line, with the chicken antibodies giving a 0.7 pH unit increase, while the rabbit antibodies reveal a small 0.3 pH unit increase (Table 4.1). The chicken antibodies, however, also revealed a 0.6 pH unit increase in the pH of the lysosome of the MCF-10AneoT cell line (Table 4.1). This was

not evident using the rabbit antibodies, possibly due to the large standard deviation caused by the high background labelling associated with the use of the rabbit anti-DNP antibody. The results obtained with the chicken anti-DNP IgY, therefore, show that, while the pH values of the early endosome remained similar in both cell lines, the pH of both the late endosome and lysosome increased in the *ras*-transfected MCF-10AneoT cell line relative to the "normal" MCF-10A cell line. Furthermore, a one-tailed student's *t*-test performed on these pH values determined that differences between the values obtained were significant within a confidence interval of 95%. The difference in pH between the late endosome and lysosome in either of the cell lines, using either the rabbit or chicken antibodies (Table 4.1), was found to be not significant in a one-tailed student's *t*-test, i.e. the late endosome and lysosome have a similar pH in either cell line. Combined late endosome and lysosome average labelling density and pH values are also indicated in Table 4.1 to allow easier comparison of DAMP EM results with those obtained using OGD and fluorescent microscopy. The labelling density of the nucleus was also found to be significantly different between the MCF-10A and MCF-10AneoT cell lines (using the one-tailed student's *t*-test within a confidence interval of 95%), possibly indicating that the nucleus and, therefore, the cytosol of the MCF-10AneoT cell line is more alkaline.

4.4 Discussion

Besides the work of Sloane *et al.* (1994b), which showed overall alkalinisation of MCF-10A cells after *ras*-transfection, it has been previously reported that the lysosomes of *ras*-transfected fibroblasts have a more alkaline pH than those of non-transfected cell lines (Jiang *et al.*, 1990). These studies used FITC-dextran pulse-chased into cells for 18–24 h. With prolonged incubations, however, it has been shown that endocytosed materials distribute equally between late endosomes and lysosomes (Griffiths *et al.*, 1990a). The results obtained by Jiang *et al.* (1990) may, therefore, reflect a pH increase in both the late endosome and lysosome. Such results agree with those obtained in the present study using OGD, which shows alkalinisation of the late endosome/lysosome in MCF-10AneoT cells (pH 5.5 ± 0.6) when compared to those of the MCF-10A cell line (pH 4.8 ± 0.6). The pH of early endosomes, however, is similar in both cell lines (MCF-10A pH 6.0 ± 0.7; MCF-10AneoT pH 6.1 ± 0.4).

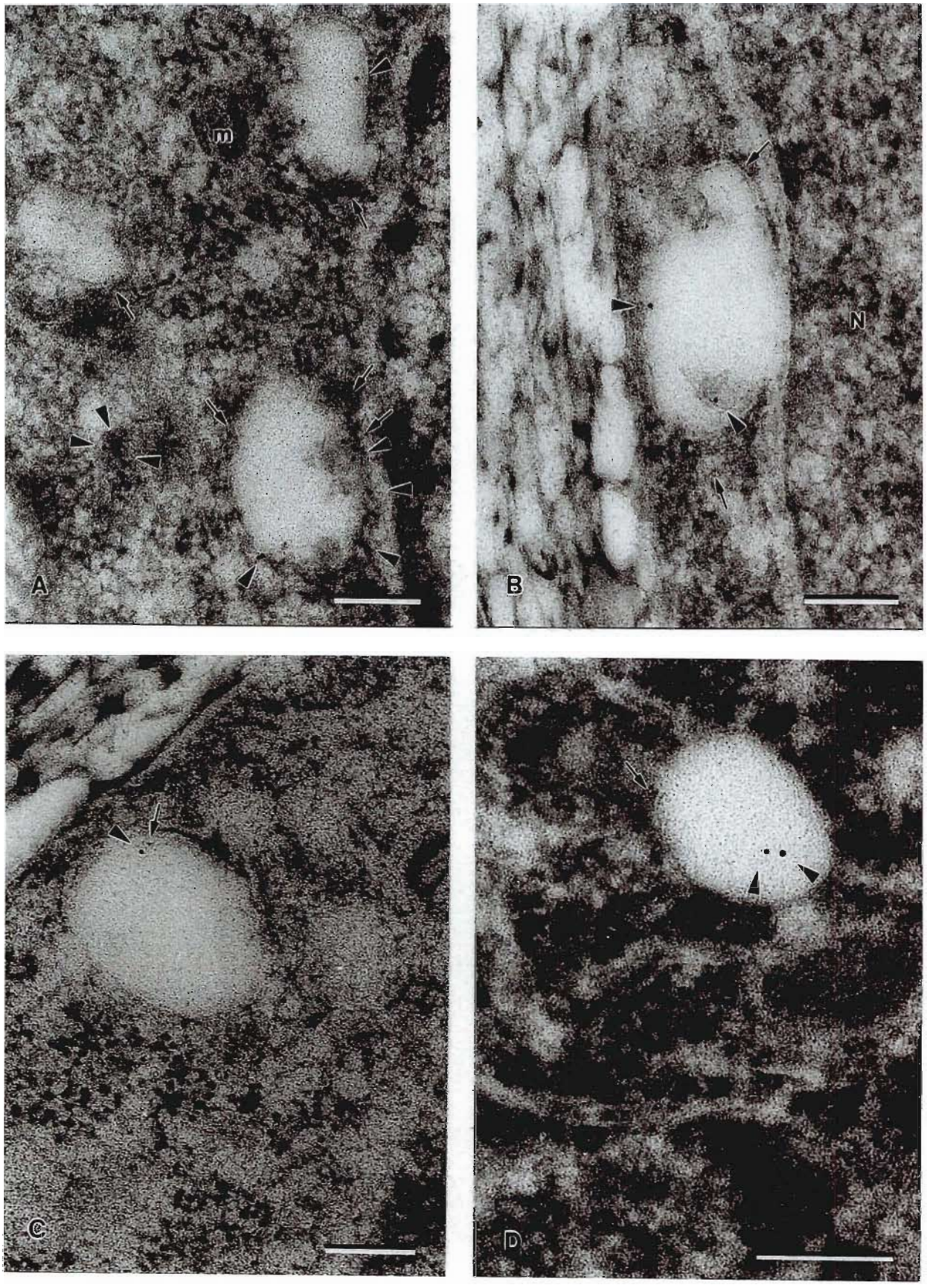
m
A
N
B
C
D

Figure 4.9 **Immunolabelling for DAMP and EEA1 in early endosomes of MCF-10A and MCF-10AneoT cell lines.**
Arrowheads indicate labelling for DAMP (10 nm) while arrows indicate labelling for EEA1 (5 nm). A and B show early endosomes of the MCF-10A cell line. C and D show early endosomes of the MCF-10AneoT cell line. The presence of DAMP is detected using rabbit anti-DNP (A and C) and chicken anti-DNP IgY (B and D). m = mitochondria; N = nucleus; bar = 200 nm.

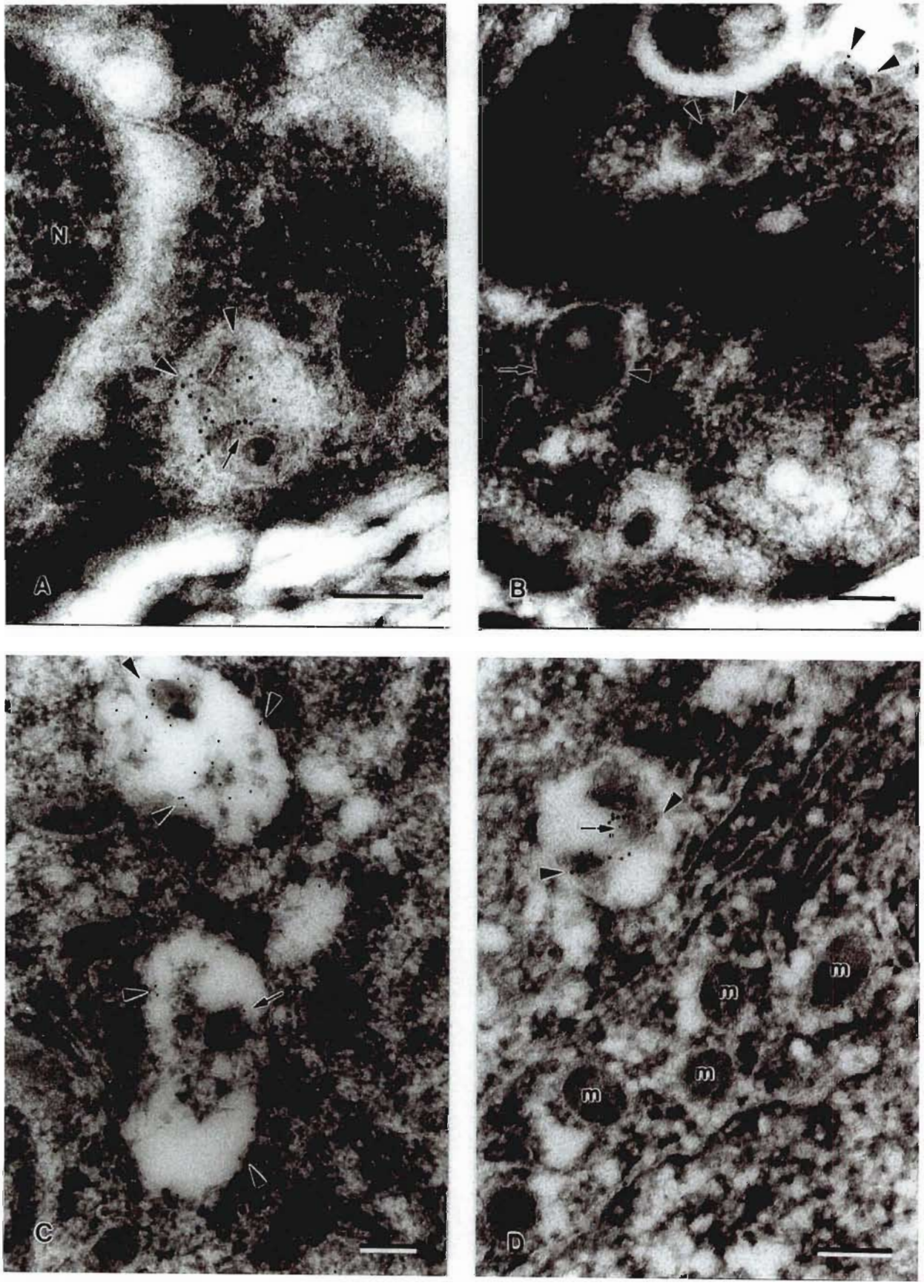
N
A
B
C
D
m
m
m
m

Figure 4.10 **Immunolabelling for DAMP and CI-MPR in late endosomes of MCF-10A and MCF-10AneoT cell lines.**
Arrowheads indicate labelling for DAMP (10 nm) while arrows indicate labelling for CI-MPR (5 nm). A and B show late endosomes of the MCF-10A cell line. C and D show late endosomes of the MCF-10AneoT cell line. The presence of DAMP is detected using rabbit anti-DNP (A and C) and chicken anti-DNP IgY (B and D). m = mitochondria; N = nucleus; bar = 200 nm.

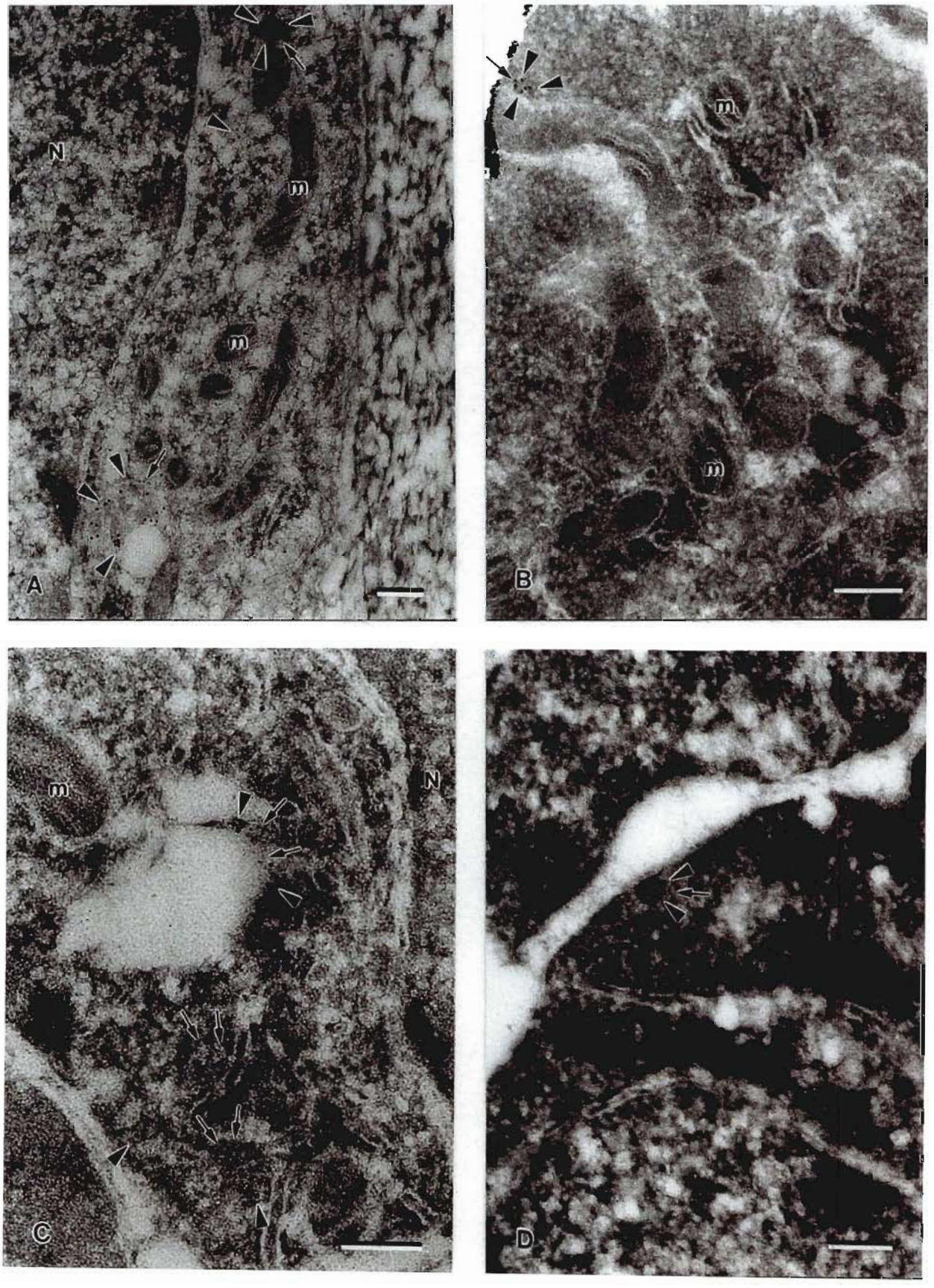
N
m
m
A
m
m
B
m
N
C
D

Figure 4.11 **Immunolabelling for DAMP and LAMP-2 in lysosomes of MCF-10A and MCF-10AneoT cell lines.**
Arrowheads indicate labelling for DAMP (10 nm) while arrows indicate labelling for LAMP-2 (5 nm). A and B show lysosomes, defined as small electron-dense organelles which are acidic and label for LAMP-2, of the MCF-10A cell line. C and D show lysosomes of the MCF-10AneoT cell line. The presence of DAMP is detected using rabbit anti-DNP (A and C) and chicken anti-DNP IgY (B and D). m = mitochondria; N = nucleus; bar = 200 nm.

Table 4.1 **pH values of the early endosome, late endosome and lysosome of the MCF-10A and MCF-10AneoT cell lines determined using rabbit and chicken anti-DNP-antibodies.**

	MCF-10A					
	Rabbit anti-DNP IgG			Chicken anti-DNP IgY		
	n	D	pH	n	D	pH
EE	5	26.8 ± 6.7	6.2 ± 0.1	6	15.1 ± 4.8	6.0 ± 0.2
LE	5	161.6 ± 22.4	5.4 ± 0.1	8	227.7 ± 19.3	4.5 ± 0.2
Lys	6	159.7 ± 135.0	5.4 ± 0.6	5	240.0 ± 54.8	4.4 ± 0.1
LE+Lys	11	160.5 ± 96.5	5.4 ± 0.4	13	232.4 ± 71.5	4.5 ± 0.2
nuc	16	4.4 ± 0.5		19	1.5 ± 0.1	
	MCF-10AneoT					
	Rabbit anti-DNP IgG			Chicken anti-DNP IgY		
	n	D	pH	n	D	pH
EE	5	24.8 ± 8.8	6.3 ± 0.2	6	13.7 ± 4.8	6.0 ± 0.2
LE	7	39.3 ± 6.9	5.7 ± 0.1	7	78.9 ± 12.8	5.2 ± 0.1
Lys	8	102.5 ± 61.9	5.4 ± 0.3	8	150.0 ± 70.7	5.0 ± 0.3
LE+Lys	15	73 ± 54.7	5.6 ± 0.3	15	126.3 ± 66.7	5.1 ± 0.3
nuc	20	2.0 ± 0.8		21	1.2 ± 0.1	

Abbreviations: EE = early endosome; LE = late endosome; Lys = lysosome; nuc = nucleus; n = number of organelles; D = labelling density in gold probes/μm^2.

The pH of the early endosome established by both OGD and DAMP uptake experiments appears to agree with the pH 6.0-6.2 range previously reported in the literature (Maxfield and Yamashiro, 1991). The literature also indicates that the pH of both the late endosome and lysosome fall between pH 4.0-5.0, with the lysosome generally having a pH slightly lower than the late endosome (Kornfeld and Mellman, 1989). With the DAMP system and using the chicken antibodies in the non-transfected cell line (MCF-10A), the pH values of the late endosome and lysosome fall within the normal range (pH 4.0-5.0) and are similar to each other. That the late endosome and lysosome may have similar pH values has been confirmed in recent reviews (Gruenberg, 2001) and may be attributed to the mixing of their fluid-phase contents, due to direct transient fusion processes (Mullock *et al.*, 1998; Bright *et al.*, 2005) equalising any differences in pH. Nevertheless, the chicken antibodies show that the lysosome has at least a 0.1 pH unit decrease in pH from the late endosome, in both

the transfected and non-transfected cell lines, whereas this was evident only in the *ras*-transfected cell line when rabbit antibodies are used. The reliability of the results obtained using either antibody is not easily assessed when considering the overlapping pH values recorded in the literature, and the similarity in pH values determined, in this study, for these organelles.

The results of the present DAMP study, using chicken antibodies, indicate that there is a significant increase in the pH of the late endosome (± 0.7 pH units) and lysosome (± 0.6 pH units) in the *ras*-transfected MCF-10AneoT cell line compared to the MCF-10A cell line, which are similar to the results obtained using OGD (± 0.7 pH unit increase). The combined pH values obtained for the late endosome/lysosome using DAMP uptake and labelling with chicken anti-DNP IgY (MCF-10A pH 4.5 ±0.2; MCF-10AneoT pH 5.1 ± 0.3) are, however, lower than those obtained using OGD uptake (MCF-10A pH 4.8 ± 0.6; MCF-10AneoT pH 5.5 ± 0.6), although they still fall with the standard deviation of the pH values obtained using OGD uptake. Results obtained using the rabbit anti-DNP antibodies, however, show that only the late endosome is slightly more alkaline (± 0.3 units) in the *ras*-transfected cell line, which does not agree with the results obtained using OGD uptake. The combined pH values for the late endosome/lysosome using rabbit anti-DNP IgG (MCF-10A pH 5.4 ± 0.4; MCF-10AneoT pH 5.6 ± 0.3) do not indicate that alkalinisation has occurred in the MCF-10AneoT cell line, in contrast to the results obtained from both OGD uptake and those from labelling with chicken antibodies. This discrepancy in pH values is most likely due to higher non-specific labelling obtained using the rabbit anti-DNP, which would influence the pH values determined using these antibodies.

High background labelling (non-specific labelling) may also increase the labelling density on the nucleus (and thus the labelling density assumed to be equivalent to pH 7.0). Since the nucleus generally has the lowest labelling density and is a relatively large organelle, any non-specific labelling may increase the apparent labelling on the nucleus disproportionately to the labelling densities on other organelles, so the pH determined for acidic organelles may be more alkaline than their actual pH. This seems to be the case for pH values obtained with the rabbit antibodies. The formula for pH calculation assumes that the background labelling is uniformly distributed, and that using a ratio of labelling

densities may compensate for such background. Unfortunately, this is often not the case, since certain cellular proteins may attract more non-specific labelling than others. Antibodies of low specificity (i.e. the rabbit anti-DNP antibodies) may, therefore, give unreliable results. The results obtained using chicken anti-DNP IgY were thus considered more reliable than those using the rabbit anti-DNP antibodies, therefore, as they produced less background and required lower antibody concentrations for optimal labelling, indicating that they were of higher titre and possibly higher specificity than the rabbit antibodies.

Immunolabelling with chicken anti-DNP IgY antibodies, on the other hand, required the use of a secondary antibody. This usually provides an amplification effect that, it could be argued, may affect the pH values determined. Despite using a ratio of labelling densities in the pH determination formula, which should cancel out any amplification effects (provided steric hindrance is not a factor in labelling of organelles and that the labelling is specific), results may have been slightly affected, since the pH determined using the chicken antibodies is slightly lower than the pH determined using OGD uptake. The combined pH of the late endosome and lysosome (using DAMP), however, fall within the standard deviation of the pH of the late endosome/lysosome (using OGD).

The slightly lower pH values obtained using DAMP and anti-DNP IgY (when compared to OGD pH values) may also be due to the assumption that the pH of the nucleus, used as the reference organelle, is neutral (pH 7.0). Sloane *et al.* (1994b), however, indicated that the cytosol is alkalinised in *ras*-transfected MCF-10AneoT cells. This cytosolic alkalinisation after *ras*-transfection has also been observed in other cell lines (Ostad *et al.*, 1996; Arends *et al.*, 1994; Ritter *et al.*, 1992). The pH of the nucleus may similarly be more alkaline, as the nucleus is accessible to the cytoplasm via the nuclear pores. If the labelling density for the nucleus is consequently lower than that assumed to be equivalent to pH 7.0, this may affect the pH values determined for all organelles and the actual pH of acidic organelles in the MCF-10AneoT cell line may actually be more alkaline than reflected in the calculated pH. This may explain the slight discrepancy in pH observed using DAMP uptake and labelling with anti-DNP IgY, compared to OGD uptake.

Based on the results obtained using OGD uptake and DAMP uptake with labelling using chicken anti-DNP antibodies, it is concluded that the organelles of the MCF-10A cell line,

after transfection with the c-Ha-*ras* oncogene, become more alkaline and that this alkalinisation affects late endosomes and lysosomes most.

There are a number of ways that mutationally activated Ras may effect the alkalinisation of the endosome-lysosome system. Recruitment of the GDP/GTP exchange factor ADP-ribosylation factor nucleotide binding site opener (ARNO) and Arf6 to endosomal membranes is dependent on luminal acidification by V-ATPases, an early step in vesicle trafficking regulation (Maranda *et al.*, 2001; Sun-Wada *et al.*, 2004). The activity of Arf fusion proteins are controlled by the protein products of the activated *ras* oncogene, as are the movements of vesicles via effects on Rho and other Ras subfamily proteins downstream of Ras in the Ras signal transduction pathway (Section 1.1.1). Any change in the activity of such intermediates may result in altered trafficking of the V-ATPases responsible for acidification, causing overall alkalinisation of the organelles of the endosome-lysosome system. Ras may also have an effect on the alkalinity of such vesicles via its effect on Rac1 and its signalling pathway, which are activated by mSOS-1 interaction with the E subunit of V-ATPases (Miura *et al.*, 2001). All such effects on vesicular trafficking and endosome-lysosome pH may cause alteration of processing and trafficking of lysosomal proteases and facilitate the acquisition of the invasive phenotype. The phenotypic change to a more fibroblast-like, chemotactically responsive cell type (Kinch *et al.*, 1995), as seen to accompany *ras*-transfection of the MCF-10A cell line (Basolo *et al.*, 1991), may similarly be directly due to *ras*-transfection, and the effects of the mutated gene product on Rac and Rho (Section 1.1.1).

Studies in yeast have indicated that reversible dissociation of the V_1 and V_0 domains represents an important mechanism for directly controlling V-ATPase activity, since glucose deprivation causes a rapid dissociation of V-ATPases from approximately 80% assembled to approximately 20% assembled. This process is reversible and independent of new protein synthesis (Kane, 1995). There is also evidence that this occurs in mammalian cells, and that the effect of glucose is mediated by PI(3)K, a downstream product of Ras (Myers and Forgac, 1993; Sautin *et al.*, 2005). As mentioned in Section 1.1.1, Ras may also regulate Tc10 (a Rho protein responsible for GLUT4 translocation and glucose transport). This intermediate may, therefore, be important in controlling the pH of the endosome-lysosome system by controlling the amount of glucose available to the cell.

Since the intracellular V-ATPases are electrogenic, vacuolar acidification could also be controlled, not by alteration of trafficking of the various pumps, but through the regulation of counterion conductance, which occurs through the action of a parallel Cl^- channel. This Cl^- channel has been shown to be regulated by PKA-dependent phosphorylation (Bae and Verkman, 1990; Mulberg *et al.*, 1991; Forgac 1998). Since Ras may indirectly control PKA activity, this suggests that these channels may represent an important control point for endosomal and lysosomal pH regulation.

The work reported in this chapter has provided evidence that *ras*-transfection may cause alkalinisation of the cytosol, and almost certainly causes alkalinisation of late endosomes and lysosomes in MCF-10AneoT cells compared to the "normal" MCF-10A cell line. Such alkalinisation of the endosome-lysosome system may be influenced by a number of factors that regulate intracellular pH. Alteration of endosome-lysosome pH may decrease the efficiency of processing of lysosomal enzymes, and their efficiency of dissociation from receptors (as described in Chapter 1), resulting in the altered trafficking of lysosomal enzymes. As mentioned in Section 1.1.1, the effects of mutationally activated Ras on Rac and Rho, and cytosolic alkalinisation, may also affect the cytoskeleton and cytoskeleton-regulated vesicular trafficking. The fusogenicity of various organelles, their shape and microtubule and cytoskeleton-regulated position in the cell may also be affected. Due to the potential effect of activated Ras on fusion factors (e.g. Arfs and Rabs) and on the structure and size of organelles, it is important to establish the identity of the various organelles using reliable markers, morphology and pH. The identity and nature of the peripheral organelles are especially important, since their appearance seems to be associated with progression to the malignant phenotype (as can be seen with the OGD uptake studies where the MCF-10AneoT cells contain a greater number of peripherally located acidic organelles than the MCF-10A cells). The morphology of cells may be affected by the presence of weak bases, such as DAMP, that upon prolonged incubation may cause vesicle swelling and distortion (Mallya *et al.*, 1992) as well as the uncoupling of membrane recycling processes. For this reason it was important to repeat studies without the inclusion of DAMP, in order to confirm the identity, position and morphological features of the organelles of the endosome-lysosome system in the absence of any interfering chemicals. The following chapter, therefore, takes a closer look at the morphology of the endosomal and lysosomal organelles, and the effects of *ras*-transfection on their localisation within the cell.

CHAPTER 5

CONFIRMATION OF IDENTITY, LOCALISATION AND MORPHOLOGY OF ORGANELLES OF THE ENDOSOME-LYSOSOME SYSTEM

5.1 Introduction

It became evident during the pH studies (Chapter 4) that improved ultrastructural preservation was required, since cells that had undergone (2,4-dinitroanilino)-3'-amino-*N*-methyldipropylamine (DAMP) treatment displayed disrupted internal morphology in many organelles, possibly caused by extraction of internal membranes and vesicular swelling, one of the disadvantages of the DAMP system (Mallya *et al.*, 1992). An improved buffering system (Santama *et al.*, 1998) was, therefore, used to confirm the identity, localisation and morphology of the organelles of the endosome-lysosome system in both MCF-10A and MCF-10AneoT cell lines.

In the pH studies reported in Chapter 4, many of the organelles with a multilamellar morphology (and thus, purportedly, late endosomes) did not label for the cation-independent mannose-6-phosphate receptor (CI-MPR), generally associated with the late endosome. DAMP molecules may have masked or distorted epitopes due to their high concentration in acidic late endosomes, thus affecting the recognition of such antigens during immunolabelling procedures. Furthermore, since DAMP is a weak base it may have affected the trafficking of receptors to the late endosome, thereby contributing to the low labelling density seen for CI-MPR. It was, therefore, considered prudent to repeat all the marker labelling experiments, including labelling for CI-MPR, in the absence of DAMP. This had the following advantages: 1) double labelling for two markers could be performed to confirm that CI-MPR and/or lysosome-associated membrane protein-2 (LAMP-2) do not co-localise with early endosome antigen 1 (EEA1) in the early endosome, that CI-MPR co-localises with LAMP-2 in the late endosome, that EEA1 is not present in the late endosome, and that neither EEA1 or CI-MPR is present in the lysosome which labels for LAMP-2, 2) the internal morphology of organelles and their localisation in the cell could be better determined, without the interfering influence of DAMP, using a technique that improves preservation of ultrastructure.

As mentioned in Section 1.1.1, Ras family proteins (Rac and Rho) may affect cytoskeletal elements and thus influence vesicle trafficking, location and endosome-lysosome fusion (Bretscher, 1993; Hall, 1994; Sahai and Marshall, 2002). It is also vital for the movements of vesicles containing newly synthesised proteolytic enzymes from the *trans* Golgi network (TGN) to elements of the endocytic system. The activity of many elements of the cytoskeletal system is also pH dependent (e.g. microtubule depolymerisation) (Heuser, 1989). In order to explain the possible effects of *ras*-transfection and altered pH on the cytoskeleton in the *ras*-transfected MCF-10AneoT cell line, the role of the cytoskeletal elements involved in endosome-lysosome trafficking are reviewed below.

5.1.3 The role of microtubules and actin in endocytosis and secretion

In mammalian cells, endocytosis is responsible for the uptake of essential nutrients from the external environment and the retrieval of secreted proteins and lipids (Mellman, 1996). After internalisation, efficient sorting of endocytosed proteins and lipids for degradation or recycling to the plasma membrane is required. The actin and microtubule cytoskeletal networks mediate both the generation and the movement of vesicular carriers containing endocytosed material, as well as maintenance of the characteristic spatial distribution and morphology of endocytic organelles within the cell. There is, therefore, a link between the membrane targeting, docking and fusion machinery and the machinery that governs organelle movement and position (Mellman, 1996; Murray and Wolkoff, 2003).

Microtubules determine the distribution of the endoplasmic reticulum (ER) and Golgi and facilitate vesicle transport along the secretory pathway (Lippincott-Schwartz, 1998). In the endocytic pathway, association of organelles with microtubules and microtubule-associated proteins (MAPs) is necessary for the proper positioning of late endosomes and lysosomes (Matteoni and Kreis, 1987; Gruenberg *et al.*, 1989; McGraw *et al.*, 1993). Efficient transport of cargo between early and late endosomes is dependent on the MAP dynein, which moves the organelles in the minus direction toward the interior of the cell (Aniento *et al.*, 1993). The rate of endocytosis, and the morphology and motility of early endosomes on microtubules is regulated by Rab5 (also responsible for early endosome homotypic and heterotypic fusion) (Bucci *et al.*, 1992; D'Arrigo *et al.*, 1997; Nielson *et al.*, 1999). Rab5, in turn, is regulated by upstream factors, including phosphatidylinositol

3-kinase [PI(3)K], Akt and Ras (Li *et al.*, 1995; 1997; Barbier *et al.*, 1998; Simonsen *et al.*, 1998), which thus regulate early endosome fusion processes.

The mitogen activated protein kinase (MAPK) or extracellular signal-related kinase (ERK) is involved in the transmission of signals between the plasma membrane receptors and the nucleus. MAPK has been shown to phosphorylate and regulate cytoskeletal components such as MAP2, MAP4 and caldesmon (Ray and Sturgill, 1987; Hoshi *et al.*, 1992; Childs *et al.*, 1992; Drechsel *et al.*, 1992). MAPs, which bind to and stabilise microtubules, are phosphorylated in response to cell stimulation by a variety of mitogens and this inhibits their capacity to stabilise microtubules (Jameson and Caplow, 1981). MAPK activation is triggered not only by a large number of mitogens but also by activated Ras, by indirect methods that have been shown to affect microtubule stabilisation (Gupta *et al.*, 1992; Reszka *et al.*, 1995). *Ras*-transfection that results in the production of activated Ras proteins may, therefore, influence the stabilization of the microtubule network via MAPK, and thus affect the position of organelles within the cell.

Actin polymerisation plays a key role in the topography and dynamics of the plasma membrane. The cortical actin cytoskeleton is involved in cell motility, adhesion, stabilisation of microvilli, formation of ruffles, and endocytosis (Arpin *et al.*, 1994; Bretscher, 1991; Cunningham, 1995; Louvard, 1989; Leffers *et al.*, 1993). It is implicated in the early events of endocytosis in both yeast and mammalian cells (Riezman, 1993; Lamaze *et al.*, 1997; Pol *et al.*, 1997), i.e. in the initial uptake of receptors via clathrin-coated pits (Merrifield, 2004). Actin also enhances enzyme and endocytosed material delivery to the late endosome, downstream of a microtubule requirement (Durrbach *et al.*, 1996), and has been implicated in facilitating fusion of late endosomes and lysosomes (van Deurs *et al.*, 1995).

Another, and more indirect, role of the cortical actin cytoskeleton in events at the plasma membrane, is that it may constitute a barrier for exocytosis. Disassembly of cortical actin seems to be required for the interactions of an organelle with the plasma membrane, leading to fusion and release of the organelle's contents to the cell exterior (Bretscher, 1991; Muallem *et al.*, 1995; van Deurs *et al.*, 1996; Andrews, 2000). Defects in the normal actin cytoskeleton assembly have, therefore, been correlated with increased motility and

metastatic potential (Janmey and Chaponnier, 1995) and may explain the increased secretion of proteases, such as cathepsin B (Sloane *et al.*, 1994a).

Rac and Rho are involved in regulating the actin reorganisation that results in secretion when mast cells are activated (Norman *et al.*, 1994; Price *et al.*, 1995). The pathways regulated by these two proteins to promote exocytosis of granules may similarly provide a mechanism whereby mutated Ras, upstream in the signalling cascade involving Rac and Rho, may induce the secretion of lysosomes, observed in the MCF-10AneoT cell line.

Norman *et al.* (1996) showed that the activity of either Rho or Rac is required for exocytosis, since inhibition of secretion was only observed when both proteins are inhibited. The two cytoskeletal responses elicited by Rac and Rho may also be evoked independently of each other, i.e. actin polymerisation can occur in the absence of an assembled cortical actin cytoskeleton, and conversely, establishment of the cortical actin cytoskeleton can occur when actin polymerisation is otherwise inhibited (Norman *et al.*, 1994). The pathways to exocytosis and to the cytoskeleton are, therefore, divergent but are controlled by a common upstream regulator, an activator of Rac and/or Rho (in the case of *ras*-transfection this may be Ras). The shared pathway from Rac and Rho to a common downstream fusogenic effector could be mediated by a common target protein for Rho and Rac, possibly one of the GTPase activating proteins (GAPs) (Boguski and McCormick, 1993; Lancaster *et al.*, 1994). The divergent pathways could be mediated by specific target and/or accessory proteins, such as bcr and n-chimaerin for Rac and p190 for Rho (Diekman *et al.*, 1991; Ridley *et al.*, 1993; Brunton *et al.*, 2004). Exocytosis, however, requires activation of other small GTPase fusion proteins, Rab11, Arf6 and Rac1 (Fensome *et al.*, 1996; Trischler *et al.*, 1999; Bader *et al.*, 2004). The effects of mutationally activated Ras on Rac and Rho could, therefore, influence fusion processes and thus the enhanced secretion of lysosomal enzymes seen in the *ras*-transfected cell line (MCF-10AneoT).

In this chapter, the localisation and identity of the peripheral organelle seen in MCF-10AneoT cells is probed and confirmed as far as possible, in the absence of DAMP. The ultrastructure of the early endosome, late endosome and lysosome is also examined in the absence of DAMP, their identity being confirmed using the currently accepted markers (EEA1 for the early endosome, CI-MPR and LAMP-2 for the late endosome, and LAMP-2

for the lysosome) (Section 1.4). Finally, the possible mechanism of lysosomal enzyme translocation to the cell surface, and the mechanism of subsequent fusion with the cell membrane, to release proteolytic enzymes, is discussed.

5.2 Immunoelectron microscopy for the ultrastructure of endocytic organelles

Subsequent to the DAMP uptake studies reported in Chapter 4, an improved buffering system reported to enhance preservation of the cytoskeleton and the internal ultrastructure of organelles (e.g. the multilamellar late endosome) (Santama *et al.*, 1998) during fixation was employed. An increased amount of glutaraldehyde in the fixative (from that described in Chapter 4) was also used in an attempt to improve the preservation of the ultrastructure of the cells. As in the previous study using DAMP, the organelles were identified by immunolabelling with antibodies to EEA1 (early endosome), CI-MPR (late endosome) and LAMP-2 (late endosome and lysosome).

5.2.1 Reagents

Reagents used for cell culture as described in Section 2.9.1.

Reagents for preparation of formvar-coated nickel grids as described in Section 2.12.1.

Reagents for immunolabelling as described in Section 2.13.1.

130 mM PIPES, 60 mM HEPES, 20 mM EGTA, 4 mM $MgCl_2$, pH 7.3 (2x PHEM). PIPES (9 g), HEPES (2.68 g), EGTA (1.875 g) and $MgCl_2.6H_2O$ (0.163 g) were dissolved in 180 ml of $d.H_2O$, adjusted to pH 7.3 with NaOH and made up to 200 ml. The solution was aliquotted and stored frozen.

65 mM PIPES, 30 mM HEPES, 10 mM EGTA, 2 mM $MgCl_2$, pH 7.3 (PHEM). 2x PHEM (50 ml) was diluted with $d.H_2O$ (45 ml), adjusted to pH 7.3 if necessary and made up to 100 ml.

16% (m/v) Paraformaldehyde stock solution. Prepared as described in Section 2.10.1.

8% (m/v) Paraformaldehyde in PHEM, pH 7.3. Paraformaldehyde stock solution (25 ml) was added to 2x PHEM (12.5 ml), adjusted to pH 7.3 with 1 M HCl and made up to 50 ml with d.H_2O. The solution was stored at -10°C until required.

4% (m/v) Paraformaldehyde, 0.5% (v/v) glutaraldehyde in PHEM, pH 7.3. Paraformaldehyde stock solution (25 ml) and glutaraldehyde [400 µl of 25% (v/v)] were added to 2x PHEM (50 ml), made up to 90 ml with d.H_2O, adjusted to pH 7.3 with 1 M HCl and made up to 100 ml. The solution was stored at -10°C until required.

20 mM Glycine in PHEM, pH 7.3. Glycine (15 mg) was dissolved in PHEM (10 ml).

10% (m/v) Gelatin in PHEM, pH 7.3. Microbiological grade gelatin (10 g) was added to PHEM (100 ml) and dissolved by heating. The volume was made up to 100 ml (if necessary) with d.H_2O, the solution chilled rapidly on ice and stored at 4°C.

Antibodies. Monoclonal mouse anti-EEA1 was used at 5 µg/ml, rabbit anti-CI-MPR was used at 1/40 dilution, mouse anti-LAMP-2 was used at 1/200 dilution, and rabbit anti-mouse was used at 1/200 dilution. All antibody dilutions were made using 1% (v/v) fish skin gelatin, 0.8% (m/v) BSA, 20 mM gelatin in PBS (FBG) (Section 2.13.1).

Protein A-gold (PAG). 5 nm PAG was used at 1/300 dilution, 10 nm PAG was used at 1/300 dilution, dilutions being made in FBG immediately before use.

5.2.2 Procedure

MCF-10A and MCF-10AneoT cells were grown as described in Section 2.9.2. The cells were fixed with 4% (m/v) paraformaldehyde, 0.5% (v/v) glutaraldehyde in PHEM (30 min, RT). The fixative was removed and replaced by 8% (m/v) paraformaldehyde in PHEM. The monolayers were carefully scraped off the bottom of the flasks using a rubber policeman and transferred to Eppendorf tubes. The cells were stored overnight in fixative (4°C), pelleted and the excess fixative removed. Residual free aldehyde groups were quenched with 20 mM glycine in PHEM (2 x 15 min). The cells were pelleted, excess glycine removed, 10% (m/v) gelatin in PHEM was added and allowed to infiltrate

(2 h, 37°C). The cells were pelleted, excess gelatin removed and the pellets chilled rapidly on ice. A thin layer of PHEM was placed over the gelatin to prevent drying out. The gelatin blocks were cut into 1 mm^3 cubes under buffer, dehydrated and embedded in LR White as described in Section 2.11.2. The resin blocks were sectioned as described in Section 2.12.2 and the grids immunolabelled, using FBG as blocking agent, as described in Section 2.13.2.

5.2.3 Results

The early endosome was identified by the presence of immunolabelling for the marker EEA1, found on the outer membrane (Fig. 5.1, small arrows). The membrane localisation of EEA1 is consistent with its function as a Rab5 effector protein that acts as a tethering protein in early endosome fusion (Stenmark *et al.*, 1996). As seen in Fig. 5.1, early endosomes are simple, electron-translucent organelles that do not label for either CI-MPR or LAMP-2 (results not shown). Small numbers of CI-MPR may, however, be present in these organelles, as these proteins traffic through the early endosome en route to the late endosome (Ludwig *et al.*, 1991). Not all electron-translucent organelles label for EEA1 (Fig. 5.1A), therefore, not all electron-translucent organelles are necessarily early endosomes, assuming the different fixation used in this study had no deleterious effect on the antigenicity of the target antigen. Since very few membrane-bound EEA1 molecules would be present within the plane of sectioning, and labelling efficiency usually does not exceed 10% (Griffiths, 1993), it is also possible that not all early endosomes would be detected using immunolabelling. The identity of the electron-translucent organelles (Fig. 5.1A) without EEA1 labelling, therefore, cannot be confirmed. The average diameter of the early endosomes in the MCF-10AneoT (0.25-0.52 μm) (Fig. 5.1B) is slightly larger than that of the MCF-10A cells (0.13-0.4 μm) (Fig. 5.1A). In both the MCF-10A and MCF-10AneoT cell lines, the diameter and morphology of the early endosome without the presence of DAMP (Fig. 5.1) appears similar to those with DAMP (0.2-0.4 μm) (Fig. 4.9). Such diameters, however, are only approximate averages, as stereological studies were not performed. Also of note, is the close proximity (which may lead to fusion) of three electron-translucent organelles with each other (Fig. 5.1A, centre) and with a late endosome, identified by its distinctive internal multilamellar morphology and lack of labelling for EEA1 (Fig. 5.1A, large arrow). The multilamellar morphology is, however,

much better preserved with the improved buffering system and fixation method used in this study [4% paraformaldehyde (m/v), 0.5% glutaraldehyde (v/v) in PHEM] (Fig. 5.1A, large arrow) than that used in the previous study with DAMP (4% (m/v) paraformaldehyde, 0.05% (v/v) glutaraldehyde in 200 mM HEPES) (Fig. 4.10). Since the different buffering system and fixation method and the omission of DAMP was instituted simultaneously, it is difficult to assess the relative contribution of DAMP to the poor ultrastructure of the late endosome in earlier studies (compare Fig. 4.10 and Fig. 5.1). The multilamellar membranous structures observed in these and other cell types, fixed in a variety of ways and embedded in different types of resins, have also been observed in unfixed cells prepared by vitrification for cryoultramicrotomy and are, therefore, not an artefact of fixation (McDowall *et al.*, 1989).

Positive identification of late endosomes is confirmed through immunolabelling for CI-MPR (Fig. 5.2, arrows) as in the previous study, and now by the additional labelling for LAMP-2 (Fig. 5.2, arrowheads). Much of the confusion in the literature in distinguishing the late endosome from the lysosome has occurred because of the localisation of LAMP-2 to both organelles. Inadequate preservation of the distinctive internal morphology of the late endosome during fixation, and the difficulty of keeping the internal structure of the organelle intact during sectioning and immunolabelling has also contributed to the confusion in the literature. In the MCF-10A cell line (Fig. 5.2A) it can be seen that much of the internal structure of the late endosomes has possibly been extracted during sectioning. This does not seem to have occurred to such an extent in sections of the MCF-10AneoT cell line (Fig. 5.2B), so that these late endosomes appear to be more electron-dense than those in Fig. 5.2A. The multilamellar structure, though less extracted in the MCF-10AneoT cells (Fig. 5.2B) than in the MCF-10A cells (Fig. 5.2A), seems to be less defined in the MCF-10AneoT cells, reminiscent of what was seen in the cells treated with DAMP (Fig. 4.10). It may, therefore, be possible that such a lack of definition could, similar to that seen in the presence of DAMP, be due to the relative alkalinisation of the *ras*-transfected cell line, and the resultant partial disruption of membrane trafficking in these cells. Although not obvious from the photographs selected (Fig. 4.10 and 5.2), DAMP treatment did not seem to affect the diameter of the late endosomes of the MCF-10A cell line (0.3-0.6 μm for both treated and untreated cells). Some swelling was, however, observed in the late endosomes of the MCF-10AneoT cell line with DAMP treatment (0.3-0.46 μm compared to 0.3-0.7 μm).

Evidence of possible homotypic fusion between late endosomes, and heterotypic fusion between late endosomes and lysosomes or other, unidentified organelles [possibly endosome carrier vesicles (ECVs)] was also seen (Fig. 5.2A). Performing triple labelling with CI-MPR, LAMP-2 and markers for other organelle types [e.g. lysobisphosphatidic acid (LBPA) for the ECV] could potentially identify these unlabelled organelles.

The labelling densities of the various antigens (EEA1, CI-MPR and LAMP-2) (Fig. 5.1, 5.2 and 5.3) are similar to those seen in studies using DAMP (Fig. 4.9, 4.10 and 4.11). It may, therefore, be assumed that DAMP did not interfere significantly with antigen recognition and the labelling density of the organelle markers. The peripheral organelles observed in the MCF-10AneoT cells are found in both DAMP treated (Fig. 4.11C and D) and untreated cells (Fig. 5.3C and D). DAMP exposure was, therefore, not long enough to allow major disruption of microtubule and membrane trafficking and result in a redistribution of normally perinuclear organelles to the cell periphery. Although DAMP treatment may have caused some swelling of organelles, and thereby disruption of internal morphology, the short-term exposure to DAMP also does not seem to have affected localisation of the marker complement.

The peripherally situated small, electron-dense organelles seen in the *ras*-transfected cells (Fig. 5.3C and D) seem to be equivalent to the small, acidic, electron-dense peripheral organelles seen in the DAMP studies (Fig. 4.11C and D), especially since both label for LAMP-2. These peripheral organelles seen in the MCF-10AneoT cell line (Fig. 4.11C and D) may, therefore, be lysosomes as they fit the current definition of a lysosome as a small, acidic, electron-dense structure which contains LAMP-2 (Fig. 5.3, arrowheads), but not CI-MPR (Fig. 5.2 arrows) or EEA1 (results not shown). In the MCF-10AneoT cell line these "lysosomes" were found in the periphery of the cell and seemed to fuse with the plasma membrane (Fig. 5.3C and D). This peripheral localisation is not as frequent in the "normal" MCF-10A cell line (Fig. 5.3A and B) and, therefore, suggests an involvement of these peripheral lysosomes in the premalignant phenotype.

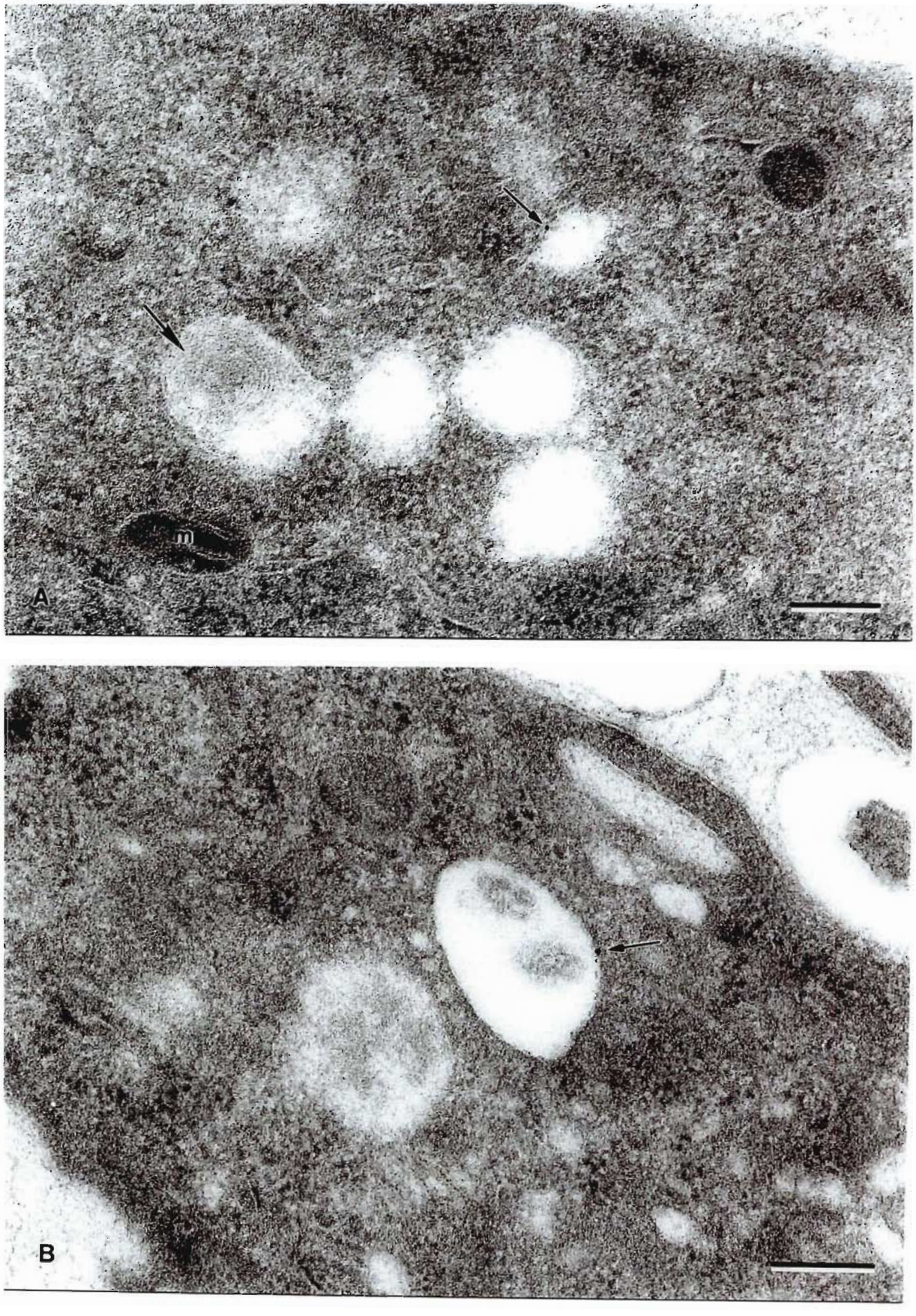
m
A
B

Figure 5.1 **Structure and localisation of the early endosome in (A) MCF-10A and (B) MCF-10AneoT cell lines.**
Small arrow indicates early endosomes labelled for EEA1, which is not present in the late endosome (large arrow). m = mitochondria; bar = 200 nm.

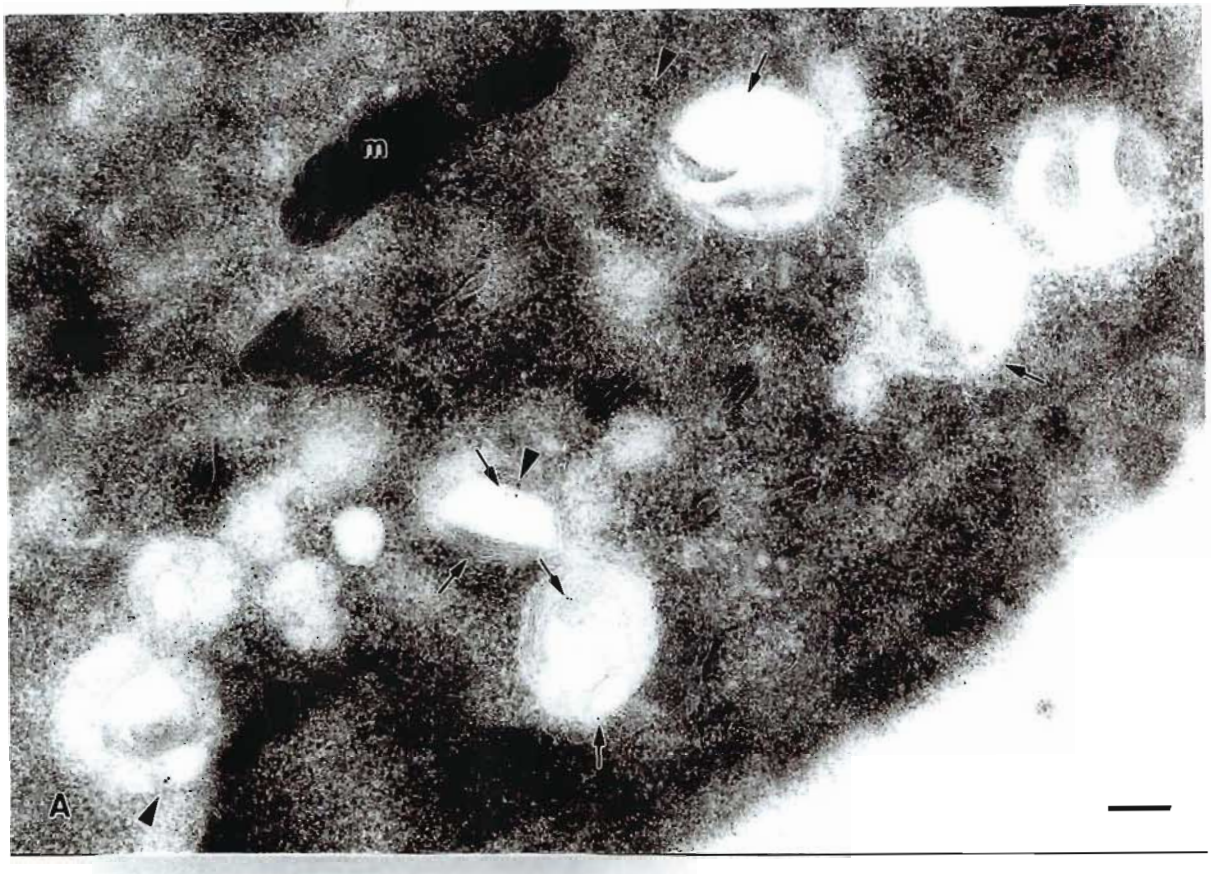
m
A

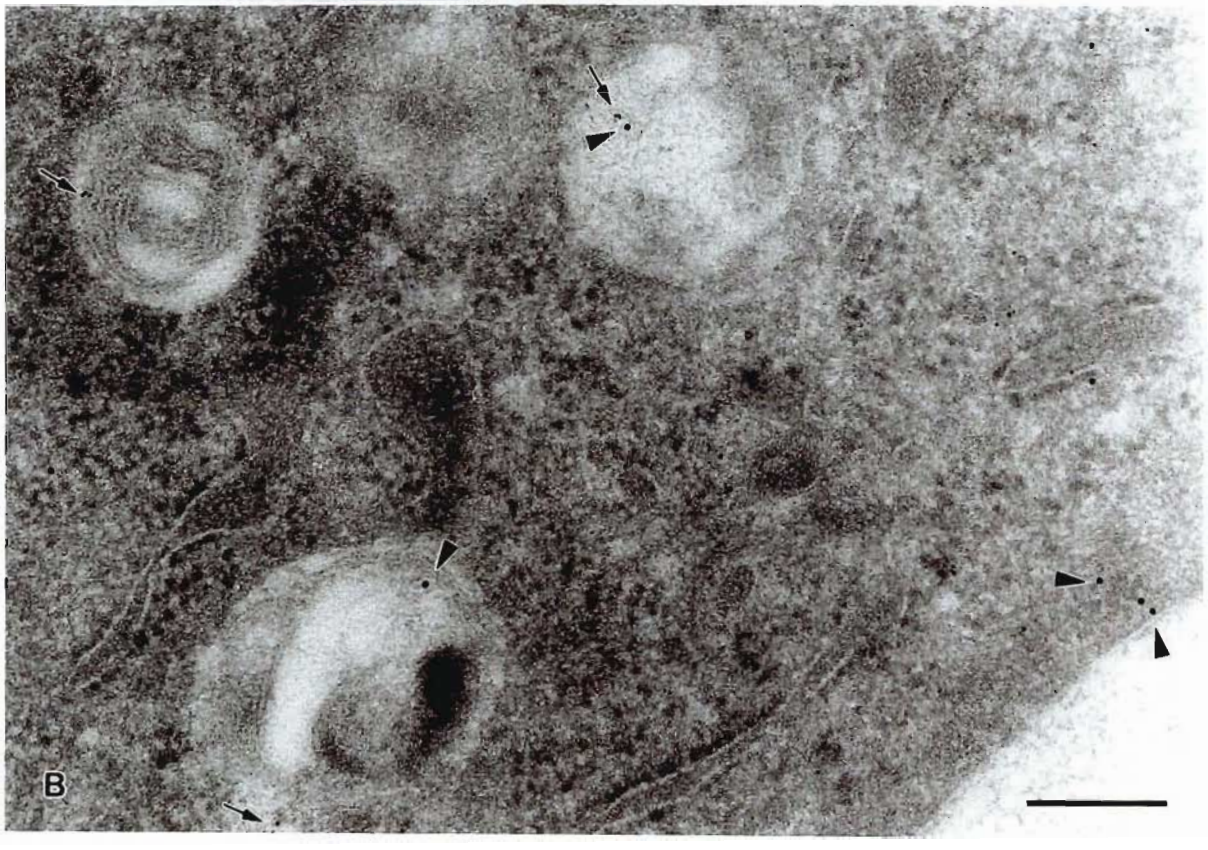
B

Figure 5.2 **Structure and localisation of late endosomes and lysosomes in (A) MCF-10A and (B) MCF-10AneoT cell lines.**
Late endosomes label for CI-MPR (arrows) and/or LAMP-2 (arrowheads). Lysosomes label only for LAMP-2. m = mitochondria; bar = 200 nm.

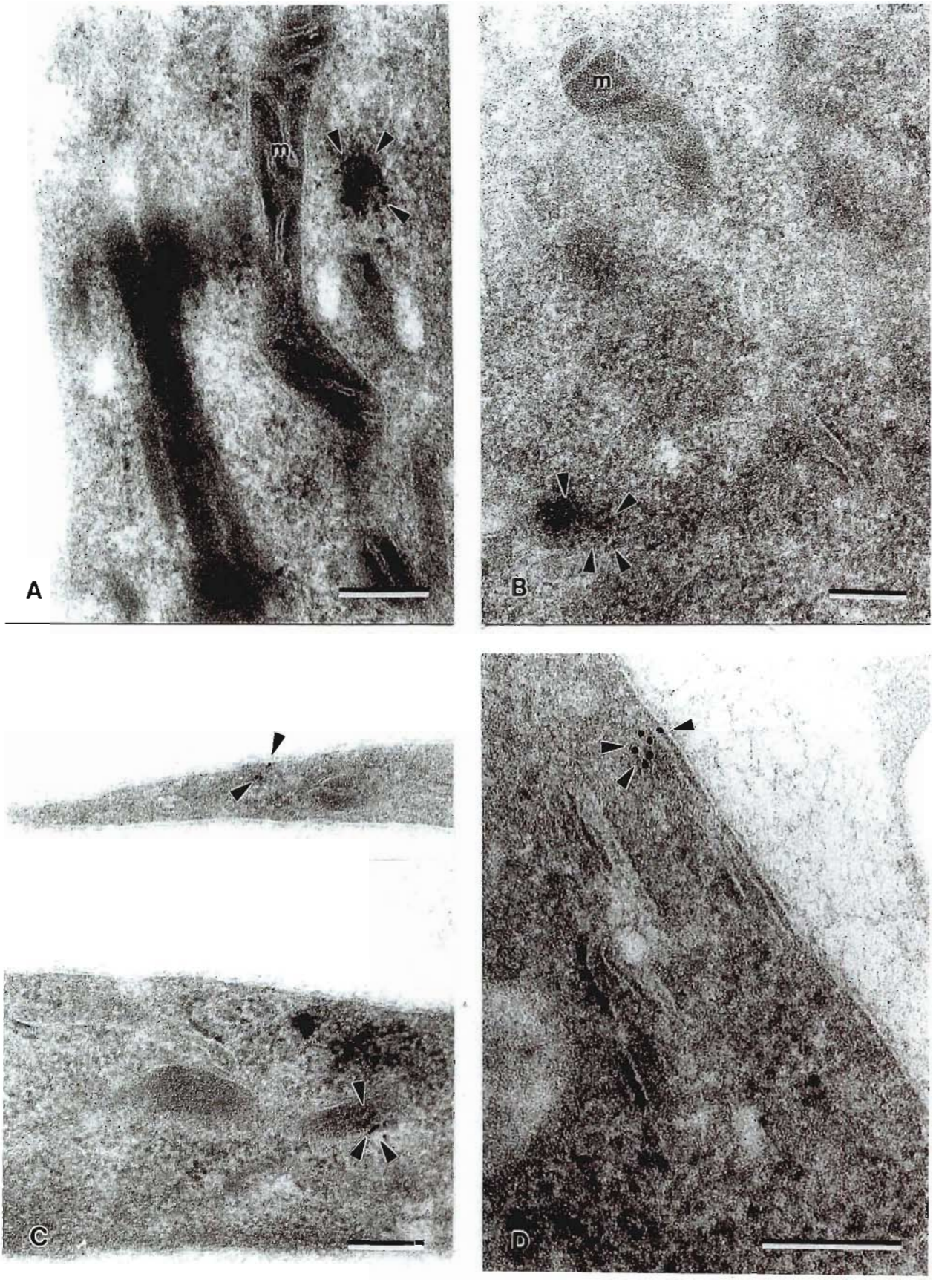
m
A
m
B
C
D

Figure 5.3 **Structure and localisation of lysosomes in (A and B) MCF-10A and (C and D) MCF-10AneoT cell lines.**
Labelling for LAMP-2 (arrowheads) identifies lysosomes. m = mitochondria; bar = 200 nm.

5.3 Discussion

In the presence and absence of DAMP, the early endosome, as defined by the presence of EEA1, seems to have a relatively simple morphology in both the *ras*-transfected MCF-10AneoT and non-transfected MCF-10A cell lines, appearing as an electron-translucent organelle, with no internal membranous structures. Similarly, the morphology of the lysosome, as defined by the presence of LAMP-2 and the lack of CI-MPR, is also simple, being a small electron-dense organelle with no internal structures. The late endosome, containing both CI-MPR and LAMP-2, however, has a complex morphology, and is extremely pleiomorphic. This pleiomorphic organisation may contain cisternal, tubular and vesicular regions with many membrane invaginations (Griffiths *et al.*, 1988). The late endosome usually, therefore, appears to be either multivesicular or multilamellar. The functional differences and composition of these different types of inner membranes has, however, only recently been discovered (see Fig. 1.3) (Gruenberg, 2003).

The outer, or limiting membrane of the late endosome contains high amounts of LAMP-1, which is believed to be protected from degradation by lysosomal enzymes by its high level of glycosylation, which also protects the outer membrane from degradation (Griffiths *et al.*, 1988). The internal membranes contain LBPA, which is a poor substrate for phospholipases and is, therefore, resistant to degradation (Kobayashi *et al.*, 1998; 2001). Negatively charged phospholipids, in particular LBPA, facilitate the degradation of several glycolipids by presenting lipids and proteins that need to be degraded to digestive enzymes (Wilkening *et al.*, 1998). The internal membranes also contain LAMP-3 (Escola *et al.*, 1998), and constitutes the predominant area in which CI-MPR and LAMP-2 is located (this study; Griffiths *et al.*, 1988; Kobayashi *et al.*, 1998). CI-MPRs are recycled back to the Golgi from these internal late endosome membranes, a process that should occur slowly since there are numerous internal membranes, and only molecules that are present on the limiting outer membrane would be available for transport. CI-MPR recycling is very efficient, however, although the mechanism by which the movement of CI-MPR from the inner membranes to the outer membrane occurs is unknown. The effect of *ras*-transfection on the trafficking of CI-MPR is similarly unknown.

In this Chapter it was shown that LAMP-2 positive organelles of the MCF-10A cell line are redistributed towards the periphery of the cell after *ras*-transfection. Experimental protocols that result in the depolymerisation of microtubules or disturb the dynein-kinesin

balance affect lysosomal positioning. Examples include: nocodoazole-induced dispersion of lysosomes (Matteoni and Kreis, 1987) and the dramatic redistribution of lysosomes to a peripheral position upon cytoplasmic acidification/alkalinisation, or overexpression of dynamitin or KIF2β, or the elimination of cytoplasmic dynein expression (Heuser, 1989; Parton *et al.*, 1991; Busch *et al.*, 1994; Burkhardt *et al.*, 1997; Santama *et al.*, 1998; Harada *et al.*, 1998). Anti-kinesin antibody-induced inhibition of radial lysosomal movement (Hollenbeck and Swanson, 1990) and blocking of lysosome transport to the cell periphery by mutations in the ATP-binding domain of overexpressed kinesin may also affect the position of organelles (Nakata and Hirokawa, 1995). All these result in the translocation of lysosomes from a perinuclear position to the periphery of the cell via affects on microtubules. It has been shown that the microtubule network is destabilised in the MCF-10AneoT cell line (Elliott, 1993; Nishimura *et al.*, 1998). Since the cytoplasm is alkalinised in the MCF-10AneoT cell line (Chapter 4; Sloane *et al.*, 1994b), which directly affects microtubule polymerisation/depolymerisation (Heuser, 1989), this could be one mechanism by which the movement of lysosomes towards the cell surface may be facilitated after *ras*-transfection. The effect of constitutively activated Ras on Rac and Rho could also result in the relocation of organelles to the cell periphery (Section 1.1.1). These organelles, by their morphology, pH value, labelling for LAMP-2 and lack of labelling for CI-MPR may be tentatively identified as lysosomes. Additional evidence for the identification of the peripheral organelle as lysosomes is that they also contain mature active lysosomal enzymes (cathepsins D and B), distinguishing them from constitutive secretory vesicles that would contain precursor enzymes (Elliott, unpublished data).

Agents that depolymerise actin filaments increase the secretion of vesicles (Bader *et al.*, 2004). The pH of the cytosol may also influence the actin cytoskeleton and thus the fusion of vesicles with the plasma membrane. *In vitro*, alkalinisation of the cytosol causes a loss of elongation factor-1α (EF-1α) mediated F-actin crosslinking and an increase in single filament binding (i.e. the binding of EF-1α to actin changes from a multivalent interaction with filaments, forming bundles, to a monovalent binding interaction where EF-1α binds to single filaments). This may result in stress fibre breakdown (Liu *et al.*, 1996), and the simultaneous breakdown of the cortical actin cytoskeleton, allowing fusion of organelles with the plasma membrane. Alkalinisation of the cytoplasm and the subsequent actin cytoskeleton depolymerisation may thus facilitate peripheral lysosomes fusion with the

plasma membrane, increasing the invasive malignant phenotypes of *ras*-transfected cell lines by allowing the secretion and surface expression of cathepsins B and D and LAMP-2 (Sameni *et al.*, 1995).

Malignant transformation has been associated with an increased secretion of lysosomal enzymes, invasion and metastasis (Andrews, 2000). This increased secretion has been attributed to the mis-trafficking of enzymes from the TGN to a constitutive secretory pathway (Prence *et al.*, 1990). Regulated exocytosis has, however, also been shown to occur in cells previously thought to exhibit only constitutive exocytosis, e.g. fibroblasts and epithelial cells (Chavez *et al.*, 1996; Ninomiya *et al.*, 1996; Rodriguez *et al.*, 1997). Studies have also shown that an increased lysosomal pH increases lysosomal secretion (Tapper and Sundler, 1990) by decreasing the lysosomal Ca^{2+} concentration (and thus increasing the cytosolic Ca^{2+} concentration) (Andrews, 2000; Christensen *et al.*, 2002). The peripheral lysosomes also do not label for Rab11 (fusiogenic factor linked to regulated secretory organelles) and are, therefore, probably not regulated secretory organelles (Elliott, unpublished results). Secretion of proteolytic enzymes from exocytosed lysosomes in the MCF-10AneoT cell line may thus be regulated by Ca^{2+} concentrations, although constitutive secretion cannot be ruled out.

Invasiveness is characterised, not only by the secretion of proteolytic enzymes that degrade the extracellular matrix (ECM), but also by cell motility. The actin cytoskeleton remodelling necessary for cell motility is modulated by tyrosine kinase and MAPK activity. MAPK activity stimulates myosin light chain kinase (MLCK) activation and phosphorylation of the myosin light chain (MLC), which is presumed to induce actin-myosin contraction (Fincham *et al.*, 2000). Tyrosine kinase-induced actin-myosin contraction also contributes to the release of focal adhesions during cell detachment (Crowley and Horwitz, 1995). Rho binding kinase (ROK) can, however, replace the activity of MLCK by directly phosphorylating MLC (Amano *et al.*, 1996), and can elevate MLC phosphorylation by inhibiting the MLC phosphatase (Kimura *et al.*, 1996). Usually cell motility is a tightly regulated event that occurs only in certain cell types after stimulation by cytokines or hormones. In the case of *ras*-transfection, however, the stimulatory signals could be bypassed by constitutively activated Ras, which is upstream of MAPK and ROK in the Ras signalling pathway, allowing cell motility and (with the addition of proteolytic activity) invasion.

Metastasis is the dissemination of tumours caused by the invasion of tumour cells into- and back out of the blood vascular system. Highly metastatic human colon tumour cells express more LAMP molecules on the cell surface than their low metastatic counterparts (Saitoh *et al.*, 1992). Mac-3, which is identical to murine LAMP-2, was originally identified as a macrophage cell surface molecule (Ho and Springer, 1983). Additionally, increased amounts of LAMP-1 and LAMP-2 are found on the cell surface of activated platelets (Febbraio and Silverstein, 1990; Silverstein and Febbraio, 1992). Similarly, the MCF-10AneoT cell line also expresses LAMP-2 on the plasma membrane (Sameni *et al.*, 1995). These results imply that surface expression of lysosomal membrane proteins is achieved by fusion of the lysosomal membrane with the plasma membrane. The presence of lysosomal membrane proteins may not, however, simply be a by-product of lysosome-plasma membrane fusion. Cytotoxic T-lymphocytes (CTLs) exocytose granules during specific interaction with target cells. After granules fuse with the plasma membrane, lysosomal membrane glycoproteins apparently protect the plasma membrane from the contents of the granules. These results indicate that lysosomal membrane glycoproteins are utilised when the cytoplasm and the cell membrane need protection from hydrolases and other lethal proteins (Peters *et al.*, 1991). In the case of tumourigenic cells, the presence of LAMPs on the cell surface may, therefore, protect the cell from proteolysis by its secreted proteolytic enzymes.

Highly metastatic tumour cells also adhere more efficiently to E-selectin-expressing cells (Sawada *et al.*, 1993a,b). This suggests that LAMP molecules on the cell surface are critical because they bind to and thus present ligands (e.g. E-selectin) for the adhesion molecules present on the cell surface of other cells. In tumour metastasis, tumour cells aggregate with platelets in blood circulation (Nicolson, 1989). Such aggregated tumour cells could subsequently be trapped in capillaries, which could trigger the activation of endothelial cells to express E-selectin on the cell surface. Tumour cells are, therefore, slowed down in the bloodstream by the binding of LAMPs to E-selectin, leading to stronger adhesion to endothelial cells through integrins and counter-receptor interactions [e.g. through ezrin, radixin, and moesin (ERM)]. This is a similar process to that which occurs at inflammatory sites (Lawrence and Springer, 1991; Ley *et al.*, 1991; Ivetic and Ridley, 2004). It is possible that these events result in the lodging of tumour cells in capillary beds at junctions between endothelial cells, establishing metastasis. Therefore,

all the mechanisms described here that result in the surface expression or release of proteases and LAMP-2 in the premalignant MCF-10AneoT cell line could be ways in which the cells prepare themselves for metastasis.

The work presented in this chapter confirms the identity of the organelles of the endosome-lysosome system, for which the pH was established using Oregon Green® 488 dextran (OGD) and DAMP (Chapter 4). It was confirmed that the presence, or absence, of DAMP did not seem to influence the labelling densities of the various markers. Results also show that the morphology of these organelles was compromised by the presence of the weak base DAMP (although they are still recognisable). The improved buffering and fixation system used in the present study, in conjunction with the absence of DAMP, however, vastly improved the ultrastructure of the various organelles. The findings of this and Chapter 4 suggest that *ras*-transfection caused an increase in cellular pH, which effected the peripheral localisation of lysosomes and fusion of lysosomes with the plasma membrane (by disrupting microtubules and the actin cytoskeleton), resulting in the release of lysosomal enzymes to the cell exterior and the invasive phenotype.

CHAPTER 6

GENERAL DISCUSSION

Tumour cell invasion and metastasis require the destruction of the extracellular matrix (ECM) during local invasion, angiogenesis, intravasation and extravasation (Liotta *et al.*, 1983). This process is mediated by the multiple degradative activities of proteolytic enzymes (Mignatti *et al.*, 1986). There are five classes of proteolytic enzymes [matrix metalloproteinases (MMPs) and serine-, aspartic-, threonine- and cysteine proteases] and members of all the classes have been implicated in the progression and invasive activities of animal and human tumours (e.g. Garcia *et al.*, 1996; Chambers and Matrisian, 1997; DeClerk *et al.*, 1997; Johnsen *et al.*, 1998; Lochter *et al.*, 1998; Yan *et al.*, 1998; Rao, 1996). These enzymes can act directly, or indirectly by activating other proteases, to degrade the ECM. Local ECM degradation is facilitated by proteases secreted from the tumour cell, some of which become bound to the cell surface, e.g. the urokinase-type plasminogen activator (uPA), tissue-type plasminogen activator (tPA) and plasminogen, the transmembrane matrix metalloproteinases (MT-MMPs) and cathepsin B and D (Roldan *et al.*, 1990; Hajjar *et al.*, 1994; Nomura *et al.*, 1995; Sameni *et al.*, 1995). Latent precursor forms of membrane-associated proteases may be activated by soluble proteases (Okumura *et al.*, 1991; Kobayashi *et al.*, 1991) and secreted precursors may be activated by membrane-associated proteases (Kobayashi *et al.*, 1993; Llano *et al.*, 1999). In addition, the cleaved propeptides of cathepsin L and D act as autocrine growth factors or mitogens (Kasai *et al.*, 1993; Fusek and Vetvicka, 1994). Cathepsin D also acts as a key paracrine mitogen, independent of its catalytic activity, to stimulate tumour-fibroblast interactions. This allows fibroblast proliferation, motility and invasion that, in addition to the invasive properties of the tumour cells, leads to cancer progression (Laurent-Matha *et al.*, 2005).

6.1 Altered trafficking of proteolytic enzymes due to *ras*-transfection and pH alteration

The normal trafficking of proteases, via either the cation-independent mannose-6-phosphate receptor (CI-MPR) or the cation-dependent mannose-6-phosphate receptor (CD-MPR), to organelles within the endosome-lysosome system, appears to alter following transfection of MCF-10A breast epithelial cells with oncogenic c-Ha-*ras* (MCF-10AneoT). The expression of cathepsin B and L of MCF-10AneoT cells is increased and constitutive cathepsin B secretion is 2.5-fold greater (Lah *et al.*, 2000; Rozhin *et al.*, 1994). Lysosomal enzyme-containing vesicles seem more peripherally distributed in the cytoplasm than in normal cells and the lysosomal enzymes (cathepsins B, D and L) also no longer co-localise in all vesicles, as is the case in the non-transfected MCF-10A cell line (Sameni *et al.*, 1995; Moin *et al.*, 1994). Both cathepsin B and D can become plasma membrane-associated while remaining functionally active (Sloane *et al.*, 1994a). Such altered trafficking seems to be typical of tumour cells, and this may further be reflected in alterations in the enzyme complement of different lysosomes, leading to lysosomal sub-populations (Moin *et al.*, 1994).

Lysosomal enzyme trafficking can occur independently of MPRs. This has been demonstrated in macrophages, HepG2 cells, U937 monocytes and I-cell disease (Diment *et al.*, 1988; Rijnboutt *et al.*, 1991; Braulke *et al.*, 1987; Glickman and Kornfeld, 1993) and may also explain the differential trafficking of cathepsins D and B observed in the MCF-10AneoT cell line. This hypothesis is reinforced by the findings of Capony *et al.* (1994), who showed that cathepsin D secretion in some metastatic human breast cancer cell lines, contrary to what is found in normal mammary cells, including the MCF-10A cell line, is not increased by ammonium chloride (a weak base) treatment, which inhibits the synthesis of mannose-6-phosphate (M-6-P) groups on the lysosomal proenzymes and also inhibits MPR-dependent trafficking by preventing acidic pH-dependent dissociation of MPR/lysosomal enzyme complexes (Capony *et al.*, 1994; Isidoro *et al.*, 1997). The alternate trafficking route of these enzymes was shown to involve membrane-association. Subsequently, the presence of other pro-enzyme receptors for cathepsin D (e.g. prosaposin) and cathepsin L were shown to traffic these enzymes in an MPR-independent manner (Gopalakrishnan *et al.*, 2004; Zhu and Conner, 1994; McIntyre and Erickson, 1993; Ahn *et al.*, 2003; Laurent-Matha *et al.*, 1998). It remains to be seen by which mechanism enzyme/membrane association occurs in the *ras*-transformed MCF-10AneoT cells. In this

study, these cells have been shown to have an altered pH regulation, which may affect MPR-dependent trafficking and perhaps may favour, or modify, pro-cathepsin/membrane interactions.

Many mechanisms, besides that of vesicle alkalinisation, have been proposed to explain the altered trafficking seen after *ras*-transfection, the strongest candidates being the phosphatidylinositol-3-kinases [PI(3)Ks]. Rho, a downstream target of Ras, appears to mediate the activation of PI(3)K (Fig. 1.1) (Kumagai *et al.*, 1993). PI(3)K, in turn, has been implicated in the trafficking of MPR-ligand complexes from the *trans* Golgi network (TGN) towards late endosomes and lysosomes (Davidson, 1995). Wortmannin, a PI(3)K inhibitor, causes almost complete extracellular mis-targeting of pro-cathepsin D which, in the cell line studied, is normally trafficked to lysosomes in a CI-MPR-dependent manner. The most probable explanation for this is that wortmannin directly interferes with CI-MPR trafficking. This could occur through the prevention of CI-MPR recruitment into clathrin-coated vesicles (CCVs) on the TGN, inhibition of budding or fusion events, or by the prevention of receptor recycling (Davidson, 1995).

6.2 The effect of *ras*-transfection on cellular pH

To maintain the intracellular pH near neutrality, most mammalian cells actively secrete H^+ in exchange for extracellular Na^+, a process mediated by Na^+/H^+ exchanger proteins (NHEs). NHEs are integral membrane phospho-glycoproteins with 10–12 transmembrane domains and a large carboxyl-terminal hydrophilic domain facing the cytoplasm (Noel and Pouysségur, 1995; Yun *et al.*, 1995). Seven members of the NHE family have been identified to date, and these are distinct from the Na^+/K^+-ATPase and vacuolar H^+-ATPase (V-ATPase) pumps. NHE-1, thought to be the "housekeeping" isoform, is found on the plasma membranes of virtually all animal cells and functions primarily in pH and cell volume regulation (Grinstein *et al.*, 1992; Noel and Pouyssegur, 1995; Orlowski and Grinstein, 1997; Counillon and Pouyssegur, 2000). NHE-2,3,4 are expressed in kidney and gut tissues, where NHE-3 is found on the apical membranes of epithelial cells and is thought to play a central role in transepithelial reabsorption of Na^+ (D'Souza *et al.*, 1998; van Dyke, 1995). NHE-5,6,7 function in brain tissue, mitochondria and the TGN, respectively (Numata *et al*, 1998; Izumi *et al.*, 2003).

Growth factor receptor occupancy (which could be bypassed by the presence of activated Ras) and the activation of Rho, and hence of PI(3)K, besides affecting the trafficking of lysosomal enzymes, results in the activation of NHEs on the cell surface (NHE-1). This is accomplished by increasing the affinity of the exchanger proteins for protons at an internal pH-sensitive regulatory site (Paris and Pouysségur, 1984; Moolenar *et al.*, 1984; Swann and Witaker, 1985). The affinity of NHE-1 for protons follows a Monod-Wyman-Changeaux mechanism, i.e. the dimeric transporter oscillates between two conformations possessing, respectively, a high and a low affinity for protons. Both conformations have the same affinity for sodium. Growth signals modify the balance between the 2 existing conformations to those with increased affinity for protons (Lacroix *et al.*, 2004). Growth factors, serum and phorbol esters also increase the basal phosphorylation state of NHE-1 resulting in its activation and inducing cytosolic alkalinisation (Sardet *et al.*, 1990; Pewitt *et al.*, 1990; Haystead *et al.*, 1989).

NHE-1 is stimulated upon activation of a receptor tyrosine kinase (RTK) via epidermal growth factor (EGF), and G protein-coupled receptors (GCRs) and protein kinase C (PKC) via α-thrombin (Birnbaumer *et al.*, 1990). Both RTK and GCR stimulate phosphorylation of NHE-1, and thus the activation of NHE-1, exclusively on serine residues (Sardet *et al.*, 1990; 1991). Raf1-kinase or mitogen activated protein kinase (MAPK) integrates signals from PKC and RTK (Morrison *et al.*, 1988; Anderson *et al.*, 1990) and may activate NHE through a Raf1-mitogen activated protein kinase kinase (MEK) -dependent mechanism (Hooley *et al.*, 1996). Usually Ha-*ras* induced stimulation of NHE-1 is PKC-dependent (Wolfman and Makara, 1987; Huang *et al.*, 1988; Wadsworth *et al.*, 1997), although LPA may also be required (Vexler *et al.*, 1996). There have, however, been reports of Ha-*ras*-induced NHE-1 stimulation occurring through a PKC-independent mechanism (Maly *et al.*, 1989; Wöll *et al.*, 1993), which probably involves Janus kinase 2 and calmodulin (Garnovskaya *et al.*, 2003).

Mitogenic signals that stimulate NHE, leading to intracellular alkalinisation, are thought to be one prerequisite for the initiation of cell proliferation (Doppler *et al.*, 1987; Grinstein *et al.*, 1989, 1992; Gillies *et al.*, 1992; Lang *et al.*, 2000). Another consequence of the activation of NHE is an increase in cell volume, which may participate in the regulation of cell proliferation (Lang *et al.*, 1992a,b). Similarly, a constitutively active Ras, which may arise from mutation of Ras or viral transfection with the activated Ha-*ras* oncogene, may

activate NHE and lead to intracellular alkalinisation (Hagag *et al.*, 1987; Maly *et al.*, 1989; Ritter *et al.*, 1992; Kaplan and Boron, 1994) and increased cell volume (Meyer *et al.*, 1991; Ritter *et al.*, 1993), although increased NHE-1 activity may not be essential for transformation to occur (Lin *et al.*, 1996). Since the MCF-10AneoT cell line contains activated Ha-*ras*, has an increased growth rate and larger cell volume (Basolo *et al.*, 1991), the activation of NHE-1 may explain the general alkalinisation of the cytosol and morphological transformation of the *ras*-transformed cell lines, via the effects of pH on the cytoskeleton. It would not, however, explain why the pH of specific organelles, such as the late endosome and lysosome, may be affected (unless these are a function of the cytosolic pH).

The activated NHE-1 of *ras*-transfected cells may pump Na^+ constitutively into the cytosol with a subsequent increase in cell volume (a phenotype seen in the MCF-10AneoT cell line). This increase in intracellular cation concentration may diminish endosomal acidification (Moriyama *et al.*, 1992), especially since H^+ is being constitutively pumped out of the cell. In addition, reversible dissociation of the V_1 and V_0 domains of V-ATPases may be induced by glucose deprivation (Kane, 1995). Due to the rapid cell division that the *ras*-transfected cells exhibit (Basolo *et al.*, 1991), glucose deprivation may more easily affect the *ras*-transfected than the non-transfected cell line. Evidence for this may be that MCF-10AneoT cells express the pro-enzyme forms of cathepsin B, D and L on their surface (Sloane *et al.*, unpublished data), a condition potentially induced by low glucose concentrations (Tournu *et al.*, 1998). This may explain why it may be difficult to demonstrate great pH differences between the MCF-10A and MCF-10AneoT cell lines, as the pH differences may depend upon how rapidly cell division is occurring in the particular cell line. Also, Cl^- channel activity is regulated by protein kinase A (PKA), which is activated by *ras*-transfection (Bae and Verkman, 1990; Mulberg *et al.*, 1991), so that V-ATPase action that relies on Cl^- counterion conductance may be retarded. This could result in alkalinisation of the late endosome and lysosome. It may, therefore, be any one of these three mechanisms, or a combination, which results in alkalinisation of the late endosome and lysosome in *ras*-transfected cells. Fig. 6.1 provides a summary of how the results obtained in this study contribute to the understanding of the mechanisms involved with the invasive phenotype, in the context of the reviewed literature.

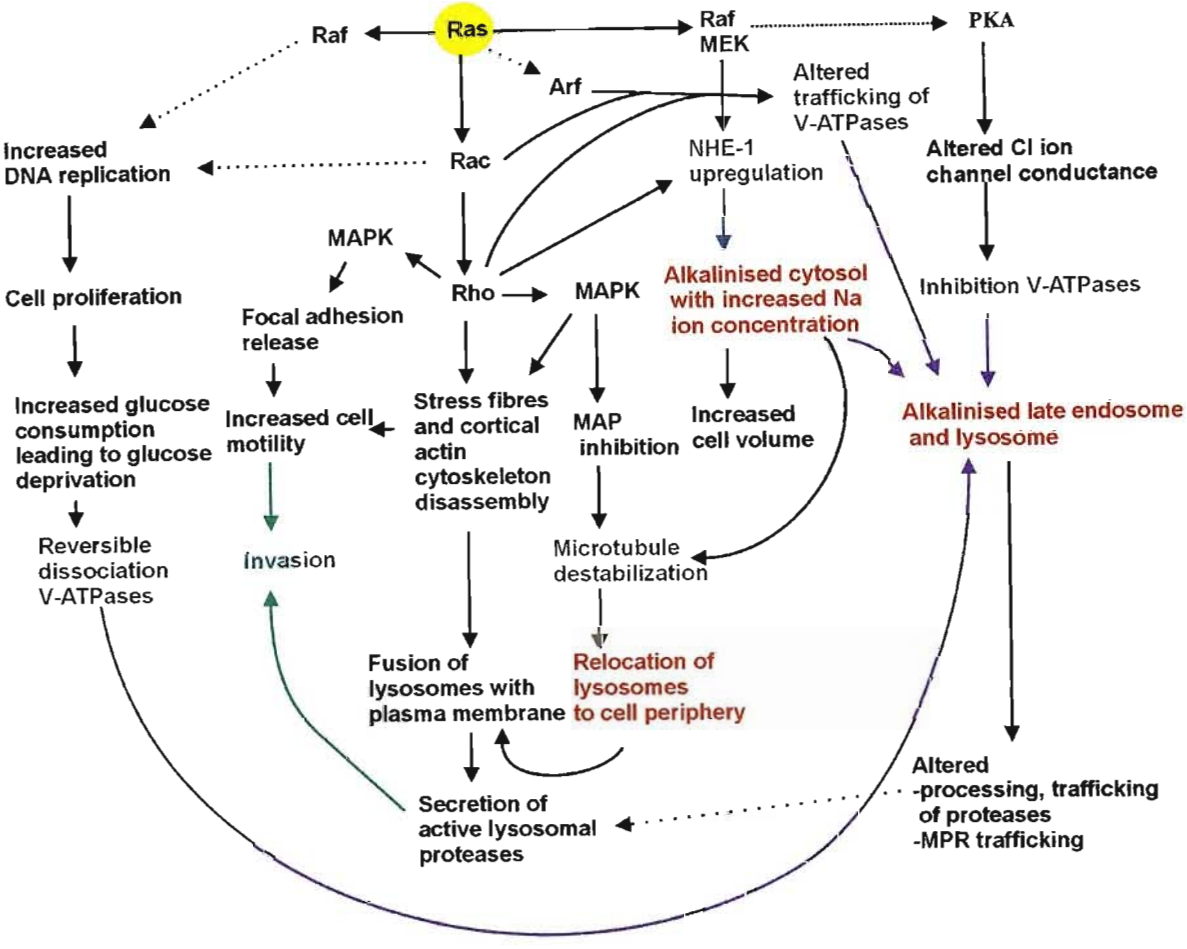

Figure 6.1 **Summary of effect of *ras*-transfection on cellular alkalinisation and invasion.** Diagram showing how the results obtained in this study (red) contribute to the understanding of the mechanisms involved with the invasive phenotype (green), in the context of the literature reviewed in this thesis (black, blue, purple, brown). Constitutively active Ras (yellow) may lead to upregulation of NHE-1 (blue) resulting in cytosolic alkalinisation (red), which may also contribute to microtubule destabilisation (brown) resulting in translocation of lysosomes to the cell periphery (red). Altered trafficking, reversible dissociation and/or inhibition of V-ATPases (purple) are the most likely mechanisms that lead to late endosome-lysosome alkalinisation (red), and the more alkaline cytosol (red) may also mean that there are fewer protons in the cell available for late endosome-lysosome acidification. The altered processing and trafficking of proteases resulting from late endosome-lysosome alkalinisation (red) and the relocation of lysosomes to the cell periphery (red) may lead to the secretion of these proteases, contributing to invasion (green). Abbreviations: MAPK = mitogen activated protein kinase; MEK = MAPK kinase; MAP = microtubule associated protein; PKA = protein kinase A; NHE-1 = Na^+/H^+-exchanger-1; V-ATPase = vacuolar H^+-ATPase; MPR = mannose-6-phosphate receptor.

In the present study on the effects of *ras*-transfection and pH of the endosome-lysosome system on cellular function, the following goals were achieved: 1) antibodies to be used for pH determination of endocytic organelles were developed and characterised, 2) these antibodies were applied to the MCF-10A and MCF-10AneoT cell lines, 3) the pH and morphology of the early endosome, late endosome and lysosome (using specific markers), was determined, and it was found that the late endosome and lysosome of the MCF-10AneoT cell line are alkalinised, 4) the peripheral lysosomal enzyme-containing organelles, the appearance of which accompanied *ras*-transfection, were as far as possible identified as lysosomes. In conclusion, it would seem that the increase in late endosome and lysosome pH and lysosome translocation towards the cell periphery is the result of *ras*-transfection (Fig. 6.1). *Ras*-transfection may also result in the downstream activation of NHE-1, which alters the cytosolic pH. The translocation of lysosomes to the cell periphery may be caused by the cytoskeleton, which may be affected by both pH and Ras downstream proteins (e.g. Rac and Rho).

Insights into how cancer cells become malignant allow novel strategies for the treatment of cancer to be developed. There are numerous therapeutic approaches currently available to treat cancer (e.g. irradiation, chemotherapy and immunotherapy), but the following section will be limited to those approaches where the insights gained by this study may find some application.

6.3 Cancer therapy

Drugs that inhibit the actions of a specific oncogene (in this case *ras*) or the proteases involved in malignancy are under constant development. Inhibition of the transporters responsible for the altered pH regulation of cancer cells, in combination with other anticancer agents, could also provide new therapeutic targets. Preferably, these drugs should ultimately result in the regression back to a normal phenotype, or in the total destruction of tumour cells with little or no toxicity to normal cells. The development of immunotherapy, however, as a way to use the patient's immune system to combat cancer, has come to the fore as the least toxic method of cancer treatment.

6.3.1 Ras inhibitors

Drugs aimed at Ras family proteins have predominantly been designed to inhibit the post-translational farnesylation event, which allows oncogenic Ras proteins to embed themselves within the plasma membrane and activate their signal transduction cascades to bring about cellular transformation. The drugs fall into two broad categories: 1) those that are derived from natural metabolites (e.g. bacterial manumycin and fungal gliotoxin); 2) synthetic peptidomimetic compounds that are structural analogues of the Ras family protein CaaX motif (Symons, 1995).

The peptidomimetic compounds show great promise in cancer therapy. They are non-toxic and may be synthesised in a way that increases their hydrophobicity to improve cellular uptake. They may also be used at very low concentrations that do not inhibit farnesylation of non-Ras proteins, e.g. nuclear lamins (Lerner *et al.*, 1995). These advantages make them more popular than conventional chemotherapeutic drugs that broadly target rapidly dividing cells. Certain peptidomimetics have the added advantage of being resistant to degradation by cellular proteases (Gibbs *et al.*, 1994). In addition to the above inhibitory compounds, monoterpenes, such as plant limonene, have been successfully used as competitive inhibitors of farnesyltransferase (FTase) in inhibiting the formation of mammary carcinomas induced by mutationally activated *ras* (Gould *et al.*, 1994).

Inhibitors of 3-hydroxy-3-methylglutaryl-coenzyme A reductase (HMG-CoA reductase inhibitors or statins) are usually used for the treatment of lipid disorders, although there is evidence that they may also be useful for treating Alzheimer's disease and osteoporosis (Simons *et al.*, 2001; Wolozin *et al.*, 2000; Coons, 2002). The potential of statins for cancer treatment is also under investigation. Statins inhibit HMG-CoA reductase, an enzyme that catalyses the conversion of HMG-CoA into mavelonate. The downstream product of the mavelonate pathway is farnesylpyrophosphate (FPP), a precursor of products such as cholesterol, ubiquinones and geranylgeranylpyrophosphate (GGPP) (Goldstein and Brown, 1990). FTase and geranylgeranyltransferase (GGTase) catalyse the addition of farnesyl and geranylgeranyl moieties from FPP and GPP to proteins (prenylation). Ras, Rho and the small G proteins use prenylation for activation (Section 1.1.1). Inhibitors of HMG-CoA reductase thus block the mevalonate pathway and consequently, Ras activation by decreasing the *in vivo* pools of FPP and GGPP (Gibbs *et al.*, 1994).

In vitro studies have also shown that statins can inhibit tumour growth by inducing either G1-arrest, G2-M-arrest or cell death via apoptosis (Jakobisiak *et al.*, 1991; Rao *et al.*, 1999; Park *et al.*, 2001; Kim *et al.*, 2000; Dimitroulakos *et al.*, 2001). Lovastatin (a drug of the statin family) arrests G1-S transition by increasing the expression of the cyclin-dependent kinase (Cdk) inhibitors p21 and p27 (Chang *et al.*, 1998; Gray-Bablin *et al.*, 1997; Weiss *et al.*, 1999; Hirai *et al.*, 1997; Laufs *et al.*, 1999). Besides G1 arrest, overexpression of p27 also induces apoptosis (Katayose *et al.*, 1997). Statins may also suppress the expression of MMP-9, uPA and uPAR (Wang *et al.*, 2000; Ganne *et al.*, 2000). Studies on numerous cell lines have demonstrated the ability of statins to reduce invasiveness in matrigel, cell migration and the ability of cells to attach to the ECM (Matar *et al.*, 1999; Prasanna *et al.*, 1996; Wang *et al.*, 2000; Kusama *et al.*, 2001; DeNoyelle *et al.*, 2001; Alonso *et al.*, 1998; Jani *et al.*, 1993; Wong *et al.*, 2001; Vincent *et al.*, 2001). *In vivo* studies have, furthermore, shown that statins can reduce metastasis (Matar *et al.*, 1999; Alonso *et al.*, 1998; Jani *et al.*, 1993; Kort *et al.*, 1989, Kusama *et al.*, 2002).

Since inhibition of Ras farnesylation was originally thought to be the mechanism by which statins prevented tumour growth, specific inhibitors of FTase (FTIs) were developed. FTIs reverse the morphological changes induced by constitutively active Ras, block anchorage-independent growth and induce apoptosis (Rose *et al.*, 2001; Suzuki *et al.*, 1998; Lebowitz *et al.*, 1997a; Wang and Macaulay, 1999; Gu *et al.*, 1999). It was originally presumed that FTase inhibitors only targeted Ras, but later reports suggest that RhoB may in fact be the critical target molecule. Unlike other Rho proteins that can only be geranylgeranylated, RhoB has the ability to exist in both geranylgeranylated and farnesylated forms (Lebowitz *et al.*, 1995) and FTIs result in decreased levels of farnesylated RhoB and increased levels of geranylgeranylated RhoB (Lebowitz *et al.*, 1997b). RhoB associates with intracellular vesicles via geranylgeranyl-, and with the plasma membrane via farnesyl moieties and cycles between the plasma membrane and the endosomal/prelysosomal vesicles in a similar manner to the geranylgeranylated Rab proteins (Adamson *et al.*, 1992). RhoB is thus a short-lived protein whose cellular localisation is affected by FTase inhibition and is necessary for Ras to maintain the transformed phenotype, since dominant inhibitory RhoB mutants inhibit Ras focal adhesion complex formation (Armstrong, 1995). Also, the kinetics of peptidomimetic-induced reversion of anchorage-independent growth in soft agar of v-Ha-*ras*-transformed human pancreatic adenocarcinoma cells is too rapid to be accounted for by a loss of membrane associated Ras protein (Kohl *et al.*, 1994). The short

half-life of RhoB (2 to 3 h) indicates that >95% of the vesicle bound protein could be depleted within the 18-24 h period required before phenotypic reversion is detectable. Ras, on the other hand, is a more stable protein and has a half-life of approximately 24 h (Armstrong, 1995). This mechanism has been questioned, however, since both geranylgeranylated and farnesylated RhoB can suppress tumour growth (Chen *et al.*, 2000).

The exact mechanisms whereby statins and FTIs inhibit cancer growth are yet to be established. This can probably be explained by cell line specificity and variations in experimental models. Also, differences in the mechanism of *ras*-transformation between murine and human cells have recently been discovered (Hamad *et al.*, 2002), meaning that mechanisms that were established using murine models (which have been very popular) need to be re-evaluated. Whatever the mechanisms of statin and FTI action, however, these drugs are undergoing successful clinical trials, especially in combination with other chemotherapeutics (reviewed Haluska *et al.*, 2002; Graaf *et al.*, 2004).

6.3.2 pH regulation

Tumour growth, invasion and metastasis are aided by intracellular alkalinisation and extracellular acidosis. Intracellular alkalinisation, among other effects discussed previously, prevents apoptosis while extracellular acidosis leads to the activation of secreted proteases that have acidic pH optima (e.g. cathepsins and MMPs) to degrade the ECM.

Tumour cells with low metastatic potential (e.g. MCF-10AneoT) have been shown to preferentially use NHE-1 for cytosolic pH regulation, while highly metastatic cells use plasma membrane V-ATPases that normally reside in acidic vesicles (Sennoune *et al.*, 2004). The presence of such V-ATPases in the plasma membrane are, therefore, involved in the acquisition of a more metastatic phenotype. In both c-Ha-*ras* transformants and highly metastatic cell lines apoptosis is inhibited by the prevention of intracellular acidosis, which is required by the pH-dependent endonucleases to induce DNA fragmentation, thus ensuring tumour cell survival (Ostad *et al.*, 1996; Lang *et al.*, 2000; Izumi *et al.*, 2003). Drugs that inhibit NHE-1 and V-ATPases, therefore, show promise as anticancer therapeutic agents.

NHE inhibitors generally fall into two classes. The first is amiloride and its derivatives that non-specifically inhibit all NHE isoforms and the second is guamidine and its derivatives, of which benzoylguamidine is specific for NHE-1 (Izumi *et al.*, 2003). The drug troglitazone has also been shown to inhibit NHE-1 in breast carcinoma-derived cell lines, inducing cellular acidosis and resulting in decreased proliferation (Turturro *et al.*, 2004).

V-ATPase inhibitors include: *N*-ethyl-maleimide, 7-nitro-1,2,3-benzoxadiazolyl-4-aminochloride, concanamycin A, bafilomycin A and salicylihalamide A, which is mammalian V-ATPase specific (Galloway *et al.*, 1983; Huss *et al.*, 2002; Bowman and Bowman, 2002; Xie *et al.*, 2004). Bafilomycin A1 and concanamycin A have been shown to inhibit growth and induce apoptosis in various human cell lines (e.g. Bowman *et al.*, 1988; Zhang *et al.*, 1992a,b; Drose *et al.*, 1993) and bafilomycin A1 has also been shown to increase the sensitivity of tumour cells to irradiation (Paglin *et al.*, 2001) and to enhance the effect of the anticancer drug TAS-103 (Torigoe *et al.*, 2002).

Overexpression of V-ATPases on the cell surface and increased cytosolic pH have, besides their involvement in invasion and metastasis, been implicated in the multidrug resistance (MDR) of many tumour cells (Murakami *et al.*, 2001; Moriyama, 1996). The ionophore monensin (see Section 4.3) has been used to overcome MDR in human breast tumour cell lines (Shaik *et al.*, 2004) and to inhibit the proliferation of various cancer cell lines (Park *et al.*, 2002a,b, 2003a,b,c). In cells with MDR, the weak bases daunomycin, doxorubicin and vinblastine (anticancer agents) accumulate in acidic vesicles and are removed from the cell via exocytosis, reducing their action (Willingham *et al.*, 1986). The V-ATPase inhibitor bafilomycin A1 prevents the accumulation of these anticancer agents (Marquardt and Center, 1991; Martinez-Zaguilan *et al.*, 1999; Raghunand *et al.*, 1999).

The prevention of extracellular acidosis by NHE and V-ATPase inhibitors may also decrease invasion by reducing the activity of secreted proteases. Further inhibition of proteases, thus preventing the spread of tumours, may provide another strategy that may be used in cancer therapy. The local containment of these tumours then allows for surgical removal.

6.3.3 Cysteine protease inhibitors

Evidence on the role of the endogenous cysteine protease inhibitors in tumours remains contradictory, as inhibitor activity is sometimes elevated and sometimes decreased in tumours. The effect not only depends on the balance between proteases and their endogenous inhibitors, but also on the kinetics of the interactions between the proteases and their inhibitors. Lah *et al.* (1989) have shown that stefin A, purified from human sarcoma, has reduced inhibitory activity against papain and cathepsin B. This seems to be because of higher inhibition constants, reflecting a slower rate of association and a faster rate of dissociation between the enzyme and inhibitors. Cysteine protease inhibitors are frequently secreted from tumours, but often do not seem to have the desired effect of inhibiting proteolysis. It is suggested that this may be a physiological attempt by the tumour to regulate the balance between the proteases and inhibitors. The inhibitors may function as a "reservoir" for the secreted proteases, protecting them from autocatalytic breakdown, and releasing them in an activated form (Turk *et al.*, 1994; Berquin and Sloane, 1994).

Endogenous protease inhibitors occur naturally, and appear always to be proteinaceous, while non-physiological inhibitors are either chemically synthesised or produced by other organisms. In the MCF-10AneoT cell line, degradation of the ECM may occur both intracellularly and extracellularly, partially due to the activity of cathepsin B, found in the endocytic pathway and outside the cell, contributing to invasion (Premzl *et al.*, 2003). Synthetic cathepsin B inhibitors that target intracellular activity are more effective at reducing invasion than those that inhibit only extracellular cathepsin B, though inhibitors of both intracellular and extracellular activity are most effective (Bervar *et al.*, 2003; Szpaderska and Frankfater., 2001; Premzl *et al.*, 2003).

Chicken cystatin inhibits both cathepsin B and L, and since its partial internalisation by tumour cells can also inhibit intracellular cysteine proteases, it can substantially reduce invasion (Premzl *et al.*, 2003; Sameni *et al.*, 2000). This inhibition, however, occurs only at concentrations that are not viable for *in vivo* use. A delivery system resulting in high intracellular levels of inhibitor could improve the therapeutic potential of cystatin. The incorporation of cystatin into poly(lactide-co-glycolide) nanoparticles (PLGA NPs) has been shown to internalise more rapidly into cells than free cystatin, protect the inhibitor against proteolytic degradation and aggregation, and enable a sustained inhibitor release

into cells (Cegnar *et al.*, 2004). PLGA NP technology could also be used with other inhibitors but further study is required to lower toxicity, increase loading capacity and prolong the release of the active ingredient before clinical trials can be contemplated.

Prodrug inhibitors, which require activation by proteases, represent an alternative approach. This type of inhibitor utilises the phenotypic characteristic of malignant cells, the expression of proteases on the cell surface. In one such case, cathepsin B is used to trigger the action of α-haemolysin, a pore-forming toxin resulting in permeabilisation and cell death (Panchal *et al.*, 1996).

Another approach has been to inhibit the secretion of the proteases rather than their activity. One study used estramustine to prevent the secretion of type IV collagenase from mouse melanoma and human prostate carcinoma, thereby preventing the invasion of ECM barriers by interfering with the microtubular system responsible for the intracellular vesicular traffic and thus preventing the secretion of the protease (Wang and Stearns, 1988). The PI(3)K inhibitor, wortmannin, inhibits Rac1 activation by preventing guanine nucleotide exchange, interfering with Rho functioning and the sorting and transport of lysosomal proteases (Symons, 1995; Brown *et al.*, 1995) and could similarly be used to prevent protease secretion.

The use of protease inhibitors appears to have limited application, however, owing to the fact that prolonged administration of these compounds may lead to toxicity. Protease inhibitors are also often relatively non-specific and many of the target proteases are involved in normal, non-pathological tissue remodelling and repair, reproduction, menstruation and blood coagulation (Marbaix *et al.*, 1996). Despite the toxicity associated with the use of protease inhibitors in chemotherapy, a number of protease inhibitors have undergone limited clinical trials. Examples are, Batimastat, a metalloproteinase inhibitor (Brown, 1994), α_1-antitrypsin inhibitor, hirudin (a thrombin inhibitor) (DeClerck and Imren, 1994) and the Bowman-Birk soybean proteinase inhibitor (Kennedy, 1994). Unfortunately, the therapeutic application of proteinase inhibitors has met with very little success and their application is likely to be very limited. The alternative approach is to use immunotherapy

6.3.4 Immunotherapy

$CD8^+$ cytotoxic T lymphocytes (CTLs) are able to lyse tumour cells directly upon recognition of the peptide-MHC class I complexes expressed by a tumour. This enables them to eradicate large tumour masses *in vivo*, and resulted in much attention being given to the role of $CD8^+$ CTLs in cancer immunity (reviewed by Pardoll and Topalian, 1998; Davis *et al.*, 2003; Mapara and Sykes, 2004). Less attention has been given to $CD4^+$ T helper (Th) cells for immunotherapy.

Reports on cytokine-secreting tumour cell vaccines, however, provide evidence for the participation of Th cells in generating and maintaining anti-tumour immunity (Topalian, 1994). Generating autoantibodies against autoantigens for vaccination of cancers, where vaccination with a tumour specific antigen induces both autoimmunity and tumour eradication, depends on both antibody and $CD4^+$ T cells. Furthermore, the immune response to less immunogenic proteins displays a more pronounced dependency on "help" from $CD4^+$ T cells (Overwijk *et al.*, 1999). The fact that the multiple antigens expressed by a certain tumour elicits an immune response in a cancer patient, has made it evident that the recognition of tumour antigens is not the limiting step in immune responses against tumours. Rather, it seems to be the effectors (i.e. cytokines) of the immune system that are responsible for the failure of the cancer patient's immune system to prevent or control cancer (Sahin *et al.*, 1997).

During the early stages of tumour development, inflammatory-like responses cause the infiltration of macrophages and polymorphonuclear cells, which in turn produce chemokines and cytokines. These stimulants induce the accumulation and expansion of T lymphocytes at the tumour site, resulting in either tumour eradication or progression. Many solid tumours are characterised by tumour-infiltrating lymphocytes (TILs) consisting of $CD4^+$ and $CD8^+$ T cells, which can be divided into tumour-specific and tumour-non-specific T cells (Goedegebuure and Eberlein, 1995).

Tumour-nonspecific TILs have specificity for non-tumour cells, within the tumour environment. The function of these cells is unknown but they could potentially affect the functional activity of tumour-specific T cells (Goedegebuure and Eberlein, 1995). $CD4^+$ T cells can be functionally distinguished and classified as Th0, Th1, and Th2 cells. $CD4^+$ Th1 cells produce interleuken-2 (IL-2) and interferon-γ (IFN-γ), and consequently support

the development of a cellular immune response. Th2 cells, on the other hand, produce IL-4, IL-5 and IL-10 and are critical for the development of a humoral immune response (Goedegebuure and Eberlein, 1995). The effect of an anti-tumour immune response, however, is also determined by the net effect of both the stimulatory and inhibitory responses. An understanding of the developmental pathways of $CD4^+$ TILs is, therefore, very important in the context of immunotherapy for cancer (Goedegebuure and Eberlein, 1995). Fig. 6.2 describes the integrated immune response to tumour cells, and explains the importance of the $CD4^+$ T cells in lending help to CTLs, IgG responses and maintaining immune memory.

Many vaccines have so far been designed to generate $CD8^+$ T cell responses. The importance of $CD4^+$ T cells should not be ignored, however, as they lend help to CTLs, induce IgG responses and maintain immune memory. They can also directly lyse target cells, or kill target cells via cytokine secretion (Pardoll and Topalian, 1998; Pieper *et al.*, 1999).

An important feature of either spontaneous or experimentally induced autoimmunity is the ability to break tolerance, which is highly dependent on the autoantigen chosen (Pardoll, 1999). Therefore, induction of autoimmune responses against tissue-specific self-antigens as a strategy for cancer immunotherapy would depend significantly on which antigen is chosen. Tumour antigens can be divided into four groups: 1) antigens unique to an individual patient's tumour; 2) antigens common to a histologically similar group of tumours; 3) tissue-differentiation antigens; 4) ubiquitous antigens expressed by normal and tumour cells (Berzofsky *et al.*, 2004). To specifically target tumours, the antigen must be expressed only on tumour cells e.g. mutated Ras and p53, and intensive research is underway to find other tumour-specific antigens. The major problem in inducing an anti-tumour response, however, is to break self-tolerance and many strategies have been developed. These include: inoculation with dendritic cells (APCs) already presenting tumour antigens and/or cytokines and the use of adjuvants (reviewed by Davis *et al.*, 2003; Berzofsky *et al.*, 2004).

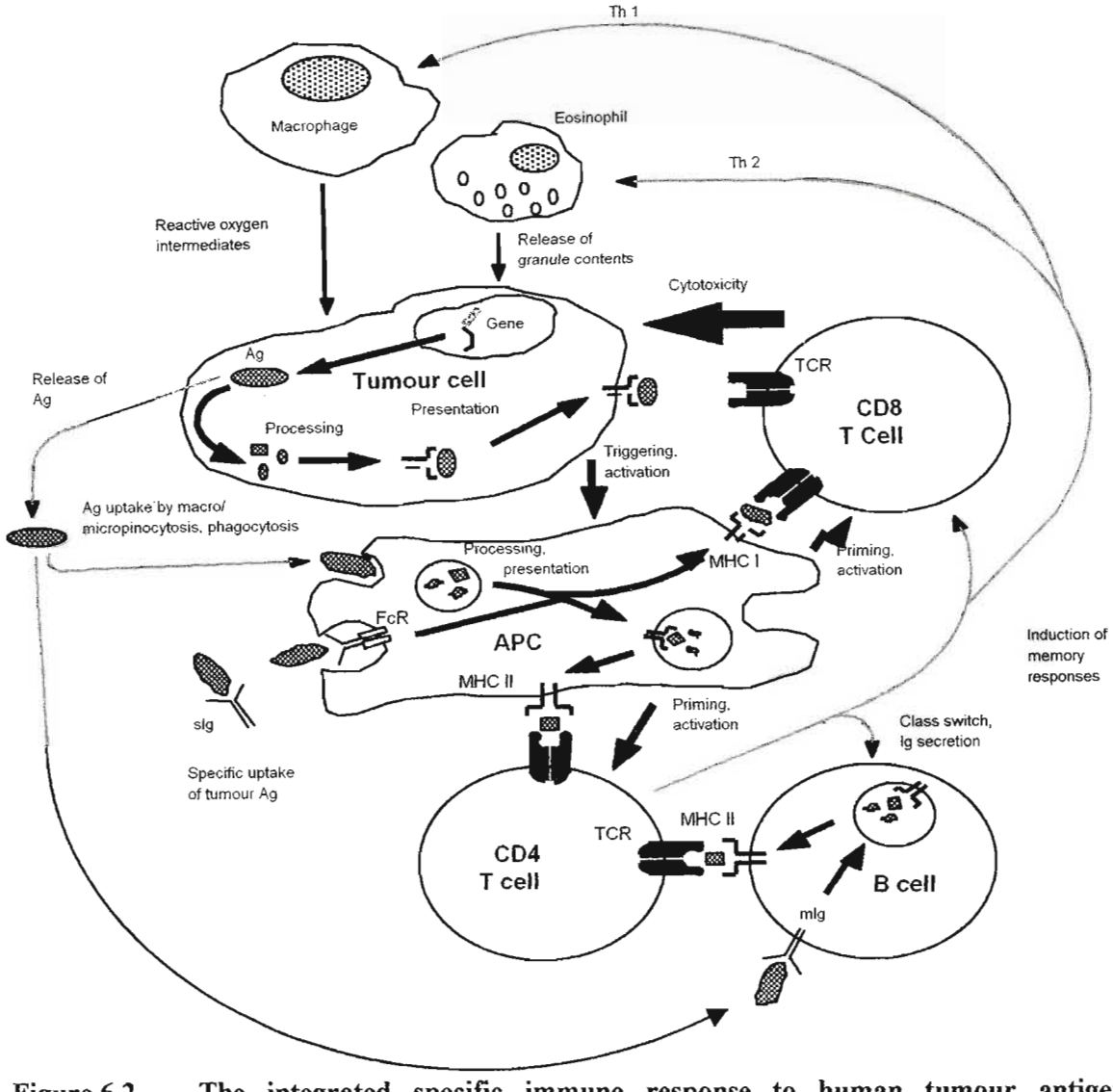

Figure 6.2 **The integrated specific immune response to human tumour antigens, involving $CD4^+$, $CD8^+$ T cells, B cells and APCs.**
(a) Tumour antigens are released by secretion, shedding, or tumour cell lysis, and are captured by APCs, by either (b) macro/micropinocytosis, phagocytosis or (e) via Fc-receptor mediated endocytosis of soluble immunoglobulin-antigen complexes. Endocytosed antigens are (d) processed and presented by either (e) MHC class I or (f) MHC class II molecules for priming and activation of $CD8^+$ and $CD4^+$ T cells respectively. (g) Uptake of antigen by B cells also occurs and is driven by membrane immunoglobulin leading to MHC class II antigen presentation to $CD4^+$ T cells. Antigen presentation to $CD4^+$ T cells by both (f) APCs and (g) B cells is critical for the immune response as it induces (h) class switching and the production and secretion of IgG and IgA antibodies by B cells and (i) long lasting T cell memory responses. In addition, (e) priming and activation of $CD8^+$ T cells by the APC, triggers (j) the cytotoxic activity of $CD8^+$ T cells inducing tumour cell lysis and augmentation of the immune response. (k) Primed $CD4^+$ T cells at sites of tumour metastasis, orchestrate effector function, involving, (l) Th1 cells that activate macrophages to produce reactive oxygen intermediates and (m) Th2 cells that activate eosinophils to release their granule contents (adapted from Moolman, 2002). Abbreviations: APC = antigen presenting cell; Ags = antigens; sIg = soluble immunoglobulin; MHC I = MHC class I; MHC II = MHC class II; mIg = membrane immunoglobulin.

Another strategy has been to modify the antigen. Any alterations in the structure of the self-antigen could make it more immunogenic. Belleli *et al.* (1990) inhibited tumour growth rate, invasion and metastasis in both B16 melanoma and Lewis lung carcinoma by inoculating mice with papain. Papain is a cysteine protease, and the antibodies produced against papain cross-reacted with both cathepsin B and H. Other modification strategies include: mutation of tumour antigens and addition of DNP to tumour cells (Houghton and Guevara-Patiño, 2004; Berd 2001; 2003)

Cationisation of the target antigen could also be used to alter the immunogenicity of self-antigens, although no research to date has been performed to discover if this is feasible for cancer immunotherapy. Work by Farmer *et al.* (1993) on human mononuclear cells showed that an antigen-specific proliferative response to cationised diphtheria toxoid is detected much earlier and at lower antigen concentrations than for the native antigen. This response was found to be HLA-DR-dependent with elevated production of a number of cytokines (IL-1β, IL-2 and IFN-γ). The enhanced proliferative response was attributed to $CD4^+$ Th cells. Their results demonstrate that cationisation of antigens enhances the ability to generate a cell-mediated immune response in humans, and could, therefore, be used in the design of immunotherapeutic treatments. If anti-self antibodies are required, the results reported in this thesis on raising anti-ovalbumin (anti-OVA) antibodies in chickens (Chapter 3) indicates that the anti-self response generated by inoculation with the cationised derivative may produce a more sustained, high titre response.

6.4 The way forward

Initially this study intended to determine which organelles of the endosome-lysosome system were alkalinised due to *ras*-transfection. As is the case with all scientific studies, each result poses further questions. These include:

- What is the pH of the other endosome-lysosome system organelles, such as the endosome carrier vesicle (ECV) or the recycling endosome? Are these organelles alkalinised in the MCF-10AneoT cell line relative to the MCF-10A cell line? These questions could be answered using the (2,4-dinitroanilino)-3'-amino-*N*-methyldipropylamine (DAMP) technique, described in this thesis, and Rab11 as a marker for the recycling endosome. A unique marker for the ECV is not yet available and, therefore, a combination of labelling for lysobisphosphatidic acid (LBPA) (which

is also present in the late endosome and lysosome) and morphology may be used to distinguish the ECV from other organelles of the endosome-lysosome system.

- Are the late endosome and lysosome (and possibly other organelles) of other *ras*-transfected cell lines alkalinised? This would help to establish whether the effects of *ras* on pH are universal to all cell types or limited only to human and murine fibroblasts, as determined by Jiang *et al.* (1990), and human breast epithelial cells. This could be determined by applying Oregon Green® 488 dextran (OGD) uptake and/or the DAMP technique to *ras*-transfected cell lines established from different organs (e.g. oesophagus) from different species.
- What is the distribution of lysosome-associated membrane protein-1 (LAMP-1) in the MCF-10A and MCF-10AneoT cell lines? Do organelles containing LAMP-1 also move to the periphery and cell surface in MCF-10AneoT cells? Does LAMP-1 co-localise with LAMP-2 and/or cathepsin B and D in the *ras*-transfected and non-transfected cell lines? These questions could be answered by immunolabelling for electron microscopy (EM). If differences in the localisation of LAMP-1 and LAMP-2 are found, this could indicate functional differences between the two proteins and the organelles that contain them.
- Is PI(3)K overexpressed in the MCF-10AneoT cell line? Would wortmannin, an inhibitor of PI(3)K, return the MCF-10AneoT cell line phenotype to the "normal" phenotype displayed by the MCF-10A cell line? PI(3)K is a downstream product of Ras (see Fig. 1.1) and seems to play a pivotal role in affecting vesicular trafficking, the regulation of the actin cytoskeleton, and monogenesis (Siddhanta *et al.*, 1998). Furthermore, PI(3)K has been implicated in the trafficking of lysosomal enzymes (Davidson, 1995). PI(3)K also acts to activate Na^+/H^+ exchange (Paris and Pouysségur, 1984; Moolenar *et al.*, 1984), resulting in an increase in the cytosolic pH. The expression of PI(3)K could be examined using western and northern blotting techniques. The effects of wortmannin treatment on protease trafficking and the morphology of the MCF-10AneoT cell line could be detected by immunolabelling for cathepsins and LAMPs (both EM and fluorescence microscopy), as well as for tubulin and actin (fluorescent microscopy). An alternative to immunolabelling to detect any changes in the actin cytoskeleton would be the use of fluorescent-tagged phalloidin, a mushroom poison that binds with high affinity to microfilaments.

- Now that markers for the early endosome, late endosome and lysosome of the MCF-10A and MCF-10AneoT cell lines have been defined, what is the cellular distribution of the cathepsins? The localisation of cathepsins B and D have been established (Sameni *et al.*, 1995; Moin *et al.*, 1994; Sloane *et al.*, 1994a,b; Elliott and Sloane, 1996). Cathepsin H, on the other hand, is enriched in the early endosomes of macrophages (Claus *et al.*, 1998), but the distribution and expression of cathepsin H is relatively unknown for the *ras*-transfected MCF-10AneoT cell line. The relative distribution of cathepsin H may be determined using immunolabelling for EM.
- Will cationisation of a self-antigen to elicit an immune response be a feasible approach for cancer immunotherapy? It would first have to be determined if the anti-self response declines when inoculations cease (Chapter 3) before testing whether cationisation of self-antigens, specific for a tumour type, are effective for anti-tumour immune responses without inducing autoimmune disease. Cationisation could also be useful for passive immunisation, i.e. immunotherapies where the antibodies to tumour antigens are introduced into the patient. The increased antibody titres produced using inoculation of cationised antigens into *in vitro* systems could decrease production costs for pharmaceutical companies. This issue may be addressed by comparing the antibody titres produced using cationised and non-cationised tumour antigens *in vitro*, the relative specificity of the antibodies produced, their effectiveness in reducing tumours and the production costs involved in raising these antibodies.

There are many unanswered questions, and research such as this illuminates a small aspect of the greater study into the cause, effects and treatment of cancer. A better understanding of the cellular mechanisms of cancer can only lead to the development of better treatment for cancer victims, and ultimately either vaccines or cures which would make cancer a non-lethal disease.

REFERENCES

Abbas A.K., Lohr J., Knoechel B. and Nagabhushanam V. (2004). T cell tolerance and autoimmunity. Autoimmun. Rev. 3: 471-475.

Achkar C., Gong Q., Frankfater A. and Bajkowski A.S. (1990). Differences in targeting and secretion of cathepsin B and L by BALB/3T3 fibroblasts and moloney murine sarcoma virus transformed BALB/3T3 fibroblasts. J. Biol. Chem. 265: 13650-13654.

Adamson P., Paterson H.F. and Hall A. (1992). Intracellular localization of the $P21^{rho}$ proteins. J. Cell Biol. 119: 617-627.

Ahn K., Yeyeodu S., Collette J., Madden V., Arthur J., Li L. and Erickson A.H. (2002). An alternate targeting pathway for procathepsin L in mouse fibroblasts. Traffic 3: 147-159.

Akasaki K. and Tsuji H. (1998). Purification and characterization of a soluble form of lysosome-associated membrane glycoprotein-2 (LAMP-2) from rat liver lysosomal contents. Biochem. Mol. Biol. Int. 46: 197-205.

Akifusa S., Ohguchi M., Koseki T., Nara K., Semba I., Yamoto K., Okahashi N., Merino R., Núñez G., Hanada N., Takehara T. and Nishihara T. (1998). Increase in Bcl-2 level promoted by CD40 ligation correlated with inhibition of B cell apoptosis induced by vacuolar type H^+-ATPase inhibitor. Exp. Cell Res. 238: 82-89.

Allison A.C. and Young M.R. (1969). Vital staining and fluorescence microscopy. In Lysosomes in Biology and Pathology volume 2. (Eds. Dingle J.T. and Fell H.B.), 600-628.

Alonso D.F., Farina H.G., Skilton G., Gabri M.R., De Lorenzo M.S. and Gomez D.E. (1998). Reduction of mouse mammary tumor formation and metastasis by lovastatin, an inhibitor of the mavelonate pathway of cholesterol synthesis. Breast Cancer Res. Treat. 50: 83-93.

Altmann K.G. (1993). Effect of cationization on anti-hapten antibody responses in sheep and mice. Immunol. Cell Biol. 71: 517-525.

Altstiel L. and Branton D. (1983). Fusion of coated vesicles with lysosomes: measurement with a fluorescent assay. Cell 32: 921-929.

Amano M., Ito M., Kimura K., Fukata Y., Chihara K., Nakano T., Matsuura Y. and Kaibuchi K. (1996). Phosphorylation and activation of myosin by Rho-associated kinase (Rho-kinase). J. Biol. Chem. 271: 20246-20249.

Anderson N.G., Maller J., Tonk N. and Sturgill T. (1990). Requirement for integration of signals from two distinct phosphorylation pathways for activation of MAP kinase. Nature 343: 651-653.

Anderson R.G.W. (1989). Postembedding detection of acidic compartments. Methods Cell Biol. 31: 463-472.

Anderson R.G.W. and Orci L. (1988). A view of acidic intracellular compartments. J. Cell Biol. 106: 539-543.

Anderson R.G.W. and Pathak R.K. (1985). Vesicles and cisternae in the *trans* Golgi apparatus of human fibroblasts are acidic compartments. Cell 40: 635-643.

Anderson R.G.W., Falck J.R., Goldstein J.L. and Brown M.S. (1984). Visualization of acidic organelles in intact cells by electron microscopy. Proc. Nat. Acad. Sci. USA 81: 4824-4838.

Andrews N.W. (2000). Regulated secretion of conventional lysosomes. Trends Cell Biol. 10: 316-321.

Aniento F., Emans N., Griffiths G. and Gruenberg J. (1993). Cytoplasmic dynein-dependent vesicular transport from early to late endosomes. J. Cell Biol. 123: 1373-1387.

Apple R.J., Domen P.L., Muckerheide A. and Michael J.G. (1988). Cationization of protein antigens IV: increased antigen uptake by antigen-presenting cells. J. Immunol. 140: 3290-3295.

Arends M.J., McGregor A.H. and Wyllie A.H. (1994). Apoptosis is inversely related to necrosis and determined net growth in tumors bearing constitutively expressed myc, ras, and HPV oncogenes. Am. J. Pathol. 144: 1045-1057.

Arends M.J., Morris R.G. and Wyllie A.H. (1990). Apoptosis. The role of the endonuclease. Am. J. Pathol. 136: 593-608

Arighi C.N., Hartnell L.M., Aguilar R.C., Haft C.R. and Bonifacino J.S. (2004). Role of the mammalian retromer in sorting of the cation-independent mannose 6-phosphate receptor. J. Cell. Biol. 165: 123-133.

Armstrong S.A. (1995). Geranylgeranyltransferase I transfers farnesyl as efficiently as geranylgeranyl to RhoB. J. Biol. Chem. 270: 764-7868.

Arpin M., Algrain M. and Louvard D. (1994). Membrane-actin microfilament connections: an increasing diversity of players related to band 4.1. Curr. Opin. Cell Biol. 6: 136-141.

Augenbraun E., Sulzer D., Rayport S., Setlik W. and Holtzman E. (1990). Experiments on the use of DAMP to study retina and cultured neurons. J. Histochem. Cytochem. 38: 1927-1931.

Bader M., Doussau F., Chasserot-Golaz S., Vitale N. and Gasman S. (2004). Coupling actin and membrane dynamics during calcium-regulated exocytosis: a role for Rho and ARF GTPases. Biochim. Biophys. Acta 1742: 37-49.

Bae H.R. and Verkman A.S. (1990). Protein kinase A regulates chloride conductance in endocytic vesicles from proximal tubule. Nature 348: 637-639.

Bagshaw R.D., Mahuran D.J. and Callahan J.W. (2005). A proteomic analysis of lysosomal integral membrane proteins reveals the diverse composition of the organelle. Mol. Cell. Proteomics 4: 133-143.

Bakker A.C., Webster P., Jacob W.A. and Andrews N.W. (1997). Homotypic fusion between aggregated lysosomes triggered by elevated $[Ca^{2+}]_i$ in fibroblasts. J. Cell Sci. 110: 2227-2238.

Baranski T.J., Faust P.I. and Kornfeld S. (1990). Generation of a lysosomal enzyme targeting signal in the secretory protein pepsinogen. Cell 63: 281-291.

Barasch J., Gerhon M.D., Nunez E.A., Tamir H. and Al-Awqati Q. (1988). Thyrotropin induces the acidification of the secretory granules of parafollicular cells by increasing the chloride conductance of the granular membrane. J. Cell Biol. 107: 2137-2147.

Barasch J., Kiss B., Prince A., Saiman L., Gruenert D. and Al-Awqati Q. (1991). Defective acidification of intracellular organelles in cystic fibrosis. Nature 352: 70-73.

Barbacid M. (1987). *Ras* Genes. Ann. Rev. Biochem. 56: 779-827.

Barbier M.A., Kohn A.D., Roth R.A. and Stahl P.D. (1998). Protein kinase B/akt and Rab5 mediate Ras activation of endocytosis. J. Biol. Chem. 273: 19367-19370.

Barriocanal J.G., Bonifacino J.S., Yuan L. and Sandoval I.V. (1986). Biosynthesis, glycosylation, movement through the Golgi system, and transport to lysosomes by an *N*-linked carbohydrate-independent mechanism of three lysosomal integral membrane proteins. J. Biol. Chem. 261: 16755-16763.

Barry M.A. and Eastman A. (1992). Endonuclease activation during apoptosis: the role of cytosolic Ca^{2+} and pH. Biochem. Biophys. Res. Commun. 186: 782-789.

Basolo F., Elliot J., Tait L., Chen Q.C., Maloney T.M., Russo I.H., Pauley R., Momiki S., Caamano J., Klein-Szanto A.J.P., Koszalka M. and Russo J. (1991). Transformation of human breast epithelial cells by c-Ha-*ras* oncogene. Mol. Carcinog. 4: 25-35.

Bass P.S., Drake A.F., Wang Y., Thomas J.H. and Davies D.R. (1990). Cationization of bovine serum albumin alters its conformation as well as its charge. Lab. Inves. 62: 185-188.

Basu S.K., Goldstein J.L., Anderson R.G.W. and Brown M.S. (1981). Monensin interrupts the recycling of low density lipoprotein receptors in human fibroblasts. Cell 24: 493-502.

Bellelli A., Mattioni M., Rusconi V., Sezzi M.L. and Bellelli L. (1990). Inhibition of tumor growth, invasion and metastasis in papain-immunized mice. Invasion Metastasis 10: 142-169.

Berd D. (2001). Autologous, hapten-modified vaccine as a treatment for human cancers. Vaccine 19: 2565-2570.

Berd D. (2003). Contribution of dead cells to the immunogenicity of an autologous, hapten-modified melanoma vaccine. Vaccine 21: 795-797.

Berneman A., Guilbert B., Eschrich S. and Avrameas S. (1993). IgG auto- and polyreactivities of normal human sera. Mol. Immunol. 16:1499-1510.

Berquin I.M. and Sloane B.F. (1994). Cysteine proteases and tumor progression. Persp. Drug Disc. Design 2: 371-388.

Bervar A., Zajc I., Sever N., Katunuma N., Sloane B.F. and Lah T.T. (2003). Invasiveness of transformed human breast epithelial cell lines is related to cathepsin B and inhibited by cysteine proteinase inhibitors. Biol. Chem. 384: 447-455.

Berzofsky J.A., Terabe M., Oh S., Belyakov I.M., Ahlers J.D., Janik J.E. and Morris J.C. (2004). Progress on new vaccine strategies for the immunotherapy and prevention of cancer. J. Clin. Invest. 1515-1525.

Bickel U., Lee V.M., Trojanowski J.Q. and Pardridge W.M. (1994). Development and *in vitro* characterization of a cationized monoclonal antibody against βA4 protein: a potential probe for Alzheimer's disease. Bioconjug. Chem. 5: 119-125.

Birnbaumer L., Abramowitz J. and Brown A.M. (1990). Receptor-effector coupling by G proteins. Biochim. Biophys. Acta 1031: 163-224.

Boguski M.S. and McCormick F. (1993). Proteins regulating Ras and its relatives. Nature 366: 643-654.

Border W.A., Ward H.J., Kamil E.S. and Cohen A.H. (1982). Induction of membranous nephropathy in rabbits by administration of an exogenous cationic antigen. J. Clin. Inves. 69: 451-461.

Boss W.F., Morré D.J. and Mollenhauer H.H. (1984). Monensin-induced swelling of Golgi apparatus cisternae mediated by a proton gradient. Eur. J. Cell Biol. 34: 1-8.

Bottger G., Nagelkerken B. and van der Sluijs P. (1996). Rab4 and Rab7 define distinct nonoverlapping endosomal compartments. J. Biol. Chem. 271: 29191-29197.

Bowman B.J. and Bowman E.J. (2002). Mutations in subunit c of the vacuolar ATPase confer resistance to bafilomycin and identify a conserved antibiotic binding site. J. Biol. Chem. 177: 3965-3972.

Boyer R.F. (1993). In Modern Experimental Biochemistry (second edition). Benjamin/Cummings Publishing Co., California, 42-51.

Bradford M.M. (1976). A rapid and sensitive method for the quantitation of microgram quantities of protein utilizing the principle of protein-dye binding. Anal. Biochem. 72: 248-254.

Braell W.A. (1987). Fusion between endocytic vesicles in a cell-free system. Proc. Natl. Acad. Sci. USA 84: 1137-1141.

Braulke T., Geuze H.J., Slot J.W., Hasilik A. and von Figura K (1987). On the effects of weak bases and monensin on sorting and processing of lysosomal enzymes in human cells. Eur. J. Cell Biol. 43: 316-132.

Bretscher A. (1991). Microfilamemt structure and function in the cortical cytoskeleton. Annu. Rev. Cell Biol. 7: 337-374.

Bretscher A. (1993). Microfilaments and membranes. Curr. Opin. Cell Biol. 5: 653-660.

Bright N.A., Gratian M.J. and Luzio J.P. (2005). Endocytic delivery to lysosomes mediated by concurrent fusion and kissing events in living cells. Curr. Biol. 15: 360-365.

Bright N.A., Reaves B.J., Mullock B.M. and Luzio J.P. (1997). Dense core lysosomes can fuse with late endosomes and are re-formed from the resultant hybrid organelles. J. Cell Sci. 110: 2027-2040.

Brorson S.H., Roos N. and Skjorten F. (1994). Antibody penetration into LR White sections. Micron. 25: 453-460.

Brown J.B., DeWald D.B., Emr S.D., Plutner H. and Balch W.E. (1995). Role for phosphatidylinositol 3-kinase in the sorting and transport of newly synthesized lysosomal enzymes in mammalian cells. J. Cell Biol. 130: 781-796.

Brown P.D. (1994). Preclinical and clinical studies on the matrix metalloproteinase inhibitor, batimastat (BB-94). Ann. NY Acad. Sci. 732: 217-221.

Brunner G., Heidrich H.G., Golecki J.R., Bauer H.C., Suter D., Pluckhahn P. and Ferber E. (1977). Fractionation of membrane vesicles II. A simple method for separation of membrane vesicles bearing different enzymes by free flow electrophoresis. Biochim. Biophys. Acta. 471: 195-212.

Brunton V.G., MacPherson I.R.J and Frame M.C. (2004). Cell adhesion receptors, tyrosine kinases and actin modulators: a complex three-way circuitry. Biochim. Biophys. Acta 1692: 121-144.

Bucci C., Parton R.G., Mather I.H., Stunnenburg H., Simons K., Hoflack B. and Zerial M. (1992). The small GTPase rab5 functions as a regulatory factor in the early endocytic pathway. Cell 70: 715-728.

Burck K.B., Liu E.T. and Larrick J.W. (1988). In Oncogenes: An Introduction to the Concept of Cancer Genes. Springer-Verlag, New York.

Burd C.G. and Emr S.D. (1998). Phosphatidylinositol(3)-phosphate signaling mediated by specifc binding to RING FYVE domains. Mol. Cell 2: 157-162.

Burkhardt J.K., Echeverri C.J., Nilsson T. and Vallee R.B. (1997). Overexpression of the dynamitin (p50) subunit of the dynactin complex disrupts dynein-dependent maintenance of membrane organelle distribution. J. Cell Biol. 139: 469-484.

Busch G.L., Schreiber R., Dartch P.C., Völkl H., vom Dahl S., Häussinger D. and Lang F. (1994). Involvement of microtubules in the link between cell volume and pH of acidic cellular compartments in rat and human hepatocytes. Proc. Natl. Acad. Sci. USA 91: 9165-9169.

Butor C., Griffiths G., Aronson Jr. N.N. and Varki A. (1995). Co-localisation of hydrolytic enzymes with widely disparate pH optima: implications for the regulation of lysosomal pH. J. Cell Sci. 108: 2213-2219.

Callaghan J., Simonsen A., Gaullier J.M., Toh B.H. and Stenmark H. (1999). The endosome fusion regulator earlyendosomal autoantigen 1 (EEA1) is a dimer. Biochem. J. 338: 539-543.

Caplan M.J., Stow J.L., Newman A.P., Madri J., Anderson H.C., Farquhar M.G., Palade G.E. and Jamieson J.D. (1987). Dependence on pH of polarized sorting of secreted proteins. Nature 329: 632-635.

Capony F., Braulke T., Rouget C., Roux S., Montcourrier P. and Rochefort H. (1994). Specific mannose 6-phosphate receptor-independent sorting of pro-cathepsin D in breast cancer cells. Exp. Cell Res. 215: 154-163.

Carlsson S.R. and Fukuda M. (1989). Structure of human lysosomal membrane glycoprotein 1: assignment of disulfide bonds and visualization of its domain arrangement. J. Biol. Chem. 264: 20526-20531.

Carlsson S.R. and Fukuda M. (1990). The polylactosaminoglycans of human lysosomal membrane glycoproteins, lamp-1 and lamp-2: localization on the peptide backbones. J. Biol. Chem. 265: 20488-20495.

Carlsson S.R., Lycksell P.O. and Fukuda M. (1993). Assignment of O-glycan attachment sites to the hinge-like regions of human lysosomal membrane glycoproteins lamp-1 and lamp-2. Arch. Biochem. Biophys. 304: 65-73.

Carlsson S.R., Roth J., Piller F. and Fukuda M. (1988). Isolation of human lysosomal membrane glycoproteins, h-lamp-1 and h-lamp-2. J. Biol. Chem. 263: 18911-18919.

Carragher N.O. and Frame M.C. (2004). Focal adhesion and actin dynamics: a place where kinases and proteases meet to promote invasion. Trends Cell Biol. 14: 241-249.

Casciola-Rosen L.A. and Hubbard A.L. (1991). Hydrolases in intracellular compartments of rat liver cells. Evidence for selective activation and/or delivery. J. Biol. Chem. 266: 4341-4347.

Casten L.A. and Pierce S.K. (1988). Receptor-mediated B cell antigen processing. Increased antigenicity of a globular protein covalently coupled to antibodies specific for B cell surface structures. J. Immunol. 140: 404-410.

Causton B.E. (1984). The choice of resins for electron immunocytochemistry. In Immunolabelling for Electron Microscopy. (Eds. Polak J.M. and Varndell I.M.). Elsevier Science Publishers, BV, 30-53.

Cegnar M., Premzl A., Zavašnik-Bergant V., Kristl J. and Kos J. (2004). Poly(lactide-co-glycolide) nanoparticles as a carrier system for delivering cysteine protease inhibitor cystatin into tumor cells. Exp. Cell Res. 301: 223-231.

Chambers A.F. and Matrisian L.M. (1997). Changing views of the role of matrix metalloproteinases in metastasis. J. Natl. Cancer Inst. 89: 1260-1270.

Chang E.H., Furth M.E., Scolnick E.M. and Lowry D.R. (1982). Tumorigenic transformation of mammalian cells induced by a normal human gene homologous to the oncogene of Harvey murine sarcoma virus. Nature 297: 479-483.

Chang M.Y., Jan M.S., Won S.J. and Liu H.S. (1998). Ha-rasVal12 oncogene increases susceptibility of NIH/3T3 cells to lovastatin. Biochem. Biophys. Res. Commun. 248: 62-68.

Chavez R.A., Miller S.G. and Moore H.P. (1996). A biosynthetic regulated secretory pathway in constitutive secretory cells. J. Cell Biol. 133: 1177-1191.

Chavrier P., Parton R.G., Hauri H.P., Simons K. and Zerial M. (1990). Localization of low molecular weight GTP binding proteins to exocytic and endocytic compartments. Cell 62: 317-329.

Chen J.W., Murphy T.L., Willingham M.C., Pastan I. and August J.T. (1985). Identification of two lysosomal membrane glycoproteins. J. Biol. Chem. 101: 85-95.

Chen S.H., Bubb M.R., Yarmola E.G., Zuo J., Jiang J., Lee B.S., Lu M., Gluck S.L., Hurst I.R. and Holliday L.S. (2004). Vacuolar H^+-ATPase binding to microfilaments: regulation in response to phosphatidylinositol 3-kinase activity and detailed characterization of the actin-binding site in subunit B. J. Biol. Chem. 279: 7988-7998.

Chen Z., Sun J., Pradines A., Favre G., Adnane J. and Sebti S.M. (2000). Both farnesylated and geranylgeranylated RhoB inhibit malignant transformation and suppress human tumor growth in nude mice. J. Biol. Chem. 275: 17974-17978.

Chiang S.H., Baumann C.A., Kanzaki M., Thurmond D.C., Watson R.T., Neudauer C.L., Macara I.G., Pessin J.E. and Saltiel A.R. (2001). Insulin-stimulated GLUT4 translocation requires the CAP-dependent activation of Tc10. Nature 410: 944-948.

Childs T.J., Watson M.H., Sanghera J.S., Campbell D.L., Pelech S.L. and Mak A.S. (1992). Phosphorylation of smooth muscle caldesmon by mitogen-activated protein (MAP) kinase and expression of MAP kinase in differentiated smooth muscle cells. J. Biol. Chem. 267: 22853-22859.

Christensen K.A., Myers J.T. and Swanson J.A. (2002). pH-dependent regulation of lysosomal calcium in macrophages. J. Cell Sci. 115: 599-607.

Christoforidis S., McBride H.M., Burgoyne R.D. and Zerial M. (1999a). The rab5 effector EEA1 is a core component of endosome docking. Nature 397: 621-625.

Christoforidis S., Miaczynska M., Ashman K., Wilm M., Zhao L., Yip S.C., Waterfield M.D., Backer J.M. and Zerial M. (1999b). Phosphatidylinositol-3-OH kinases are Rab5 effectors. Nat. Cell Biol. 1: 249-252.

Chrzanowska-Wodnicka M. and Burridge K. (1996). Rho-stimulated contractility drives the formation of stress fibres and focal adhesions. J. Cell Biol. 133: 1403-1415.

Ciardiello F., McGeady M.L., Kim N., Basolo F., Hynes N., Langton B.C., Yokozaki H., Saeki T., Elliott J.W., Masui H., Mendelsohn J., Houle H., Russo J. and Salomon D.S. (1990). Transforming growth factor-α expression is enhanced in human mammary epithelial cells transformed by an activated c-Ha-*ras* protooncogene but not by the c-*neu* protooncogene, and overexpression of the transforming growth factor-α complementary DNA leads to transformation. Cell Growth and Differentiation 1: 407-420.

Clague M.J. (1998). Molecular aspects of the endocytic pathway. Biochem. J. 336: 271-282.

Claus V., Jahraus A., Tjelle T., Berg T., Kirschke H., Faulstich H. and Griffiths G. (1998). Lysosomal-enzyme trafficking between phagosomes, endosomes, and lysosomes in J774 macrophages. Enrichment of cathepsin H in early endosomes. J. Biol. Chem. 273: 9842-9851

Coetzer T.H.T. (1985). Preparation and characterisation of antibodies against mouse Ig (all classes). In Internal Report Bioclones, (Pty.) Ltd. Immunology group, Stellenbosch.

Cohen I.R. (1991). Autoimmunity to chaperonins in the pathogenesis of arthritis and diabetes. Annu. Rev. Immunol. 9: 567-89.

Cohen I.R. (1992). The cognitive paradigm and immunological homunculus. Immunol. Today 13: 490-494.

Cook N.R. and Davidson H.W. (2001). In vitro assays of vesicular transport. Traffic 1: 19-25.

Coons J.C. (2002). Hydroxymethylglutaryl-coenzyme A reductase inhibitors in oseoporosis management. Ann. Pharmacother. 36: 326-330.

Corbeil L.B., Bastida-Corcuera F.D. and Beveridge T.J. (1997). *Haemophilus somnus* immunoglobulin binding proteins and surface fibrils. Infect. Immun. 65: 4250-4257.

Corbel C. (1996). The avian model in the study of tolerance to self. In: Immunology and developmental biology of the chicken. (Eds. O. Vainio and B.A. Imhof). Springer-Verlag Berlin, 95-106.

Corley-Cain C. and Murphy R.F. (1988). A chloroquine-resistant Swiss 3T3 cell line with a defect in late endocytic acidification. J. Cell Biol. 106: 269-277.

Corley-Cain C., Spie D.M. and Murphy R.F. (1988). Regulation of endocytic pH by the Na^{+},K^{+}-ATPase in living cells. Proc. Natl. Acad. Sci. USA 86: 544-548.

Courtoy P.J. (1991). Dissection of endosomes. In Trafficking of Membrane Proteins. (Eds. Steer J.C. and Harford J.). Academic Press, New York, 103-156.

Courtoy P.J., Quintart J. and Baudhuin P. (1984). Shift of equilibrium density induced by 3,3'-diaminobenzidine cytochemistry: a new procedure for the analysis and purification of peroxidase-containing organelles. J. Cell Biol. 98: 870-876.

Cox A.D., Garcia A.M., Westwick J.K., Kowalczyk J.J., Lewis M.D., Brenner D.A. and Der C.J. (1994). The CAAX peptidomimetic compound B581 specifically blocks farnesylated, but not geranylgeranylated or myristylated, oncogenic Ras signalling and transformation. J. Biol. Chem. 269: 19203-19206.

Crowley E. and Horwitz A.F. (1995). Tyrosine phosphorylation and cytoskeletal tension regulate the release of fibroblast adhesions. J. Cell Biol. 131: 525-537.

Cunningham C.C. (1995). Actin polymerization and intracellular solvent flow in cell surface blebbing. J. Cell Biol. 129: 1589-1599.

Cuozzo J.W. and Sahagian G.G. (1994). Lysine is common determinant for mannose phosphorylation of lysosomal proteins. J. Biol. Chem. 269: 14490-14496.

D'Arrigo A., Bucci C., Toh B.H. and Stenmark H. (1997). Microtubules are involved in bafilomycin A1-induced tubulation and Rab5-dependent vacuolation of early endosomes. Eur. J. Cell Biol. 72: 95-103.

D'Souza S., Garcia-Cabado A., Yu F., Teter K., Lukacs G., Skorecki K., Moore H.P., Orlowski J. and Grinstein S. (1998). The epithelial sodium-hydrogen antiporter Na^{+}/H^{+} exchanger 3 accumulates and is functional in recycling endosomes. J. Biol. Chem. 273: 2035-2043.

Dahms N.M. (1996). Insulin-like growth factor II/cation-independent mannose 6-phosphate receptor and lysosomal enzyme recognition. Biochem. Soc. Trans. 24: 136-141.

Dahms N.M., Lobel P. and Kornfeld S (1989). Mannose-6-phosphate receptors and lysosomal enzyme targeting. J. Biol. Chem. 264: 12115-12118.

Darnell J., Lodish H. and Baltimore D. (1986). In Molecular Cell Biology. Scientific American Books, New York.

Daro E., van der Sluijs P., Galli T. and Mellman I. (1996). Rab 4 and cellubrevin define distinct populations of endosomes on the pathway of transferrin recycling. Proc. Natl. Acad. Sci. USA 93: 9559-9564.

Davey J., Hurtley S.M. and Warren G. (1985). Reconstitution of an endocytic fusion event in a cell-free system. Cell 43: 643-652.

Davidson H.W. (1995). Wortmannin causes mistargeting of procathepsin D. evidence for the involvement of a phosphatidylinositol 3-kinase in vesicular transport to lysosomes. J. Cell Biol. 130: 797-805.

Davis I.D., Jefford M., Parente P. and Cebon J. (2003). Rational approaches to human cancer immunotherapy. J. Leuk. Biol. 73: 3-29.

De Duve C. (1983). Lysosomes revisited. Eur. J. Biochem. 137: 391-397.

De Duve C., de Barsy T., Poole B., Trouet A., Tulkens P. and van Hoof F. (1974). Lysosomotropic agents. Biochem. Pharmacol. 23: 2495-2531.

Dearman R.J., Caddick H., Basketter D.A. and Kimber I. (2000). Divergent antibody isotype responses induced in mice by systemic exposure to proteins: a comparison of ovalbumin with bovine serum albumin. Food Chem. Toxicol. 38: 351-60.

Debnath J., Mills K., Collins N., Reginato S., Muthuswamy S.K. and Brugge J.S. (2002). The role of apoptosis in creating and maintaining luminal space within normal and oncogene-expressing mammary acini. Cell 111: 29-40.

Debnath J., Muthuswamy S.K. and Brugge J.S. (2003). Morphogenesis and oncogenesis of MCF-10A mammary epithelial acini grown in three-dimensional basement membrane cultures. Methods. 30: 256-268.

Decker R.S., Decker M.L., Thomas V. and Fuseler J.W. (1985). Responses of cultured cardiac myocytes to lysosomotropic compounds and methylated amino acids. J. Cell Sci. 74: 119-135.

DeClerck Y.A. and Imren S. (1994). Protease inhibitors: role and potential therapeutic use in human cancer. Eur. J. Cancer 30A: 2170-2180.

DeClerck Y.A., Imren S., Montgomery A.M., Mueller B.M., Reisfeld R.A. and Laug W.E. (1997). Proteases and protease inhibitors in tumor progression. Adv. Exp. Med. Biol. 425: 89- 97.

Dennison C. (2003). In A Guide to Protein Isolation. Kluwer Academic Publishers, Netherlands, 162-170.

DeNoyelle C., Vasse M., Korner M., Mishal Z., Ganne F., Vannier J.P., Soria J. and Soria C. (2001). Cerivastatin, an inhibitor of HMG-CoA reductase, inhibits the signaling pathways involved in the invasiveness and metastatic properties of highly invasive breast cancer cell lines: an in vitro study. Carcingogenesis 22: 1139-1148.

Der C.J., Finkel T. and Cooper G.M. (1986). Biological and biochemical properties of human rasH genes mutated at codon 61. Cell 44: 167-176.

Diaz E., Schimöller F. and Pfeffer S.R. (1997). A novel Rab9 effector required for endosome to TGN transport. J. Cell Biol. 138: 283-290.

Diaz R., Mayorga L. and Stahl P. (1988). *In vitro* fusion of endosomes following receptor-mediated endocytosis. J. Biol. Chem. 263: 6093-6100.

Dickson R.B., Hanover J.A., Willingham M.C. and Pastan I. (1983). Prelysosomal divergence of transferrin and epidermal growth factor during receptor-mediated endocytosis. Biochem. 22: 5667-5674.

Diekman D., Brill S., Garret M.D., Totty N., Hsuan J., Monfries C., Hall C., Lim L. and Hall A. (1991). Bcr encodes a GTPase activating protein for p21-rac. Nature 351: 400-402.

Diesenhofer J. (1981). Crystallographic refinement and atomic models of a human Fc fragment and its complex with fragment B of protein A *from Staphylococcus aureus* at 2.9- and 2.8-A resolution. Biochem. 20: 2361-2369.

Diment S., Leech M.S. and Stahl P.D. (1988). Cathepsin D is membrane-associated in macrophage endosomes. J. Biol. Chem. 263: 6901-6907.

Dimitroulakos J., Ye L.Y., Benzaquen M., Moore M.J., Kamel-Reid S., Freedman M.H., Yeger H. and Penn L.Z. (2001). Differential sensitivity of various pediatric cancers and squamous cell carcinomas to lovastatin-induced apoptosis: therapeutic implications. Clin. Cancer Res. 7: 158-167.

Dong J.M., Prence E.M. and Sahagian G.G. (1989). Mechanism for selective secretion of a lysosomal protease by transformed mouse fibroblasts. J. Biol. Chem. 264: 7377-7383.

Doppler W., Jaggi R., and Groner B. (1987). Induction of v-*mos* and activated Ha-*ras* oncogene expression in quiescent NIH 3T3 cells causes intracellular alkalinisation and cell-cycle progression. Gene 54: 147-153.

Draye J.P., Quintart J., Cowley P. and Baudheim P. (1987). Relations between plasma membrane and lysosomal membrane of covalently labeled plasma membrane protein. Eur. J. Biochem. 170: 395-403.

Drechsel D.N., Hyman A.A., Cobb M.H. and Kirschner M.W. (1992). Modulation of the dynamic instability of tubulin assembly by the microtubule-associated protein tau. Mol. Biol. Cell 3: 1141-1154.

Drose S., Bindseil K.U., Bowman E.J., Siebers A., Zeeck A. and Altendorf K.. (1993). Inhibitory effect of modified bafilomycins and concanamycins on P- and V-type adenosinetriphosphatases. Biochemistry. 32: 3902-3906.

Dunn K.W. and Maxfield F.R. (1992). Delivery of ligands from sorting endosomes to late endosomes occurs by maturation of sorting endosomes. J. Cell Biol. 117: 301-310.

Dunn K.W., McGraw T.E. and Maxfield F.R. (1989). Iterative fractionation of recycling receptors from lysosomally destined ligands in an early sorting endosome. J. Cell Biol. 109: 3303-3314.

Durrbach A., Louvard D. and Coudrier E. (1996). Actin filaments facilitate two steps of endocytosis. J. Cell Sci. 109: 457-465.

Dutartre H., Davoust J., Gorvel J.P. and Chavrier P. (1996). Cytokinesis arrest and redistribution of actin-cytoskeleton regulatory components in cells expressing the Rho GTPase CDC42Hs. J. Cell Sci. 109: 367-377.

Egan S.E., Broere J.J., Jarolim L., Wright J.A. and Greenberg A.H. (1989). Co-regulation of metastatic and transforming activity of normal and mutant ras genes. Int. J. Cancer 43: 443-448.

Elenbaas B., Spirio L., Koerner F., Fleming M.D., Zimonjic D.B., Donaher J.L., Popescu N.C., Hahn W.C. and Weinberg R.A. (2001). Human breast cancer cells generated by oncogenic transformation of primary mammary epithelial cells. Genes Dev. 15: 50-65.

Elliott E. (1993). A study of proteinases of invasive cells using cryoultramicrotomy and immunogold labelling. PhD thesis volume 2, University of Natal, Pietermaritzburg, South Africa.

Elliott E. and Sloane B.F. (1996). The cysteine protease cathepsin B in cancer. Persp. Drug Disc. Design 6: 12-32.

Engvall E. and Perlmann P. (1971). Enzyme-linked immunosorbent assay (ELISA): quantitative assay of immunoglobulin G. Immunocytochemistry 8: 871-874.

Escola J.M., Kleijmeer M.J., Stoorvogel W., Griffith J.M., Yoshie O. and Geuze H.J. (1998). Selective enrichment of tetraspan proteins on the internal vesicles of multivesicular endosomes and on exosomes secreted by human B lymphocytes. J. Biol. Chem. 273: 20121-20127.

Esser V., Kuwajima M., Britton C.H., Krishnan K., Foster D.W. and McGarry J.D. (1993). Inhibitors of mitochondrial carnitine palmitoyltransferase I limit the action of proteases on the enzyme: isolation and partial amino acid analysis of a truncated form of the rat liver isozyme. J. Biol. Chem. 268: 5810-5816.

Farmer J.L., Roberts L.A., Rydzinski M.E. and Hilty M.D. (1993). Human immune response to cationized proteins I: characterization of the *in vitro* response to cationized diphtheria toxoid. Cell. Immunol. 146: 186-197.

Febbraio M. and Silverstein R.L. (1990). Identification and characterization of LAMP-1 as an activation-dependent platelet surface glycoprotein. J. Biol. Chem. 265: 18531-18537.

Feng Y., Press B. and Wandinger-Ness A. (1995). Rab7: an important regulator of late endocytic membrane traffic. J. Cell Biol. 131: 1435-1452.

Fensome A., Cunningham E., Prosser S., Khoon Tan S., Swigart P., Thomas G., Hsuan J. and Cockcroft S. (1996). ARF and PITP restore GTP-γ-S-stimulated protein secretion from cytosol-depleted HL60 cells by promoting PIP_2 synthesis. Curr. Biol. 6: 730-738.

Ferguson T.A., Peters T., Reed R., Pesce A.J. and Michael J.G. (1983). Immunoregulatory properties of antigenic fragments from bovine serum albumin. Cell. Immunol. 78: 1-12.

Fincham V.J., James M., Frame M.C. and Winder S.J. (2000). Active ERK/MAP kinase is targeted to newly forming cell-matrix adhesions by integrin engagement and v-Src. EMBO J. 19: 2911-2923.

Fishkes H. and Rudnick G. (1982). Bioenergetics of serotonin transport by membrane vesicles derived from platelet dense granules. J. Biol. Chem. 257: 5671-5677.

Forgac M. (1998). Structure, function and regulation of the vacuolar (H^+)-ATPases. FEBS Lett. 440: 258-263.

Forsgren A. and Sjöquist J. (1966). Protein A from *S. Aureus*. I. Pseudo-immune reaction with human γ-globulin. J. Immunol. 97: 822-831.

Fuchs R., Male P. and Mellman I. (1989). Acidification and ion permeabilities of highly purified rat liver endosomes. J. Biol. Chem. 264: 2212-2220.

Fukuda M. (1994). Biogenesis of the lysosomal membrane. In Subcellular Biochemistry volume 22: Membrane Biogenesis. (Eds. Maddy A.H. and Harris J.R.). Plenum Press, New York, 199-229.

Fuller S.J., Storey E., Li Q.X., Smith A.I., Beyreuther K. and Masters C.L. (1995). Intracellular production of βA4 amyloid of Alzheimer's disease: modulation by phosphoramidon and lack of coupling to the secretion of the amyloid precursor protein. Biochem. 34: 8091-8098.

Fusek M. and Vetvicka V. (1994). Mitogenic function of human procathepsin D: the role of the pro-peptide. Biochem. J. 303: 775-780.

Futai M., Oka T., Sun-Wada G.H., Moriyama Y., Kanazawa H. and Wada Y. (2000). Luminal acidification of diverse organelles by V-ATPase in animal cells. J. Exp. Biol. 203: 107-116.

Futter C.F., Pearse A., Hewlett L.J. and Hopkins C.R. (1996). Multivesicular endosomes containing internalized EGF-EGF receptor complexes mature and then fuse directly with lysosomes. J. Cell Biol. 132: 1011-1023.

Gallagher J.S. and Voss E.W. (1969). Molecular weight of a purified chicken antibody. Immunochem. 6: 199-206.

Galloway C.J., Dean G.E., Marsh M., Rudnick G. and Mellman I. (1983). Acidification of macrophage and fibroblast endocytic vesicles *in vitro*. Proc. Natl. Acad. Sci. USA 80: 3334-3338.

Ganley I.G., Carroll K., Bittova L. and Pfeffer S. (2004). Rab9 GTPase regulates late endosome size and requires effector interaction for its stability. Mol. Biol. Cell. 15: 5420-5430.

Ganne F., Vasse M., Beaudeux J.L., Peynet J., Francois A., Mishal Z., Chartier A., Tobelem G., Vannier J.P., Soria J. and Soria C. (2000). Cerivastatin, an inhibitor of HMG-CoA reductase, inhibits urokinase/urokinase-receptor expression and MMP-9 secretion by peripheral blood monocytes – a possible protective mechanism against atherothrombosis. Thromb. Haemost. 84: 680-688.

Garcia M., Platet N., Liaudet E., Laurent V., Derocq D., Brouillet J.P. and Rochefort H. (1996). Biological and clinical significance of cathepsin D in breast cancer metastasis. Stem Cells 14: 642-650.

Garnovskaya M.N., Mukhin Y.V., Vlasova T.M. and Raymond J.R. (2003). Hypertonicity activates Na^+/H^+ exchange through Janus kinase 2 and calmodulin. J. Biol. Chem. 278: 16908-16915.

Gauthier V.J., Mannik M. and Striker G.E. (1982). Effect of cationized antibodies in preformed immune complexes on deposition and persistence in renal glomeruli. J. Exp. Med. 156: 766-777.

Geuze H.J., Slot J.W. and Strous G.J.A.M. (1983). Intracellular site of asialoglycoprotein receptor-ligand uncoupling: double-label immunoelectron microscopy during receptor-mediated endocytosis. Cell 32: 277-287.

Geuze H.J., Stoorvogel W., Strous G.J., Bleekemolen J.E. and Mellman I. (1988). Sorting of mannose 6-phosphate receptors and lysosomal membrane proteins in endocytic vesicles. J. Cell Biol. 107: 2491-2501.

Gibbs J.B. (1991). Ras C-terminal processing enzymes – new drug targets. Cell 65: 1-4.

Gibbs J.B., Oliff A. and Kohl N.E. (1994). Farnesyltransferase inhibitors: Ras research yields a potential cancer therapeutic. Cell 77: 175-178.

Gillies B., Martinez-Zaguilan R., Peterson E.P. and Perona R. (1992). The role of intracellular pH in mammalian cell proliferation. Cell Physiol. Biochem. 2: 159-167.

Girod J., Fenart L., Regina A., Dehouck M.P., Hong G., Scherrmann J.M., Cecchelli R. and Roux F. (1999). Transport of cationized anti-tetanus Fab'2 fragments across an in vitro blood-brain barrier model: involvement of the transcytosis pathway. J. Neurochem. 73: 2002-2008.

Glickman J.N. and Kornfeld S. (1993). Mannose 6-phosphate-independent targeting of lysosomal enzymes in I-cell disease B lymphocytes. J. Cell Biol. 123: 99-108.

Goedegebuure P.S. and Eberlein T.J. (1995). The role of $CD4^+$ tumor-infiltrating lymphocytes in human solid tumors. Immunol. Res. 14: 119-131.

Goldstein J.L. and Brown M.S. (1990). Regulation of the mevalonate pathway. Nature 343: 425-430.

Goldstein J.L., Brown M.S., Anderson A.G.W., Russell D.W. and Schneider W.J. (1985). Receptor-mediated endocytosis: concepts emerging from the LDL receptor system. Annu. Rev. Cell Biol. 1: 1-39.

Good A.H., Wofsy L., Henry C. and Kimura J. (1980). Preparation of hapten modified protein antigens. In Selected Methods in Cellular Immunology. (Eds. Mishell B.B. and Shiigi S.M.). WH Freeman and Co., San Francisco, 343-350.

Goodnow C.C., Cyster J.G., Hartley S.B., Bell S.E., Cooke M.P., Healy J.I., Akkaraju S., Rathmell J.C., Pogue S.L. and Shokat K.P. (1995). Self-tolerance checkpoints in B lymphocyte development. Adv. Immunol. 59: 279-368.

Goodnow C.C., Sprent J., Fazekas de St Groth B. and Vinuesa C.G. (2005). Cellular and genetic mechanisms of self tolerance and autoimmunity. Nature 435: 590-597.

Gopalakrishnan M.M., Grosch H-W., Locatelli-Hoops S., Werth N., Smolenovà E., Nettersheim M., Sandhoff K. and Hasilik A. (2004). Purified recombinant human prosaposin forms oligomers that bindprocathepsin D and affect its autoactivation. Biochem. J. 383: 507–515.

Gorvel J.P., Chavrier P., Zerial M. and Gruenberg J. (1991). Rab5 controls early endosome fusion *in vitro*. Cell 64: 915-925.

Gottlieb R.A., Gruol D.L., Zhu J.Y. and Engler R.L. (1996). Preconditioning rabbit cardiomyocytes: role of pH, vacuolar proton ATPase, and apoptosis. J. Clin. Invest. 97: 2391-2398.

Gould M.N., Moore C.J., Zhong R., Wang B., Kennan W.S. and Haag J.D. (1994). Limonene chemoprevention of mammary carcinoma induction following direct *in situ* transfer of v-H-*ras*. Cancer Res. 54: 3540-3543.

Goverman J., Woods A., Larson L., Weiner L.P., Hood L. and Zaller D.M. (1993). Transgenic mice that express a myelin basic protein-specific T cell receptor develop spontaneous autoimmunity. Cell 72: 551-560.

Graaf M.R., Richel D.J., van Noorden C.J.F. and Guchelaar H. (2004). Effects of statins and farnesyltransferase inhibitors on the development and progression of cancer. Cancer Treat. Rev. 30: 609-641.

Grady J.K., Chasteen N.D. and Harris D.C. (1988). Radicals from "Good's" buffers. Anal. Biochem. 173: 111-115.

Graham N.A. and Asthagiri A.R. (2004). Epidermal growth factor-mediated T-cell factor/lymphoid enhancer factor transcriptional activity is essential but not sufficient for cell cycle progression in nontransformed mammary epithelial cells. J. Biol. Chem. 279: 23517-23524.

Granger B.L., Green S.A., Gabel C.A., Howe C.L., Mellman I. and Helenius A. (1990). Characterization and cloning of lgp110, a lysosomal membrane glycoprotein from mouse and rat cells. J. Biol. Chem. 265: 12036-12043.

Gray-Bablin J., Rao S. and Keyomarsi K. (1997). Lovastatin induction of cyclin-dependent kinase inhibitors in human breast cells occurs in a cell cycle-independent fashion. Cancer Res. 57: 604-609.

Greenfield E.A., Nguyen K.A. and Kuchroo V.K. (1998). CD28/B7 costimulation: a review. Crit. Rev. Immunol. 18: 389-418.

Griffiths G. (1993). In Fine Structure Immunocytochemistry. Springer-Verlag, Berlin.

Griffiths G. (1996). On vesicles and membrane compartments. Protoplasma 195: 37-58.

Griffiths G. and Gruenberg J. (1991). The arguments for pre-existing early and late endosomes. Trends Cell Biol. 1: 5-9.

Griffiths G., Back R. and Marsh M. (1989). A quantitative analysis of the endocytic pathway in baby hamster kidney cells. J. Cell Biol. 109: 2703-2720.

Griffiths G., Hoflack B., Simons K., Mellman I. and Kornfeld S. (1988). The mannose 6-phosphate receptor and the biogenesis of lysosomes. Cell. 52: 329-341.

Griffiths G., Hollinshead R., Hemmings B.A. and Nigg E.A. (1990a). Ultrastructural location of the regulatory (RII) subunit of cyclic AMP-dependent protein kinase to subcellular compartments active in endocytosis and recycling of membrane receptors. J. Cell Sci. 96: 691-703.

Griffiths G., Matteoni R., Back R. and Hoflack B. (1990b). Characterization of the cation-independent mannose 6-phosphate receptor enriched pre-lysosomal compartment in NRK cells. J. Cell Sci. 95: 441-461.

Griffiths G., Quinn P. and Warren G. (1983). Dissection of the Golgi complex. 1. Monensin inhibits the transport of viral membrane proteins from medial to trans Golgi cisternae in baby hamster kidney cells infected with Semliki Forest virus. J. Cell Biol. 96: 835-850.

Grinstein S., Rotin D. and Mason M. (1989). Na^+/H^+ exchange and growth factor-induced cytosolic pH changes. Role in cellular proliferation. Biochim. Biophys. Acta 988: 73-97.

Grinstein S., Woodside M., Sardet C., Pouyssegur J. and Rotin D. (1992). Activation of the Na^+/H^+ antiporter during cell volume regulation. Evidence for a phosphorylation-independent mechanism. J. Biol. Chem. 267: 23823-23828.

Gruber G. (2003), Introduction: a close look at the vacuolar ATPase. J. Bioenerg. Biomembr. 35: 277-280.

Gruenberg J. (2001). The endocytic pathway: a mosiac of domains. Nature Reviews Mol. Cell Biol. 2: 721-730.

Gruenberg J. (2003). Lipids in endocytic membrane transport and sorting. Curr. Opin. Cell Biol. 15: 382–388.

Gruenberg J. and Howell K.E. (1985). Immuno-isolation of vesicles using antigenic sites either located on the cytoplasmic or the exoplasmic domain of an implanted viral protein. A quantitative analysis. Eur. J. Cell Biol. 38: 312-321.

Gruenberg J. and Howell K.E. (1986). Reconstitution of vesicle fusions occurring in endocytosis with a cell-free system. EMBO J. 5: 3091-3101.

Gruenberg J. and Howell K.E. (1987). An internalized transmembrane protein resides in a fusion-competent endosome for less than 5 minutes. Proc. Natl. Acad. Sci USA 84: 5758-5762.

Gruenberg J. and Howell K.E. (1989). Membrane traffic in endocytosis: insights from cell-free assays. Annu. Rev. Cell Biol. 5: 453-481.

Gruenberg J. and Maxfield F.R. (1995). Membrane transport in the endocytic pathway. Curr. Opin. Cell Biol. 7: 552-563.

Gruenberg J., Griffiths G. and Howell K.E. (1989). Characterization of the early endosome and putative endocytic carrier vesicles *in vivo* and with an assay of vesicle fusion *in vitro*. J. Cell Biol. 108: 1301-1316.

Gu F. and Gruenberg J. (1999). Biogenesis of transport intermediates in the endocytic pathway. FEBS Lett. 452: 61-66.

Gu W.Z., Tahir S.K., Wang Y.C., Zhang H.C., Cherian S.P., O'Connor S., Leal J.A., Rosenberg S.H. and Ng S.C. (1999). Effect of novel CAAX peptidomimetic farnesyltransferase inhibitor on angiogenesis in vitro and in vivo. Eur. J. Cancer 35: 1394-1401.

Guevara-Patiño J.A., Turk M.J., Wolchok J.D. and Houghton A.N. (2003). Immunity to cancer through immune recognition of altered self: studies with melanoma. Adv. Cancer Res. 90: 157-177.

Gupta S.K., Gallego C., Johnson G.L. and Heasley L.E. (1992). MAP kinase is constitutively activated in gip2 and src transformed rat 1a fibroblasts. J. Biol. Chem. 267: 7987-7990.

Hagag N., Lacal J.C., Graber M., Aaronson S. and Viola M.V. (1987). Microinjection of Ras p21 induces a rapid rise in intracellular pH. Mol. Cell Biol. 7: 1984-1988.

Hajjar K.A., Jacovina A.T. and Chacko J. (1994). An endothelial cell receptor for plasminogen/tissue plasminogen activator. I. Identity with annexin II. J. Biol. Chem. 296: 21191-21197.

Hall A. (1994). Small GTP-binding proteins and the regulation of the actin cytoskeleton. Annu. Rev. Cell Biol. 10: 31-54.

Haluska P., Dy G.K. and Adjei A.A. (2002). Farnesyl transferase inhibitors as anticancer agents. Eur. J. Cancer 38: 1685-1700.

Hamad N.M., Elconin J.H., Karnoub A.E., Bai W., Rich J.N., Abraham R.T., Der C.J. and Counter C.M. (2002). Distinct requirements for Ras oncogenesis in human versus mouse cells. Genes Dev. 16: 2045-2057.

Hanna J. Carroll K. and Pfeffer S.R. (2002). Identification of residues in TIP47 essential for Rab9 binding. Proc. Natl. Acad. Sci. USA 99: 7450-7454.

Hanson J.B., Olson R. and Webster P (1997). Association of tissue factor pathway inhibitor with human umbilical vein endothelial cells. Blood 90: 3568-3578.

Harada A., Takei Y., Kanai Y., Yanaka Y., Nonaka S. and Hirokawa N (1998). Golgi vesiculation and lysosome dispersion in cells lacking cytoplasmic dynein. J. Cell Biol. 141: 51-59.

Hasilik A. (1992). The early and late processing of lysosomal enzymes: proteolysis and compartmentation. Experientia 48: 130-151.

Haugland R.P. (2002). In Molecular Probes Handbook of Fluorescent Probes and Research Chemicals. (Eds. Gregory J.). 9th Ed. Molecular Probes Inc., USA.

Hayashi M., Yamamoto A. and Moriyama Y. (2002). The internal pH of synaptic-like microvesicles in rat pinealocytes in culture. J. Neurochem. 82: 698-704.

Haylett T. and Thilo L. (1986). Limited and selected transfer of plasma membrane glycoproteins to membranes of secondary lysosomes. J. Cell Biol. 103: 1249-1256.

Haystead T.A.J., Sim A.T.R., Carling D., Honnor R.C., Tsukitani Y., Cohen P. and Hardie D.G. (1989). Effects of the tumor promoter okadaic acid on intracellular protein phosphorylation and metabolism. Nature 337: 78-81.

Hengst L. and Reed S.I. (1996). Translational control of p27Kip1 accumulation during the cell cycle. Science 271: 1861-1864.

Hengst L., Dulic V., Slingerland J.M., Lees E. and Reed S.I. (1994). A cell cycle-regulated inhibitor of cyclin-dependent kinases. Proc. Natl. Acad. Sci. USA 91: 5291-5295.

Hermanson G.T., Mallia A.K. and Smith P.K. (1992). In Immobilized Affinity Ligand Techniques. Academic Press Inc., San Diego.

Heuser J. (1989). Changes in lysosome shape and distribution correlated with changes in cytoplasmic pH. J. Cell Biol. 108: 855-864.

Hilden S.A., Ghoshroy K.B. and Madias N.E. (1990). Na^+-H^+ exchange, but not Na^+-K^+-ATPase is present in endosome-enriched microsomes from rabbit renal cortex. Am. J. Physiol. 258: F1311-F1319.

Hillmer S., Joachim S. and Robinson D.G. (1991). Rapid polymerization of LR White for immunocytochemistry. Histochem. 95: 315-318.

Himeno M., Noguchi Y., Sasaki H., Tanaka Y., Furuno K., Kono A., Sasaki Y. and Kato K. (1989). Isolation and sequencing of a cDNA clone encoding 107 kDa sialglycoprotein in rat liver lysosomal membranes. FEBS Lett. 244: 351-356.

Hirai A., Nakamura S., Noguchi Y., Yasuda T., Kitagawa M., Tatsuno I., Oeda T., Tahara K., Terano T., Narumiya S., Kohn L.D. and Saito Y. (1997). Geranylgeranylated rho small GTPase (s) are essential for the degradation of p27Kip1 and facilitate the progression from G1 to S phase in growth-stimulated rat FRTL-5 cells. J. Biol. Chem. 272: 13-16.

Ho M.K. and Springer T.A. (1983). Tissue distribution, structural characterization, and biosynthesis of Mac-3, a macrophage surface glycoprotein exhibiting molecular weight heterogeneity. J. Biol. Chem. 258: 636-642.

Hollenbeck P.J. and Swanson J.A. (1990). Radial extension of macrophage tubular lysosomes supported by kinesin. Nature 346: 864-866.

Holtzmann E. (1989). In Lysosomes. Plenum Press, New York.

Hong G., Bazin-Redureau M.I., Gires P. and Scherrmann J.M. (1998). Hepatic disposition and toxicity of cationized goat immunoglobulin G and fab fragments in isolated perfused rat liver. Drug Metab. Dispos. 26: 661-669.

Hong G., Bazin-Redureau M.I. and Scherrmann J.M. (1999). Pharmacokinetics and organ distribution of cationized colchicine-specific IgG and Fab fragments in rat. J. Pharm. Sci. 88: 147-153.

Hong G., Chappey O., Niel E. and Scherrmann J.M. (2000). Enhanced cellular uptake and transport of polyclonal immunoglobulin G and fab after their cationization. J. Drug Target. 8: 67-77.

Hooley R., Yu C.Y., Symons M. and Barber D.L. (1996). Gα13 stimulates Na^+-H^+ exchange through distinct Cdc42-dependent and RhoA-dependent pathways. J. Biol. Chem. 271: 6152-6158.

Hopkins C.R., Gibson A., Shipman M. and Miller K. (1990). Movement of internalized ligand-receptor complexes along a continuous endosomal reticulum. Nature 346: 335-339.

Hordijk P.L., ten Klooster J.P., Van der Kammen R.A., Michiels F., Oomen L.C. and Collard J.G. (1997). Inhibition of invasion of epithelial cells by Tiam1-Rac signaling. Science 278: 1464-1466.

Hornick C.A., Hamilton R.L., Spaziani E., Enders G.H. and Havel R.J. (1985). Isolation and characterization of multivesicular bodies from rat liver hepatocytes: an organelle distinct from secretory vesicles of the Golgi apparatus. J. Cell Biol. 100: 1558-1569.

Hoshi M., Ohta K., Gotoh Y., Mori A., Murofushi H., Sakai H. and Nishida E. (1992). Mitogen-activated-protein-kinase-catalyzed phosphorylation of microtubule-associated proteins, microtubule-associated protein 2 and microtubule-associated protein 4, induces an alteration in their function. Eur. J. Biochem. 203: 43-52.

Hotta K., Tanaka K., Mino A., Kohno H. and Takai Y. (1996). Interaction of the Rho family small G proteins with kinectin, an anchoring protein of the kinesin motor. Biochem. Biophys. Res. Commun. 225: 69-74.

Houghton A.N. and Guevara-Patiño J.A. (2004). Immune recognition of self in immunity against cancer. J. Clin. Invest. 114: 468-471.

Houghton A.N., Gold J.S. and Blachere N. (2001). Immunity against cancer: lessons learned from melanoma. Curr. Opin. Immunol. 13: 134-140.

Howe C.L., Granger B.L., Hull M., Green S.A., Gabel C.A., Helenius A. and Mellman I. (1988). Derived protein sequence, oligosaccharides, and membrane insertion of the 120-kD lysosomal membrane glycoprotein (lgp120): identification of a highly conserved family of lysosomal membrane glycoproteins. Proc. Natl. Acad. Sci. USA 85: 7577-7581.

Huang M., Chida K., Kamata N., Nose K., Kato M., Homma Y., Takenawa T and Kuroki T. (1988). Enhancement of inositol phospholipid metabolism and activation of protein kinase C in ras-transformed rat fibroblasts. J. Biol. Chem. 263: 17975-17980.

Huang Y., Tyler T., Saadatmandi N., Lee C., Borgstrom P. and Gjerset R.A. (2003). Enhanced tumor suppression by a p14ARF/p53 bicistronic adenovirus through increased p53 protein translation and stability. Cancer Res. 63: 3646-3653.

Hudson L. and Hay F.C. (1980). In Practical Immunology. Blackwell Scientific, Oxford.

Hunziker W. and Geuze H.J. (1996). Intracellular trafficking of lysosomal membrane proteins. BioEssays 18: 379-389.

Hunziker W. and Peters P.J. (1998). Rab17 localizes to recycling endosomes and regulates receptor-mediated transcytosis in epithelial cells. J. Biol. Chem. 273: 15734-15741.

Huss M., Ingenhorst G., König S., Gassel M., Dröse S., Zeeck A., Altendorf K. and Wieczorek H. (2002). Concanamycin A, the specific inhibitor of V-ATPases, binds to the Vo subunit c. J. Biol. Chem. 277: 40544-40548.

Isidoro C., Demoz M., De Stefanis D., Baccino F.M., Hasilik A. and Bonelli G. (1997). Differential targeting and processing of procathepsin D in normal and transformed murine 3T3 fibroblasts. Int. J. Cancer 70:310-314.

Ivetic A. and Ridley A.J. (2004). Ezrin/radixin/moesin proteins and Rho GTPase signalling in leucocytes. Immunol. 112: 165-176.

Izumi H., Torigoe T., Ishiguchi H., Uramoto H., Yoshida Y., Tanabe M., Ise T., Murakami T., Yoshida T., Nomoto M. and Kohno K. (2003). Cellular pH regulators: potentially promising molecular targets for cancer chemotherapy. Cancer Treat. Rev. 29: 541-549.

Jadot M., Dubois F., Wattiaux-de Coninck S. and Wattiaux R. (1997). Supramolecular assemblies from lysosomal matrix proteins and complex lipids. Eur. J. Biochem. 249: 862-869.

Jadot M., Wattiaux R., Mainferme F., Dubois F., Claessens A. and Wattiauw-De Coninck S. (1996). Soluble form of LampII in purified rat liver lysosomes. Biochem. Biophys. Res. Commun. 223: 353-359.

Jakab M., Fürst J., Gshwentner M., Bottà G., Garavaglia M., Bazzini C., Rodighierp S., Meyer G., Eichmüller S., Wöll E., Chwatal S., Ritter M. and Paulmichl M. (2002). Mechanisms sensing and modulating signals arising from cell swelling. Cell. Physiol. Biochem. 12: 235-258.

Jakobisiak M., Bruno S., Skierski J.S. and Darzynkiewicz Z. (1991). Cell cycle-specific effects of lovastatin. Proc. Natl. Acad. Sci. USA 88: 3628-3632.

Jameson L. and Caplow M. (1981). Modification of microtubule steady-state dynamics by phosphorylation of the microtubule-associated proteins. Proc. Natl. Acad. Sci. USA 78: 3413-3417.

Janeway Jr C.A. (2001). How the immune system protects the host from infection. Microbes Infect. 3: 1167-1171.

Jani J.P., Specht S., Stemmler N., Blanock K., Singh S.V., Gupta V. and Katoh A. (1993). Metastasis of B16F10 mouse melanoma inhibited by lovastatin, an inhibitor of cholesterol biosynthesis. Invasion Metastasis 13: 314-324.

Janmey P.A. and Chaponnier C. (1995). Medical aspects of the actin cytoskeleton. Curr. Opin. Cell Biol. 7: 111-117.

Jasani B., Thomas N.D., Navabi H., Millar D.M., Newman G.R., Gee J. and Williams E.D. (1992). Dinitrophenyl (DNP) hapten sandwich staining (DHSS) procedure: a 10 year review of its principle reagents and applications. J. Immunol. Methods 50: 193-198.

Jasani B., Wynford-Thomas D., and Williams E.D. (1981). Use of monoclonal anti-hapten antibodies for immunolocalization of tissue antigens. J. Clin. Path. 34: 1000-1012.

Jiang L.W., Maher V.M., McCormick J.J. and Schindler M. (1990). Alkalinization of the lysosomes is correlated with *ras* transformation of murine and human fibroblasts. J. Biol. Chem. 265: 4775-4777.

Johnsen M., Lund L.R., Romer J., Almholt K. and Dano K. (1998). Cancer invasion and tissue remodeling: common themes in proteolytic matrix degradation. Curr. Opin. Cell Biol. 10: 667-671.

Johnson I. (1992). Optical properties of fluorescent probes. In Molecular Probes Handbook of Fluorescent Probes and Research Chemicals. (Eds. Larison K.D.). 5th Ed. Molecular probes Inc., USA.

Johnson R.G., Pfister D., Carty S.E. and Scarpa A. (1979). Biological amine transport in chromaffin ghosts. Coupling to the transmembrane proton and potential gradients. J. Biol. Chem. 254: 10963-10972.

Kane P.M. (1995). Disassembly and reassembly of the yeast vacuolar H(+)-ATPase *in vivo*. J. Biol. Chem. 270: 17025-17032.

Kane P.M. and Stevens T.H. (1992). Subunit composition, biosynthesis and assembly of the yeast vacuolar proton-translocating ATPase. J. Bioeng. Biomembr. 24: 383-370.

Kaplan D.L. and Boron W.F. (1994). Long-term expression of c-H-*ras* stimulates Na-H and Na(+)-dependent Cl-HCO_3 exchange in NIH-3T3 fibroblasts. J. Biol. Chem. 269: 4116-4124.

Kasai M., Shirasawa T., Kitamura M., Ishido K., Kominami E. and Hirokawa K. (1993). Proenzyme form of cathepsin L produced by thymic epithelial cells promotes proliferation of immature thymocytes in the presence of IL-1, IL-7, and anti-CD3 antibody. Cell. Immunol. 150: 124-136.

Kataoka T., Muroi M., Ohkuma S., Waritani T., Magae J., Takatsuki A., Kondo S., Yamasaki M. and Nagai K. (1995). Prodigiosin 25-C uncouples vacuolar type H^+-ATPase, inhibits vacuolar acidification and affects glycoprotein processing. FEBS Lett. 359: 53-59.

Katayose Y., Kim M., Rakkar A.N., Li Z., Cowan K.H. and Seth P. (1997). Promoting apoptosis: a novel activity accociated with the cyclin-dependent kinase inhibitor p27. Cancer Res. 57: 5441-5445.

Kawahata K., Misaki Y., Yamauchi M., Tsunekawa S., Setoguchi K., Miyazaki J. and Yamamoto K. (2002). Generation of $CD4^+CD25^+$ regulatory T cells from autoreactive T cells simultaneously with their negative selection in the thymus and from nonautoreactive T cells by endogenous TCR expression. J. Immunol. 168: 4399-4405.

Kawasaki-Nishi S., Nishi T. and Forgac M. (2001). Yeast V-ATPase complexes containing different isoforms of the 100-kDa a- subunit differ in coupling efficiency and in vivo dissociation. J. Biol. Chem. 276: 17941-17948.

Kennedy A.R. (1994). Prevention of carcinogenesis by protease inhibitors. Cancer Res. 54: 1999s-2005s.

Kiess W., Blickenstaff G.D., Sklar M.M., Thomas C.L., Nissley S.P. and Sahagian G.G. (1988). Biochemical evidence that the type II insulin-like growth factor is identical to the cation-independent mannose 6-phosphate receptor. J. Biol. Chem. 263: 9339-9344.

Kim J.S., Pirnia F., Choi Y.H., Nguyen P.M., Knepper B., Tsokos M., Schulte T.W., Birrer M.J., Blagosklonny M.V., Schaefer O., Mushinski J.F. and Trepel J.B. (2000). Lovastatin induces apoptosis in a primitive neuroectodermal tumor cell line in association with RB down-regulation and loss of the G1 checkpoint. Oncogene 19: 6082-6090.

Kimura K., Ito M., Amano M., Chihara K., Fukata Y., Nakafuku M., Yamamori B., Feng J., Nakano T., Okawa K., Iwamatsu A. and Kaibuchi K. (1996). Regulation of myosin phosphatase by Rho and Rho-Associated kinase (Rho-kinase). Science 273: 245-248.

Kinch M.S., Clark G.J., Der C.J. and Burridge K. (1995). Tyrosine phosphorylation regulates the adhesions of Ras-transformed breast epithelia. J. Cell Biol. 130: 461-471.

Knight K.L and Crane M.A. (1994). Generating the antibody repertoire in rabbit. Adv. Immunol. 56: 179-218.

Kobayashi H., Moniwa N., Sugimura M., Shinohara H., Ohi H. and Terao T. (1993). Effects of membrane-associated cathepsin B on the activation of receptor-bound prourokinase and subsequent invasion of reconstituted basement membranes. Biochim. Biophys. Acta 1178: 55-62.

Kobayashi H., Schmitt M., Goretzki L., Chucholowski N., Calvete J., Kramer M., Gunzler W.A., Janicke F. and Graeff H. (1991). Cathepsin B efficiently activates the soluble and the tumor cell receptor-bound form of the proenzyme urokinase-type plasminogen activator (pro- uPA). J. Biol. Chem. 266: 5147-5152.

Kobayashi T., Stang E., Fang K.S., de Moerloose P., Parton R.G. and Gruenberg J. (1998). A lipid associated with the antiphospholipid syndrome regulates endosome structure/fuction. Nature 392: 193-197.

Kobayashi T., Startchev K, Whitney A.J. and Gruenberg J. (2001). Localization of lysobisphosphaditic acid-rich membrane domains in late endosomes. Biol. Chem. 382: 483-485.

Kohl N.E., Wilson F.R., Mosser S.D., Giuliani E., deSolms S.J., Conner M.W., Anthony N.J., Holtz W.J., Gomez R.P., Lee T.J., Smith R.L., Graham S.L., Hartman G.D., Gibbs J.B. and Oliff A. (1994). Protein farnesyltransferase inhibitors block the growth of *ras*-dependent tumors in nude mice. Proc. Natl. Acad. Sci. USA 91: 9141-9145.

Kornfeld S. (1992). Structure and function of the mannose-6-phosphate/insulin-like growth factor II receptors. Annu. Rev. Biochem. 61: 307-330.

Kornfeld S. and Mellman I. (1989). The biogenesis of lysosomes. Annu. Rev. Cell Biol. 5: 483-525.

Kort W.J., Hulsmann W.C. and Stehman T.E. (1989). Modulation of metastatic ability by inhibition of cholesterol synthesis. Clin. Exp. Metastasis 7: 517-523.

Koyama A., Inage H., Kobayashi M., Nakamura H., Narita M. and Tojo S. (1986a). Effect of chemical modification of antigen on characteristics of immune complexes and their glomerular localization in the murine renal tissues. Immunol. 58: 535-540.

Koyama A., Inage H., Kobayashi M., Narita M. and Tojo S. (1986b). Effect of chemical cationization on glomerular localization of immune complexes in active models of serum sickness nephritis in rabbits. Immunol. 58: 529-534.

Kozma R., Ahmed S., Best A. and Lim L. (1995). The Ras-related protein Cdc42Hs and bradykinin promote formation of peripheral actin microspikes and filopodia in Swiss 3T3 fibroblasts. Mol. Cell Biol. 15: 1942-1952.

Kreis T. and Vale R. (1993). In Guidebook to the Extracellular Matrix and Adhesion Proteins. Oxford University Press, Oxford, 27,88.

Kumagai N., Morii N., Fujisawa K., Nemoto Y. and Narumiya S. (1993). ADP-ribosylation of *rho* p21 inhibits lysophosphatidic acid-induced protein tyrosine phosphorylation and phosphatidylinositol 3-kinase activation in cultured Swiss 3T3 cells. J. Biol. Chem. 268: 24535-24538.

Kurts C., Sutherland R.M., Davey G., Li M., Lew A.M., Blanas E., Carbone F.R., Miller J.F. and Heath W.R. (1999). CD8 T cell ignorance or tolerance to islet antigens depends on antigen dose. Proc. Natl. Acad. Sci. USA 96: 12703-12707.

Kusama T., Mukai M., Iwasaki T., Tatsuta M., Matsumoto Y., Akedo H., Inoue M. and Nakamura H. (2002). 3-Hydroxy-3-methylglutaryl-coenzyme A reductase inhibitors reduce human pancreatic cancer cell invasion and metastasis. Gastroenterology 122: 308-317.

Kusama T., Mukai M., Iwasaki T., Tatsuta M., Matsumoto Y., Akedo H. and Nakamura H. (2001). Inhibition of epidermal growth factor-induced RhoA translocation and invasion of human pancreatic cancer cells by 3-hydroxy-3-methylglutaryl-coenzyme A reductase inhibitors. Cancer Res. 61: 4885-4891.

Kutateladze T.G., Ogburn K.D., Watson W.T., de Beer T., Emr S.D., Burd C.G. and Overduin M. (1999). Phosphatidylinositol 3-phosphate recognition by the FYVE domain. Mol. Cell 3: 805-811.

Lacroix J., Poet M., Maehrel C. and Counillon L. (2004). A mechanism for the activation of the Na/H exchanger NHE-1 by cytoplasmic acidification and mitogens. EMBO Rep. 5: 91-96.

Lah T.T., Bervar A., Zajc I., Sever N., Levičar N., Filipič M. and Kos J. (2000). Cathepsins B and L and their inhibitors in relation to invasiveness and tumorigenicity of human breast tumor cell lines. Int. J. Biol. Markers 15: S27.

Lah T.T., Clifford K.M., Helmer N.A., Day N., Moin K., Honn K.V., Crissman J.D. and Sloane B.F. (1989). Inhibitory properties of low molecular mass cysteine proteinase inhibitors from human sarcoma. Biochem. Biophys. Acta. 993: 63-73.

Lamaze C., Chuang T.H., Terlecky L.J., Bokoch G.M. and Schmid S.L. (1996). Regulation of receptor-mediated endocytosis by Rho and Rac. Nature 382: 177-179.

Lamaze C., Fujimoto L.M., Yin H.L. and Schmid S.L. (1997). The actin cytoskeleton is required for receptor-mediated endocytosis in mammalian cells. J. Biol. Chem. 272: 20332-20335.

Lancaster C.A., Taylor-Harris P.M., Self A.J., Brill S., van Erp H.E. and Hall A. (1994). Characterization of RhoGAP. A GTPase-activating protein for Rho-related small GTPases. J. Biol. Chem. 269: 1137-1142.

Land H., Parada L.F. and Weinberg R.A. (1983). Tumorigenic conversion of primary embryo fibroblasts requires at least two cooperating oncogenes. Nature 304: 596-602.

Lang F., Ritter M., Gamper N., Huber S., Fillon S., Tanneur V., Lepple-Wienhues A., Szabo I. and Gulbins E. (2000). Cell volume in the regulation of cell proliferation and apoptotic cell death. Cell Physiol Biochem. 10: 417-428.

Lang F., Ritter M., Wöll E., Bichler I., Häussinger D., Offner F. and Grunicke H.H. (1992b). Ion transport in the regulation of cell proliferation in ras oncogene expressing 3T3 NIH fibroblasts. Cell Physiol. Biochem. 2: 213-219.

Lang F., Ritter M., Wöll E., Weiss H., Häussinger D., Hoflacher J., Maly K. and Grunicke H.H. (1992a). Altered cell volume regulation in *ras* oncogene expressing NIH fibroblasts. Pflügers Arch. 420: 424-427.

Lanzavecchia A. (1995). How can cryptic epitopes trigger autoimmunity? J. Exp. Med. 181: 1945-1948.

Larsson M., Majeed M., Ernst J.D., Magnusson K.E., Stendahl O. and Forsum U. (1997). Role of annexins in endocytosis of antigens in immature human dendritic cells. Immunol. 92: 501-511.

Laufs U., Marra D., Node K. and Liao J.K. (1999). 3-Hydroxy-3-methylglutaryl-coenzyme A reductase inhibitors attenuate vascular smooth muscle proliferation by preventing rho GTPase-induced down-regulation of p27 (Kip1). J. Biol. Chem. 274: 21926-21931.

Laurent-Matha V., Farnoud M.R., Lucas A., Rougeot C., Garcia M. and Rochefort H. (1998). Endocytosis of pro-cathepsin D into breast cancer cells is mostly independent of mannose-6-phosphate receptors. J. Cell Sci. 111: 2539-2549.

Laurent-Matha V., Maruani-Herrmann S., Prebois C., Beaujouin M., Glondu M., Noel A., Alvarez-Gonzalez M.L., Blacher S., Coopman P., Baghdiguian S., Gilles C., Loncarek J., Freiss G., Vignon F. and Liaudet-Coopman E. (2005). Catalytically inactive human cathepsin D triggers fibroblast invasive growth. J. Cell Biol. 168: 489-499.

Lawrence M.B. and Springer T.A. (1991). Leukocytes roll on a selectin at physiologic flow rates: distinction from and prerequisite for adhesion through integrins. Cell 65: 859-873.

Lebowitz P.F., Casey P.J., Prendergast G.C. and Thissen J.A. (1997b). Farnesyltransferase inhibitors alter the prenylation and growth-stimulation function of RhoB. J. Biol. Chem. 272: 15591-15594.

Lebowitz P.F., Davide J.P. and Prendergast G.C. (1995). Evidence that farnesyltransferase inhibitors suppress Ras transformation by interfering with Rho activity. Mol. Cell. Biol. 15: 6613-6622.

Lebowitz P.F., Sakamuro D. and Prendergast G.C. (1997a). Farnesyl transferase inhibitors induce apoptosis of Ras-transformed cells denied substratum attachment. Cancer Res. 57: 708-713.

Lee H.J. and Pardridge W.M. (2003). Monoclonal antibody radiopharmaceuticals: cationization, pegylation, radiometal chelation, pharmacokinetics, and tumor imaging. Bioconjug Chem. 14: 546-553.

Leffers H., Nielson M.S., Anderson A.H., Honore B., Madsen P., Vanderkerckhove J. and Celis J.E. (1993). Identification of two human RhoD GDP dissociation inhibitor proteins whose overexpression leads to disruption of the actin cytoskeleton. Exp. Cell Res. 209: 165-174.

Lerner E.C., Qian Y., Hamilton A.D. and Sebti S.M. (1995). Disruption of oncogenic K-Ras4B processing and signalling by a potent geranylgeranyltransferase I inhibitor. J. Biol. Chem. 270: 26770-26773.

Leunissen J.L.M. and de Mey J.R. (1989). Preparation of gold probes. In Immunolabelling in Cell Biology. (Eds. Verkleij A.J. and Leunissen J.L.M.). CRC Press, Florida, 3-16.

Levitz S.M., Nong S., Seetoo K.F., Harrison T.S., Spiezer R.A. and Simons E.R. (1999). *Cryptococcus neoformans* resides in an acidic phagolysosome of human macrophages. Infect. Immun. 67: 885-890.

Lewis V., Green S.A., Marsh M., Vihko P., Helenius A. and Mellman I. (1985). Glycoproteins of the lysosomal membrane. J. Cell Biol. 100: 1839-1847.

Ley K., Gaehtgens P., Fennie C., Singer M.S., Lasky L.A. and Rosen S.D. (1991). Lectin-like cell adhesion molecule 1 mediates leukocyte rolling in mesenteric venules in vivo. Blood 77: 2553-2555.

Li G., D'Souza-Schorey C., Barbieri M.A., Cooper J.A. and Stahl P.D. (1997). Uncoupling of membrane ruffling and pinocytosis during Ras signal transduction. J. Biol. Chem. 272: 10337-10340.

Li G., D'Souza-Schorey C., Barbieri M.A., Roberts R.L. and Stahl P.D. (1995). Evidence for phosphatidylinositol 3-kinase as a regulator of endocytosis via activation of Rab5. Proc. Natl. Acad. Sci. USA 92: 10207-10211.

Li J. and Eastman A. (1995). Apoptosis in interleukin-2 dependent cytotoxic T lymphocyte cell line is associated with intracellular acidification. J. Biol. Chem. 270: 3203-3211.

Lin R., Mamula M.J., Hardin J.A. and Janeway Jr C.A. (1991). Induction of autoreactive B cells allows priming of autoreactive T cells. J. Exp. Med. 173: 1433-1439.

Lin S.X., Mallet W.G., Huang A.Y. and Maxfield F.R. (2004). Endocytosed cation-independent mannose 6-phosphate receptor traffics via the endocytic recycling compartment en route to the trans-Golgi network and a subpopulation of late endosomes. Mol. Biol. Cell 15: 721-733.

Lin X., Voyno-Yasenetskaya T.A., Hooley R., Lin C.Y., Orlowski J. and Barber D.L. (1996). Gα12 differentially regulates Na^+-H^+ exchanger isoforms. J. Biol. Chem. 271: 22604-22610.

Liotta L.A., Rao C.N. and Barsky S.H. (1983). Tumor invasion and the extracellular matrix. Lab. Invest. 49: 636-649.

Lippincott-Schwartz J. (1998). Cytoskeletal proteins and Golgi dynamics. Curr. Opin. Cell Biol. 10: 52-59.

Lippincott-Schwartz J. and Fambrough D.M. (1987). Cycling of the integral membrane glycoprotein, LEP100, between plasma membrane and lysosomes: kinetic and morphological analysis. Cell 49: 669-677.

Lippincott-Schwartz J., Cole N.B., Marotta A., Conrad P.A. and Bloom G.S. (1995). Kinesin is the motor for microtubule-mediated Golgi-to-ER membrane traffic. J. Cell Biol. 128: 293-306.

Liu G., Edmonds B.T. and Condeelis J. (1996). pH, EF-1α and the cytoskeleton. Trends Cell Biol. 6: 168-171.

Llano E., Pendas A.M., Freije J.P., Nakano A., Knauper V., Murphy G. and Lopez-Otin C. (1999). Identification and characterization of human MT5-MMP, a new membrane-bound activator of progelatinase A overexpressed in brain tumors. Cancer Res. 59: 2570-2576.

Lobel P., Fujimoto K., Ye R.D., Griffiths G. and Kornfeld S. (1989). Mutations in the cytoplasmic domain of the 275 kDa mannose-6-phosphate receptor differentially alter lysosomal enzyme sorting and endocytosis. Cell 57: 787-796.

Lochter A., Sternlicht M.D., Werb Z. and Bissell M.J. (1998). The significance of matrix metalloproteinases during early stages of tumor progression. Ann. NY Acad. Sci. 23: 180-193.

Lohr J., Knoechel B., Nagabhushanam V. and Abbas A.K. (2005). T-cell tolerance and autoimmunity to systemic and tissue restricted self-antigens. Immunol. Rev. 204: 116-127.

Lorenzo K., Ton P., Clark J.L., Coulibaly S. and Mach L. (2000). Invasive properties of murine squamous carcinoma cells: secretion of matrix-degrading cathepsins is attributable to a deficiency in the mannose 6-phosphate/insulin-like growth factor II receptor. Cancer Res. 60: 4070-4076.

Louvard D. (1989). The function of the major cytoskeletal components of the brush border. Curr. Opin. Cell Biol. 1: 51-57.

Lowry D.R. and Willumsen B.M. (1993). Function and regulation of Ras. Annu. Rev. Biochem. 62: 851-891.

Ludwig T., Griffiths G. and Hoflack B. (1991). Distribution of newly synthesized lysosomal enzymes in the endocytic pathway of normal rat kidney cells. J. Cell Biol. 115: 1561-1572.

Luo X. and Sawadogo M. (1996). Antiproliferative properties of the USF family of helix-loop-helix transcription factors. Proc. Natl. Acad. USA 93: 1308-1313.

Lütcke A., Jansson S., Parton R.G., Chavrier P., Valencia A., Huber L., Lehtonen E. and Zerial M. (1993). Rab17, a novel small GTPase, is specific for epithelial cells and is induced during cell polarization. J. Cell Biol. 121: 553-564.

Lutz W., Leon J. and Eilers M. (2002). Contributions of Myc to tumorigenesis. Biochim. Biophys. Acta 1602: 61-71.

Luzio J.P., Poupon V., Lindsay M.R., Mullock B.M., Piper R.C. and Pryor P.R. (2003). Membrane dynamics and the biogenesis of lysosomes. Mol. Membr. Biol. 20: 141-54.

Luzio J.P., Rous B.A., Bright N.A., Pryor P.R. and Mullock B.M. (2000). Lysosome-endosome fusion and lysosome biogenesis. J. Cell Sci. 113: 1515-1524.

Madhaus I.H. (1988). Regulation of intracellular pH in eukaryotic cell. Biochem. J. 250: 1-8.

Maeji N.J., Tribbick G., Bray A.M. and Geysen H.M. (1992). Simultaneous multiple synthesis of peptide-carrier conjugates. J. Immun. Methods. 146: 83-90.

Malecz N., McCabe P.C., Spaargaren C., Qiu R., Chuang Y. and Symons M. (2000). Synaptojanin2, a novel Rac1 effector that regulates clathrin-mediated endocytosis. Curr. Biol. 10: 1383-1386.

Malliri A. and Collard J.G. (2003). Role of Rho-family proteins in cell adhesion and cancer. Curr. Opin. Cell Biol. 15: 583-589.

Mallya S.K., Partin J.S., Valdizan M.C. and Lennarz W.J. (1992). Proteolysis of the major yolk glycoproteins is regulated by acidification of the yolk platelets in sea urchin embryos. J. Cell Biol. 117: 1211-1221.

Maly K., Überall F., Loferer H., Doppler W., Oberhuber H., Groner B. and Grunicke H.H. (1989). Ha-*ras* activates the Na^+/H^+ antiporter by a protein kinase C-independent mechanism. J. Biol. Chem. 264: 11839-11842.

Mamula M.J., Lin R., Janeway Jr C.A. and Hardin J.A. (1992). Breaking T cell tolerance with foreign and self co-immunogens. A study of autoimmune B and T cell epitopes of cytochrome c. J. Immunol. 149: 789-795.

Manoni M., Tribioli C., Lazzari B., DeBellis G., Patrosso C., Pergolizzi R., Pellegrini M., Maestrini E., Rivella S., Vezzoni P. and Toniolo D. (1991). The nucleotide sequence of a CpG island demonstrates the presence of the first exon of the gene encoding the human lysosomal membrane lamp2 and assigns the gene to Xq24. Genomics 9: 551-554.

Mapara M.Y. and Sykes M. (2004). Tolerance and cancer: mechanisms of tumor evasion and strategies for breaking tolerance. J. Clin. Oncol. 22: 1136-1151.

Maranda B., Brown D., Bourgoin S., Casanova J.E. Vinay P., Ausiello D.A. and Marshansky V. (2001). Intra-endosomal pH-sensitive recruitment of the Arf-nucleotide exchange factor ARNO and Arf6 from cytoplasm to proximal tubule endosomes. J. Biol. Chem. 276: 18540-18550.

Marbaix E., Kokorine I., Moulin P., Donnez J., Eeckhout Y. and Courtoy P.J. (1996). Menstrual breakdown of human endometrium can be mimicked *in vitro* and is selectively and reversibly blocked by inhibitors of matrix metalloproteinases. Proc. Natl. Acad. Sci USA 93: 9120-9125.

Marquardt D. and Center M.S. (1991). Involvement of vacuolar H^+-adenosine triphosphatase activity in multidrug resistance in HL60 cells. J. Natl. Cancer Inst. 83: 1098-1102.

Marsh M., Bolzau E. and Helenius A. (1983). Penetration of Semliki Forest virus from acidic prelysosomal vacuoles. Cell 71: 931-940.

Marsh M., Griffiths G., Dean G.E., Mellman I. and Helenius A. (1986). Three-dimensional structure of endosomes in BHK-21 cells. Proc. Natl. Acad. Sci. USA 83: 2899-2903.

Marsh M., Schmid S., Kern H., Harms E., Male P., Mellman I. and Helenius A. (1987). Rapid analytical and preparative isolation of functional endosomes by free flow electrophoresis. J. Cell Biol. 104: 875-886.

Martin J.L., Weenink S.M. and Baxter R.C. (2003). Insulin-like growth factor-binding protein-3 potentiates epidermal growth factor action in MCF-10A mammary epithelial cells. Involvement of p44/42 and p38 mitogen-activated protein kinases. J. Biol. Chem. 278: 2969-2976.

Martin S.F., Dudda J.C., Dellattre V., Bachtanian E., Leicht C., Burger B., Weltzien H.U. and Simon J.C. (2004). Fas-mediated inhibition of $CD4^+$ T cell priming results in dominance of type 1 $CD8^+$ T cells in the immune response to the contact sensitizer trinotrophenyl. J. Immunol. 173: 3178-3185.

Martin S.S., Haruta T., Morris A.J., Klippel A., Williams L.T. and Olefsky J.M. (1996a). Activated phosphatidylinositol 3'-kinase is sufficient to mediate actin rearrangement and GLUT4 translocation in 3T3- L1 adipocytes. J. Biol. Chem. 271: 17605-17608.

Martin S.S., Rose D.W., Saltiel A.R., Klippel A., Williams LT and Olefsky J.M. (1996b). Phosphatidylinositol 3'-kinase is necessary and sufficient for insulin-stimulated stress fibre breakdown. Endocrinology 137: 5045-5054.

Martinez-Zaguilan R., Raghunand N., Lynch R.M., Bellamy W., Martinez G.M., Rojas B., Smith D., Dalton W.S. and Gillies R.J. (1999). pH and drug resistance. I. Functional expression of plasmalemmal V-type H^+-ATPase in drug-resistant human breast carcinoma cell lines. Biochem. Pharmacol. 57: 1037-1046.

Matar P., Rozados V.R., Binda M.M., Roggero E.A., Bonfil R.D. and Scharovsky O.G. (1999). Inhibitory effect of lovaststin on spontaneous metastases derived from a rat lymphoma. Clin. Exp. Metastasis 17: 19-25.

Mattei M.G., Matteson J., Chen J.W., Williams M.A. and Fukuda M. (1990). Two human lysosome membrane glycoproteins, h-lamp-1 and h-lamp-2 are encoded by genes localized to chromosome 13q34 and chromosome Xq24-25, respectively. J. Biol. Chem. 265: 7548-7551.

Matteoni R. and Kreis T.E. (1987). Translocation and clustering of endosomes and lysosomes depends on microtubules. J. Cell Biol. 105: 1253-1265.

Matzinger P. (1994). Tolerance, danger, and the extended family. Annu. Rev. Immunol. 12: 991-1045.

Matzinger P. (2002). The danger model: a renewed sense of self. Science 296: 301-305.

Maxfield F.R. (1982). Weak bases and ionophores rapidly and reversibly raise the pH of endocytic vesicles in cultured mouse fibroblasts. J. Cell Biol. 95: 676-681.

Maxfield F.R. and Yamashiro J.D. (1991). Acidification of organelles and the intracellular sorting of proteins during endocytosis. In Trafficking of Membrane Proteins. Academic Press, New York, 157-181.

Mayor S., Presley J.F. and Maxfield F.R. (1993). Sorting of membrane components from endosome and subsequent recycling to the cell surface occurs by a bulk flow process. J. Cell Biol. 121: 1257-1269.

McBride H.M., Rybin V., Murphy C., Giner A., Teasdale R. and Zerail M. (1999). Oligomeric complexes link Rab5 effectors with NSF and drive membrane fusion via interactions between EEA1 and syntaxin 13. Cell 98: 377-386.

McDowall A., Gruenberg J., Romisch K. and Griffiths G. (1989). The structure of organelles of the endocytic pathway in hydrated cryosections of cultured cells. Eur. J. Cell Biol. 49: 281-294.

McGraw T.E., Dunn K.W. and Maxfield F.R. (1993). Isolation of a temperature-sensitive variant Chinese hamster ovary cell line with a morphologically altered endocytic recycling compartment. J. Cell Physiol. 155: 579-594.

McIntyre G.F. and Erickson A.H. (1993). The lysosomal proenzyme receptor that binds procathepsin L to microsomal membranes at pH 5 is a 43-kDa integral membrane protein. Proc. Natl. Acad. Sci USA 90: 10588-10592.

McKay I.A., Marshall C.J., Cales C. and Hall A. (1986). Transformation and stimulation of DNA synthesis in NIH-3T3 cells are a titratable function of normal p21N-ras expression. EMBO J. 5: 2617-2621.

McLauchlan H., Newell J., Morrice N., Osborne A., West M. and Smythe E. (1998). A novel role for Rab5-GDI in ligand sequestration into clathrin coated pits. Curr. Biol. 8: 34-45.

Mellman I. (1996). Endocytosis and molecular sorting. Annu. Rev. Cell Dev. Biol. 12: 575-625.

Méresse S., Gorvel J.P. and Chavrier P. (1995). The rab7 GTPase resides on a vesicular compartment connected to lysosomes. J. Cell Sci. 108: 3349-3358.

Merighi A. (1992). Post-embedding electron microscopic immunocytochemistry. In Electron Microscopic Immunocytochemistry: Principles and Practice. (Eds. Polak J.M. and Priestly J.V.). Oxford University Press, Oxford, 51-87.

Merithew E., Stone C., Eathiraj S. and Lambright D.G. (2003). Determinants of Rab5 interaction with the N terminus of early endosome antigen 1. J. Biol. Chem. 278: 8494-8500.

Merlo G.R., Basolo F., Fiore L., Duboc L. and Hynes N.E. (1995). p53-Dependent and p53-independent activation of apoptosis in mammary epithelial cells reveals a survival function of EGF and insulin. J. Cell Biol. 128: 1185-1196.

Merrifield C.J. (2004). Seeing is believing: imaging actin dynamics at single sites of endocytosis. Trends Cell Biol. 14: 352-358.

Metzger D.W., McNutt R.M., Collins J.T., Buchanan J.M., van Cleave V.H. and Dunnick W.A. (1997). Interleukin-12 acts as an adjuvant for humoral immunity through interferon-γ-dependent and –independent mechanisms. Eur. J. Immunol. 27: 1958-1965.

Meuller S.C. and Hubbard A.L. (1986). Receptor-mediated endocytosis of asialoglycoproteins by rat hepatocytes: receptor positive and receptor-negative endosomes. J. Cell Biol. 102: 932-942.

Meyer M., Maly K., Überall F., Hoflacher J. and Grunicke H. (1991). Stimulation of K^+ transport systems by Ha-ras. J. Biol. Chem. 266: 8230-8235.

Michael J.G. (1991). Cationization of protein antigens VI: effect of cationization on the immunoregulatory properties of a bovine serum peptide, a.a. 506-589. Cell. Immunol. 138: 121-129.

Mignatti P., Robbins E. and Rifkin D.B. (1986). Tumor invasion through the human amniotic membrane: requirement for a proteinase cascade. Cell 47: 487-498.

Millot C., Millot J.M., Morjani H., Desplaces A. and Manfait M. (1997). Characterization of acidic vesicles in multidrug-resistant and sensitive cancer cells by acridine orange staining and confocal microspectrofluorometry. J. Histochem. Cytochem. 45: 1255-1264.

Mills I.G., Jones A.T. and Clague M.J. (1998). Involvement of the endosomal autoantigen EEA1 in homotypic fusion of early endosomes. Curr. Biol. 8: 881-884.

Mitchell H., Choudhury A., Pagano R.E. and Leof E.B. (2004). Ligand-dependent and -independent transforming growth factor-β receptor recycling regulated by clathrin-mediated endocytosis and Rab11. Mol. Biol. Cell 15: 4166-4178.

Miura K., Miyazawa S., Furuta S., Mitsushita J., Kamijo K., Ishida H., Miki T., Suzukawa K., Resau J., Copeland T.D. and Kamata T. (2001). The Sos1-Rac1 signalling. Possible involvement of a vacuolar H^+-ATPase E subunit. J. Biol. Chem. 276: 46276-46283.

Miwako I., Yamamoto A., Kitamura T., Nagayama K. and Ohashi M. (2001). Cholesterol requirement for cation-independent mannose 6-phosphate receptor exit from multivesicular late endosomes to the Golgi. J. Cell. Sci. 114: 1765-1776.

Moin K., Day N.A., Sameni M., Hasnain S., Hirama T. and Sloane B.F. (1992). Human tumor cathepsin B: comparison with normal human liver cathepsin B. Biochem. J. 285: 427-434.

Moin K., Sameni M., Elliott E., Ziegler G. and Sloane B.F. (1994). *Ras* oncogene alters localisation of cathepsins. In Proteinases Involved in Cancer. (Eds. Suzuki M. and Hiwasa T.) Monduzzi Editore, Bologne, 51-88.

Montcourrier P., Mangeat P.H., Valembois C., Salazar G., Sahuquet A., Duperray C. and Rochefort H. (1994). Characterization of very acidic phagosomes in breast cancer cells and their association with invasion. J. Cell Sci. 107: 2381-2391.

Moolenar W.H., Tertoolen L.G.K. and de Laat S.W. (1984). Phorbol ester and diacylglycerol mimic growth factors in raising cytoplasmic pH. Nature 312: 371-373.

Moolman L (2002). Induction of auto-antibodies to cathepsin B. M.Sc. dissertation, University of Natal, Pietermaritzburg, South Africa.

Morewood C.R., Elliott E., Dennison C. and Bruton A.G. (1992). Further modifications of the LKB 7800 series KnifeMaker for improved reproducibility in breaking "cryo" knives. J. Microsc. 168: 111-114.

Morgan D.O., Edman J.C., Standring D.N., Fried V.A., Smith M.C., Roth R.A. and Rutter W.J. (1987). Insulin-like growth factor II receptor as a multifunctional binding protein. Nature 329: 301-307.

Morimoto C. and Borel Y. (1983). Hapten-specific carrier-dependent tolerance induction in man *in vitro*. Cell. Immunol. 82: 415-421.

Moriyama Y. (1996). Membrane energization by proton pumps is important for compartmentalization of drugs and toxins: a new type of active transport. J. Exp. Biol. 199: 1447-1454.

Moriyama Y. and Nelson N. (1989). Lysosomal H+-translocating ATPase has a similar subunit structure to chromaffin granule H+-ATPase complex. Biochim. Biophys. Acta 980: 241-247.

Moriyama Y., Maeda M. and Futai M. (1992). Involvement of a non-proton pump factor (possibly Donnan-type equilibrium) in maintenance of an acidic pH in lysosomes. FEBS Lett. 302: 18-20.

Morrison D.K., Kaplan D.R., Rapp U. and Roberts T.M. (1988). Signal transduction from membrane to cytoplasm: growth factors and membrane-bound oncogene products increase Raf-1 phosphorylation and associated protein kinase activity. Proc. Natl. Acad. Sci. USA 85: 8855-8859.

Mu F.T., Callaghan J.M., Steele-Mortimer O., Stenmark H., Parton R.G., Campbell P.L., McCluskey C., Yeo J.P., Tock E.P.C. and Toh B.H. (1995). EEA1, an early endosome-associated protein. EEA1 is a conserved α-helical peripheral membrane protein flanked by cysteine 'fingers' and contains a calmodulin-binding IQ motif. J. Biol. Chem. 270: 13503-13511.

Muallem S., Kwiatkowska K., Xu X. and Yin H.L. (1995). Actin filament disassembly is a sufficient trigger for exocytosis in nonexcitable cells. J. Cell Biol. 128: 589-598.

Muckerheide A., Apple R.J., Pesce A.J. and Michael J.G. (1987a). Cationization of protein antigens I: alteration of immunogenic properties. J. Immunol. 138: 833-837.

Muckerheide A., Domen P.L. and Michael J.G. (1987b). Cationization of protein antigens II: alteration of regulatory properties. J. Immunol. 138: 2800-2804.

Muckerheide A., Pesce A.J. and Michael J.G. (1990). Cationization of protein antigens V: effect of the degree of cationization on patterns of immune responsiveness. Cell. Immunol. 127: 67-77.

Mukherjee S., Ghosh R.N. and Maxfield F.R. (1997). Endocytosis. Physiol. Rev. 77: 759-803.

Mulberg A.E., Tulk B.M. and Forgac M. (1991). Modulation of coated vesicle chloride channel activity and acidification by reversible protein kinase A-dependent phosphorylation. J. Biol. Chem. 266: 20590-20593.

Mullock B.M., Bright N.A., Fearson C.W., Gray S.R. and Luzio J.P. (1998). Fusion of lysosomes with late endosomes produces a hybrid organelle of intermediate density and is NSF dependent. J. Cell Biol. 140: 591-601.

Mullock B.M., Perez J.H., Kuwana T., Gray S.R. and Luzio J.P. (1994). Lysosomes can fuse with a late endosomal compartment in a cell-free system from rat liver. J. Cell Biol. 126: 1173-1182.

Murakami T., Shibuya I., Ise T., Chen Z.S., Akiyama S., Nakagawa M., Izumi H., Nakamura T., Matsuo K., Yamada Y. and Kohno K. (2001). Elevated expression of vacuolar proton pump genes and cellular pH in cisplatin resistance. Int. J. Cancer 93: 869-874.

Murphy C., Saffrich R., Grummt M., Gournier H., Rybin V., Rubino M., Auvinen P., Lütcke A., Parton R.G. and Zerial M. (1996). Endosome dynamics regulated by a Rho protein. Nature 384: 427-432.

Murphy R.F. (1991). Maturation models for endosome and lysosome biogenesis. Trends Cell Biol. 1: 77-82.

Murray J.W. and Wolkoff A.W. (2003). Roles of the cytoskeleton and motor proteins in endocytic sorting. Adv. Drug Deliv. Rev. 55: 1385-1403.

Muschel R.J., Williams J.E., Lowry D.R. and Liotta L.A. (1985). Harvey ras induction of metastatic potential depends upon oncogene activation and the type of recipient cell. Am. J. Pathol. 121: 1-8.

Muthuswamy S.K., Li D., Lelievre S., Bissell M.J. and Brugge J.S. (2001). ErbB2, but not ErbB1, reinitiates proliferation and induces luminal repopulation in epithelial acini. Nat. Cell Biol. 3: 785-792.

Mwandumba H.C., Russell D.G., Nyirenda M.H., Anderson J., White S.A., Molyneux M.E. and Squire S.B. (2004). Mycobacterium tuberculosis resides in nonacidified vacuoles in endocytically competent alveolar macrophages from patients with tuberculosis and HIV infection. J. Immunol. 172: 4592-4598.

Myers M. and Forgac M. (1993). Assembly of the peripheral domain of the bovine vacuolar H(+)-adenosine triphosphatase. J. Cell. Physiol. 156: 35-42.

Naim J.O. and van Oss C.J. (1991). The generation of antibody in mice to tufsin: a naturally occurring phagocytosis stimulating tetrapeptide. Immunol. Invest. 20: 351-364.

Nair P., Schaub B.E. and Rohrer J. (2003). Characterization of the endosomal sorting signal of the cation-dependent mannose 6-phosphate receptor. J Biol Chem. 278: 24753-24758.

Nakata T. and Hirokawa N. (1995). Point mutations of adenosine triphosphate-binding motif generated rigor kinesin that selectively blocks anteretrograde lysosome membrane transport. J. Cell Biol. 131: 1039-1053.

Nelson N. (1992). Organellar proton-ATPases. Curr. Opin. Cell Biol. 4: 654-660.

Neumann D., Wikstrom L., Watowich S.S. and Lodish H.F. (1993). Intermediates in degradation of the erythropoietin receptor accumulate and are degraded in lysosomes. J. Biol. Chem. 268: 13639-13649.

Newman G.R. and Jasani B. (1984). Post-embedding immunoenzyme techniques. In Immunolabelling for Electron Microscopy. (Eds. Polak JM and Varndell IM). Elsevier Science Publishers BV, 54-70.

Newman G.R., Jasani B. and Williams E.D. (1982). The preservation of ultrastucture and antigenicity. J. Microsc. 127: RP5-RP6.

Newman G.R., Jasani B. and Williams E.D. (1983). A simple postembedding system for the rapid demonstration of tissue antigens under the electron microscope. Histochem. J. 15: 543-555.

Nicolson G.L. (1989). Metastatic tumor cell interactions with endothelium, basement membrane and tissue. Curr. Opin. Cell Biol. 1: 1009-1019.

Nielson E., Severin F., Backer J.M., Hyman A.A. and Zerial M. (1999). Rab5 regulates motility of early endosomes on microtubules. Nature Cell Biol. 1: 376-382.

Nimnual A.S., Taylor L.J. and Bar-Sagi D. (2003). Redox-dependent downregulation of Rho by Rac. Nat. Cell Biol. 5: 236-241.

Ninomiya Y., Kishimoto T., Miyashita Y. and Kasai H. (1996). Ca^{2+}-dependent exocytic pathways in Chinese Hamster Ovary fibroblasts revealed by a caged-Ca^{2+} compound. J. Biol. Chem. 271: 17751-17754.

Nishimura Y., Sameni M. and Sloane B.F. (1998). Malignant transformation alters intracellular trafficking of lysosomal cathepsin D in human breast epithelial cells. Path. Onc. Res. 4: 283-296.

Nobes C.D. and Hall A. (1995). Rho, Rac, and Cdc42 GTPases regulate the assembly of multimolecular focal complexes associated with actin stress fibers, lamellipodia, and filopodia. Cell 81: 53-62.

Nobes C.D., Hawkins P., Stephens L. and Hall A. (1995). Activation of the small GTP-binding proteins Rho and Rac by growth factor receptors. J. Cell Sci. 108: 225-233.

Noel J. and Pouyssegur J. (1995). Hormonal regulation, pharmacology, and membrane sorting of vertebrate Na^+/H^+ exchanger isoforms. Am. J. Physiol. 268: C283-C296.

Noguchi Y., Himeno M., Sasaki H., Tanaka Y., Kono A., Sasaki Y. and Kato K. (1989). Isolation and sequencing of a cDNA clone encoding 96 kDa sialglycoprotein in rat liver lysosomal membranes. Biochem. Biophys. Res. Commun. 164: 1113-1120.

Nomura H., Sato H., Seiki M., Mai M. and Okada Y. (1995). Expression of membrane-type matrix metalloproteinase in human gastric carcinomas. Cancer Res. 55: 3263-3266.

Norman J.C., Price L.S, Ridley A.J., Hall A. and Koffer A. (1994). Actin filament organization in activated mast cells is regulated by heterodimeric and small GTP-binding proteins. J. Cell Biol. 126: 1005-1015.

Norman J.C., Price L.S., Ridley A.J. and Koffer A. (1996). The small GTP-binding proteins, Rac and Rho, regulate cytoskeletal reorganization and exocytosis in mast cells by parallel pathways. Mol. Biol. Cell 7: 1429-1442.

Numata M., Petrecca K., Lake N. and Orlowski J. (1998). Identification of a mitochondrial Na^+/H^+ exchanger. J. Biol. Chem. 273: 6951-6959.

Ochieng J., Basolo F., Albini A., Melchiori A., Watanabe H., Elliott J., Raz A., Parodi S. and Russo J. (1991). Increased invasive, chemotactic and locomotive abilities of c-Ha-ras transformed human breast epithelial cells. Invasion Metastasis 11: 38-47.

Ohkuma S. and Poole B. (1978). Fluorescence probe measurement of the intralysosomal pH in living cells and the perturbation of pH by various agents. Proc. Natl. Acad. Sci. USA 75: 3327-3331.

Ohkuma S., Moriyama Y. and Takano T. (1982). Identification and characterization of a proton pump on lysosomes by fluorescein-isothiocyanate-dextran fluorescence. Proc. Natl. Acad. Sci. USA 79: 2758-2762

Okumura Y., Sato H., Seiki M. and Kido H. (1991). Proteolytic activation of the precursor of membrane-type 1 matrix metalloproteinase by human plasmin. A possible cell surface activator. FEBS Lett. 402: 181-184.

Olson L.J., Dahms N.M. and Kim J.J. (2004a). The N-terminal carbohydrate recognition site of the cation-independent mannose 6-phosphate receptor. J. Biol. Chem. 279: 34000-34009.

Olson L.J., Yammani R.D., Dahms N.M. and Kim J.J. (2004b). Structure of uPAR, plasminogen, and sugar-binding sites of the 300 kDa mannose 6-phosphate receptor. EMBO J. 23: 2019-2028.

Olson M.F., Ashworth A. and Hall A. (1995). An essential role for Rho, Rac, and Cdc42 GTPases in cell cycle progression through G_1. Science 269: 1270-1272.

Orci L., Halban P., Perrelet A., Amherdt A., Ravazzola M. and Anderson R.G.W. (1994). pH-independent and -dependent cleavage of proinsulin in the same secretory vesicle. J. Cell Biol. 126: 1149-1156.

Orci L., Ravazzola M. and Anderson R.G.W. (1987). The condensing vacuole of exocrine cells is more acidic than the mature secretory vesicle. Nature. 326: 77-79.

Orci L., Ravazzola M., Amherdt M., Madsen O., Vassalli J.D. and Perrelet A. (1985). Direct identification of prohormone conversion site in insulin-secreting cells. Cell. 42: 671-681.

Orlowski J. and Grinstein S. (1997). Na^+/H^+ exchangers of mammalian cells. J. Biol. Chem. 272: 22373-22376.

Orsel J.G., Sincock P.M., Krise J.P. and Pfeffer S.R. (2000). Recognition of the 300-kDa mannose 6-phosphate receptor cytoplasmic domain by 47-kDa tail-interacting protein. Proc. Natl. Acad. Sci. USA 97: 9047-9051.

Ostad M., Shu W., Kong L and Liu B. C. (1996). Ha-ras oncogene expression abrogates a pH dependent endonuclease activity of apoptosis in normal rat kidney cells. Cancer Lett. 98: 175-182.

Overwijk W.W., Lee D.S., Surman D.R., Irvine K.R., Touloukian C.E., Chan C., Carrol M.W., Moss B., Rosenberg S.A. and Restifo N.P. (1999). Vaccination with a recombinant vaccinia virus encoding a "self" antigen induces autoimmune vitiligo and tumor cell destruction in mice: requirement for $CD4^+$ T lymphocytes. Proc. Natl. Acad. Sci USA 96: 2982-2987.

Paglin S., Hollister T., Delohery T., Hackett N., McMahill M., Sphicas E., Domingo D. and Yahalom J. (2001). A novel response of cancer cells to radiation involves autophagy and formation of acidic vesicles. Cancer Res. 61: 439-444.

Panchal R.G., Cusack E., Cheley S. and Bayley H. (1996). Tumor protease-activated, pore-forming toxins from a combinatorial library. Nature Biotech. 14: 852-856.

Pardoll D.M. (1999). Inducing autoimmune disease to treat cancer. Proc. Natl. Acad. Sci USA 96:5340-5342.

Pardoll D.M. and Topalian S.L. (1998). The role of $CD4^+$ T cell responses in antitumor immunity. Curr. Opin. Immunol. 10: 588-594.

Pardridge W.M., Bickel U., Buciak J., Yang J. and Diagne A. (1994c). Enhanced endocytosis and anti-human immunodeficiency virus type 1 activity of anti-rev antibodies after cationization. J. Infect. Dis. 169: 55-61.

Pardridge W.M., Bickel U., Buciak J., Yang J., Diagne A. and Aepinus C. (1994a). Cationization of a monoclonal antibody to the human immunodeficiency virus REV protein enhances cellular uptake but does not impair antigen binding of the antibody. Immunol. Lett. 42: 191-195.

Pardridge W.M., Buciak J., Yang J. and Diagne A. (1994b). Treatment of human immunodeficiency virus-infected lymphocytes with cationized human immunoglobulins. J. Infect. Dis. 170: 563-569.

Pardridge W.M., Buciak J., Yang J. and Wu D. (1998). Enhanced endocytosis in cultured human breast carcinoma cells and in vivo biodistribution in rats of a humanized monoclonal antibody after cationization of the protein. J. Pharmacol. Exp. Ther. 286: 548-554.

Pardridge W.M., Kang Y.S., Yang J. and Buciak J.L. (1995). Enhanced cellular uptake and in vivo biodistribution of a monoclonal antibody following cationization. J. Pharm. Sci. 84: 943-948.

Paris S. and Pouysségur J. (1984). Growth factors activate the Na^+/H^+ antiporter in quiescent fibroblasts by increasing its affinity for intracellular H^+. J. Biol. Chem. 259: 10989-10994.

Park C., Lee I. and Kang W.K. (2001). Lovastatin-induced E2F-1 modulation and its effect on prostrate cancer cell death. Carcinogenesis 22: 1727-1731.

Park W.H., Jung C.W., Park J.O., Kim K., Kim W.S., Im Y.H., Lee M.H., Kang W.K. and Park K. (2003b). Monensin inhibits the growth of renal cell carcinoma cells via cell cycle arrest or apoptosis. Int. J. Oncol. 22: 855-860.

Park W.H., Kim E.S., Jung C.W., Kim B.K. and Lee Y.Y. (2003c). Monensin-mediated growth inhibition of SNU-C1 colon cancer cells via cell cycle arrest and apoptosis. Int. J. Oncol. 22: 377-382.

Park W.H., Kim E.S., Kim B.K. and Lee Y.Y. (2003a). Monensin-mediated growth inhibition in NCI-H929 myeloma cells via cell cycle arrest and apoptosis. Int. J. Oncol. 23: 197-204.

Park W.H., Lee M.S., Park K., Kim E.S., Kim B.K. and Lee Y.Y. (2002b). Monensin-mediated growth inhibition in acute myelogenous leukemia cells via cell cycle arrest and apoptosis. Int. J. Cancer 101: 235-242.

Park W.H., Seol J.G., Kim E.S., Kang W.K., Im Y.H., Jung C.W., Kim B.K. and Lee Y.Y. (2002a). Monensin-mediated growth inhibition in human lymphoma cells through cell cycle arrest and apoptosis. Br. J. Haematol. 119: 400-407.

Parton R.G., Dotti C.G., Bacallao R., Kurtz I., Simons K. and Prydz K. (1991). pH-induced microtubule-dependent redistribution of late endosomes in neuronal and epithelial cells. J. Cell Biol. 113: 261-274.

Pearse B.M. and Robinson M.S. (1990). Clathrin, adaptors, and sorting. Annu. Rev. Cell Biol. 6: 151-171.

Peng L., Carlton G.J. and Burnett J.W. (1986). Stability of antibody attachment in immunosorbent chromatography. Enzyme Microb. Technol. 8: 681-685.

Peters P.J., Borst J., Oorschot V., Fukuda M., Kräbenbül O., Tschopp J., Slot J.W. and Geuze H.J. (1991). Cytotoxic T lymphocytes granules are secretory lysosomes, containing both perforin and granzymes. J. Exp. Med. 173: 1099-1109.

Pewitt E.B., Hegde R.S., Haas M. and Palfrey H.C. (1990). The regulation of Na/K/2Cl cotransport and bumetanide binding in avian erythrocytes by protein phosphorylation and dephosphorylation. Effects of kinase inhibitors and okadaic acid. J. Biol. Chem. 265: 20747-20756.

Pieper R., Christian R.E., Gonzales M.I., Nishimura M.I., Gupta G., Settlage R.E., Shabanowtz J., Rosenberg S.A., Hunt D.F. and Topalian S.L. (1999). Biochemical identification of a mutated human melanoma antigen recognized by $CD4^+$ T cells. J. Exp. Med. 189: 757-765.

Pillay C.S., Elliott E. and Dennison C. (2002). Endolysosomal proteolysis and its regulation. Biochem. J. 363: 417-429.

Piper R.C. and Luzio J.P. (2001). Late endosomes: sorting and partitioning in multivesicular bodies. Traffic 2: 612-621.

Pisoni R.L. and Theone J.G. (1991). The transport systems of mammalian lysosomes. Biochim. Biophys. Acta. 1071: 351-373.

Pohlmann R., Boeker M.W.C. and von Figura K. (1995). The two mannose 6-phosphate receptors transport distinct complements of lysosomal proteins. J. Biol. Chem. 270: 27311-27318.

Pol A., Ortega D. and Enrich C. (1997). Identification of cytoskeleton-associated proteins in isolated rat liver endosomes. Biochem. J. 327: 741-746.

Polson A., Coetzer T., Kruger J., von Maltzahn E. and van der Merwe K.J. (1985). Improvements in the isolation of IgY from the yolks of eggs laid by immunized eggs. Immunol. Invest. 14: 323-327.

Polson A., Potgieter G.M., Largier J.F., Mears E.G.F. and Joubert F.J. (1964). The fractionation of protein mixtures by linear polymers of high molecular weight. Biochim. Biophys. Acta. 82: 463-475.

Polyak S., Chen H., Hirsch D., George I., Hershberg R. and Sperber K. (1997). Impaired class II expression and antigen uptake in monocytic cells after HIV-1 infection. J. Immun. 159: 2177-2188.

Prasanna P., Thibault A., Liu L. and Samid D. (1996). Lipid metabolism as a target for brain cancer therapy: synergistic activity of lovastatin and sodium phenylacetate against human glioma cells. J. Neurochem. 66: 710-716.

Premzl A. and Kos J. (2003). Cysteine and aspartic proteases cathepsins B and D determine the invasiveness of MCF10A neoT cells. Radiol. Oncol. 37: 241-248.

Premzl A., Zavašnik-Bergant V., Turk V. and Kos J. (2003). Intracellular and extracellular cathepsin B facilitate invasion of MCF-10A neoT cells through reconstituted extracellular matrix in vitro. Exp. Cell Res. 283: 206-214.

Prence E.M., Dong J.M. and Sahagian G.G. (1990). Modulation of the transport of a lysosomal enzyme by PDGF. J. Cell Biol. 110: 319-326.

Prendergast G.C. and Gibbs J.B. (1993). Pathways of Ras function: connections to the actin cytoskeleton. Adv. Cancer Res. 62: 35-64.

Press B., Feng Y., Hoflack B. and Wandinger-Ness A. (1998). Mutant Rab7 causes the accumulation of cathepsin D and cation-independent mannose 6-phosphate receptor in an early endocytic compartment. J. Cell Biol. 140: 1075-1089.

Pressman B.C. (1976). Biological applications of ionophores. Annu. Rev. Biochem. 45: 501-530.

Price L.S., Norman J.C., Ridley A.J. and Koffer A. (1995). Small GTPases, Rac and Rho, as regulators of secretion in mast cells. Curr. Biol. 5: 68-73.

Qyang Y., Luo X., Lu T., Ismail P., Krylov D., Vinson C. and Sawadogo M. (1999). Cell-type-dependent activity of the ubiquitous transcription factor USF in cellular proliferation and transcriptional activation. Mol. Cell. Biol. 19: 1508-1517.

Rabinowitz S., Horstman H., Gordon S. and Griffiths G. (1992). Immunocytochemical characterization of the endocytic and phagolysosomal compartments in peritoneal macrophages. J. Cell Biol. 116: 95-112.

Raghunand N., Martinez-Zaguilan R., Wright S.H. and Gillies R.J. (1999). pH and drug resistance. II. Turnover of acidic vesicles and resistance to weakly basic chemotherapeutic drugs. Biochem. Pharmacol. 57: 1047-1058.

Rao R.N. (1996). Targets for cancer therapy in the cell cycle pathway. Curr. Opin. Oncol. 8: 516-524.

Rao S., Porter D.C., Chen X., Herliczek T., Lowe M. and Keyomarsi K. (1999). Lovastatin-mediated G1 arrest is through inhibition of the proteosome, independent of hydroxymethylglutaryl-CoA reductase. Proc. Natl. Acad. Sci. USA 96: 7797-7802.

Rash J.E. (1986). Glutaraldehyde chemistry: fixation reactions consume oxygen and are inhibited by tissue anoxia. J. Cell Biol. 87: 234-238.

Ray L.B. and Sturgill T.W. (1987). Rapid stimulation by insulin of a serine/threonine kinase in 3T3-L1 adipocytes that phosphorylates microtubule-associated protein 2 in vitro. Proc. Natl. Acad. Sci. USA 84: 1502-1506.

Read S.M. and Northcote D.H. (1981). Minimization of variation in the response to different proteins of the Coomassie Blue dye-binding assay for protein. Anal. Biochem. 116: 53-64.

Reddy S.T., Chai W., Childs R.A., Page J.D., Feizi T. and Dahms N.M. (2004). Identification of a low affinity mannose 6-phosphate-binding site in domain 5 of the cation-independent mannose 6-phosphate receptor. J. Biol. Chem. 279: 38658-38667.

Reszka A.A., Seger R., Diltz C.D., Krebs E.G. and Fischer E.H. (1995). Association of mitogen-activated protein kinase with the microtubule cytoskeleton. Proc. Natl. Acad. Sci. USA 92: 8881-8885.

Reynaud C.A., Bertocci B., Dahan A. and Weill J.C. (1994). Formation of the chicken B cell repertoire – ontogeny, regulation of Ig gene rearrangement, and diversification by gene conversion. Adv. Immunol. 57: 353-378.

Ridley A.J. and Hall A. (1992). The small GTP-binding protein Rho regulates the assembly of focal adhesions and actin stress fibres in response to growth factors. Cell 70: 389-399.

Ridley A.J. and Hall A. (1994). Signal transduction pathways regulating Rho-mediated stress fibre formation: requirement for a tyrosine kinase. EMBO J. 13: 2600-2610.

Ridley A.J., Paterson H.F., Johnston C.L., Diekmann D. and Hall A. (1992). The small GTP-binding protein Rac regulates growth factor-induced membrane ruffling. Cell 70: 400-410.

Ridley A.J., Self A.J., Kasmi F., Paterson H.F., Hall A., Marshall C.J. and Ellis C. (1993). Rho family GTPase-activating proteins p190, bcr, and RhoGAP show distinct specificities *in vitro* and *in vivo*. EMBO J. 12: 5151-5160.

Riederer M.A., Soldati T., Shapiro A.D., Lin J. and Pfeffer S. (1994). Lysosome biogenesis requires Rab9 function and receptor recycling from endosomes to the *trans* Golgi network. J. Cell Biol. 125: 573-582.

Riezman H. (1993). Yeast endocytosis. Trends Cell Biol. 273-277.

Rijnboutt S.W., Kal A.J., Geuze H.J., Aerts H. and Strous G.J. (1991). Mannose 6-phosphate-independent targeting of cathepsin D to lysosomes in HepG2 cells. J. Biol. Chem. 266: 23586-23592.

Rijnboutt S.W., Stoorvogel H.J., Geuze H.J. and Strous G.J. (1992). Identification of subcellular compartments involved in biosynthetic processing of cathepsin D. J. Biol. Chem. 267: 15665-15672.

Ritter M., Wöll E., Häussinger D. and Lang F. (1992). Effects of bradykinin on cell volume and intracellular pH in NIH 3T3 fibroblasts expressing the *ras* oncogene. FEBS Lett. 307: 367-370.

Ritter M., Wöll E., Waldegger S., Häussinger D., Lang H.J., Scholz W., Scholkens B. and Lang F. (1993). Cell shrinkage stimulates bradykinin-induced cell membrane potential oscillations in NIH 3T3 fibroblasts expressing the *ras*-oncogene. Pflügers Arch. 423: 221-224.

Robertson D., Monaghan P., Clarke C. and Atherton A.J. (1992). An appraisal of low-temperature embedding by progressive lowering of temperature into Lowicryl HM20 for immunocytochemical studies. J. Microsc. 168: 85-100.

Rodriguez A., Webster P., Ortego J. and Andrews N.W. (1997). Lysosomes behave as Ca^{2+}-regulated exocytic vesicles in fibroblasts and epithelial cells. J. Cell Biol. 137: 93-104.

Roederer M., Barry J.R., Wilson R.B. and Murphy R.F. (1990). Endosomes can undergo an ATP-dependent density increase in the absence of dense lysosomes. Eur. J. Cell Biol. 51: 229-234.

Roederer M., Bowser R. and Murphy R.F. (1987). Kinetics and temperature dependence of exposure of endocytosed material to proteolytic enzymes and low pH: evidence for a maturation model for the formation of lysosomes. J. Cell Physiol. 131: 200-209.

Rohrer J., Schweizer A., Johnson K.F. and Kornfeld S. (1995). A determinant in the cytoplasmic tail of the cation-independent mannose-6-phosphate receptor prevents trafficking to lysosomes. J. Cell Biol. 130: 1297-1306.

Roitt I. (1994). In Essential Immunology. Blackwell Scientific Publications, Oxford.

Roldan A.L., Cubellis M.V., Masucci M.T., Behrendt N., Lund L.R., Dano K., Appella E. and Blasi F. (1990). Cloning and expression of the receptor for human urokinase plasminogen activator, a central molecule in cell surface, plasmin dependent proteolysis. EMBO J. 9: 467-474.

Rose W.C., Lee F.Y., Fairchild C.R., Lynch M., Monticello T., Kramer R.A. and Manne V. (2001). Preclinical antitumor activity of BMS-214662, a highly apoptotic and novel farnesyltransferase inhibitor. Cancer Res. 61: 7507-7517.

Roth J. (1984). The protein A-gold technique for antigen localization in tissue sections by light and electron microscopy. In Immunolabelling for Electron Microscopy. (Eds. Polak J.M. and Varndell I.M.). Elsevier Science Publishers BV.

Rowland G.F., Polson A., van der Merwe K.J. (1986). Antibodies from chicken eggs. S. Afr. J. Sci. 82: 339.

Rozhin J., Sameni M., Ziegler G. and Sloane B.F. (1994). Pericellular pH affects distribution and secretion of cathepsin B in malignant cells. Cancer Res. 54: 6517-6525.

Ruley H.E. (1983). Adenovirus early region 1A enables viral and cellular transforming genes to transform primary cells in culture. Nature 304: 602-606.

Russo J., Tait L. and Russo H. (1991). Morphological expression of cell transformation induced by c-Ha-*ras* oncogene in human breast epithelial cells. J. Cell Sci. 99: 453-463.

Sahai E. and Marshall C.J. (2002). Rho-GTPases and cancer. Nature Reviews Cancer 21: 133-142.

Sahara H. and Shastri N. (2003). Second class minors: molecular identification of the autosomal *H46* histocompatability locus as a peptide presented by major histocompatability complex class II molecules. J. Exp. Med. 197: 375-385.

Sahin U., Türeci Ö. and Pfreundschuh M. (1997). Serological identification of human tumor antigens. Curr. Opin. Immunol. 9: 709-716.

Saitoh O., Wang W.C., Lotan R. and Fukuda M. (1992). Differential glycosylation and cell surface expression of lysosomal membrane glycoproteins in sublines of a human colon cancer exhibiting distinct metastatic potentials. J. Biol. Chem. 267: 5700-5711.

Salzman N.H. and Maxfield F.R. (1988). Intracellular fusion of sequentially formed endocytic compartments. J. Cell Biol. 106: 1083-1091.

Sameni M., Elliott E., Ziegler G., Fortgens P.H., Dennison C. and Sloane B.F. (1995). Cathepsin B and D are localized at the surface of human breast cancer cells. Pathol. Oncol. Res. 1: 43-53.

Sameni M., Moin K. and Sloane B.F. (2000). Imaging proteolysis by living human breast cancer cells. Neoplasia 2: 496-504.

Sanger F. (1945). The free amino groups of insulin. Biochem. J. 39: 507-515.

Sanger F. and Thompson E.O.P. (1953). The amino-acid sequence in the glycylchain of insulin. 2. The investigation of peptides from enzymatic hydrolysates. Biochem. J. 53: 366-374.

Santama N., Krijnse-Locker J., Griffiths G., Noda Y., Hirokawa N. and Dotti C.G. (1998). KIF2β, a new kinesin superfamily protein in non-neuronal cells, is associated with lysosomes and may be implicated in their centrifugal translocation. EMBO J. 17: 5855-5867.

Sapperstein S.K., Walter D.M., Grosvenor A.R., Heuser J.E. and Waters M.G. (1995). p115 is a general vesicular transport factor related to the yeast endoplasmic to Golgi transport factor Uso1p. Proc. Natl. Acad. Sci. USA 92: 522-526.

Sardet C., Counillon L., Franchi A. and Pouysségur J. (1990). Growth factors induce phosphorylation of the Na^+/H^+ antiporter, glycoprotein of 110 kD. Science 247: 723-726.

Sardet C., Fafournoux P. and Pouysségur J. (1991). α-Thrombin, epidermal growth factor, and okadaic acid activate the Na^+/H^+ exchanger, NHE-1, by phosphorylating a set of common sites. J. Biol. Chem. 266: 19166-19171.

Sautin Y.Y., Lu M., Gaugler A., Zhang L. and Gluck S.L. (2005). Phosphatidylinositol 3-kinase-mediated effects of glucose on vacuolar H^+-ATPase assembly, translocation, and acidification of intracellular compartments in renal epithelial cells. Mol. Cell Biol. 25: 575-89.

Savina A., Fader C.M., Damiani M.T. and Colombo M.I. (2005). Rab11 promotes docking and fusion of multivesicular bodies in a calcium-dependent manner. Traffic 6: 131-143.

Sawada R., Lowe J.B. and Fukuda M. (1993a). E-selectin dependent adhesion efficiency of colonic carcinoma cells is increased by genetic manipulation of their cell surface lamp-1 expression levels. J. Biol. Chem. 268: 12675-12681.

Sawada R., Tsuboi S. and Fukuda M. (1993b). Differential E-selectin dependent adhesion efficiency in sublines of a human colon cancer exhibiting distinct metastatic potentials. J. Biol. Chem. 269: 1425-1431.

Schiff R.I. and Gennaro Jr. J.F. (1979). The role of the buffer in the fixation of biological specimens for transmission and scanning electron microscopy. Scanning 2: 135-148.

Schilizzi B.M., Kroesen B.J., The T.H. and de Leij L. (1992). Increased production of antigen specific B lymphocytes during *in vitro* immunization using carrier-specific T helper hybridomas. J. Immun. Methods. 153: 49-56.

Schneider D.L. (1981). ATP-dependent acidification of intact and disrupted lysosomes. Evidence for an ATP-driven proton pump. J. Biol. Chem. 256: 3858-3864.

Scott M.G. and Fleischman J.B. (1982). Preferential idiotype-isotype associations in antibodies to dinitrophenyl antigens. J. Immun. 128: 2622-2628.

Seaman M.N. (2004). Cargo-selective endosomal sorting for retrieval to the Golgi requires retromer. J. Cell. Biol. 165: 111-122.

Segre M. and Segre D. (1994). Behavior of the idiotypic network in conventional immune responses III: Detection and enumeration of cells producing idiotypic and anti-idiotypic antibodies by a spot ELISA technique. Cell. Immunol. 159: 40-48.

Sennoune S.R., Bakunts K., Martinez G.M., Chua-Tuan J.L., Kebir Y., Attaya M.N. and Martinez-Zaguilan R. (2004). Vacuolar H^+-ATPase in human breast cancer cells with distinct metastatic potential: distribution and functional activity. Am. J. Physiol. Cell Physiol. 286: C1443-1452.

Shaik M.S., Chatterjee A. and Singh M. (2004). Effects of monensin liposomes on the cytotoxicity, apoptosis and expression of multidrug resistance genes in doxorubicin-resistant human breast tumour (MCF-7/dox) cell-line. J. Pharm. Pharmacol. 56: 899-907.

Shekhar P.V.M., Welte R, Christman J.K., Wang H. and Werdell J (1997). Altered P53 conformation: a novel mechanism of wild-type *p53* functional inactivation in a model for early human breast cancer. Int. J. Oncol. 11: 1087-1094.

Siddhanta U., McIlroy J., Shah A., Zhang Y. and Backer J.M. (1998). Distinct roles for the p110α and hVPS34 phosphatidylinositol 3'-kinases in vesicular trafficking, regulation of the actin cytoskeleton, and mitogenesis. J. Cell Biol. 143: 1647-1659.

Silverstein R.L. and Febbraio M. (1992). Identification of lysosome-associated membrane protein-2 as an activation-dependent platelet surface glycoprotein. Blood 80: 1470-1475.

Simons M., Keller P., Dichgans J. and Schulz J.B. (2001). Cholesterol and Alzheimer's disease: is there a link. Neorology 57: 1089-1093.

Simonsen A., Gaullier J.M., D'Arrigo A. and Stenmark H. (1999). The Rab5 effector EEA1 interacts directly with syntaxin-6. J. Biol. Chem. 274: 28857-28860.

Simonsen A., Lippe R., Christoforidis S., Gaullier J.M., Brech A., Callaghan J., Toh B.H., Murphy C., Zerial M. and Stenmark H. (1998). EEA1 links PI(3)K function to Rab5 regulation of endosome fusion. Nature 394: 494-498.

Singh R.R., Ebling F.M., Albuquerque D.A., Saxena V., Kumar V., Giannini E.H., Marion T.N., Finkelman F.D. and Hahn B.H. (2002). Induction of autoantibody production is limited in nonautoimmune mice. J. Immunol. 169: 587-594.

Sloane B.F., Moin K., Sameni M., Tait L., Rozhin J. and Ziegler G. (1994a). Membrane association of cathepsin B can be induced by transfection of human breast epithelial cells with c-Ha-*ras* oncogene. J. Cell Sci. 107: 373-384.

Sloane B.F., Sameni M., Cao L., Berquin I., Rozhin J., Ziegler G., Moin K. and Day N. (1994b). Alterations in processing and trafficking of cathepsin B during malignant progression. In Biological Functions of Proteases and Inhibitors. (Eds. Katunuma N., Travis J. and Fritz H.). Tokyo, Japan Scientific Societies Press, 131-147.

Slot J.W. and Geuze H.J. (1985). A new method of preparing gold probes for multiple-labeling cytochemistry. Eur. J. Cell Biol. 38: 87-93.

Slot J.W., Posthuma G., Chang L.Y., Krapo J.D. and Geuze H.J. (1989). Quantitative aspects of immunogold labeling in embedded and non-embedded sections. Am. J. Anat. 185: 271-281.

Snider D.P. and Segal D.M. (1989). Efficiency of antigen presentation after antigen targeting to surface IgD, IgM, MHC, Fcgamma RII, and B220 molecules on murine splenic B cells. J. Immunol. 143: 59-65.

Soldati T., Shapiro A.D., Dirac Svejstrup A.B. and Pfeffer S.R. (1994). Membrane targeting of the small GTPase Rab9 is accompanied by nucleotide exchange. Nature 369: 76-78.

Soule H., Maloney T.M., Wolman S.R., Peterson Jr W.D., Brenz R., McGrath C.M., Russo J., Pauly R.J., Jones R.F. and Brooks S.C. (1990). Isolation and characterization of a spontaneously immortalized human breast epithelial cell line MCF-10. Cancer Res. 50: 6075-6086.

Spiotto M.T., Fu Y. and Schreiber H. (2003). Tumor immunity meets autoimmunity: antigen levels and dendritic cell maturation. Curr. Opin. Immunol. 15: 725-730.

Stampfer M.R. and Yaswen P. (2000). Culture models of human mammary epithelial cell transformation. J. Mamm. Gland Biol. Neoplasia 5: 365-378.

Steele M.G. and Herscowitz H.B. (1993). Suppression of murine IgM, IgG, IgA and IgE antibody responses by alveolar macrophages. Immunol. 80: 62-67.

Steinhoff U., Burkhart C., Arnheiter H., Hengartner H. and Zinkernagel R. (1994). Virus or a hapten-carrier complex can activate autoreactive B cells by providing linked T help. Eur. J. Immunol. 24: 773-776.

Steinman R.M., Brodie S.E. and Cohn Z.A. (1976). Membrane flow during pinocytosis. J. Cell Biol. 68: 665-687.

Stenmark H., Aasland R., Toh B.H. and D'Arrigo A. (1996). Endosomal localization of the autoantigen EEA1 is mediated by a zinc-binding FYVE finger. J. Biol. Chem. 271: 24048-24054.

Stinchcombe J.C. and Griffiths G.M. (1999). Regulated secretion from hemopoietic cells. J. Cell Biol. 147: 1-5.

Stoorvogel W., Strous G.J., Geuze H.J., Oorschot A. and Schwartz A.L. (1991). Late endosomes derive from early endosomes by maturation. Cell 65: 417-427.

Storrie B. and Desjardins M. (1996). The biogenesis of lysosomes: is it a kiss and run, continuous fusion and fission process? BioEssays 18: 895-903.

Strous G.J.A.M. and Lodish H.F. (1980). Intracellular transport of secretory and membrane proteins in hepatoma cells infected by vesicular stomatitis virus. Cell 22: 709-717.

Sumner J.P., Dow J.A., Earley F.G., Klein U., Jager D. and Wieczorek H. (1995). Regulation of the plasma membrane V-ATPase activity by dissociation of peripheral subunits. J. Biol. Chem. 270: 5649-5653.

Sun-Wada G.H., Wada Y. and Futai M. (2003). Lysosome and lysosome-related organelles responsible for specialized functions in higher organisms, with special emphasis on vacuolar-type proton ATPase. Cell Struct. Funct. 28: 455-463.

Sun-Wada G.H., Wada Y. and Futai M. (2004). Diverse and essential roles of mammalian vacuolar-type proton pump ATPase: toward the physiological understanding of inside acidic compartments. Biochim. Biophys. Acta. 1658: 106-114.

Suzuki N., Del Villar K. and Tamanoi F. (1998). Farnesyltransferase inhibitors induce dramatic morphological changes of KNRK cells that are blocked by microtubule interfering agents. Proc. Natl. Acad. Sci. USA 95: 10499-10504.

Swann K. and Witaker M. (1985). Stimulation of the Na^+/H^+ exchanger of sea urchin eggs by phorbol ester. Nature 314: 274-277.

Symons M. (1995). The Rac and Rho pathways as a source of drug targets for Ras-mediated malignancies. Curr. Opin. Biotech. 6: 668-674.

Symons M. (1996). Rho family GTPases: the cytoskeleton and beyond. TIBS 21: 178-181.

Szentirmay M.N., Yang H.X., Pawar S.A., Vinson C. and Sawadogo M. (2003). The IGF2 receptor is a USF2-specific target in nontumorigenic mammary epithelial cells but not in breast cancer cells. J. Biol. Chem. 278: 37231-37240.

Szpaderska A.M. and Frankfater A. (2001). An intracellular form of cathepsin B contributes to invasiveness in cancer. Cancer Res. 61: 3493–3500.

Tait L., Soule H.D. and Russo J. (1990). Ultrastructural and immunocytochemical characterization of an immortalized human breast epithelial cell line, MCF-10. Cancer Res. 50: 6087-6094.

Takai Y., Sasaki T., Tanaka K. and Nakanishi H. (1995). Rho as a regulator of the cytoskeleton. TIBS 20: 65-70.

Tamanoi F. (1993). Inhibitors of Ras farnesyltransferases. TIBS 18: 349-353.

Tanaka S., Yora T., Nakayama K., Inoue K. and Kurosumi K. (1997). Proteolytic processing of pro-opiomelanocortin occurs in acidifying granules of AtT-20 cells. J. Histochem. Cytochem. 45: 425-436.

Tanaka Y., Guhde G., Sute A., Eskelinen E.V., Hartmann D., Lüllman-Rauch R., Janssen P.M.L., Blanz J., von Figura K. and Saftig P. (2000). Accumulation of autophagic vacuoles and cardiomyopathy in LAMP-2 deficient mice. Nature 406: 902-906.

Tapper H. and Sundler R. (1990). Role of lysosomal and cytosolic pH in the regulation of macrophage lysosomal enzyme secretion. Biochem. J. 272: 407-414.

Tartakoff A.M. and Vassalli P. (1978). Comparative studies of intracellular transport of secretory proteins. J. Cell Biol. 79: 694-707.

Ternynck T.H. and Avrameas S. (1990). Immunoenzymatic techniques. In Volume 1 in Techniques in Immunology (Eds. Kazatchkine M. and Turner M.W.). Elsevier, Amsterdam, 32-34.

Thilo L. (1985). Quantification of endocytosis-derived membrane traffic. Biochim. Biophys. Acta 822: 243-266.

Timchak L.M., Kruse F., Marnell M.H. and Draper R.K. (1986). A thermosensitive lesion in a Chinese hamster cell mutant causing differential effects on the acidification if endosomes and lysosomes. J. Biol. Chem. 261: 14154-14159.

Tjelle T.E., Brech A., Juvet L.K., Griffiths G. and Berg T. (1996). Isolation and characterization of early endosomes, late endosomes and terminal lysosomes: their role in protein degradation. J. Cell Sci. 109: 2905-2914.

Tong P. and Kornfeld S. (1989). Ligand interactions of the cation-dependent mannose 6-phosphate receptor. Comparison with the cation-independent mannose 6-phosphate receptor. J. Biol. Chem. 264: 7970-7975.

Tooze J. and Hollinshead M. (1991). Tubular early endosomal networks in AtT20 and other cells. J. Cell Biol. 115: 635-653.

Topalian S.L. (1994). MHC class II restricted tumor antigens and the role of $CD4^+$ T cells in cancer immunotherapy. Curr. Opin. Immunol. 6: 741-745.

Torigoe T., Izumi H., Ishiguchi H., Uramoto H., Murakami T., Ise T., Yoshida Y., Tanabe M., Nomoto M., Itoh H. and Kohno K. (2002). Enhanced expression of the human vacuolar H^+-ATPase c subunit gene (ATP6L) in response to anticancer agents. J. Biol. Chem. 277: 36534-36543.

Tournu C., Obled A., Roux M.P., Deval C., Ferrara M. and Béchet D.M. (1998). Glucose controls cathepsin expression in Ras-transformed fibroblasts. Arch. Biochem. Biophys. 360: 15-24.

Towbin H., Staehlin T. and Gordon J. (1979). Electrophoretic transfer of proteins from polyacrylamide gels to nitrocellulose sheets: procedure and some applications. Proc. Natl. Acad. Sci. USA 76: 4350-4354.

Toyomura T., Murata M., Yamamoto A., Oka T., Sun-Wada G.H., Wada Y. and Futai M. (2003). From lysosomes to plasma membrane: localization of vacuolar type H^+-ATPase with the a3 isoform during osteoclast differentiation. J. Biol. Chem. 278: 22023-22030.

Triguero D., Buciak J.L. and Pardridge W.M. (1991). Cationization of immunoglobulin G results in enhanced organ uptake of the protein after intravenous administration in rats and primate. J. Pharmacol. Exp. Ther. 258: 186-192.

Trischler M., Stoorvogel W. and Ullrich O. (1999). Biochemical analysis of distinct Rab5- and Rab11- positive endosomes along the transferrin pathway. J. Cell Sci. 112: 4773-4783.

Turk B., Dolenc I., Zerovnik E., Turk D., Gubensek F. and Turk V. (1994). Human cathepsin B is a metastable enzyme stabilized by specific ionic interactions associated with the active site. Biochem. 33: 14800-14806.

Turturro F., Friday E., Fowler R., Surie D. and Welbourne T. (2004). Troglitazone acts on cellular pH and DNA synthesis through a peroxisome proliferator-activated receptor gamma-independent mechanism in breast cancer-derived cell lines. Biochem. Cell Biol. 82: 626-635.

Ullrich O., Reinsch S., Urbé S., Zerial M. and Parton R.G. (1996). Rab11 regulates recycling through the pericentriolar recycling endosome. J. Cell Biol. 135: 913-924.

Vajdy M. and Lycke N. (1995). Mucosal memory B cells retain the ability to produce IgM antibodies 2 years after oral immunization. Immunol. 86: 336-342.

Vajdy M., Sethupathi P. and Knight K.L. (1998). Dependence of antibody somatic diversification on gut-associated lymphoid tissue in rabbits. J. Immunol. 160: 2725-2729.

van Bambeke F., Carryn S., Seral C., Chanteux H., Tyteca D., Mingeot Leclercq M and Tulkens P. (2004). Cellular pharmacokinetics and pharmacodynamics of the glycopeptide antibiotic Oritavancin (LY333328) in a model of J774 mouse macrophages. Antimicrob. Agents Chemother. 48: 2853-2860.

van der Sluijs P., Hull M., Webster P., Mâle P., Goud B. and Mellman I. (1992). The small GTP-binding protein Rab4 controls an early sorting event on the endocytic pathway. Cell 70: 729-740.

van Deurs B., Holm P.K., Kayser L. and Sandvig K. (1995). Delivery to lysosomes in the human carcinoma cell line Hep-2 involves an actin filament-facilitated fusion between mature endosomes and preexisting lysosomes. Eur. J. Cell Biol. 66: 309-323.

van Deurs B., Peterson O.W., Olsness S. and Sandvig K. (1989). The ways of endocytosis. Int. Rev. Cytol. 117: 131-177.

van Deurs B., von Bülow F., Vilhardt F., Holm K. and Sandvig K. (1996). Destabilization of plasma membrane structure by prevention of actin polymerization. Microtubule-dependent tubulation of the plasma membrane. J. Cell Sci. 109: 1655-1665.

van Dyke R.W. (1988). Proton pump-generated electrochemical gradients in rat liver multivesicular bodies. J. Biol. Chem. 263: 2603-2611.

van Dyke R.W. (1995). Na^+/H^+ exchange modulates acidification of early rat liver endocytic vesicles. Am. J. Physiol. 269: C943-C954.

van Dyke R.W. and Belcher J.D. (1994). Acidification of three types of liver endocytic vesicles: similarities and differences. American J. Physiol. 266: C81-C94.

van Weert A.W.M., Dunn K.W., Geuze H.J., Maxfield F.R. and Stoorvogel W. (1995). Transport from late endosomes to lysosomes, but not sorting of integral membrane proteins in endosomes, depends on the vacuolar proton pump. J. Cell Biol. 130: 821-834.

Vergne I., Constant P. and Lanéelle G. (1998). Phagosomal pH determination by dual fluorescence flow cytometry. Anal. Biochem. 255: 127-132.

Vexler Z.S., Symons M. and Barber D.L. (1996). Activation of Na^+-H^+ exchange is necessary for RhoA-induced stress fiber formation. J. Biol. Chem. 271: 22281-22284.

Veyrat-Durebex C., Pomerleau L., Langlois D. and Gaudreau P. (2004). Internalization and trafficking of the human and rat growth hormone-releasing hormone receptor. J. Cell Physiol. 203: 335-344.

Vignal E., Blangy A., Martin M., Gaultier-Rouviere C. and Fort P. (2001). Kinectin is a key effector of RhoG microtubule-dependent cellular activity. Mol. Cell. Biol. 21: 8022-8034.

Vincent L., Chen W., Hong L., Mirshahi F., Mishal Z., Mirshahi-Khorassani T., Vannier J.P., Soria J. and Soria C. (2001). Inhibition of endothelial cell migration by cerivastatin, an HMG-CoA reductase inhibitor: contribution to its anti-angiogenic effect. FEBS Lett. 495: 159-166.

Vogelstein B., Fearon E.R., Hamilton S.R., Kern S.E., Preisinger A.C., Leppert M., Nakamura Y., White R., Smits A.M.M. and Boss J.L. (1988). Genetic alterations during colorectal-tumor development. New England J. Med. 319: 525-532.

Vojtek A.B. and Cooper J.A. (1995). Rho family members: activators of MAP kinase cascades. Cell 82: 527-529.

von Boehmer H. (2003). Dynamics of suppressor T cells: in vivo veritas. J. Exp. Med. 198: 845-859.

Wadsworth S.J., Gebauer G., van Rossum G.D. and Dhanasekaran N. (1997). Ras-dependent signaling by the GTPase-deficient mutant of $G\alpha_{12}$. J. Biol. Chem. 272: 28829-28832.

Wall D.A. and Hubbard A.L. (1985). Receptor-mediated endocytosis of asialoglycoproteins by rat liver hepatocytes: biochemical characterization of the endosomal compartments. J. Cell Biol. 101: 2104-2122.

Wang I.K., Lin-Shiau S.Y. and Lin J.K. (2000). Suppression of invasion and MMP-9 expression in NIH 3T3 and v-H-Ras 3T3 fibroblasts by lovastatin through inhibition of Ras isoprenylation. Oncology 59: 245-254.

Wang M.W. and Stearns M.E. (1988). Blocking of collagenase secretion by estramustine during *in vitro* tumor cell invasion. Cancer Res. 48: 6262-6271.

Wang W. and Macaulay R.J. (1999). Apoptosis of medulloblastoma cells in vitro follows inhibition of farnesylation using manumycin A. Int. J. Cancer 82: 430-434.

Wang Y., Pennock S., Chen X. and Wang Z. (2002). Endosomal signaling of epidermal growth factor receptor stimulates signal transduction pathways leading to cell survival. Mol. Cell. Biol. 22: 7279-7290.

Wang Z.Q. and Gluck S. (1990). Isolation and properties of bovine kidney brush border vacuolar H^+-ATPase. J. Biol. Chem. 265: 21957-21965.

Ward D.M., Leslie J.D. and Kaplan J. (1997). Homotypic lysosome fusion in macrophages: analysis using an *in vitro* assay. J. Cell Biol. 137: 665-673.

Weiss R.H., Ramirez A. and Joo A. (1999). Short-term pravastatin mediates growth inhibition and apoptosis, independently of Ras, via the signaling proteins p27Kip1 and PI3 kinase. J. Am. Soc. Nephrol. 10: 1880-1890.

White J., Kartenbeck J. and Helenius A. (1980). Fusion of Semliki Forest virus with the plasma membrane can be induced by low pH. J. Cell Biol. 8: 264-272.

Wilkening G., Linke T. and Sandhoff K. (1998). Lysosomal degradation on vesicular membrane surfaces. Enhanced glucosylceramide degradation by lysosomal anionic lipids and activators. J. Biol. Chem. 273: 30271-30278.

Willingham M.C., Cornwell M.M., Cardarelli C.O., Gottesman M.M. and Pastan I. (1986). Single cell analysis of daunomycin uptake and efflux in multidrug-resistant and –sensitive KB cells: effects of verapamil and other drugs. Cancer Res. 46: 5941-5946.

Wilson J.M., Whitney J.A. and Neutra M.R. (1991). Biogenesis of the apical endosome-lysosome complex during differentiation of absorptive epithelial cells in rat ileum. J. Cell Sci. 100: 133-143.

Wojtkowiak Z., Briggs R.C. and Hnilica L.S. (1983). A sensitive method for staining proteins transferred to nitrocellulose sheets. Anal. Biochem. 129: 486-489.

Wolfman A. and Macara I.G. (1987). Elevated levels of diacylglycerol and decreased phorbol ester sensitivity in ras-transformed fibroblasts. Nature 325: 359-361.

Wöll E., Ritter M., Scholz W., Häussinger D. and Lang F. (1993). The role of calcium in cell shrinkage and intracellular alkalinisation by bradykinin in Ha ras oncogene expressing cells. FEBS Lett. 322: 261-265.

Wolozin B., Kellman W., Ruosseau P., Celesia G.G and Siegel G. (2000). Decreased prevalence of Alzheimer disease assiocited with 3-hydroxy-3-methylglutaryl coenzyme A reductase inhibitors. Arch. Neurol. 57: 1439-1443.

Wong B., Lumma W.C., Smith A.M., Sisko J.T., Wright S.D. and Cai T.Q. (2001). Statins suppress THP-1 cell migration and secretion of matrix metalloproteinase 9 by inhibiting geranylgeranylation. J. Leukoc. Biol. 69: 959-962.

Woodman P.G. and Warren G. (1988). Fusion between vesicles from the pathway of receptor-mediated endocytosis in a cell-free system. Eur. J. Biochem. 173: 101-108.

Xie S.X., Crider B.P. and Stone D.K. (1989). Isolation and reconstitution of the chloride transporter of clathrin-coated vesicles. J. Biol. Chem. 264: 18870-18873.

Xie X.S., Padron D., Liao X., Wang J., Roth M.G. and De Brabander J.K. (2004). Salicylihalamide A inhibits the V_0 sector of the V-ATPase through a mechanism distinct from bafilomycin A_1. J. Biol. Chem. 279: 19755-19763.

Yamashiro D.J., Fluss S.R. and Maxfield F.R. (1983). Acidification of endocytic vesicles by an ATP-dependent proton pump. J. Cell Biol. 97: 929-934.

Yamashiro D.J., Tycko B., Fluss S.R. and Maxfield F.R. (1984). Segregation of transferrin to a mildly acidic (pH 6.5) para-Golgi compartment in the recycling pathway. Cell 37: 789-800.

Yan S.Q., Sameni M. and Sloane B.F. (1998). Cathepsin B and human tumor progression. Biol. Chem. 379: 113-123.

Yun C.H., Tse C.M. and Donowitz M. (1995). Chimeric Na^+/H^+ exchangers: an epithelial membrane-bound N-terminal domain requires an epithelial cytoplasmic C-terminal domain for regulation by protein kinases. Proc. Natl. Acad. Sci. USA 92: 10723-10727.

Zhang K., Wang Z.Q. and Gluck S. (1992a). Identification and partial purification of a cytosolic activator of vacuolar H^+-ATPases from mammalian kidney. J. Biol. Chem. 267: 9701-9705.

Zhang K., Wang Z.Q. and Gluck S. (1992b). A cytosolic inhibitor of vacuolar H^+-ATPases from mammalian kidney. J. Biol. Chem. 267: 14539-14542.

Zhu Y. and Conner G.E. (1994). Intermolecular association of lysosomal protein precursors during biosynthesis. J. Biol. Chem. 269: 3846-3851.

Zoller M. and Andrighetto G. (1988). Induction of tolerance towards TNP entails down-regulation of an autoimmune attack. Immunol. 63: 205-212.